CREEP BEHAVIOUR ANALYSIS OF THIN SPRAY-ON LINERS

A THESIS SUBMITTED TO
THE GRADUATE SCHOOL OF NATURAL AND APPLIED SCIENCES
OF
MIDDLE EAST TECHNICAL UNIVERSITY

BY

DOĞUKAN GÜNER

IN PARTIAL FULFILLMENT OF THE REQUIREMENTS
FOR
THE DEGREE OF DOCTOR OF PHILOSOPHY
IN
MINING ENGINEERING

MAY 2020

Approval of the thesis:

THESIS TITLE

submitted by **DOĞUKAN GÜNER** in partial fulfillment of the requirements for the degree of **Doctor of Philosophy** in **Mining Engineering, Middle East Technical University** by,

Prof. Dr. Halil Kalıpçılar
Dean, Graduate School of **Natural and Applied Sciences**   _____

Prof. Dr. Naci Emre Altun
Head of the Department, **Mining Engineering**   _____

Prof. Dr. Hasan Öztürk
Supervisor, **Mining Engineering, METU**   _____

Examining Committee Members:

Assoc. Prof. Dr. İbrahim Ferid Öge
Mining Engineering, Muğla Sıtkı Koçman University   _____

Prof. Dr. Hasan Öztürk
Mining Engineering, METU   _____

Assist. Prof. Dr. Serhat Canbolat
Petroleum and Natural Gas Engineering, Near East University   _____

Assist. Prof. Dr. Mustafa Erkayaoğlu
Mining Engineering, METU.   _____

Assist. Prof. Dr. Onur Gölbaşı
Mining Engineering, METU.   _____

Date: 28.05.2020

I hereby declare that all information in this document has been obtained and presented in accordance with academic rules and ethical conduct. I also declare that, as required by these rules and conduct, I have fully cited and referenced all material and results that are not original to this work.

Name, Last name : Doğukan Güner

Signature :

ABSTRACT

CREEP BEHAVIOUR ANALYSIS OF THIN SPRAY-ON LINERS

Güner, Doğukan
Doctor of Philosophy, Mining Engineering
Supervisor : Prof. Dr. Hasan Öztürk

May 2020, 203 pages

Thin Spray-on Liner (TSL) is a relatively thin (2–5 mm) and fast-setting liner material used by spraying onto rock surfaces to support underground excavations. Areal support materials that are sprayed onto the rock, such as shotcrete or liners, are able to generate support resistance at small rock deformations and can prevent underground rockfalls from happening in the first place. However, where large ground convergence occurs, the more flexible TSLs may provide superior support over the full range of rock deformations. In this study, the creep behaviour of two TSLs were determined in the laboratory environment. Under constant stress levels, strain-time behaviours of two TSLs were determined up to 2 months of the testing period. For this purpose, dogbone shape test samples were prepared with different curing times (1-2, 7, and 14 days) and were tested under $23 \pm 2\,°C$ laboratory conditions according to the ASTM standards. Four different constant stress levels (80%, 60%, 40%, and 20% of the tensile strength) were applied until rupture of the specimens. The resultant correlations are explained using inter-related equations to make a forecast about the service life of the material (creep rupture envelopes) were derived. The proposed correlations may offer an insight into both the effective permanent support time and the strain amount at the liner failure. Experimental data were used to construct viscoelastic and viscoplastic models. A good agreement was generally observed between the presented models and the experimental results. In

addition, the developed constitutive stress-strain-time relations were introduced to finite element software ABAQUS with a new subroutine. After verification of the implemented subroutines, the support performance of the TSLs on the global stability in the underground openings has been investigated. As a result of this study, the creep behaviours of TSLs were investigated for the first time in the literature and it has been found that TSLs are extremely sensitive to creep behaviour. The effective block bearing time of TSL's with different wedge dimension scenarios of underground excavations were determined. As a result of the numerical studies, performed in 4 different representative rock mass squeezing behaviours with different TSL application thicknesses, it was concluded that the effect of TSL on global stability was extremely small.

Keywords: Thin spray-on liner (TSL), Time-dependent, Creep, Surface support, Dogbone, Numerical modeling

ÖZ

PÜSKÜRTME İNCE KAPLAMALARIN SÜNME DAVRANIŞI ANALİZİ

Güner, Doğukan
Doktora, Maden Mühendisliği
Tez Yöneticisi: Prof. Dr. Hasan Öztürk

Mayıs 2020, 203 sayfa

Püskürtme İnce Kaplama (PİK), yeraltı kazılarının tahkimatı için kaya yüzeyine püskürtme olarak uygulanan, hızlı kür alan, göreceli olarak ince (2-5 mm) kaplamadır. Püskürtme beton veya kaplamalar gibi kaya üzerine püskürtülen bölgesel destek malzemeleri, küçük kaya deformasyonlarında tahkimat direnci oluşturabilir ve yeraltı kaya düşmelerini ilk etapta önleyebilir. Bununla birlikte, konverjansının fazla olduğu durumlarda, daha esnek olan PİK'ler püskürtme betona oranla tam alan kaya deformasyonları için üstün tahkimat özelliği sağlayabilir. Bu çalışmada laboratuvar ortamında iki farklı PİK'in sünme davranışı belirlenmiştir. Sabit gerilim seviyeleri altında, iki PİK'in gerinim-zaman davranışları her biri en fazla 2 ay sürecek deneyler ile belirlenmiştir. Bu amaçla, farklı kür sürelerine sahip (1-2, 7 ve 14 gün) köpek kemiği şeklinde test numuneleri ASTM standartlarına göre hazırlanmış ve $23 \pm 2\,°C$ laboratuvar koşullarında test edilmiştir. Numuneler, dört farklı sabit gerinim seviyesinde (çekme dayanımının % 80,% 60,% 40 ve% 20'si), yenilme gerçekleşinceye kadar bırakılmıştır. Elde edilen korelasyonlar, malzemenin servis ömrü (sünme kopması zarfları) hakkında bir tahmin yapmak için birbiriyle ilişkili denklemler kullanılarak açıklanmıştır. Önerilen korelasyonlar hem etkili kalıcı kalıcı süresi hem de kaplama yenilme anındaki gerilme miktarları hakkında

bir fikir vermektedir. Deneysel veriler viskoelastik ve viskoplastik modeller oluşturmak için kullanılmıştır. Sunulan modeller ile deneysel sonuçlar arasında genellikle iyi bir uyum gözlemlenmiştir. Buna ek olarak, bulunan temel gerilim-gerinim-zaman ilişkileri sonlu elemanlar yazılımı olan ABAQUS'e yeni bir alt rutin ile tanıtılmıştır. Oluşturulan alt rutinlerin doğrulaması yapıldıktan sonra PİK'lerin yeraltı açıklıklardaki global stabilite durumuna olan etkisi incelenmiştir. Bu çalışmanın sonucunda, PİK'lerin sünme davranışları literatürde ilk kez araştırılmış ve PİK'lerin sünme davranışına son derece duyarlı olduğu ortaya çıkarılmıştır. PİK'lerin yeraltı kazılarında etkin blok taşıma süreleri, farklı kama boyut senaryolarıyla belirlenmiştir. Gerçekleştirilen sayısal çalışmalar sonucunda, 4 farklı sıkışma davranışlarına sahip temsili kaya kütlelerindeki dairesel kesit analizlerinde farklı uygulama kalınlıklarına sahip PİK'lerin global stabilite durumuna etkisinin son derece düşük olduğu gözlemlenmiştir.

Anahtar Kelimeler: Püskürtme İnce Kaplama (PİK), Zamana bağlı, Sünme, Yüzey tahkimatı, Köpek kemiği, Sayısal modelleme

To my beloved family and my love

for their infinite support and trust

ACKNOWLEDGMENTS

First of all, I would like to express my deepest appreciation and heartfelt thanks to my advisor Prof. Dr. Hasan Öztürk for his constructive guidance, insightful wisdom, valuable suggestions and continuing patience throughout this study. I also present my special thanks to the examining committee members, Assoc. Prof. Dr. Ferid Öge, Asst. Prof. Dr. Mustafa Erkayaoğlu, Asst. Prof. Dr. Onur Gölbaşı and Asst. Prof. Dr. Serhat Canbolat for serving on the PhD thesis committee.

I express my graditude to Dr. Ahmet Güneş Yardımcı, Dr. Selahattin Akdağ, Dr. Selin Yoncacı, Deniz Tuncay, Uğur Alkan, Mahir Can Çetin, Kutay Emre Karadeniz and my dear friends who are not mentioned here for their invaluable encouragement and friendship.

Finally, I owe my loving thanks to my family. Without their encouragement and understanding it would have been impossible for me to complete this thesis. At last but not least, many thanks to my beloved love Aysu, she has always supported me and stood by me throughout this exhausting period.

TABLE OF CONTENTS

LIST OF TABLES

LIST OF FIGURES

FIGURES

CHAPTER 1

INTRODUCTION

Underground operations have high incident and severity rates compared to the other industries. It is a fact that this rate is higher in underground operations especially in small-scale mines. Underground rockfall and rockburst accidents are considered as the most significant causes of all fatal accidents in deep mines. Therefore, the stability of underground openings both during and after the excavation stages is of great concern to design engineers. According to Potvin (2006), over 90% of rockfalls causing injuries weigh less than 2 tonnes, considered as a small amount of rock mass, and more than 80% of the rockfall injuries happened within 10 m of an active development mining face in Australia. This information shows the importance of surface support in underground openings.

Since any instabilities may lead to irremediable results, rock reinforcement and supporting issues have a vital importance to ensure the safe continuation of the advance or production cycle. Rock reinforcement is widely used to describe the procedures and the materials, which restrains the movement of rock mass and enhances the mechanical properties of surrounding rock mass without deforming excessively. On the other hand, rock support elements or systems are used to provide resistance against the movement of surrounding rock mass so that the underground opening retains its integrity for a reasonable period.

Rock support elements are primarily used to prevent the movement of rock mass and large blocks, while surface support elements, which are used for preventing small-scale block-induced instabilities in the rock mass, are more favorable for the containment purposes. Surface support elements are also called as "areal support" as they cover the roof and walls of the underground openings. Wire mesh, straps, grids,

1

thick layer sprayed material (mortar and shotcrete), and Thin Spray-on Liners (TSLs) are considered as areal support elements (Thompson et al., 2012).

TSL is developed as an alternative to shotcrete, a widely used surface support material, at the beginning of the 1990's in Canada and South Africa. The recognized definition of TSL in the mining sector worldwide is "generally cement, latex, polymer-based and also reactive or non-reactive, multi-component materials applied to the rock surface sprayed by nozzle, in a layer of generally 6 mm or less (3-5mm) thickness to temporarily support the excavation " (Hadjigeorgiou, 2003). In the last decade, TSLs have gained some partial acceptance by the authorities in mining industry. However, there is still a lack of full technical knowledge about this new generation support member.

Sprayed areal supports can be able to act as an active support element when a few millimeters relative movements occur in a rock mass or blocks. Therefore, they can reinforce the rock mass at the early stages before the excavation convergence reaches large displacement values on the ground reaction curve. Wire mesh, straps, and grids are passive support elements and require substantial displacement to act as an active support element. Although shotcrete or reinforced shotcrete has more support resistance than TSLs, the TSLs can provide a better rock support in highly squeezed ground conditions (O'Donnell and Tannant, 1998). Unlike traditional brittle bolts and shotcrete, the more flexible behaviour observed in TSLs allows the distribution of loads over a larger lining area. When TSLs are used in conjunction with wire mesh, the TSL can achieve a high load-carrying capacity, which can be equal or higher than the strength of the reinforced shotcrete (Tannant, 2001).

Unlike shotcrete, which can exhibit abrupt failure due to shear and tensile loads, polyurethane/polyuria or cement-based TSLs may deform together with the rock and even maintain the support function when the surrounding rock or rock block reaches the extreme relative displacement values. Besides, the deformability capabilities of the TSLs enable them to carry the imposed load just like a suspension bridge (Tannant et al., 1999).

1.1. Problem Statement

TSLs are predicted to be sufficient for the use of areal support. However, the mechanical behaviour and the support mechanism of this relatively new support material is still not fully understood and well defined. Although some researchers in the literature conducted various laboratory, analytical, empirical, and numerical studies to reveal the effectiveness of TSLs, it is still very challenging to describe the support ability of the TSLs with a quantitative validation. A detailed and comparative review of these studies will be presented in Chapter 2.

Since the main component of TSLs is polymer-based, the studies of the related research area have stated that creep behaviour was an important design parameter that should be investigated in detail (Yılmaz et al., 2003; Kuijpers et al., 2004; Villaescusa, 2014). A comprehensive literature review shows that there is not study considering the time-dependent behaviours of TSLs. Besides, the tensile strength parameter of TSL has been used as the fundamental design parameter in numerical and analytical studies in the literature. Therefore, it was emphasized in those studies that creep tests would play a significant role in the identification of TLS design parameters.

TSLs are fast setting materials. Therefore, curing time becomes very crucial and effective in the variations of TSLs geomechanical properties. It is considered that the effect of curing time on creep behaviour should also be investigated as a complementary to a full TSL creep characterization.

Currently, when the holding function of the liner is activated under the influence of the formed wedge blocks, design engineers fail to forecast the long-term performance and the expected service life of the bagged TSL.

1.2. Key Research Objectives

This research study aims to provide an insight into the creep behaviour of thin spray-on liners. The following sub-objectives of the thesis are summarized to achieve main objective as follows:

- To complete an extensive review of the background, application areas, advantages and disadvantages of TSL, laboratory studies of TSL, and creep modeling,
- To design a laboratory creep test apparatus for TSLs,
- To perform creep experiments for two different TSL products at three different curing times, which are widely used worldwide.
- To generate creep rupture envelopes as a result of the creep tests so as to predict the long-term performance and the expected service life of tested TSLs.
- To construct nonlinear viscoplastic and viscoelastic models and to find constitutive time-dependent stress-strain relationships.
- To implement the constitutive relationships in a finite element software with a developed subroutine.
- By using the subroutine, numerical stability modeling of circular excavations with four different rock mass quality supported by TSLs with a varying thickness.

This study is motivated by the apparent lack of research on creep behaviour of TSLs in the literature. Therefore, the related researchers and design engineers may benefit from the outcomes of the current research by analyzing the long-term behaviour of TSL support and may modify or change their empirical or numerical designs, concordantly.

It is also expected from this research that TSL manufacturers may realize the importance of time-dependent mechanical behaviour of their products. By this way,

they may manufacture different TSLs for different use and life and may necessitate performing creep tests to reveal a full time-dependent performance of the products.

1.3. Research Methodology

The methodology of this research includes the following steps:

- Acquisition of the two widely used TSLs from different manufacturers.
- Setting-up of the testing apparatus and pretesting of the setup with some trial tests.
- Determination of a proper specimen preparation technique and specimen dimension.
- Performing tensile tests to determine the stress levels to be used in creep tests.
- Creep tests for two TSL products at three different curing times.
- Evaluation of test results to obtain creep rupture envelopes.
- Development of nonlinear viscoplastic and viscoelastic models
- Constructing a new subroutine in ABAQUS software for mathematical expression of the stress-strain relationship as a function of time
- Investigation of the support behaviour of TSL in a tunnel application in ABAQUS software

1.4. Thesis Outline

This thesis consists of eight chapters, which are organized as described below.

Chapter 1 introduces the research subject, problem statement, research objectives, methodology of the study, and thesis outline.

Chapter 2 presents the overview, fields of application, advantages, and disadvantages of TSLs. The laboratory and numerical studies performed for TSLs in the literature, are also presented in this part. An overview of the time-dependent models for different polymer-based materials is given at the end of this chapter.

Chapter 3 covers the laboratory studies. This chapter makes a detailed discussion on i) the preparation of laboratory creep testing apparatus for TSLs, which is capable of carrying out eight tests at the same time, ii) general information about TSLs used, iii) determination of sample type and sample preparation method to be used in creep tests, iv) tensile tests for determination of constant tensile stresses to be used in the experiments, and v) creep tests of two different TSLs with different curing time for four different constant tensile levels.

Chapter 4 concentrates on the evaluation of the test results and comparison of the tested products in terms of their time-dependent performance.

Chapter 5 presents the critical assessment and development of nonlinear viscoplastic and viscoelastic models using the laboratory test results.

Chapter 6 covers the implementation of the generated constitutive relationships in a finite element software with a new routine, and model verifications of the routine by simulating tensile creep tests.

Chapter 7 presents a numerical application in the finite element software to investigate the support behaviour of TSL in a squeezing tunnel. The application is performed for two cases in which a circular opening is unsupported and supported by the TSL.

Chapter 8 outlines the conclusion drawn from the study and provides some recommendations for future works.

CHAPTER 2

LITERATURE REVIEW

This chapter presents relevant literature studies of TSLs including background information, fields of application, advantages, and disadvantages. Laboratory and numerical studies of TSL are covered with an overview of time-dependent models at the end of this chapter.

2.1. Rock Failure

The stability behaviour of underground openings directly depend on the hosting rock mass. Knowledge regarding the rock mass involving the deformation behavior, rock mass strength, presence of discontinuities and some other parameters are required for the design of underground structures. Different forms of instabilities may occur in the excavation design due to the analyzes conducted with insufficient data or unpredictable ground conditions.

In literature, types of underground excavation instabilities can be divided into two main categories as local instabilities and global instabilities. When the failure on the surrounding rock mass takes place continuously, and the opening cannot be stable without any support, this is referred to as global instability. Global instability is a result of the critical ratio of rock mass strength to induced stress being exceeded (Villaescusa *et al.,* 2019). On the other hand, joints and discontinuity sets may also create loose blocks around openings; the dead weight of these blocks can lead to local instabilities. For the stable surrounding rock, local instabilities are the primary failure mode. The typical global and local instability modes for underground openings are presented in Figure 2.1.

Moreover, failure modes can also be classified according to the structure of the surrounding rock mass conditions as follows (Aydan, 1989):

- Failure modes involving only intact rock: rockbursting and squeezing.
- Failure modes involving discontinuities and intact rock: bending, buckling, shearing, and sliding.
- Failure modes involving only discontinuities (blocky medium only): blockfalls, sliding, toppling, sliding and toppling.

Rockbursting: Very high stressing due to depth of opening and/or seismic events of massive, hard, brittle rock creates a stress-induced failure, resulting from the combined action of initial shearing and the subsequent splitting. Rock burst is generally associated with energy and is interplayed between the elastic stored energy and the brittleness of the rock. Moreover, this failure is a combination of the behaviour of the rock mass, seismic event, and the properties of the presence discontinuities. Two principal rockburst types are classified as strain burst and fault burst.

Squeezing: The time-dependent large deformation, which occurs around the underground opening, is essentially associated with creep caused by exceeding limiting shear strength. Although this failure mode is associated only with intact rock in this classification, squeezing can occur both in massive rocks and in highly jointed rock masses as a result of overstressing. Also, heavily jointed rock masses behave as ductile.

According to Aydan (2018), the strength of the rock element is the key parameter controlling the rockbursting and squeezing failure modes.

Bending: This instability type is generally encountered in sedimentary rocks, horizontally bedded and vertically jointed. Bending failure is also associated with in-situ stresses. It can be triggered when the horizontal field stress, parallel to the bedding, is relatively low.

Buckling: Similar to bending failure, buckling is generally observed in ductile sedimentary rocks with thin layers. Besides, it can also be in some metamorphic rocks (i.e., phyllite, mica, and schists). As opposed to bending, high field stresses require in the parallel direction of the layers. Moreover, layer thickness versus span ratio should be relatively small for the occurrence of buckling failure.

Shearing and sliding: It is a combination of sliding of the unstable part along the bedding plane, relatively thick layered sedimentary rocks, and shearing of intact rock. Shearing and sliding can be seen when the field stresses are relatively higher than the uniaxial compressive strength of the rock, where buckling failure becomes impossible.

Blockfalls and sliding: In blocky rock mass excavations, blocks are formed by the intersection of three or more discontinuities. Unfavorable blocks with falling potential may be formed. Under the effect of gravity and other static and dynamic forces, back and wall wedges may either fall or slide out of their sockets. The geometry, strength characteristics, orientation and length of the planes, and stresses within the rock mass are the main factors that control the stability of formed blocks (Nomikos *et al.*, 2006)

ROCKBURSTING   **SQUEEZING FAILURE**

BUCKLING FAILURE   **TENSILE SPLITTING SHEARING AND SLIDING**
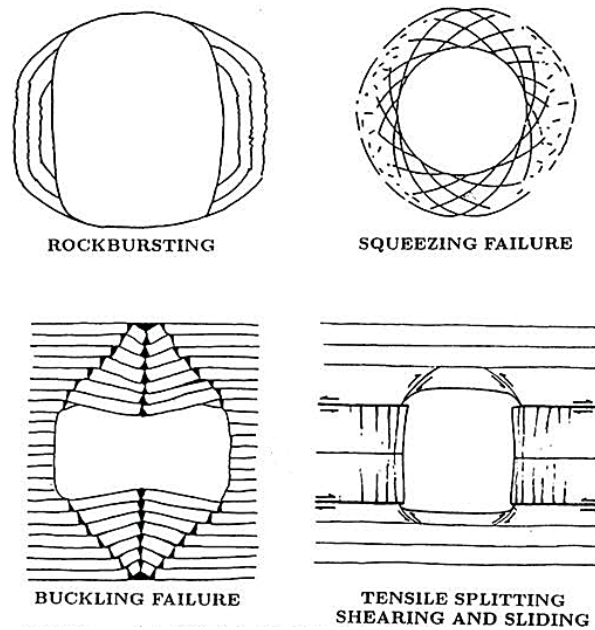
a) Global form of instabilities

BENDING FAILURE   **FLEXURAL TOPPLING SHEARING AND SLIDING**   **FLEXURAL TOPPLING**

FALLS   SLIDING   TOPPLING
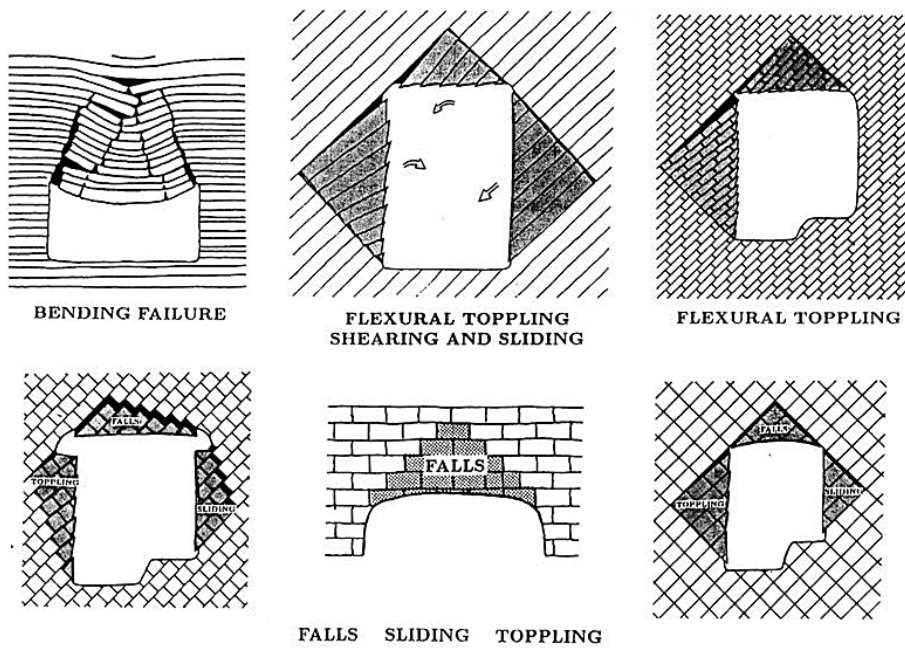
b) Local form of instabilities

Figure 2.1. Instability modes of underground openings (modified after Aydan, 1989)

10

2.2. Rock Support Types

The term rock support is used for describing the procedures and materials to sustain and improve the stability of underground openings. Rock support is a general term, covering both the effects of reinforcement and support members. Widely used rock reinforcement elements are dowels, tensioned rock bolts, and cable bolts. On the other hand, support elements are mesh, straps, sprayed material (shotcrete and thin spray-on liner), and steel sets.

Although various classifications are presented for rock supports in the literature, the most widely used rock support classification is based on its supporting character. Hoek and Wood (1987) classified the rock support systems as active rock reinforcement and passive rock support.

Mechanically anchored and resin anchored rockbolts, grouted, and friction dowels are principal types of rock reinforcement members. Rock bolts are generally used for primary support purposes, and they are considered to be the most significant and widespread support members in underground excavations. They apply positive? force to the rock mass; on the other hand, dowels requires rock movement to activate its reinforcing action.

Mechanically anchored rockbolts: These rockbolts are the oldest form of reinforcement elements used in underground excavations. They are relatively inexpensive and still most widely used for short-term (temporary) support in underground mines. Mechanically anchored rockbolts consist of three parts; expansion shell, steel bolt, and face plate. After the entire assembly is inserted into the drilled hole, rotating the end of the bolt will force the shell to expand against the rock wall of the hole, hence the anchoring force increases. Since the length of the expansion shell is limited for these rockbolts, the anchoring force is also relatively low. Pre-tension in the bolt is usually required, 70% of the ultimate bearing capacity of the rockbolt, to inhibiting the joint dilatation. However, the anchoring unit of the bolt tends to slip over time by the triggering effects of dynamic events. Groundwater also has an adverse effect on rockbolts. In some extreme cases, the service life of an

unprotected bolt may be less than one year in massive sulphides (Hoek and Wood, 1987).

Resin anchored rockbolts: These rockbolts are necessary for the conditions where the support load should be maintained. Resin products have generally both resin and catalyst in separate parts. The cartridges are pushed to the bottom of the drillhole. With the spinning action of the bolt, the plastic cover of the cartridge is broken, then resin and catalyst were mixed and set in a few minutes. In this way, the strong anchor has achieved. For some permanent applications, the number of resins can be increased, and a number of relatively slow-setting resins are inserted into the drillhole behind the fast-setting anchor cartridges.

Grouted or friction anchored dowels: If the supporting action is required very close to an advancing face, dowels become more favorable. For grouted dowels, grout application is the most critical part. "A thick grout is pumped into the drillhole by inserting the grout tube to the end of the hole and slowly withdrawing the tube as the grout is pumped in" (Hoek *et. al.,* 2000). Split set and swellex are widely used friction anchored dowels worldwide. Grouted or friction anchored dowels are placed to drillhole without pre-tension. They require substantial rock mass movements to become active, which also means that they are considered to be passive elements . Although this may be considered as a drawback, when dowels were applied close to the advancing face, adequate ground movement can be achieved in the rockmass and interlocking between rock blocks is retained.

2.2.1. Passive Rock Support and Areal Support

Passive support systems are actived in case the rock moves. Mesh, shotcrete, steel sets, straps, are the common passive support systems utilized in underground openings. Some of the rock reinforcement elements,   such as expandable friction bolt, split-sets are also passive support members as mentioned in grouted or friction anchored dowels part.

Wire mesh, shotcrete, and Thin spray-on liners can distribute the exposed loads on the larger area. Therefore, they are also considered as areal support members. They can be used in conjunction with rockbolts and other support elements. Wire mesh and shotcrete have been used extensively in underground operations since the 1950s (Morton *et al.,* 2007).

Welded and chain link are two standard wire mesh types. Chain link mesh is flexible, and it has higher elongation and load-bearing capacity than welded. The installation of the chain link mesh is difficult in an underground opening. It is not also suitable to be used in conjunction with shotcrete applications. It is more popular in slope stability and rockfall protection fields rather than underground operations. Welded meshes are produced by welding of a grid of crossing wires at their intersection points. It is more widely used, rigid and easier to install than chain link mesh.

"Gunite", accepted as the first spraying support product and later called shotcrete, has become widely used in underground excavations with the worldwide acceptance of the NATM method (Rabcewicz, 1965). During the rapid technological advancements in the mining industry the improvement in mechanical properties of shotcrete became necessary. Researches have extensively focused on the issues of the development of support systems. Especially in the last 30 years, there have been many studies for the development of different underground supports to ensure better health and safety conditions of people. As a result of increasing investments and rapid technological developments in the mining and tunneling industry, there was a need to enhance the mechanical, operational properties of shotcrete. Despite the studies carried out by many researchers in this field, improvements in these properties of shotcrete remained limited.

2.3. Overview of TSL

At the beginning of the 1980's, underground mining companies invited researchers to develop an alternative product for shotcrete due to some logistic and geotechnical drawbacks of shotcrete. MIROC (Canadian Mining Industry Research Organization) conducted a detailed research in the late 1980's to produce a new material that could

be an alternative to shotcrete for large-scale private companies. As a result of this research, they developed the first Polyurethane based TSL product called Mineguard ™. The detailed laboratory tests of this TSL continued until the end of the 1990s (Archibald et al., 1997; Archibald and Lausch., 1999). During the same period in South Africa, a latex-based TSL material called Everbond was developed (Wojno and Kuijpers, 1997). These studies have increased the interest of the world mining sector in TSLs. As TSLs have some advantages such as providing ease of use and reducing mining costs, mining companies have started to consider TSLs as an alternative of shotcrete.

After the workshop of "1st International Seminar on Mine Surface Support Liners: Membrane, Shotcrete and Mesh" organized in Perth, Australia in 2001, all products falling into the description of "thin layer of surface support made from plastic, polymer or cement-based compositions" were called as "Thin Spray-on Liner (TSL)". A general definition of TSL accepted by the whole mining society is "generally cement, latex, polymer-based and also reactive or non-reactive, multi-component materials applied to the rock surface sprayed by a nozzle, in a layer of generally 6 mm or less (3-5 mm) thickness to temporarily support the excavation" (Hadjigeorgiou, 2003).

So far, more than 40 TSL products are on the market, but currently, 19 of them are actively sold. It is known that TSL suppliers actively carry out R & D studies in order to improve the mechanical and logistic properties of the products in order to meet the demands of the companies. Table 2.1 represents the commercially available TSL products worldwide.

Table 2.1 Currently available TSL products

Product	Manufacturer	Chemistry
MasterRoc TSL 865™	BASF, International	Single-component polymer powder
Diamondguard™	Diamondguard, South Africa	Non-cementitious, elastomeric
Aero SealTM	Genrock Mining, South Africa	Cementitous, polymer
Tekflex™ Tekflex Black™ Tekflex White™	Minova International Inc.	Cementitious polymer powder, liquid
Tekflex LP™	Minova, Germany	Stabilized resin latex, cementitious
Tekflex DS-W™	Minova, Germany	Cementitious, copolymer
Capcem™ KT Fast Tekcrete™	Minova International Inc.	Cementitious
Capcem™ KT Fast 2C		Cementitious powder, polymer liquid
TamCrete SSL™	Normet, International	Non-cementitious, acrylic
Tunnel Guard™	SA Mining, South Africa	Cementitious, PP fiber, composite
Sealaport™	Sealaport, South Africa	Acrylic, 2 layer composite
Technicrete TSL	Technicrete	Cementitious, PP fiber, silica sand
PTU™ K5™	Specialty Products Inc., USA	Polyurea elastomer
Rockweb™	Spray-on Plastics, Canada	3 part Polyurea
Jennchem TL-40	Jennchem, Australia	2 part cement and polymer

In 2001, 55 different mines began to use TSLs as a surface support material (Tannant, 2001). From a survey of the leading suppliers, TSLs are currently being estimated to be used in more than 150 mines and underground openings all around the world. According to Mpunzi et al. (2015), in South Africa, the annual usage of TSL is around 7500 tonnes and it is estimated that this number will increase consistently. Moreover, for Copiapó mining accident in 2010, an experimental remote borehole installation was sent as an emergency support plan for the rescue of the 33 Chilean miners by using TSL (Rockweb).

The majority of current TSLs are two-part polyurethane/polyurea or cement-based latex products that are mixed on-site before spraying them onto rock surfaces. Figure 2.2 shows the typical applications of TSLs.

Figure 2.2 Typical Underground applications of TSLs (Ferreira and Piroddi,2012)

In the literature, various advantages and disadvantages of using TSL have been proposed in detail. Yilmaz (2011) and Guner (2014) summarized all the advantages and the disadvantages mentioned in the literature. They classified the advantages and disadvantages as presented in Figure 2.3.
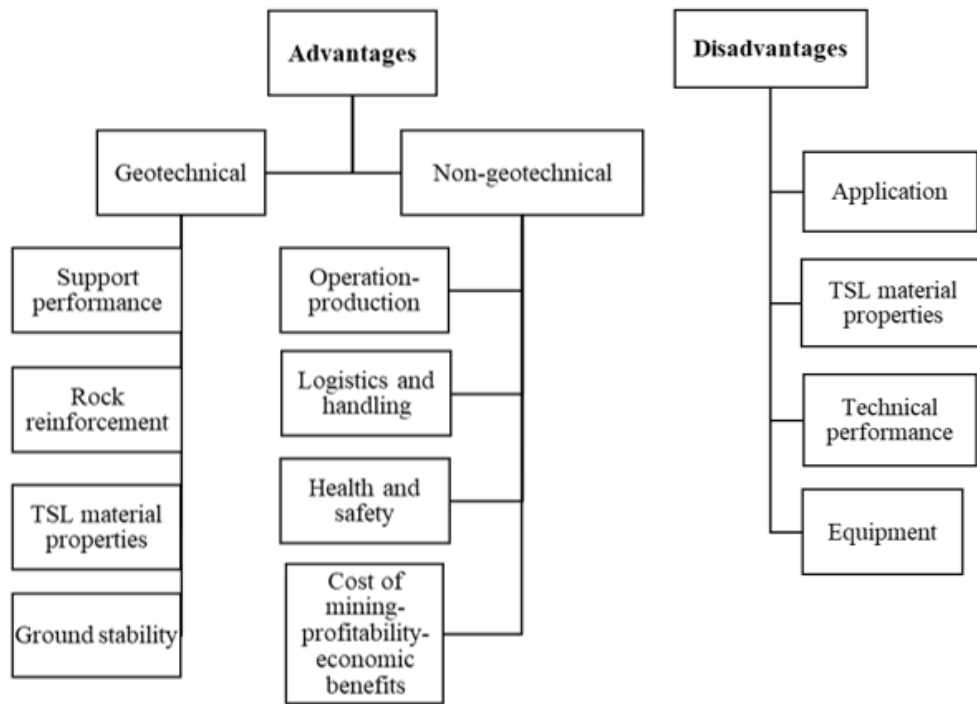
Figure 2.3 Classification of advantages and disadvantages of TSLs (modified after Yilmaz, 2011; Guner 2014)

Similar to shotcrete, TSLs are also surface support members. In the point of alternativeness, the advantages of TSLs over shotcrete are given in this section. These advantages are;

- Fast curing rate and ability to reach adequate mechanical properties in a few hours after application, (Lacerda, 2004; Hannon, 2009; Guner 2014; Wei et al., 2019)

- Discardable rebound amount and wastage during the spraying process, (Spearing et al., 2009; Smith, 2012)

- Wide displacement range (elongation ratio), (Tannant, 2001; Kuijpers et al., 2004; Lukey et al., 2008; Ozturk, 2011; Guner 2014)

- Ease of application and fast application rate, (Tannant, 2001; Pappas et al., 2003; Kuijpers et al., 2004; Yilmaz, 2011; Esterhuizen and Bosman, 2009).

- Smaller spraying equipment and less material handling, (Laurence, 2001; Tannant, 2001; EFNARC, 2008; Steyn et al., 2008; Guner 2014; Li et al., 2016;

- The decrease in the operating costs, (Tannant, 2001; Archibald, 2004; Esterhuizen and Bosman, 2009).

- Thinner thicknesses of applied material, (Tannant, 2001; Pappas et al., 2003)

Despite the mentioned advantages, there are also few drawbacks of using TSL claimed by some researchers. Those disadvantages are; lack of information about support mechanism (Guner and Ozturk 2016; Kuijpers et al., 2004) and constitutive behaviour (Tannant and Wang 2003), short shelf-life (Espley et al., 2001; Pappas et al., 2003), and the ease of crack propagation in brittle liner (Guner 2014).

2.3.1. TSL Application Areas

TSLs are traditionally used in hard rock mines, generally in Canada, South Africa, USA, and Australia. In the early twenty-first century, underground coal mines have also noticed the potential benefits of TSLs. According to Guner and Ozturk (2016), there are broad application areas for TSLs, which can assist in various forms of wall support. Table 2.2 summarizes TSL application areas.

Table 2.2 TSL application areas (Guner and Ozturk, 2016)

Application	Source
After blasting immediately (primary) supporting	Potvin et al., 2004; Espley et al., 2001
Burnt coal site	Kuijpers, 2001; Potvin et al., 2004
Face support	Carstens 2005; Potvin et al., 2004
Ground alteration (moisture, heat, humidity, chemical)	Kuijpers, 2001; Potvin et al., 2004;
Ground degradation (weathering fretting, swelling, slaking)	Spearing et al., 2009; Kuijpers 2001; Carstens and Oosthuizen, 2004
Mesh replacement	Potvin et al., 2004; Spearing et al., 2009
Pillar reinforcement	Potvin et al., 2004; Kuijpers, 2001;Ozturk and Guner 2017
Preventing weathering, spalling, and damage in the rock mass as a result of blasting	Spearing et al., 2009; Pappas et al., 2003
Prevention of rock falls	Potvin et al., 2004; Kuijpers, 2001
Protecting steel support and bolt elements from corrosion	Komurlu and Kesimal, 2014; Espley et al. 2001
Reducing seismic damage	Spearing et al., 2009; Jensen, 2013
Reducing the permeability of shotcrete linings	Hawker, 2001
Reduction in rock burst damage	Jensen 2013; Potvin et al. 2004; Spearing et al., 2009
Rehabilitation	Spearing et al., 2009; Potvin et al., 2004
Rigid ventilation seals	Potvin et al., 2004; Spearing et al., 2009
Shotcrete repair	A TSL supplier, Lacerda and Rispin, 2002
Sinking salt shafts, back of a hoist winze headworks.	A TSL supplier
Stabilization of return air tunnel	Potvin et al., 2004; Spearing et al., 2009
Support between rock anchors	Spearing et al., 2009, Potvin et al., 2004
Supporting areas with limited access and/or logistics constraints	Kuijpers 2001; Pickett and Thomas, 2013; Spearing et al; 2009; Espley et al., 2001
Temporary support (before shotcrete)	Pickett and Thomas, 2013; Potvin et al., 2004
Temporary support in TBM tunnels (poor ground)	Potvin et al., 2004; Pickett and Thomas, 2013

2.4. Support Mechanisms of TSLs

There are various support mechanisms of areal support members (TSL, shotcrete, wire mesh, wire rope lacing, and straps). Stacey (2001) reviewed the most common support mechanisms of membrane supports, also categorized by him. These categorized mechanisms can be observed as either individually or in combination for the field applications. In this manner, this part provides the mechanisms and the effects of the creep properties of TSLs on these mechanisms.

2.4.1. Promotion of block interlock

This mechanism is mainly to protect blocks in the rock mass in an unloosened state. This mechanism type involves three sub-mechanism.

i. Restriction of shear and rotational movement by bonding. The adhesion and the tensile strength of the TSL assists interlocking mechanism (Figure 2.4-a)

ii. Penetration of the liner into the cracks or joints. Low-viscosity spraying support members, especially TSLs, can prevent the movement of the rock blocks by penetrating the cracks or joints (Figure 2.4-b).

iii. Block movement prevention by shear resistance and tensile strength. Stiff and thicker shotcrete can provide high shear resistance. On the other hand, tensile strength of the TSL can promote the block interlocking mechanism (Figure 2.4-c).
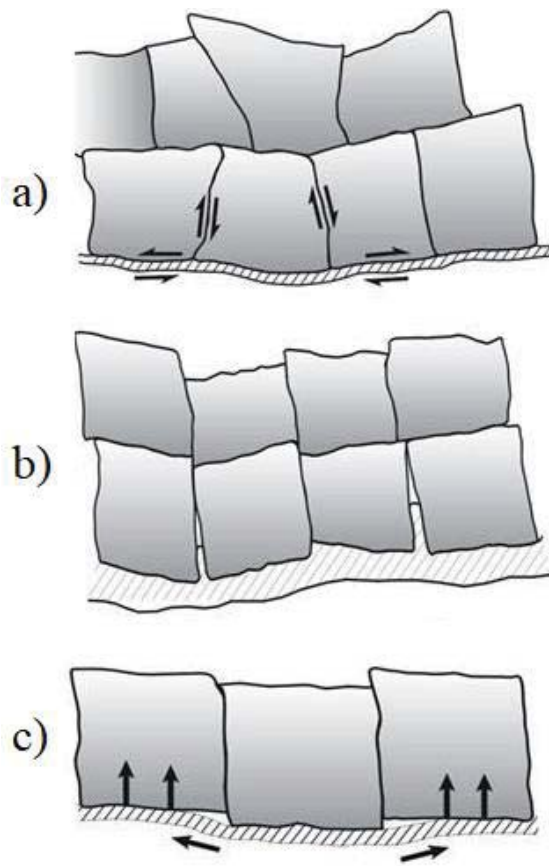
Figure 2.4 Promotion of Block Interlock mechanisms (After Stacey, 2001)

The time-dependent material properties of the TSLs directly effect the third sub-mechanism. In this case, TSL remains in tension to prevent block movement. If the acting tensile stress value is lower than the TSL's tensile strength, TSL does not fail at once. However, since TSLs are predicted to have creep sensitive behaviour, this support mechanism directly depends on tensile creep parameters

2.4.2. Airtightness

When the surface support member prevents the entry of air, the dilation is restricted. The failure on a rock mass might be prevented or mitigated by this way. This mechanism was first proposed by Coates (1966), also known as contributory support mechanism (Finn et al., 1999). However, according to Stacey (2001), the effectiveness of this mechanism under static loading conditions is questionable. On the other hand, in dynamic loading conditions, it might work to some extent. In case,

any crack or opening might be preserved in the areal support member, and in this way, the rapid air entrance into rock mass is prevented, the stability might be promoted, or the failure might be mitigated (Figure 2.5).
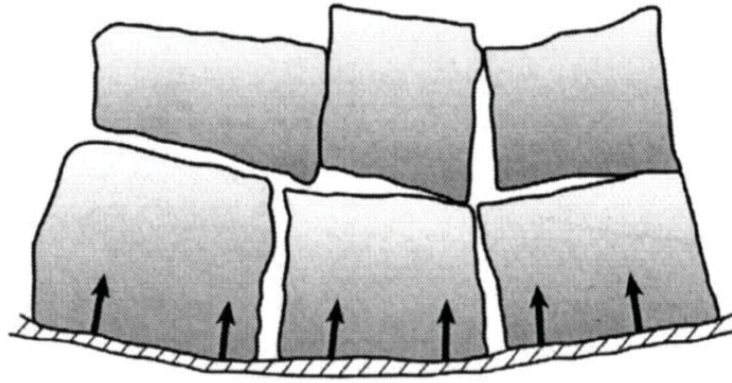
Figure 2.5 Air Tightness Mechanism (After Stacey, 2001)

This support mechanism is predicted to be more effective in dynamic conditions (deep, rockburst prone openings). Therefore, since the applied liner does not have a static load effect for a time, the impact of creep behaviour on this mechanism cannot be considered.

2.4.3. Basket mechanism

This mechanism is observed by the movement of the rock block or the debonding that occurs with the adhesion loss of the liner due to different reasons. In this mechanism, a basket is formed between stable blocks and relatively unstable small blocks, held by this basket. When the adhesion is maintained in stable blocks, and the adhesion loss is observed to some extent of unstable blocks, the tensile mechanical properties (stiffness, strength, and yielding capacity) of the TSL is key factors for supporting (Kuijpers and Toper, 2002). In this case, the tensile creep behaviour is as crucial as the tensile strength of the TSL. If the acting tensile stress on the TSL goes over the limit of creep rupture envelope, the tensile failure of the liner is inevitable no matter how strong or stiff it is. It should be noted that the cement-based stiff TSLs may fail before the formation of the basket.

2.4.4. Slab enhancement

Slabs or incipient slabs are frequently formed in brittle formations, especially close to the boundaries of deep openings. The presence of high field stresses in the parallel direction of the slabs may result in buckling failure. Moreover, layer thickness versus span ratio should be relatively small for the occurrence of buckling failure. Application of the liner can effectively thicken slabs, and increase their buckling resistance. Figure 2.6 shows the slab enhancement mechanism of the TSL. Tougher and stiffer TSLs with higher application thicknesses are predicted to be more effective in enhancing the slabs. In this support mechanism, the bending creep behaviour may have some significances.
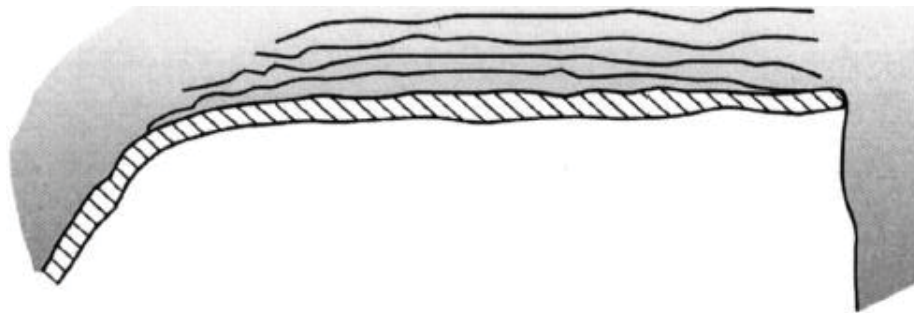
Figure 2.6 Slab Enhancement Mechanism (After Stacey, 2001)

2.4.5. Durability enhancement

Drying and wetting cycles may deteriorate some rocks, such as Basalt or Kimberlite. Due to this deterioration, the micro cracks, and then the rock fragments may be formed. The application of TSL can seal the rock and preserve the inherent strength of the rock mass (Finn et al, 1999). TSLs also have some indirect durability enhancements. They can also be effectively used when sealing is required to prevent water ingress before the shotcrete application, It should be noted that water-based TSLs may not be able to provide sealing.

2.4.6. Extended Faceplate

Faceplates are widely used to distribute the load of the rockbolt or cable bolt on the rock mass. If the bolt is inserted after the TSL application, the faceplate is located at

the top of the liner. In this case, the TSL can extend the effective area of the faceplate. Although the magnitude of the transferred load is higher in shotcrete, the cement-based stiffer TSLs can be used for this purpose as well (Figure 2.7).
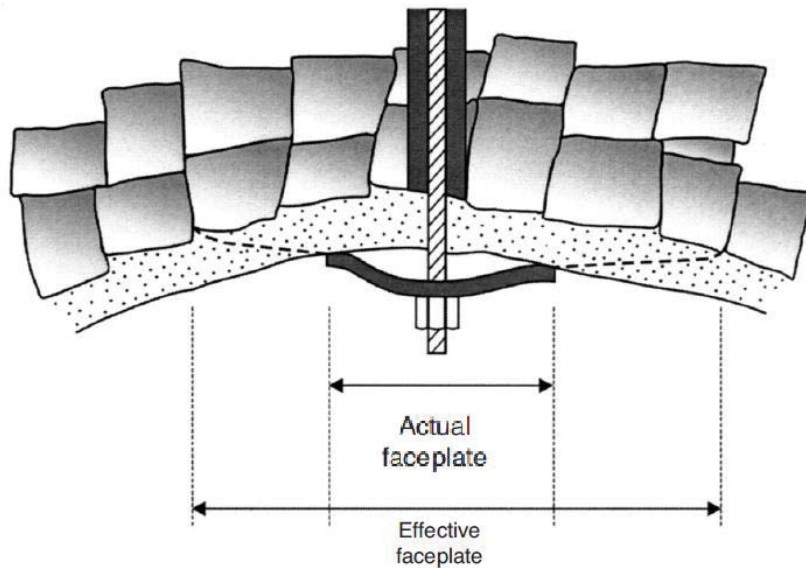
Figure 2.7 Extended Faceplate Mechanism (After Stacey, 2001)

2.5. Laboratory Studies on TSLs

In the literature, various laboratory-scale experimental setups have been proposed in order to understand the mechanical properties of TSLs and TSL-rock interactions, and to make comparisons between different TSL products. Laboratory scale tests can be divided into two subgroups namely as small and large scale. Since small-scale tests are cheaper, easier and simpler to perform than large-scale tests, researchers are mainly focused on small-scale experiments. According to Potvin (2002), large-scale tests can provide more interesting results, but the interpretation of the results is challenging in terms of TSL properties and behaviour. Moreover, most of the large scale tests are costly and time consuming; therefore, they are mainly performed only by the proposed researcher. The schematic representation of all experiments performed to indicate the mechanical properties of TSLs in the literature is presented in Figure 2.8.
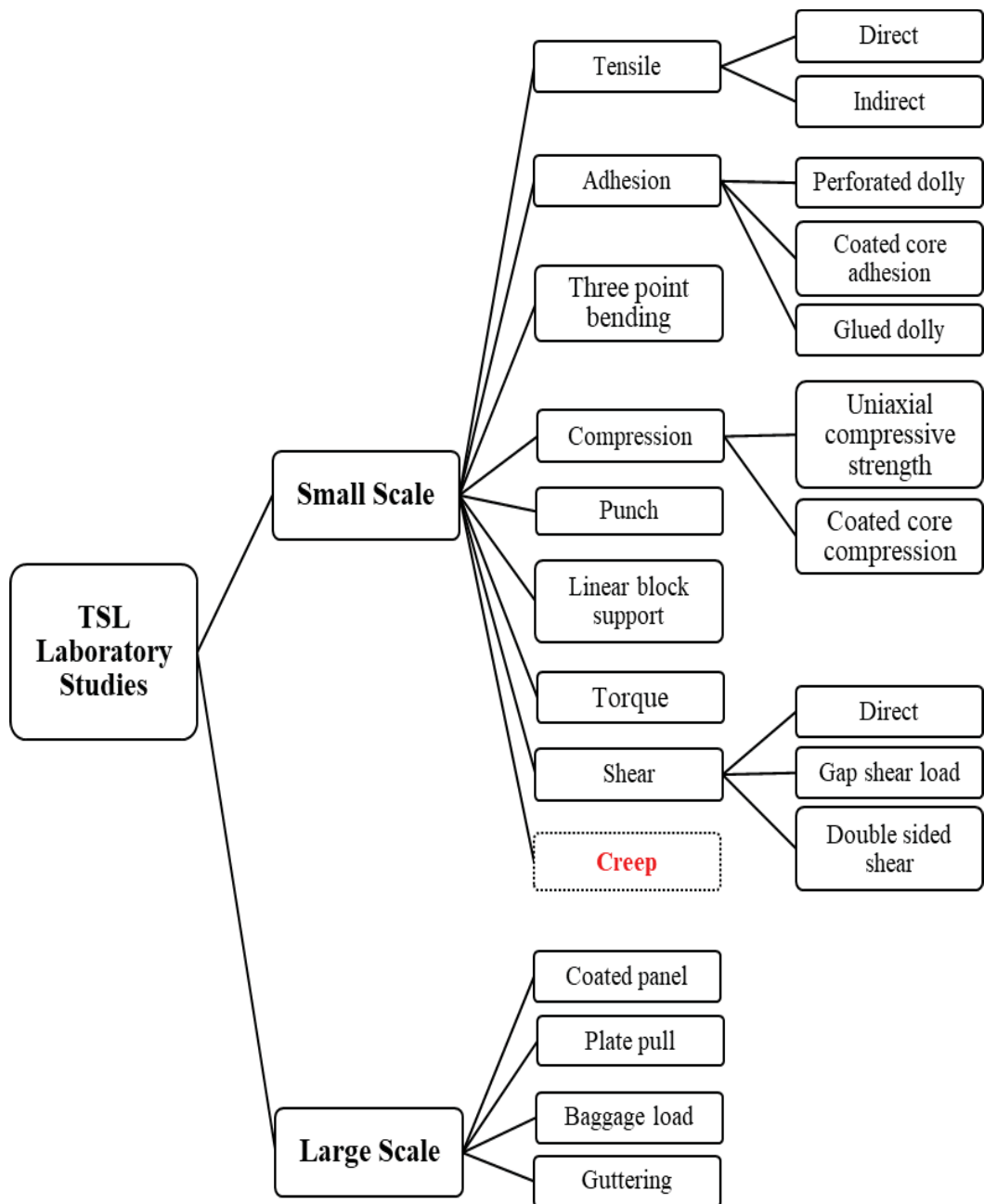
Figure 2.8 Schematic Description of Laboratory TSL Experiments in Literature

The mechanical laboratory experiments summarized in Figure 2.8 were conducted by various researchers in the literature as given in Table 2.3.

Table 2.3 Laboratory TSL experiments and Researchers

Test Type	Source
Tensile	Archibald, 2001; Guner and Ozturk, 2016; Lee et al., 2018; Mpunzi et al 2015; Ozturk, 2005; Spearing and Gelson 2002; Tannant et al., 1999; Wei et al., 2019; Yilmaz, 2011; Zhou et al., 2019
Adhesion	Chen et al., 2020; Gilbert et al., 2010; Lewis, 2001; Li et al., 2015; Li et al,, 2017; Ozturk and Tannant, 2004; Ozturk and Tannant, 2010; Spearing et al., 2001; Tannant and Ozturk, 2003; Yilmaz, 2007
Three Point bending	Mpunzi, 2012; Shan, 2017
Compression	Archibald and DeGagne, 2000; Espley et al., 1999; Gilbert et al., 2010; Kuijpers, 2001; Lau et al., 2008; Mpunzi, 2012; Ozturk, 2005; Ozturk and Guner, 2017; Ozturk and Guner, 2019; Qiao et al., 2014; Qiao et al., 2015
Punch	Kuijpers, 2001; Spearing et al., 2001; Stacey and Kasangula 2003
Linear block support	EFNARC, 2008; Lee et al, 2018
Torque	Yilmaz et al, 2003
Shear	EFNARC, 2008, Qiao et al., 2015; Saydam et al., 2004
Creep	Guner and Ozturk, 2018*; Guner and Ozturk, 2019* *Based on the outcomes of this thesis
Coated panel	Kuijpers, 2001; Naismith,and Steward, 2002
Plate pull	Archibald, 2001; Finn, 2001; Tannant et al., 1999
Baggage load	Swan and Henderson, 2001
Guttering	Zhenjun et al. 2014

Although more than 15 different tests were proposed and performed in the literature, only direct tensile (elongation) and tensile-bond (adhesion) strength test methodologies have gained general acceptance by TSL researchers (Yilmaz, 2011). As mentioned in the problem statement section, there is no creep test information in the literature to examine the time-dependent stress strain behaviour of TSLs so far.

The mechanical properties of TSLs vary according to their chemical components. Typical elastic material properties of 7-day cured TSL is presented in Table 2.4.

Table 2.4 Typical Mechanical properties of the 7- day cured TSL (Guner, 2014)

Property	Value
Tensile Strength (MPa)	2.9± 0.1
Tensile Modulus (MPa)	51.1 ± 6.4
Elongation at Break (%)	12.0 ± 2.0
Young's Modulus (MPa)	45.9 ± 6.7
Poisson's Ratio	0.37 ± 0.02
Uniaxial Compressive Strength (MPa)	>2.0

2.6. Numerical Modeling of TSLs

There are various numerical models in the literature for polymers, rock, and ground support materials, however TSL models are limited. Most of the studies performed in literature assume that TSLs have linear- elastic behaviors without any study on creep behaviour. Therefore, it is thought that the current numerical modeling studies for TSLs can be used for classification purposes rather than understanding the structural behaviour or support mechanism of TSLs.

As a result of the literature review, since there is no numerical modeling study on creep behaviour in the literature, it was decided to present the numerical model studies of the TSLs in the form of a table. Summary of numerical modeling studies performed in the literature for TSLs is presented in Table 2.5.

Table 2.5 Conducted Numerical TSL Studies in the Literature

Researchers	Model purpose	Numerical method
Tannant and Wang (2003)	Tensile, Block punch, tunnel	Discrete element
Malan and Napier (2008)	Fractured underground excavation (square)	Boundary element
Richardson et al. (2009)	Bending Double sided shear	Finite difference
Dirige and Archibald (2009)	Underground excavation (horseshoe)	Finite difference
Nater and Mena-Cabrera (2010)	Underground excavation (square)	Distinct element
Ahn (2011)	Segmential lining, effects on concrete	Finite element
Qiao (2015)	Underground pillar	Finite element
Guner and Ozturk (2016)	Tensile	Discrete element
Komurlu and Demir (2017)	Linear block support	Finite element
Lee et al. (2015, 2018)	Linear block support	Finite element
Ozturk and Guner (2019)	Compression	Discrete element

2.7. Analytical studies of TSLs

In addition to the experimental and numerical studies of TSL, the researchers also conducted the analytical studies to explain the support and failure mechanisms of TSLs. In these studies, the time dependency of the TSL is not taken into consideration, and all of the researchers, who conducted analytical studies, have accepted TSLs as linear elastic material.

Fowkes et al. (2008) investigated the effect of the elastic liner for the crack repair. They proposed an explicit solution for a simple geometry. They concluded that the liner with a much smaller shear modulus than rocks could be effectively used to repair cracks assuming that the liner penetrates the crack tip. Thus, the TSL may prevent crack coalescence, and promote the stability of opening by remaining key blocks in place.

Mason and Stacey (2008) studied the support provided to circular underground excavations by TSLs with three different models. They found that the TSL, well bonded to the rock surface, may reduce the magnitude of the stress, strain energy, displacement, and rotation in the rock at the interface. Moreover, although the flexible liner can provide better support after the movement in the rock takes place, the stiff liner is more successful in preventing the crack formation and movement of the rock mass. In this study, the TSL was assumed to be instantaneously applied at the end of the excavation and also the elastic moduli of the fractured and intact rock mass considered to be the same.

In the field applications, the combined surface support elements (multi-layer) are frequently used to provide better support performance. Mason and Abelman (2009) investigated the two-liner support system applied to a circular opening, subjected to the uniform shear stress at infinity. The elastic analytical solutions were proposed using the theory of plane strain.

The adhesive strength and the effective bond width are two significant design parameters for the evaluation of the interface property of the TSL during the support design. According to Ozturk (2012a), the maximum weight of a block (frictionless) that the TSL can be held in the roof or upper part of underground openings can be calculated by using adhesive strength and effective bond parameters. This study also provides an indirect way to find the effective bond width of liners. Moreover, the findings of this study support that the chemical interaction between the liner and the rock grain (matrix) is more significant than the mechanical interlocking to get better adhesion properties.

Ozturk (2012b), interpreted the direct pull-off adhesion tests, based on fracture mechanics to evaluate failure modes of TSLs by deriving an equation of the edge crack propagation for a generic case. This study reveals that the adhesion test geometries of TSLs, which show confined behaviour; the failure mode of the tests are edge crack propagation. Bulk cavitation of TSLs can only occur for samples that have smaller than 0.6 MPa elastic moduli.

2.8. Creep on TSL

Engineering materials can show a wide range of mechanical behaviors from a rigid solid to a viscous liquid, depending on the environmental and loading conditions. Due to the combination of these behaviors, polymers are usually referred to as time and temperature-dependent materials. This phenomenon is also known as creep (Findley *et al*. 1989). Creep can be defined as the time-dependent permanent deformation that occurs under applied constant loads. For most materials, molecules and their bonds can stretch and move at elevated temperatures, thus materials will behave more ductile. Hence, the time-dependent material properties become more significant. Unlike many materials, polymers undergo creep even at room temperature, and creep performance may become the primary design concern. Creep deformation depends on stress, time, and temperature parameters.

Creep is also an important parameter for the evaluation of durability and serviceability of cementitious materials (Zhang et al., 2014). Cementitious materials generally have less creep activity than polymers. To enhance workability of the material, polymer additives are frequently used (Göbel et al., 2018).

The creep phenomenon is generally divided into three stages; primary (transient), secondary (steady-state), and tertiary (accelerating). In the primary stage, the strain rate, $d\varepsilon/dt$, is initially high and then decreases with time. Then the material enters the secondary creep regime, in which the creep rate is constant and the slowest. Finally, the creep rate continually increases until the failure occurs (tertiary stage) (Figure 2.9). It should be noted that, as the constant load is applied, the elastic strain occurs instantaneously (ε_e), this part sometimes referred to as the zeroth stage. This strain is reversible and fully recoverable.
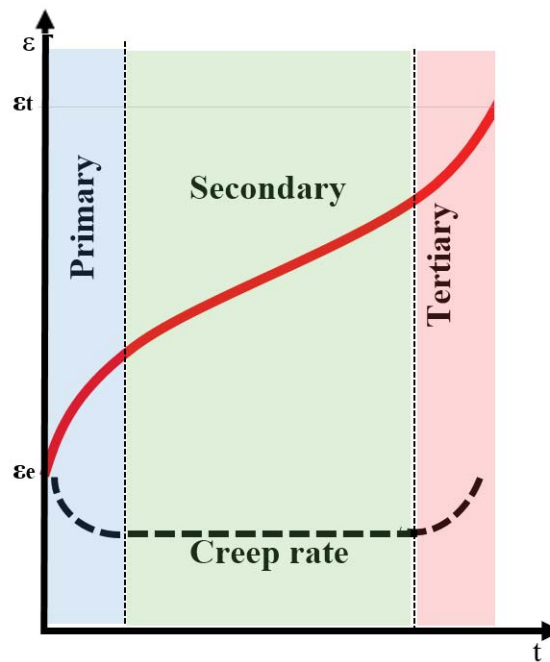
Figure 2.9 Typical time-dependent behaviour of polymeric materials.

Creep testing is commonly performed in material engineering laboratory studies. Polymers, metals, ceramics, and even some rocks show time-dependent behavior. Different creep test set-up and standards were utilized depending on the exposed loading direction during the field applications. Tensile, compression, and flexural creep tests are widely performed in polymer engineering. Tensile creep test methodology for plastics (ASTM, D2990, 2010) were followed through the laboratory studies since tensile failure is a commonly encountered failure mechanism in the field application of TSLs (Figure 2.10), and due to the polymer content of TSLs. Test results of tensile creep can be used to estimate service life in the field application, compare different TSLs, and characterize TSLs for long-term performance under constant loading conditions.

As mentioned before, in blocky rock mass excavations, wedge blocks are formed as the intersection of three or more discontinuities, joints, or bedding planes. If the orientations of these planes are against the advance direction, unfavorable wedges with falling potential may be formed. Under the effect of gravity and other static and dynamic forces, back and wall wedges may get dislocated either by falling or sliding out of their sockets. The geometry, strength characteristics, orientation, length of the

planes, and stresses within the rock mass are the main factors that control the stability of formed wedges (Curran et. al 2004; Nomikos et. al 2006). Although small scale wedges do not cause major problems in terms of global stability, it is known that they might cause many different problems apart from the engineering sides such as worker injuries and equipment losses. According to a study conducted in Australia, 90% of the injuries caused by underground wedges are caused by blocks smaller than 1 m^3 (Potvin, 2006).

Rock bolt systems are widely used to prevent falling or sliding of wedge blocks. Since sprayed surface support systems distribute the weight of the wedge in larger lining area, they can support small scale (<1m^3) wedge blocks. TSLs can enable to hold the blocks after falling or sliding out of their sockets due to their high elastic-plastic behaviour as presented in Figure 2.10.
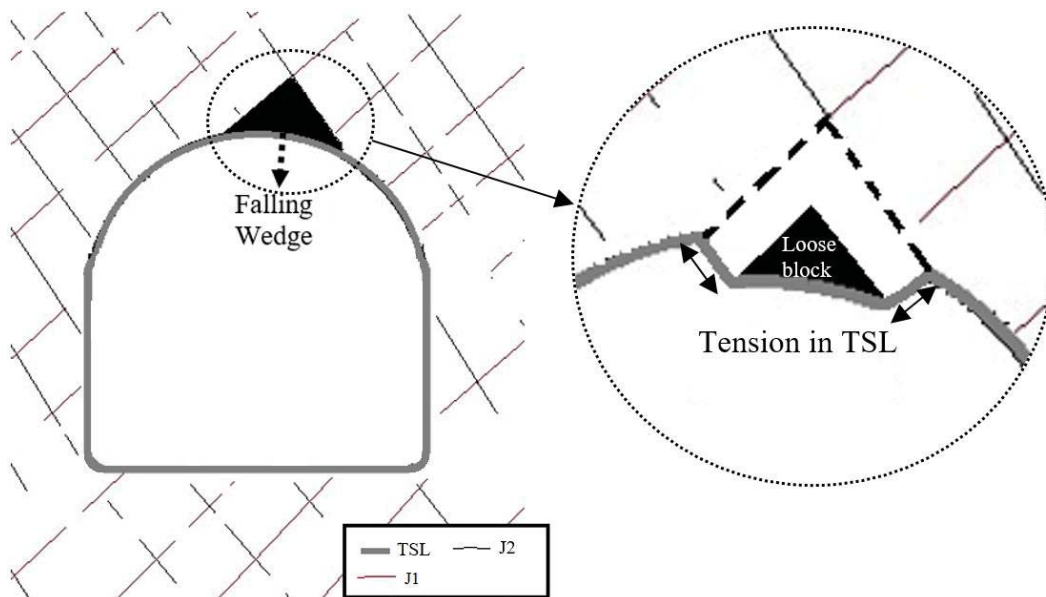
Figure 2.10 Formed Wedge and Holding Function of TSL

For this kind of failure, the primary concern of the TSL is the holding time. Since they behave as a time-dependent material, the holding behaviour is directly related to their creep properties. Due to blasting, rockburst, or earthquakes, wedges may form after the application of TSL. Therefore, the effect of curing time on creep properties is also another significant research subject.

In creep literature, the strain recovery behaviour of the material is also examined by unloading during specific experiments in order to visualize the behaviour of the material in real life. In the field applications of TSLs, there was no such condition as unloading after being under constant load due to TSLs wedge blocks. Therefore, strain recovery behaviour was excluded from the scope of this study.

2.9. Creep Models

Mechanical response predictions of the cement or polymer-based materials might be troublesome, since they may be able to show linear elastic, viscoelastic, non-linear viscoelastic, or viscoplastic behavior. Creep models are widely used to predict these mechanical responses during service life without performing long creep tests (i.e., 10 years). The other purpose of creep models is to give a physical basis to the empirical constitutive relations.

The models used to simulate the time-dependent behaviour can be categorized into two main concepts: namely, phenomenological models, and mechanical models. Phenomenological models do not take into consideration the physical meaning of the mechanisms and are not based on environmental changes. Besides, mechanical models are based on constitutive laws, closed-form relationships and general theories. Changes in the mechanisms and environmental conditions result in changes in the model's mechanical behaviour (Paraskevopoulou, 2016).

In addition to this, the other classification can be made considering empirical models, based on the curve fitting of the experimental data and rheological models, based on time-dependent behavioral functions composed of assemblages of elastic springs and viscous dash-pots. Both the empirical models and rheological models are phenomenological models.

2.9.1. Empirical Models

There are many different approaches and methods of creep behaviour modeling. None of these methods can be said to be more accurate than the others (DeMaio, 2006). In the selection of the appropriate model, the factors such as the behaviour of

the material and the intended usage of the model are generally taken into consideration. The empirical model approach is one of the widely used techniques to predict creep behavior. Empirical models do not construct from inherent material behaviour or microscale properties. Instead, the parameters of empirical model are determined by the curve fitting of the experimental data, acquired from laboratory tests. These models vary between a few parameters and over ten parameters depending on the complexity of the material behaviour and desired model sensitivity.

Among all empirical models, the most well-known and simple model is Norton and Bailey power law as follows (Bailey, 1929; Norton, 1929):

$$\dot{\varepsilon} = k\sigma^p \tag{2.1}$$

where $\dot{\varepsilon}$ is the creep rate, k and p are constants, and σ is the applied stress. This equation is also called Norton's creep law or power law. Ludwik (1909) firstly proposed the exponential creep model as given below:

$$\dot{\varepsilon} = ke^{\sigma/\sigma+} \tag{2.2}$$

where k and $\sigma+$ are material constants. Besides, the hyperbolic sine function is also using the stress dependency of the time-dependent behaviour of the material. Prandtl (1928) proposed the following equation to represent creep behaviour either nearly linear for small stresses or nonlinear for high stresses:

$$\dot{\varepsilon} = D \sin h \frac{\sigma}{\sigma+} \tag{2.3}$$

where D and $\sigma+$ are material constants. According to Findley et al. (1989), Equations 2.1-2.3 have been found adequate to describe the steady-state (secondary stage) creep behaviour in tension under constant stress and temperatures. The other creep model, which considers both primary and secondary stages, is as follows:

$$\dot{\varepsilon} = kn\sigma^p t^{n-1} \tag{2.4}$$

where k, p, and n are material constants. The empirical equations (2.1-2.4) are used for metals, rocks, composites, and polymers. However, some researchers put forward

more specific equations just for polymers, due to differences in secondary creep stage. Leaderman (1941) suggested a logarithmic equation to model the creep behaviour of bakelite as given:

$$\varepsilon = \varepsilon_0 + A \log t + Bt \tag{2.5}$$

where ε_0 is an instantaneous elastic strain, A, and B are material constants that are functions of stress, temperature, and material. Although various simple and complex equations have been introduced to describe the time-dependent model of materials, the well-known empirical creep equation is:

$$\varepsilon = \varepsilon_0 + C_0 t^{C_1} \tag{2.6}$$

where ε_0 is an instantaneous elastic strain, C_0, and C_1 are material constants, which are all functions of stress. Because of the reliability and widespread use of Eq. 2.6, it is also utilized in the modeling section of this study. It is simpler to practice and requires fewer fitting parameters. Since the creep strain keeps growing at a decreasing rate in the power function models, this approach is referred to as viscoplastic.

2.9.2. Rheological Models

Rheology, the science of deformation and flow, gives a phenomenological account of the mechanical behaviour of matter which involves its mechanical properties (Severs, 1962). The researches of the time-dependent properties of polymers are the most extensive application of the rheological models. These models can be used to simulate viscoelastic responses. The springs (Hookean element) and dashpots (Newtonian element) are the basic elements of the rheological models. Figure 2.11 shows illustrations of a spring and a dashpot element.
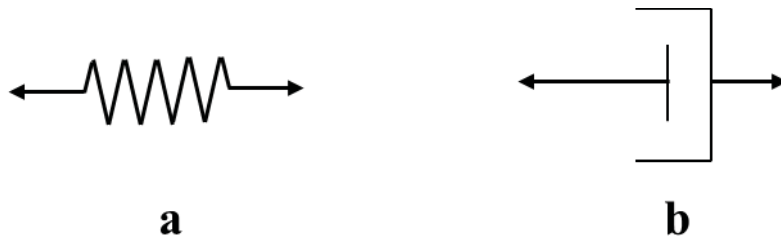
Figure 2.11 Mechanical analogues represented by elastic spring (a), viscous dashpot (b)

The spring represents the instantaneous elastic straining, governed by a constant elastic modulus or stress-strain dependent modulus for nonlinearly elastic materials. This element exhibits a linear stress-strain relationship independent of the time. Stress-strain-time relationships of the spring element are presented in Figure 2.12.
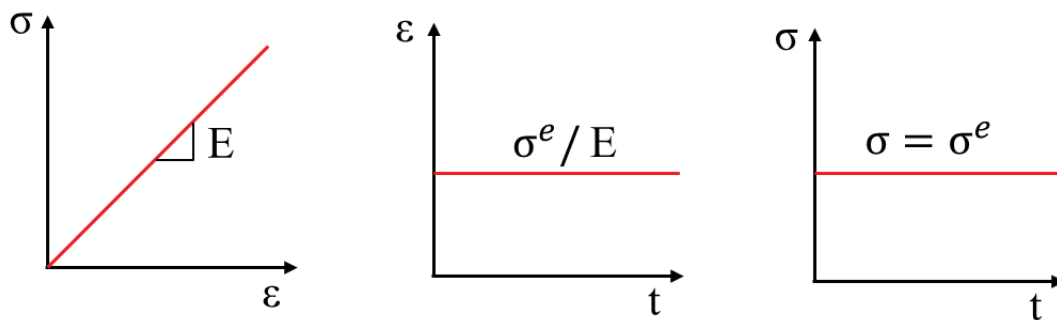
Figure 2.12 Response of a spring element (stress-strain-time)

The dashpot element is also known as a damper, or the viscous Newtonian element provides resistance to the flow of material. The response of this element depends on the rate of strain and the applied stress increment. In other words, if a stress is applied to this element, the resulting strain is time-dependent and permanent. Stress-strain-time relationships of the dashpot element are presented in Figure 2.13.
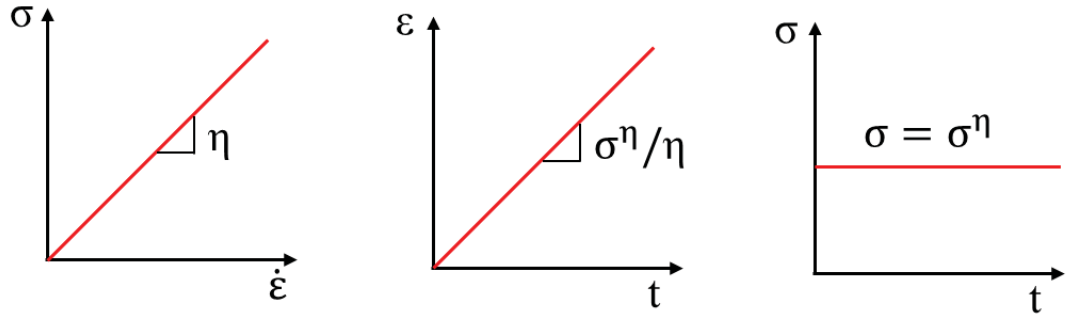
Figure 2.13 Response of a dashpot element (stress-strain-time)

The various combinations of the springs and dashpots may sufficiently capture the time-dependent viscoelastic behaviour of the material. Four basic and two generalized rheological models will be discussed in the following part.

2.9.2.1. Maxwell Model

This model consists of a spring and a dashpot element connected in series. Since the applied stress level is the same in spring and dashpot, the model is also known as iso-stress model. On the other hand, the total strain of the model is the sum of the elastic and the viscous strain. If the Maxwell model is subjected to constant stress (σ_n), at t=0, the following strain-time equation can be obtained:

$$\varepsilon_t = \frac{\sigma_n}{E} + \frac{\sigma_n}{\eta} t \qquad (2.7)$$

In Eq. (2.7), the first term, σ_n/E, represents the response of the spring. Once the load is applied, the spring can reach definite strain value. The dashpot response, the second term of the Eq. (2.7), has a constant velocity when the load is applied. When the load is removed, the spring recovers the attained strain, but the dashpot remains its attained strain. The mechanical analogue and strain-time behaviour under constant stress level of the Maxwell model are presented in Figure 2.14.
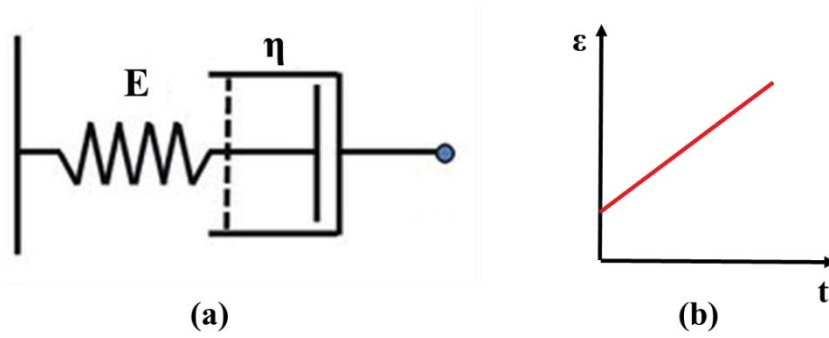
Figure 2.14 Mechanical analogue and strain-time behaviour of the Maxwell model

2.9.2.2. Kelvin-Voigt Model

The Kelvin-Voigt model is the combination of an elastic spring and a viscous dashpot element connected in parallel. In this model, the strain value is the same for each element and the total stress of the model is the sum of the elastic and viscous elements. It is possible to detect the initial elastic deformation of the Kelvin model, but the dashpot resists to the applied stress. Over time, the viscous element begins to deform and part of the applied stress level is transmitted to the spring. This causes a reduction in the dashpot's strain rate and stress value. This behaviour is called as delayed elasticity. The Kelvin model is capable of simulating the actual inelastic response of the material when being subjected to a constant load. Therefore, in rheological models, the Kelvin-Voigt unit is of great importance. When the Kelvin-Voigt model is subjected to constant stress (σ_n), at t=0, the strain-time equation can be obtained as follows:

$$\varepsilon_t = \frac{\sigma_n}{E}\left[1 - \exp(-t\frac{E}{\eta})\right] \tag{2.8}$$

The strain predicted by Eq. (2.8) tends to increase with a decreasing rate and approaches asymptotically the value of σ_n/E when t=∞. The mechanical analogue and strain-time behaviour under the constant stress level of the Kelvin-Voigt model are presented in Figure 2.15.

(a)   (b)
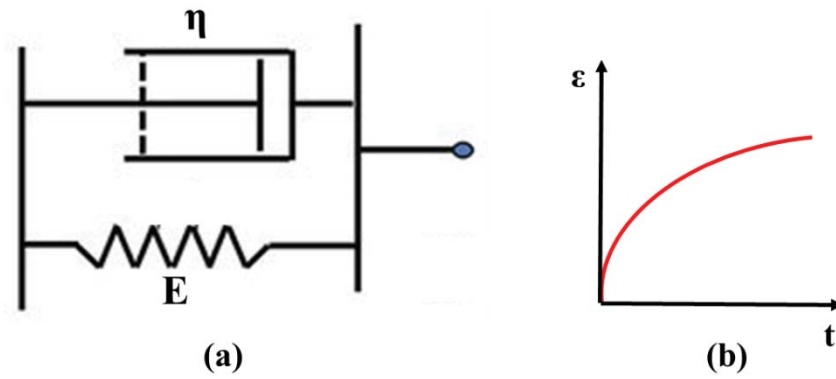
Figure 2.15 Mechanical analogue and strain-time behaviour of the Kelvin model

The retardation time (τ) can be defined as a measure of the time taken for the creep strain to accumulate. The shorter the retardation time, the more rapid the creep straining. The retardation time of the Kelvin element can be calculated by dividing the dashpot viscosity and spring stiffness (η/E). The retardation time in a single Kelvin unit can be considered as the time unit when the stress is removed. The significance of this parameter becomes apparent when the multiple Kelvin elements are used in the model.

2.9.2.3. Three-Element Standard Solid Model

The abovementioned models are the basis of the rheological models. In practice, more elements and various combinations of the Maxwell and Kelvin elements are required to obtain more realistic material behaviour. The three-element standard solid model is the combination of an elastic spring and a Kelvin-Voigt element connected in series. the strain-time equation can be obtained as follows:

$$\varepsilon_t = \frac{\sigma_n}{E_1} + \frac{\sigma_n}{E_2}\left[1 - \exp(-t\frac{E_2}{\eta})\right] \tag{2.9}$$

The mechanical analogue and strain-time behaviour under the constant stress level of the standard solid model are presented in Figure 2.16.

39
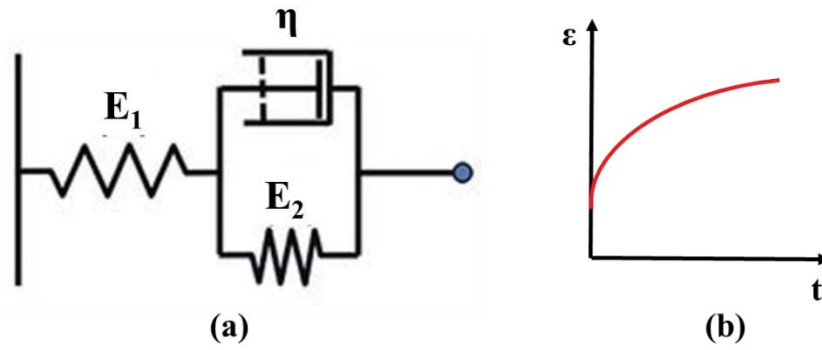
Figure 2.16 Mechanical analogue and strain-time behaviour of the standard solid model

2.9.2.4. Burgers or Four Element Model

The constitutive equations for the four-element Burger's model can be derived considering the strain response under the constant stress of a spring, a dashpot, and a Kelvin unit connected in series. Since the spring and dashpot in the Maxwell model are considered as two separate elements, the total strain at time t is the sum of the strain in the three elements.

At the beginning of the model, there is an instantaneous change in strain due to the Maxwell spring of the model. This parameter is also known as the instantaneous elastic stiffness (E_1). The Kelvin and Maxwell dashpots are responsible for the initial slope of the retarded elastic behaviour (η_1, and η_2). When the material passes on to the secondary creep stage, the Maxwell dashpot generates purely viscous response (η_1). On the other hand, the Kelvin and Maxwell springs are responsible for the interception value of the secondary creep range slope with the strain axis (E_1, E_2). In the Burger's model, the creep equation for the case of simple creep loading can be defined as:

$$\varepsilon_t(t) = \frac{\sigma_n}{E_1} + \frac{\sigma_n}{E_2}\left[1 - \exp(-t\frac{E_2}{\eta_2})\right] + \frac{\sigma_n t}{\eta_1} \qquad (2.10)$$

The creep behaviour of the Burger model is considered to be the sum of the creep behaviour of the Kelvin and Maxwell models. This model can be able to simulate

40

both the primary and secondary creep stages. The mechanical analogue and strain-time behaviour under the constant stress level of the Burger's model are presented in Figure 2.17.
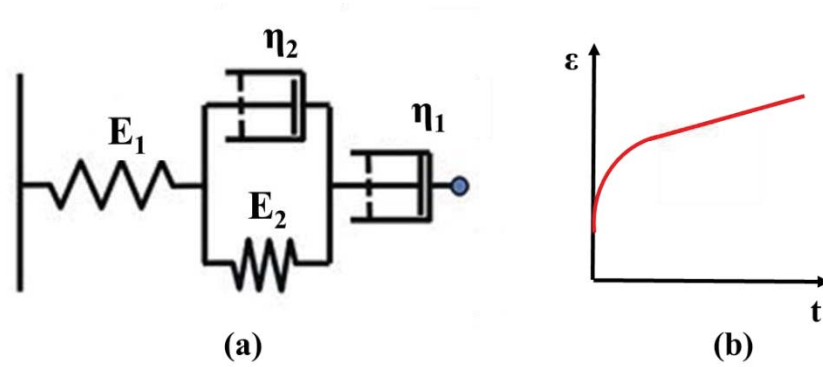
Figure 2.17 Mechanical analogue and strain-time behaviour of the Burger's model

2.9.2.5. Combinations of Three Element and Four Element Models

In addition to the given standard solid model and Burger's model, several combinations of the three and four element models are proposed in the literature. The type of their constitutive equations are the same, and they are mechanically equivalent. Findley et al., (1989) classified these models into four main groups. These groups and their mechanical analogues are presented in Figure 2.18.
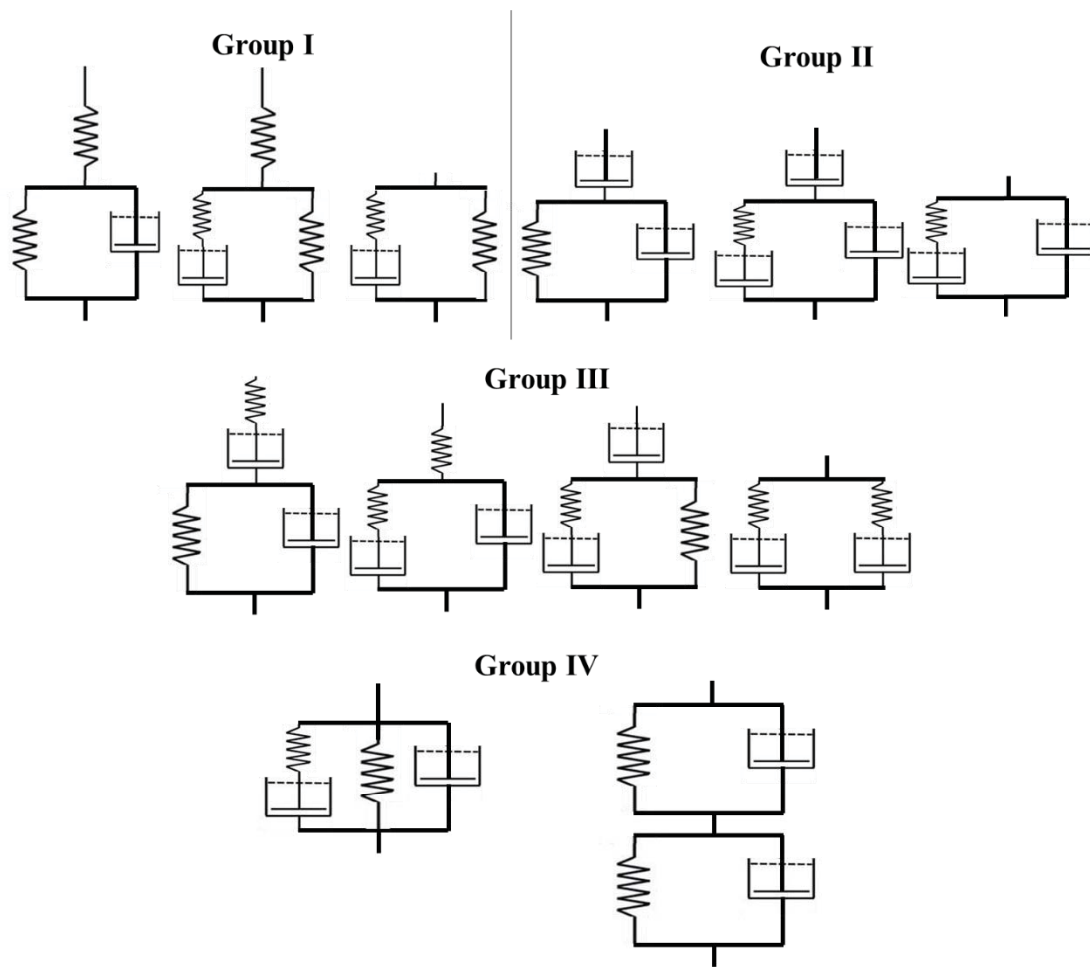
Figure 2.18 Mechanical analogues of possible three and four element models (After Findley et al., 1989)

The generic name of Group I is the standard solid. They show solid-like behaviour, which means that both the instantaneous and delayed elasticity can be simulated with these models. In addition to the time-dependent models, this group is widely used for modeling shear wave propagation. Group II shows liquid-like behaviour due to the dashpot elements. On the other hand, Group III consists of the combination of the Maxwell and Kelvin models connected in series. This group shows the instantaneous elastic behavior, viscous flow, and delayed elasticity. Group IV can simulate more complex material behaviour. The delayed elasticity can be achieved by two dashpots, therefore they have two separate retardation times.

For the practical applications of the given models, these models are widely used to simulate the material behaviour of the simple structures and single stress levels. Many engineering materials show hypervariable behaviour under various stress levels. Therefore, since these models have a single retardation time, except for Group IV, their applicability for the complex mechanical models is limited. For this reason, more complex rheological models have been put forward to achieve accurate material behaviour under different stress levels.

2.9.2.6. Generalized Models

In the literature, although the Maxwell and Kelvin chains can be combined in many ways, two variations of the generalized Maxwell and Kelvin Models are most frequently utilized. These rheological models are more complicated and more realistic, considering earlier indicated models.

The first model was generated by connecting several Maxwell models in parallel. To be able to reach an asymptotic value for strains as time approaching infinity, a free spring is also included (E_∞). This model is known as the Wiechert Model, capable of simulating the instantaneous elasticity and delayed elasticity with various retardation times. This model takes into account that the relaxation occurs at a distribution of times. Mechanical analogue of the Wiechert Model is presented in Figure 2.19(a). In practice, it is not possible to simulate the actual creep and relaxation behaviour of polymeric materials with the combination of single or double Maxwell elements connected in parallel. Preferable, as many as 5 to 15 or more elements may be necessary (Brinson and Brinson, 2015). For the Wiechert model, the derivation of the creep function in a closed form is not possible. Solutions are possible by an integral constitutive equation approach with the given stress or strain histories.
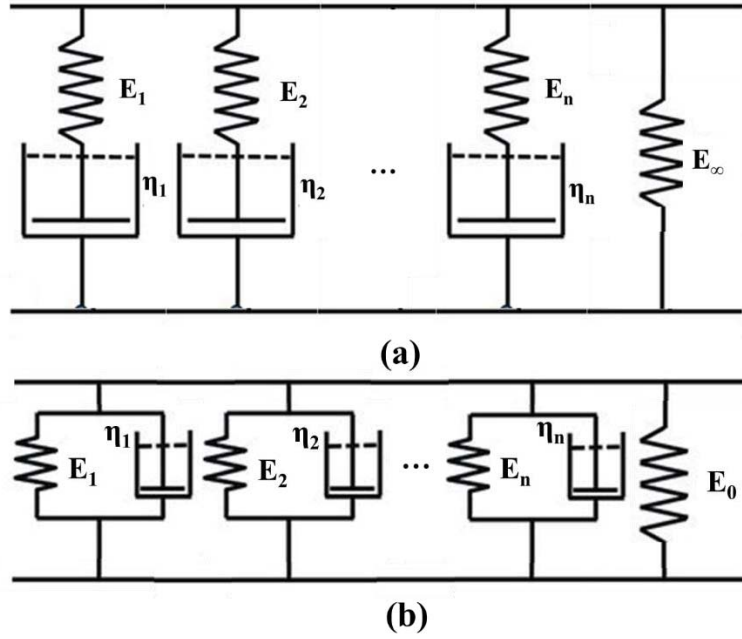
Figure 2.19 Mechanical analogues of Wiechert (a) and Generalized Voigt-Kelvin (b) model

The second generalized model can be obtained by combinations of n Kelvin units. To simulate the instantaneous elastic strain response, a linear spring element is also required (E_0). This model is named as generalized Kelvin or generalized Voigt-Kelvin solid (Figure 2.19(b)). The main assumption in this model is that the deformations of the spring and dashpot under loading are equal at any time. The constitutive equation of the viscoelastic material can be obtained by the Generalized Voigt-Kelvin model as follows:

$$\varepsilon(t) = \int_0^t \frac{1}{E_0} + \sum_{i=1}^{n} \frac{1}{E_i} \left\{1 - e^{[-(t-\tau)/\tau_i]}\right\} \dot{\sigma}(\tau) \, d\tau \qquad (2.11)$$

In the condition of creep tests, where stress is constant (σ_n) Eq. (2.11) becomes;

$$\varepsilon(t) = \frac{\sigma_n}{E_0} + \sum_{i=1}^{n} \frac{\sigma_n}{E_i} \left[1 - e^{(-t/\tau_i)}\right] \qquad (2.12)$$

Where E_0 is the instantaneous elastic modulus, η_i and E_i are the dashpot viscosity and spring stiffness of ith Kelvin element. τ_i is the retardation time (η_i/E_i).

Although the Generalized Voigt-Kelvin Model can also be solved for the case of relaxation, due to the forms of the differential equations and ease of solution, the Generalized Voigt-Kelvin is used for creep while the Wiechert model is used for relaxation.

CHAPTER 3

LABORATORY STUDIES

This chapter presents the laboratory studies performed within the scope of the thesis. This chapter covers five subsections. The first section presents the general information about the tested TSL products. The second section describes the design of the creep test setup used through this study. The third section presents the selection of appropriate sample geometry and sample preparation technique by performing various tensile tests.

Since the preparation of the representative test specimen is crucial for a comparative verification of the rest results, a laboratory-scale preparation guide of TSL is presented in the fourth section. The final section includes all the tensile and creep experiments and the resultant outputs deduced from the experiments.

In order to start the laboratory studies, TSL products were procured first. Since the shelf life of a TSL product is around 12 months, each product was supplied at different times just before the start of the experiments. The first product "Tekflex LP" was ordered from Minova CarboTech GmbH (Germany).This product is called as "TSL-1" during the study. Another TSL product, which is "MasterRoc® TSL 865"produced by BASF, is called TSL-2 in the study. TSL-2 was supplied just after the completion of the TSL-1 tests.

3.1. Brief Information About Tested TSLs

3.1.1. TSL-1

TSL-1 is a two-component mineral-organic mixture in which the liquid component is an aqueous polymer dispersion and the powder-component is a hydraulically curing powder based on a special cement, packaged in 25 kg bags. The components

were mixed with 2:1 liquid-powder ratio by mass. The tack free time of the product is measured as 30 min. The amount of TSL application is determined as 1.25 kg of mixture per m^2 and per mm thickness, as suggested by the manufacturer. Moreover, this product is classified as self-extinguishing product. Polymer dispersion and the powder-component compositions are disclosed by the manufacturer (Tekflex LP, 2019).

3.1.2. TSL-2

TSL-2 is a single-component polymer-based powder for spray application on rock-coal faces for surface support without a toxic component, packaged in 20 kg bags. Preliminary laboratory studies showed that the tack-free time of the mixture takes a few minutes. Amount of TSL application is determined as 0.9 kg of dry powder per m^2 and per mm thickness, as suggested by the manufacturer. The suggested mixing amount of the polymer powder is twice of the water by weight. Polymer powder composition disclosed by the manufacturer is as follows: 10–30% limestone, 10–30% calcium oxide, 7–13% cement, alumina, chemicals, 1–5% kaolin, 0.1–1.0% crystalline silica (by weight) (MasterRoc, 2018).

3.2. The Design of the Experimental Setup

In the laboratory studies, at least two specimens at each stress level should be tested according to the ASTM D-2990 standard. In order to investigate the time-dependent behaviour of TSL in detail for each curing time, 4 different stress levels varying from 20% to 80% of the ultimate tensile strength of the sample were considered. In other words, 8 tests were performed simultaneously for each TSL set. For this purpose, one large test frame with 80×80×280 cm dimensions was built.

When determining the height of the test table, the table was decided to be around 80 cm in height considering the sample length and estimated elongation amounts, the size of the clamps, and the weights to be connected. In addition, the dimensions of the testing room were taken into consideration in such a way that all experiments can be carried out in a single table arrangement. At this stage, the most appropriate

distance between the test units was determined so that the fall of the suspended loads due to rupture at different times did not affect the ongoing experiments. In this basis, the frame was fixed to the ground to prevent the shock effect of the weight change in the table due to falling of some weights. The top grip was attached to the table by screws and nuts. Laboratory tests were performed by dead weights attached to the bottom grip as seen in Figure 3.1.
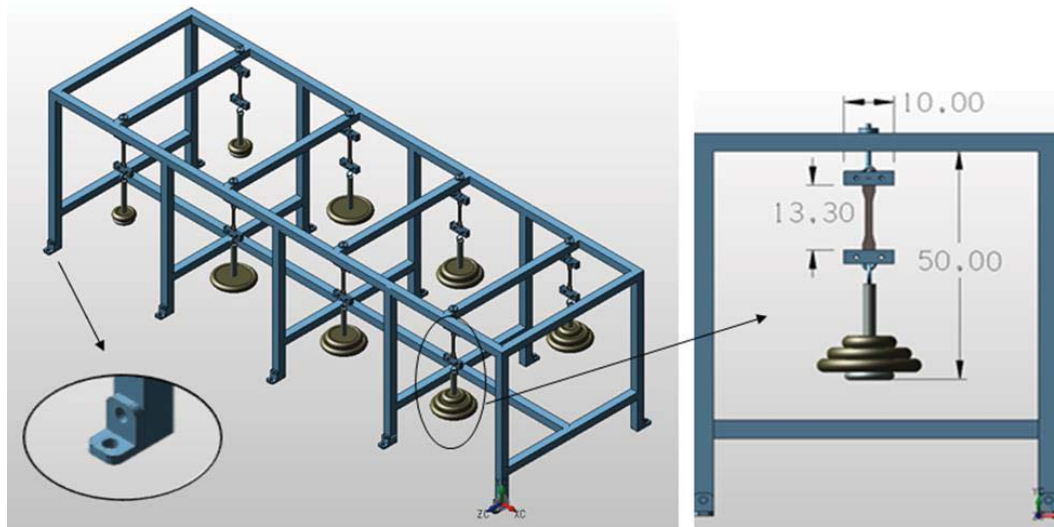
Figure 3.1 Isometric and Side View of the Tensile Creep Testing Setup (dimensions in cm)

The grips were designed to minimize eccentric loading of the specimen. The grips also served as clamps to hold and prevent sliding of the test specimens. Linear Variable Displacement Transducers (LVDT) and dial gauges were attached to the bottom grips to measure the elongation due to the total applied forces (load, grip weight). LVDT and data acquisiton systems were used for a continuous measurement. All LVDTs were calibrated with the help of the calibration certificates issued in the products and mounted on the test apparatus. Due to the long duration of the experiments, the dial gauges were utilized to crosscheck the LVDT measurements.

3.3. Determination of Sample Size and Sample Preparation Technique

Tensile testing is the most commonly used strength determination practice for TSLs in the literature. In the preparation of tensile test specimens, specimens are prepared in accordance with ASTM D-638 test standards. Two different sample geometries and two different sample preparation techniques are proposed in the available standard. In compliance with this standard where a similar sample specimen type is used, a sample size and preparation technique was introduced in this section to find out the optimum sample preparation technique for TSLs and to provide a guideline for the future studies. In this section, 48 tensile tests were carried out for 12 different samples in two different sample geometries with two different sample preparation techniques. These sample geometries stated in ASTM D-638 and used in previous studies are illustrated in Figure 3.2. Although only Type-I samples were proposed for creep test standard, a sample set was also prepared for Type-IV in this study.
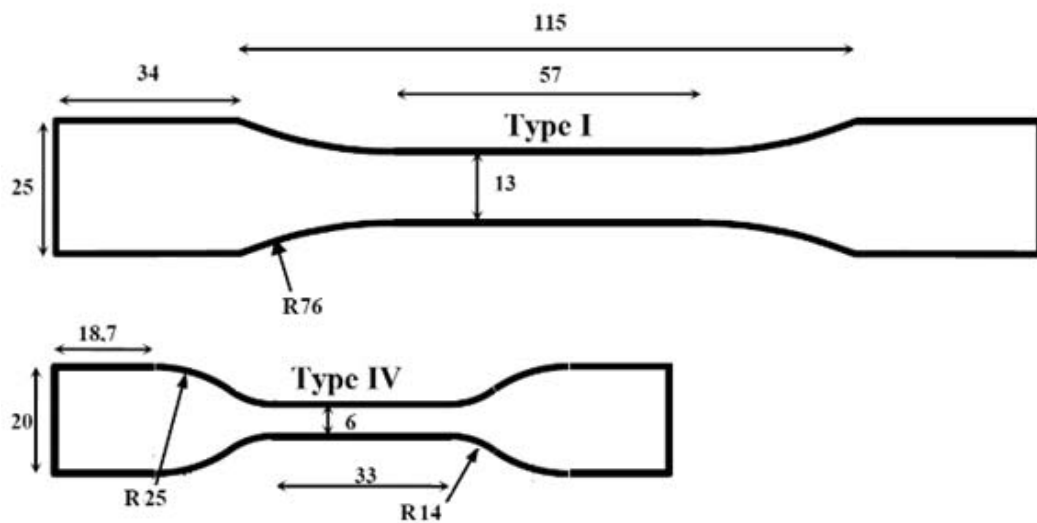
Figure 3.2 Type I and Type IV Specimen Geometries (dimensions in mm)

In addition to sample geometry, two different sample preparation techniques are included in the relevant standard and previous studies. These techniques are molding and die-cutting. The tensile tests were conducted with TSL-1. Liquid and powder components were mixed with an electric mixer at a 120 rpm for 5 minutes (Figure

50

3.3-A), then it was poured into a plexiglass plate and molds with a 4 mm thick frame by using a spatula (Figure 3.3-B and C).
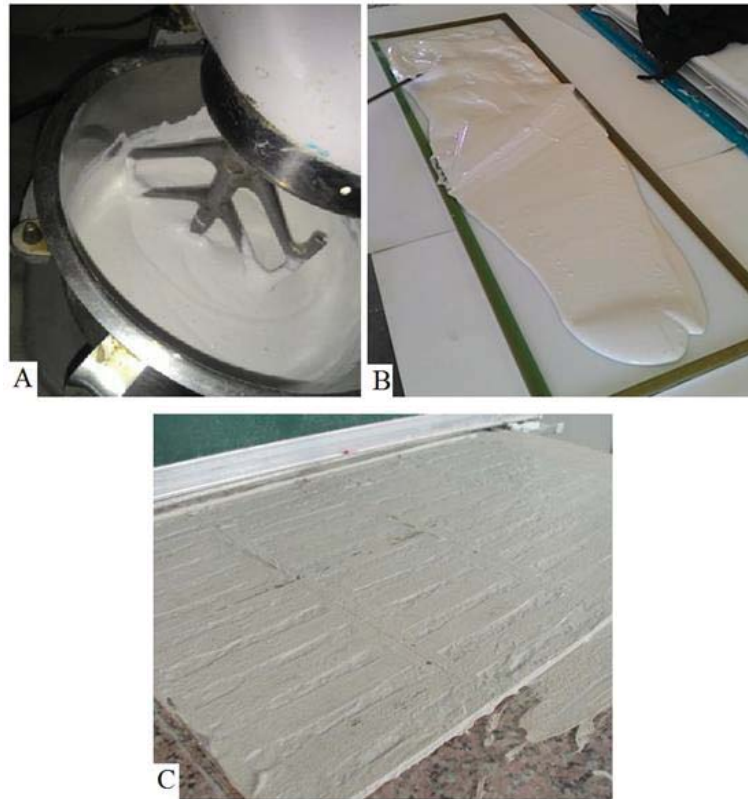
Figure 3.3 Mixing and Pouring of the TSL

After the molding process, the plate was vibrated to remove air bubbles. The mixture was allowed to cure for 7 days at 25°C in the test chamber after being poured into the plate and molds. At the end of the curing period, 12 specimens were prepared by die cutter and molding methods, for each geometry type (Figure 3.4).

Figure 3.4 Specimen Preparation by Molding and Die cutter

The tensile tests were conducted with a displacement rate of 6 mm/min, which is within the limits of the ASTM standard (5±1.25 mm/min). During the tests, the values of load, axial displacement, and time were recorded continuously. The test apparatus is shown in Figure 3.5. Due to the liquid component of the product, dimensions of the molded specimens shrink; and bending might occur. Shrinkage is an inevitable problem for such samples. At the end of the 7-day curing time, 6% shrinkage was measured in the specimens prepared by the molding technique. Since a die cutter was used at the end of the curing period, the shrinkage did not create an issue in the sample preparation process. It should be noted that each sample dimension was re-measured at the end of the curing time.

In this study, 4 different specimen sets were prepared. The test results were abbreviated according to the specimen type and the technique applied as given below:

- Type I geometry, specimens prepared by molding technique: **T-I-M**
- Type I geometry, specimens prepared by die cutting technique: **T-I-D**
- Type IV geometry, specimens prepared by molding technique: **T-IV-M**
- Type IV geometry, specimens prepared by die cutting technique: **T-IV-D**
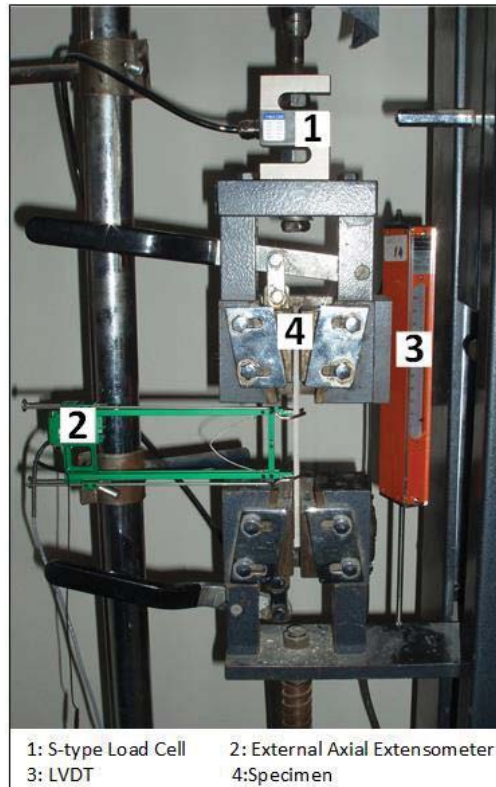
Figure 3.5 Tensile Test Set-up

The tensile tests were performed to evaluate four important parameters:

- Ultimate Tensile Strength (σ_t) in MPa
- Yield Strength (σ_t) in MPa
- Tensile modulus (E_t) in MPa
- Elongation at break in %

Yield strength is defined as the minimum stress under which a material deforms permanently, whereas tensile strength describes the maximum stress that a material can handle before rupture. In case that the applied constant load exceeds the elastic limit of the liner (yield strength), failure may take place. In field applications, the loading conditions are irreversible, which means that there is not possibility of unloading of TSL. Therefore, yield strength of a TSL product is also as significant as its ultimate tensile strength.

The test measurements allows plotting of 48 stress-strain curves. Figure 3.6 shows a representative illustration of stress–strain curves of four different test sets. All test results and specimen photos before and after tests for each set are presented in Appendix A.
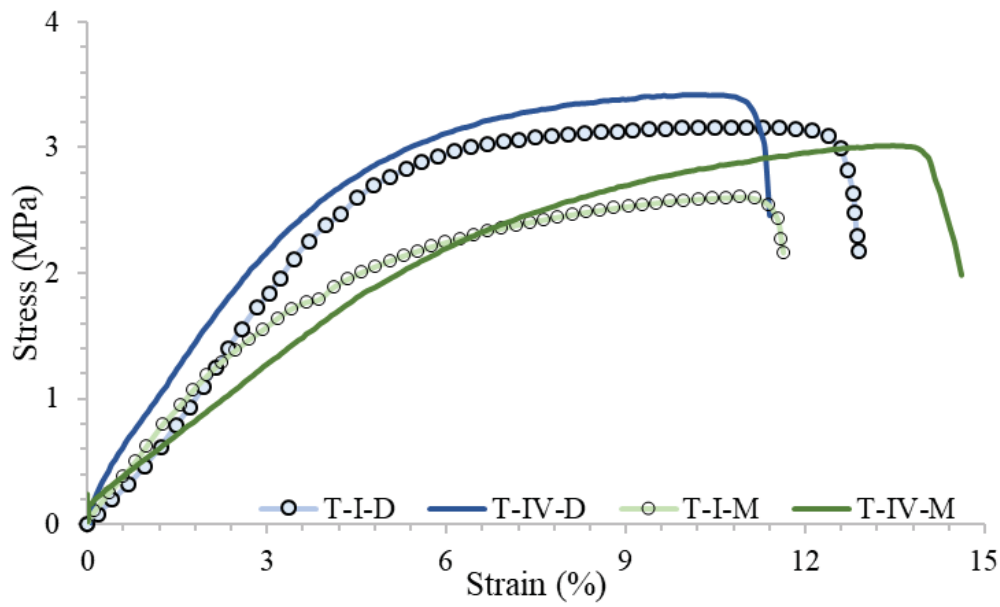
Figure 3.6 Representative Tensile Stress– Strain curves for Different Test Sets

As seen from the stress-strain curves (Figure 3.6), T-IV-D specimens have the highest ultimate tensile and yield strength values where its ultimate tensile strength is 0.7 MPa greater than the value of T-I-M specimens. Moreover, T-IV-M specimens have a higher strain capability than other sets. This might lead to a decrease on the tensile modulus values. The expected values and the standard deviations of the parameters for four test results are presented in Table 3.1. All four test sets meet the minimum requirement of ultimate tensile strength, tensile modulus and elongation at break values (σ_t >2 MPa, E_t >20 MPa, elongation at break >10%) stated in the general and special requirements of TSL document of the Experts for Specialised Construction and Concrete Systems (EFNARC).
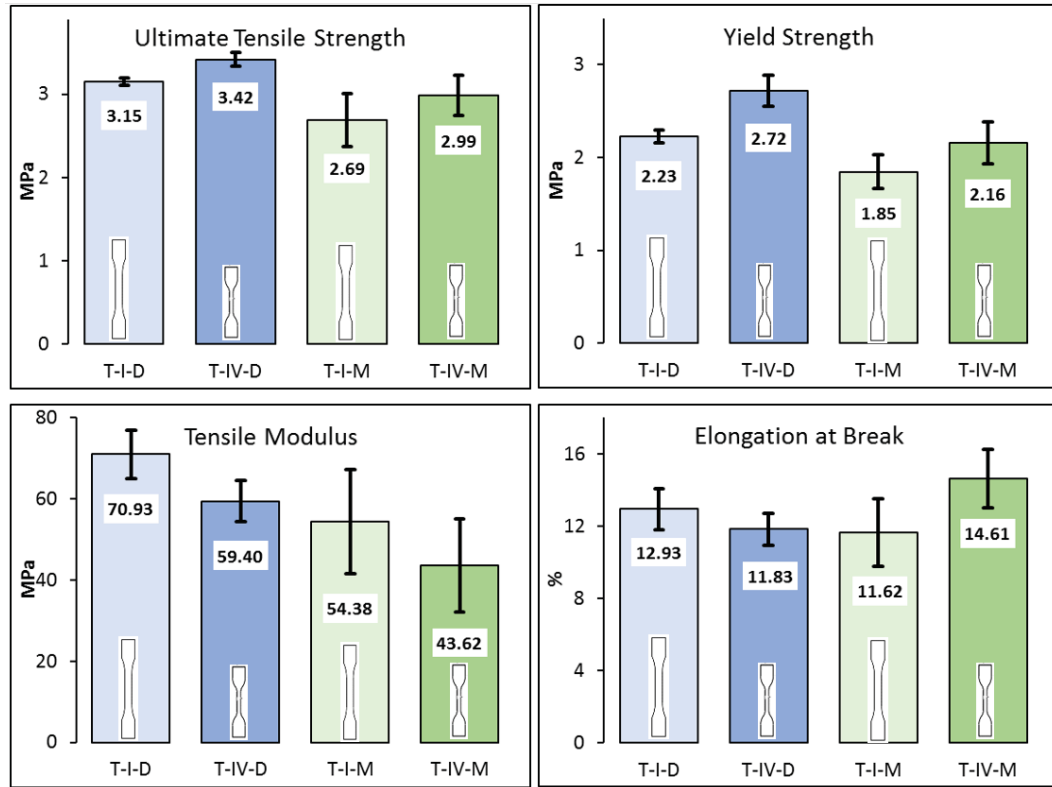
Figure 3.7 Ultimate Tensile Strength, Yield Strength, Tensile Modulus and Elongation at Break Results (error bars represent standard deviations)

Specimens prepared by die cutter have higher strength and tensile modulus values; and standard deviation of repetitive test results for each parameter is observed to be small as seen in Figure 3.7. Angular shape of the molds is expected to contribute the most to the difference between the specimen types. The corners and the gauge section of the sample mold are not filled by the fresh TSL mixture, naturally. Therefore, the mixture was carefully spread by a spatula. During the preparation phase, large air bubbles, which have a potential to create a flawed sample and a negative impact on the test results, were frequently observed. On the other hand, when preparing the sample by die cutter technique, the specimen can be cut in a proper shape directly from the cured TSL plate (Guner and Ozturk, 2017).

Moreover, Type IV specimens have higher strength and tensile modulus values due to the small specimen dimensions. As the dimensions of the gauge section decrease, the occurrence probability of a lump or air bubble decreases. Table 3.1 presents the

comparison of the tensile mechanical properties obtained from four different test sets.

Table 3.1 Comparison of four techniques

| | % Change in | | | |
	Ult. Tens. Strength	Tensile Modulus	Elongation at break	Yield Strength
T-I-D vs T-I-M	+16.93	+30.43	+11.25	+20.77
T-IV-D vs T-IV-M	+14.50	+36.17	-19.02	+25.87
T-I-D vs T-IV-D	-7.88	+19.41	+9.31	-17.94
T-I-M vs T-IV-M	-9.79	+24.67	-20.44	-14.48

As a result of this study, specimens prepared by die cutter were observed to provide more accurate results. In tensile testing, Type IV specimens prepared by die cutter was found as the most proper specimen preparation technique. In tensile creep test study, since Type-IV specimens are not suggested in the standards, Type I specimens prepared with die cutter is taken as a basis for specimen preparation and size type.

Following the sample preparation process, some preliminary control tests were performed to ensure that the creep test apparatus was operating properly. During the preliminary experiments, data acquisition system, air conditioner, power supply, LVDT and dial gauges were observed to work as intended. The general view of the testing apparatus is presented in Figure 3.8. One of the problems encountered in the preliminary test was the slippage of the sample during the experiment. In order to avoid this problem, the clamps are notched perpendicular to the sample position. The points where the samples were attached to the clamps before the experiment were marked, the changes in the post-test positions were checked. It was observed that the sample was completely prevented from slipping.

Figure 3.8 General view of the creep test setup

3.4. Laboratory-Scale TSL Preparation Guide

Specimen preparation is one of the most critical steps in laboratory testing of TSLs. Test specimens should be representative of the field application in compliance with the defined test standards; and each specimen should be identical. For this reason, it was decided to present a detailed procedure for the preparation of TSLs in the laboratory.

In all experiments conducted for TSL-1 and TSL-2, parameters such as, mixing ratio, mixing time, mixing speed, ambient conditions were kept constant. First of all, the shelf life of TSLs to be used in the experiments is limited, and it is important to comply with the shelf life and storage conditions. TSLs that are not stored in appropriate conditions or exceed their shelf life are easily understood during the sample preparation process. Such products lead to lumps during the mixing process. The shelf life of TSLs sold in packs of 20-25 kg is generally 12 months. However, if the packages are not sealed immediately after opening up and not stored at room temperature, they start to deteriorate in 15 days (dust components moisten, liquid components solidify).

Since the particle size of the powder components of TSLs is at the micron level, it is absolutely necessary to use masks and gloves during the sample preparation process.

Besides, the material safety data sheet (MSDS) must be read carefully before using the product. In general, each TSL product has its own fixed mixing ratio and the practitioner must comply with these ratios. In field applications, TSLs are mixed with the help of special equipment. However, this type of equipment could not be used in laboratory applications due to the small amount of material requirements. For this reason, different mixing techniques (on the same mixing ratio) have been applied in the laboratory studies. As a result of preliminary laboratory experiments, it has been observed that a 10% error or change in the mixing ratio has an effect of up to 40% on the mechanical material properties. Therefore, if the results of the tests with the prepared samples are compared with each other, the mixing ratio and the mixing quantities must be kept constant.

In previous studies, researchers have followed different procedures to mix TSLs. Mixing by hand mixer is not recommended. After the addition of powder and liquid components, the gel time of some TSL products can be as short as 5 minutes (TSL-2). During this limited time, the mixture should be prepared homogeneously. The mixing palette of the mixer must perform the mixing process by contacting the entire surface area of the mixing bowl evenly. Therefore, a laboratory-scale cement mixer with different speed settings is recommended as the most suitable equipment for mixing.

It was determined that the mixing process should not exceed 6 minutes regardless of the TSL product type. In this process, firstly, the components can be mixed with a slower speed (60-70 rpm) for 3 minutes. Then, the adhered fresh mixture to the inner surface of the mixing bowl is added to the mixture with the help of a spatula and mixed at higher speed (120-130 rpm) for 3 minutes for preparation of the mixture, which is recommended. Mixing speeds above the recommended value cause the formation of bubbles in the fresh TSLs, and it is determined that it is not possible to remove these air bubbles from the mixture during the molding stage. In addition, it was observed that the powder component of TSLs tends to lump at speeds less than 60 rpm.

After the mixture process of TSLs, pouring into mold or plate should be done immediately. As it is known, high adhesion strength is one of the critical features of TSLs. The mold or plate must not be made of aluminum, steel, or glass. Preferably, the use of flexible plexiglass is recommended. Although the interaction of the plexiglass mold or plate with the fresh TSL mixture is low (varies according to the products), the possibility of TSL sticking to the mold during curing time should be prevented. For this reason, it is recommended to apply a mold releasing agent (especially those that will be used in the molding process) such as mold release spray, mineral oil, as a very thin layer to sharp corners. It is recommended that the temperature and humidity values of the environment where the molding process will be performed is to be in the laboratory conditions. Also, plates with a frame 1-2 mm thicker than the intended sample thickness in the molding process are suggested. Spatula, to be used to spread the mixture and keep the thickness of the mixture constant during the molding process, is recommended to be used in the same direction.

In light of the literature review and preliminary experiments, it was observed that the size of some samples prepared by the molding technique was reduced while curing due to its water content. In addition to the decrease in the size of the samples that lost water content, bending in different directions was observed. Shrinkage is an inevitable problem in this type of water-based TSLs. Since the bent samples lost their symmetrical geometry, the results obtained in the experiments showed sizeable standard deviation values. This shrinkage problem is one of the important reasons for the selection of the die-cutting specimen preparation technique. Since TSL-2 is water-based, the shrinkage and bending problems were encountered in the preliminary test samples prepared by a molding technique. Figure 3.9 presents a typical standard and shrunken test samples.

Figure 3.9 Standard and shrunk test specimens (Guner, 2014)

The sample thickness is determined by considering the application thickness of the TSLs in the field. Since the general application thickness of TSLs in the field is 3-5 mm, researchers in the previous studies have generally prepared the samples in thicknesses of 3-5 mm. Similarly, 4 mm thick samples were prepared in this study. In the preliminary experiments, samples with different thicknesses were also tested; and it was determined that the thin samples reached relatively higher strength values with lower standard deviations. Besides, the invariability in the thickness of the prepared samples is crucial to obtain comparable test results. Samples should be prepared with a constant thickness, especially before testing, to ensure that the gauge section, the thinnest part of the sample, has a uniform thickness.

3.5. TSL Testing

This section presents tensile and creep tests for both TSL-1 and TSL-2 products. The number of experiments performed within the scope of laboratory studies are presented in detail in Table 3.2.

Table 3.2 TSL Testing Programme

	TSL-1					TSL-2			
Curing Time (days)	1	7	14	500	Total	2	7	14	Total
Tensile Tests	7	6	8	6	27	7	5	7	19
Creep Tests	8	8	8	8	32	8	8	8	24

At the beginning of the study, it was planned to conduct creep tests for two TSL products and only for 1, 7 and 14-day curing time. Since the TSL-1 product was found to be highly sensitive to creep behaviour at the end of the experiments, it was decided to find this behaviour for the aged TSL as well. Moreover, at the end of 1 day curing period, TSL-2 could not be tested due to the high elongation rate. Although the sample reached approximately 4 times of its initial length, it continued its flow behaviour and did not fail. Considering all these reasons, it was decided to apply the test program given in Table 3.2.

General information about tensile and creep test setups are given in the previous section. The general view of the tensile and creep test setups is presented in Figure 3.5 and Figure 3.8, respectively. The tensile tests were carried out just before each creep test set in order to determine the sustained load amounts to be used in the creep tests.

3.5.1. TSL-1 Testing

This section includes the tensile and the creep tests for TSL-1 with a curing time of 1, 7, 14 and 500 days. Preliminary experiments showed that the samples prepared at different times with the same mixing ratio, having the same curing time and kept under the same conditions, could show different tensile and creep behaviors. For this reason, the tensile tests and the creep test specimens were prepared with the same batch; and the tensile tests were performed just before creep tests. The tensile tests were carried out with at least 5 samples for each curing period. All the valid test results and the sample figures (before and after test) are presented in Appendix B. The average ultimate tensile strength values for TSL-1 are presented in Table 3.3.

Table 3.3 Average tensile strength values for TSL-1 for specified curing time

Curing Time (Day)	Failure Load (N)	Ult. Tensile Strength (MPa)
1	70.14 ± 1.08	1.32 ± 0.06
7	160.88 ± 5.10	2.91 ± 0.07
14	185.51 ± 7.65	3.47 ± 0.15
500	196.28 ± 8.01	3.70 ± 0.15

The relationship between ultimate tensile strength and curing time of TSLs in the literature has been defined by logarithmic functions. In this study, the relationship between the maximum tensile strength values and the curing time was consistent with the previous studies. As shown in Figure 3.10, the tensile strength parameter changes depending on the curing time, expressed in logarithmic curve function. At this point, it is seen that the performing creep tests for different curing times is necessary. Since the logarithmic relationship is evaluated in the literature only within the 30-day of curing time, experimental results with a curing time of 500 days were not included in the graph.

$$y = 0.8168\ln(x) + 1.3189$$
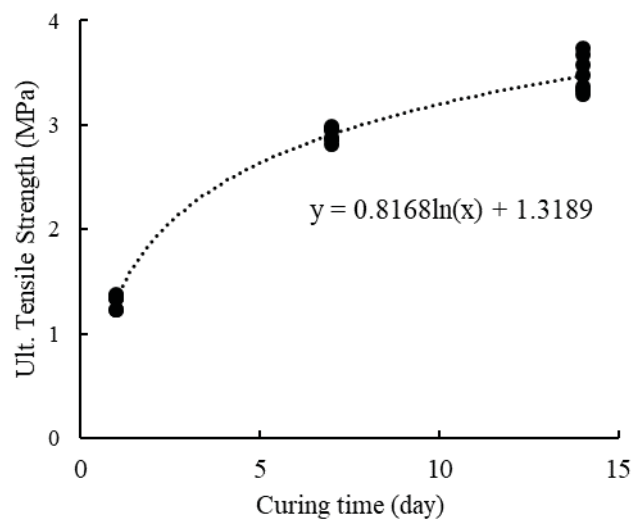
Figure 3.10 Ultimate tensile strength growth with curing time for TSL-1

62

As shown in Table 3.3, samples with a curing time of 1, 7, and 14 days of TSL-1 were failed at approximately 70 N, 161 N and 186 N, respectively. These values were taken into consideration in determining the constant loads to be used in creep tests.

As mentioned in the test set-up part, the creep test apparatus is designed to perform 8 tests simultaneously. ASTM-2990 suggests that 1000 h of testing time is good enough for plastic materials. In this study, taking the service life of the TSL into account for field applications (TSL coated production panels, tunnels), 1500 h (~2 months) testing time was estimated to be more representative. Also, at least two repetitions are recommended for each stress level according to this standard.

The calculated deadweight levels to be used in the creep tests are presented in Table 3.4. While calculating the dead weights to which the sample will be sustained, the clamps and all other apparatus holding the bottom of the sample were also taken into account.

Table 3.4 Applied dead weights in creep tests for TSL-1

Creep Test No	Required Load (%)	1-Day Req. Load (N)	Eq. Stress (MPa)	7-Day Req. Load (N)	Eq. Stress (MPa)	14-Day Req. Load (N)	Eq. Stress (MPa)	500-Day Req. Load (N)	Eq. Stress (MPa)
1 2	80	56.1	1.06	128.7	2.33	148.4	2.78	154.7	2.96
3 4	60	42.1	0.79	96.5	1.75	111.3	2.08	115.7	2.22
5 6	40	28.1	0.53	64.4	1.16	74.3	1.39	76.6	1.48
7 8	20	14	0.26	32.2	0.58	37.1	0.69	38.2	0.74

Creep tests of TSL-1 were designed to be 1500 hours for each curing time, and the total test period for TSL-1 was decided to be about 8 months. Of the 32 creep tests, 30 were completed within the planned duration. In the experiments performed under 20% of its tensile strength (0.26 MPa) during the curing period of 1 day only, no

rupture was observed. At this stress level, the strain of the samples measured in the last 30 days was around 2.2×10^{-3}. This strain was approximately 15×10^{-3} in the experiments of the same stress percentage for the curing time of 7 days. 1-day cured and tested under 0.26 MPa stress level, TSL-1 creep tests were estimated to take approximately one year to complete; these two experiments were terminated at the end of 60 days to comply with the planned test schedule. Raw displacement-time graphs and sample images obtained from TSL-1 creep tests are presented in Appendix B.

Creep strain-time and creep compliance-time graphs were plotted as a result of the creep tests for TSL-1. The material behaviour identification has an important role for the material modeling stage. For this purpose, compliance vs. time curves were also plotted. Figure 3.11 and Figure 3.12 shows compliance behaviour of TSL-1 for different stress levels and curing times. Depending on the sustained load and curing time, the rupture times vary from a few minutes to 2 months, therefore, compliance vs. time curves were divided into two parts.
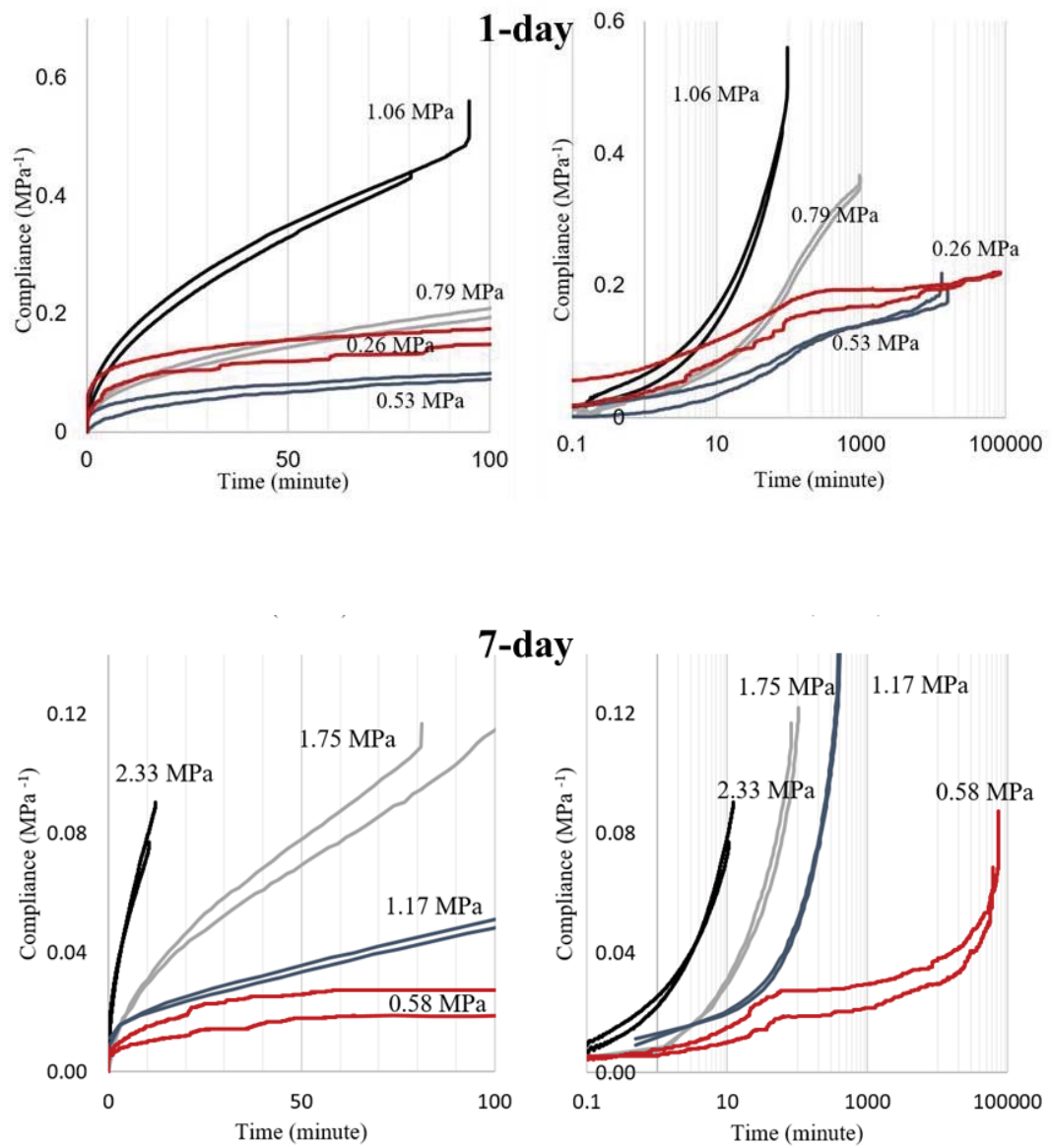
Figure 3.11 Experimental Compliance response of the TSL-1 for 1 and 7 days
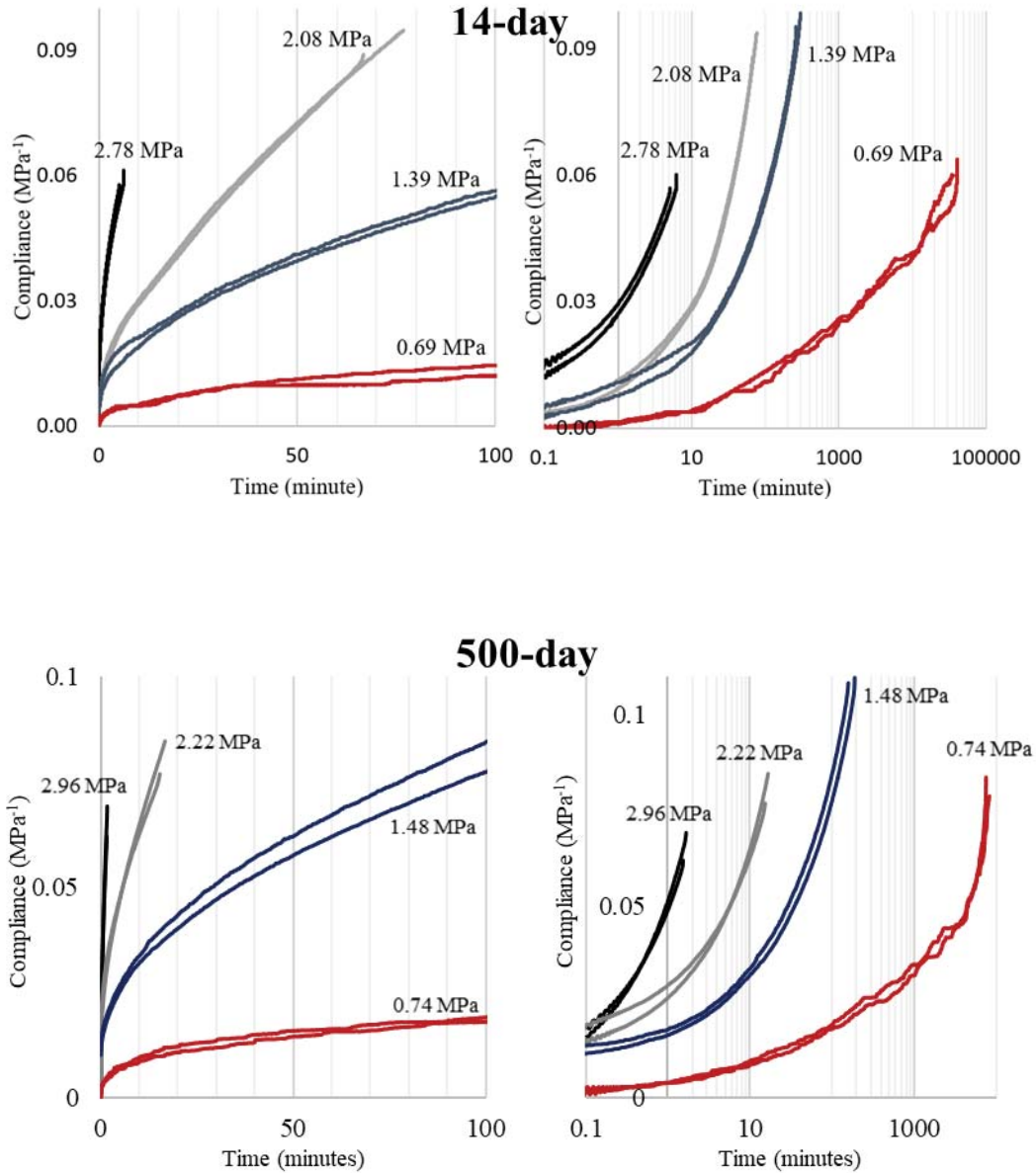
Figure 3.12 Experimental Compliance response of the TSL-1 for 14 and 500 days

The compliance behaviour of TSL for different stress levels is not identical and it is not similar either. Therefore, creep strain must be represented by different functions of time at each stress level. It should be noted that, the material behaviour also depends on the curing time. Therefore, the tested TSL can only be described by nonlinear and non-separable models in terms of the applied stress, time, and curing time.

66

The creep test results with different curing times are shown in Figure 3.13 and Figure 3.14. Depending on the sustained load and curing time, the rupture times vary from few minutes to 2 months, therefore in these figures, total strain vs. time curves were divided into two parts, the first part is up to 100 min and the second part is up to 100,000 min (2 months). 1-day cured TSL specimens tested under 20% of their tensile strength did not fail within the 2 months testing time. In contrast, all 7 and 14-day cured TSL specimens ruptured from their gauge section and provided valid test results.

According to the nonlinear curves in Figure 3.13 and Figure 3.14., it is seen that for the 1-day cured TSL under a constant tensile load of 80% of its tensile strength (1.06 MPa), the rupture is observed within 100 min and the total strain is obtained to be more than 50%. On the other hand, the liner can resist a smaller load for more than two months when the load is about 20% of its tensile strength (0.26 MPa). For 7-day cured samples, the failure takes place within 12 min under a constant tensile load of 80% of its tensile strength (2.33 MPa). As expected, when the sustained load decreases, the rupture time increases. For 7-day results, specimens fail within 55 days under a constant tensile load of 20% of its tensile strength (0.58 MPa). For the 500-day cured test set, in a case where a tensile load that is 80% of the tensile strength (2.97 MPa) is applied, the failure happens in 2 minutes with an about 20% strain. It is obvious that the elongation capability (total strain) and the rupture time parameters are inversely proportional to the curing time (Guner and Ozturk, 2018).

Results of the 500-day test indicate that the TSL-1 product behaved similar to the previous experiments at the different stress levels. The total strain values reached by the samples at the time of rupture are lower than the 14-day experiments. In addition, the samples were failed in a shorter period of time compared to the 14-day experiments. The analysis of the test results will be given in the next section.
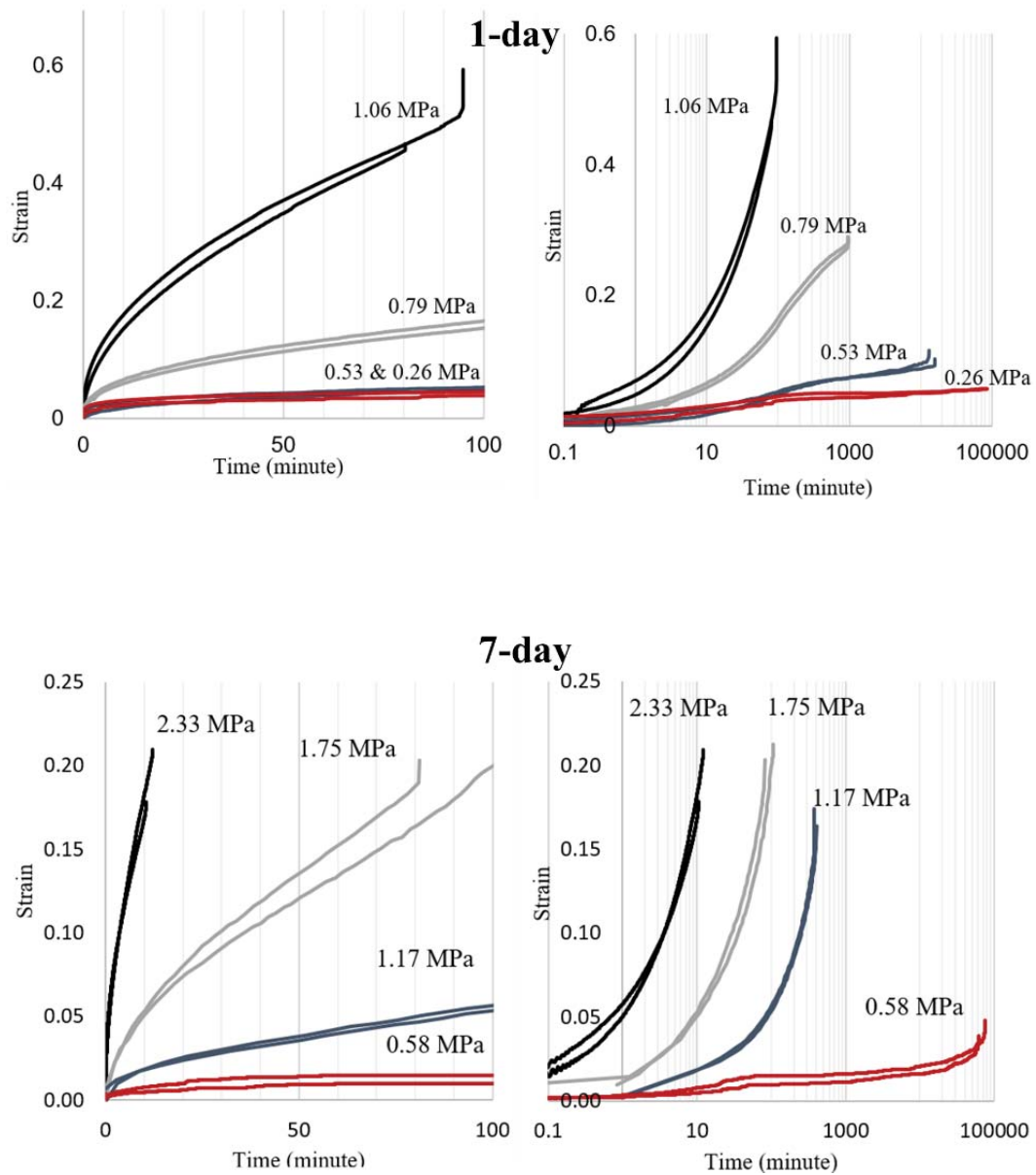
Figure 3.13 Experimental creep response of the TSL-1 for 1 and 7 days
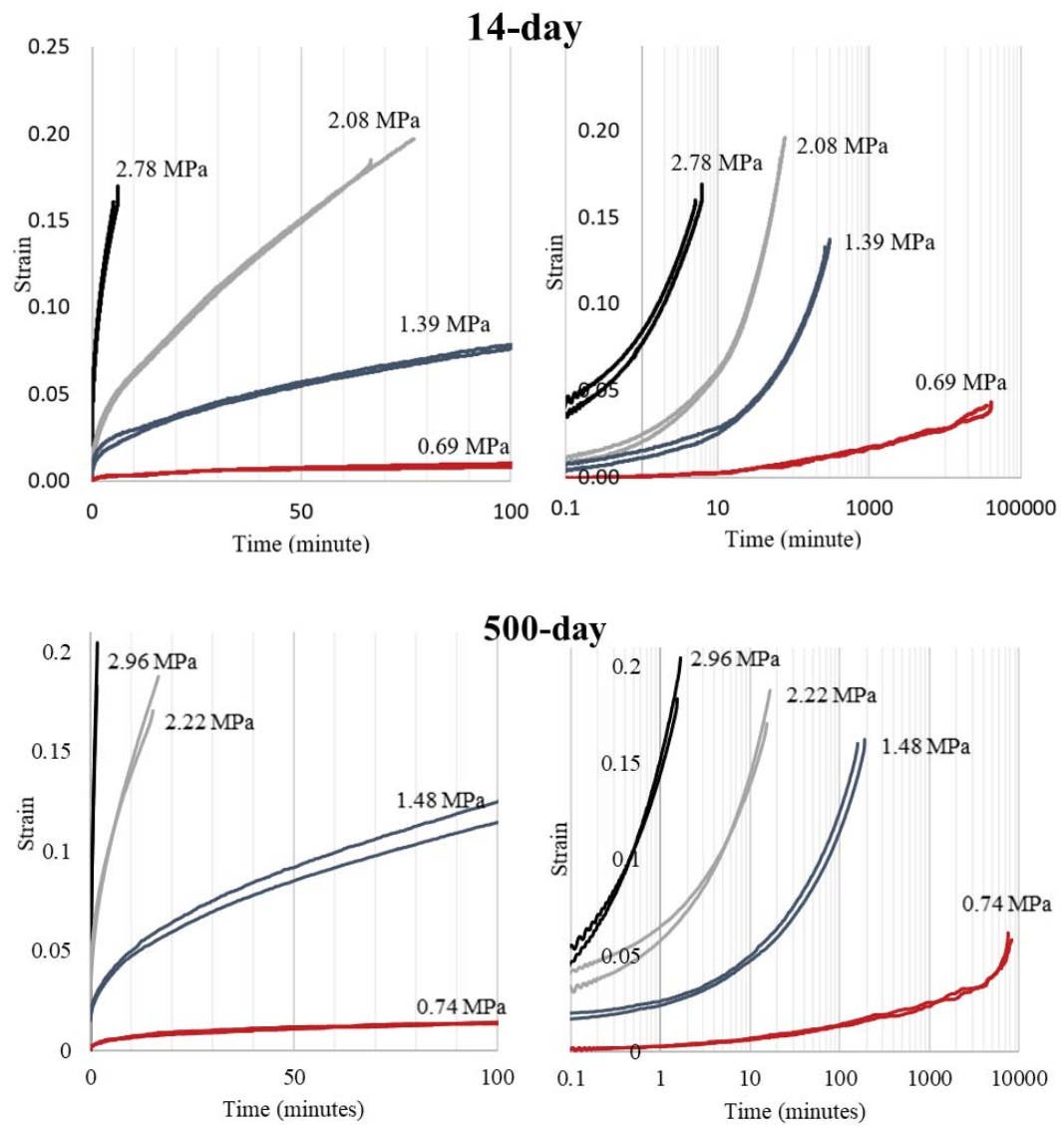
Figure 3.14 Experimental creep response of the TSL-1 for different curing times

3.5.2. TSL-2 Testing

Tensile and creep tests performed for TSL-2 with a curing time of 2, 7, and 14 days are included in this section. At the beginning of this study, it was also planned to perform creep tests with 1-day cured specimens, however, the preliminary tensile tests showed that 1-day cured specimens can have more than 300% strain. This extreme ductile behaviour caused that the specimen exceeded the testing limits of the machine. As it can be seen in Figure 3.15, the specimen reached almost 4 times the gauge length although the viscous flow behaviour was still active. After the load was removed, even though the axial strain was partially recovered due to elastic deformation, the specimen length was stabilized at around twice of its initial length. The tested specimen could barely reach a tensile stress of about 1 MPa.
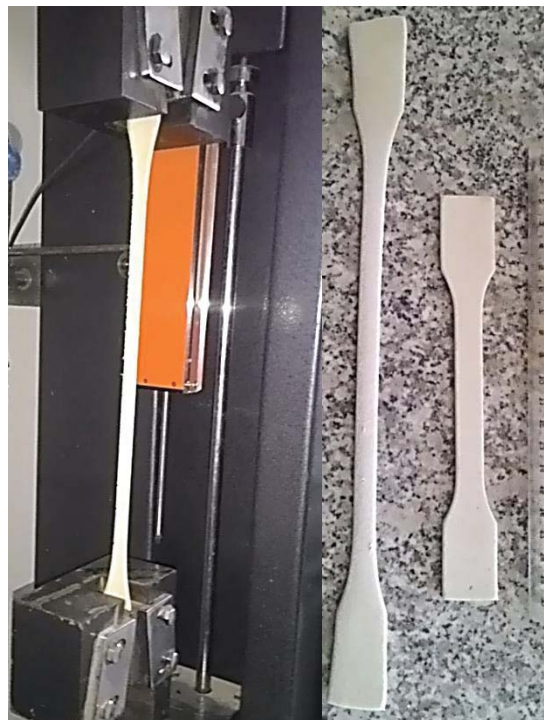
Figure 3.15 Elongation capability of 1-day cured TSL.

Since it is known that the material properties of TSLs change drastically in the first few days, depending on the curing time,1-day cured specimens were excluded from the experimental study; and 2-day cured specimens were used instead.

The tensile tests and the creep test specimens were prepared with the same batch; and the tensile tests were performed just before the creep tests. The tensile tests were carried out with at least 5 samples for each curing period. In tensile testing, a constant displacement rate was applied (6.5 mm/min). All valid test results and the sample figures (before and after test) are presented in Appendix C. The average ultimate tensile strength values for TSL-2 are presented in Table 3.5.

Table 3.5 Average tensile strength values for TSL-2 for specified curing time

Curing Time (Day)	Failure Load (N)	Ult. Tensile Strength (MPa)
2	93.24 ± 1.71	1.84 ± 0.04
7	107.13 ± 2.44	2.10 ± 0.05
14	136.86 ± 8.07	2.67 ± 0.21

As mentioned in the previous section, logarithmic functions have been defined to find out the relationship between ultimate tensile strength and curing time of TSLs in the literature. In this sense, the logarithmic tensile strength growth with curing time for TSL-2 is presented in Figure 3.16.

$$y = 0.4057\ln(x) + 1.5042$$
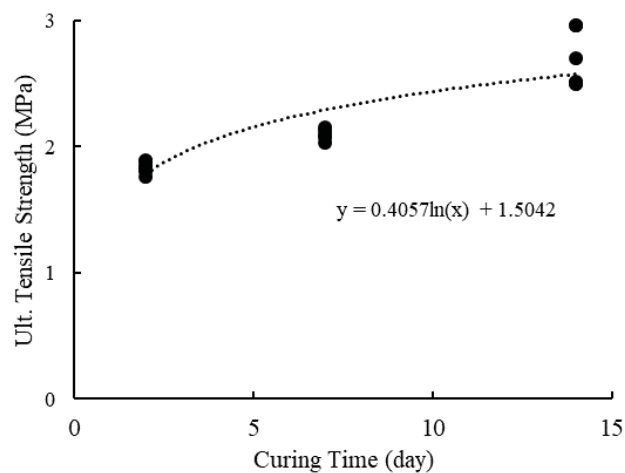
Figure 3.16 Ultimate tensile strength growth with curing time for TSL-2

As shown in Table 3.5, the samples with a curing time of 2, 7, and 14 days of TSL-2 were failed at approximately 93 N, 107 N and 137 N, respectively. These values were taken into consideration in determining the constant loads to be used in TSL-2 creep tests. To have comparable results for the two TSL products, the same laboratory conditions, specimen preparation techniques, test procedures, and test standards were maintained for TSL-2 testing.

The calculated deadweight levels to be used in the TSL-2 creep tests are presented in Table 3.6. While calculating the dead weights to which the sample will be sustained, the clamps and all other apparatus holding the bottom of the sample were also taken into account.

Table 3.6 Applied dead weights in creep tests for TSL-2

Creep Test No	Required Load (%)	2-Day Req. Load (N)	Eq. Stress (MPa)	7-Day Req. Load (N)	Eq. Stress (MPa)	14-Day Req. Load (N)	Eq. Stress (MPa)
1 2	80	74.6	1.46	85.7	1.68	109.5	2.14
3 4	60	55.9	1.10	64.3	1.26	82.1	1.60
5 6	40	37.3	0.74	42.9	0.84	54.7	1.07
7 8	20	18.6	0.37	21.4	0.42	27.4	0.53

Both tensile and creep test specimens are expected to fail from their gauge section to validate the test results. Specimens tested under 20% of their tensile strength did not fail within 2 months of testing time. The remaining TSL specimens failed from their gauge section and provided valid test results.

In the experiments performed under 20% of its tensile strength during the curing periods of 2, 7, and 14 days, the strain of the samples measured in the last 30 days is less than 0.75×10^{-3}. These six experiments were terminated at the end of 60 days to

comply with the planned test schedule. The raw displacement vs. time graphs and the sample images obtained from the TSL-2 creep tests are presented in Appendix C.

Compliance (ε/σ) vs. time curves can be used to decide on whether the material behaviour is linear or nonlinear. If the compliance is not dependent on the applied stress level, the single creep curve can describe the material behaviour. In this case, the material behaviour is linear. However, if different compliance vs. time curves are obtained, the material behaves nonlinearly. The material behaviour identification has an important role for the material modeling stage. For this purpose, compliance vs. time curves were also plotted. Figure 3.17 shows the compliance behaviour of TSL-2 for different stress levels and curing times. Depending on the sustained load and the curing time, the rupture times vary from a few minutes to 2 months. Therefore, compliance vs. time curves were divided into two parts. The compliance behaviour of TSL at different stress levels is not similar. Therefore, creep strain must be represented by different functions of time at each stress level. It should be noted that the material behaviour also depends on the curing time. Therefore, the tested TSL can only be described by nonlinear and integrated models in terms of applied stress, time, and curing time.
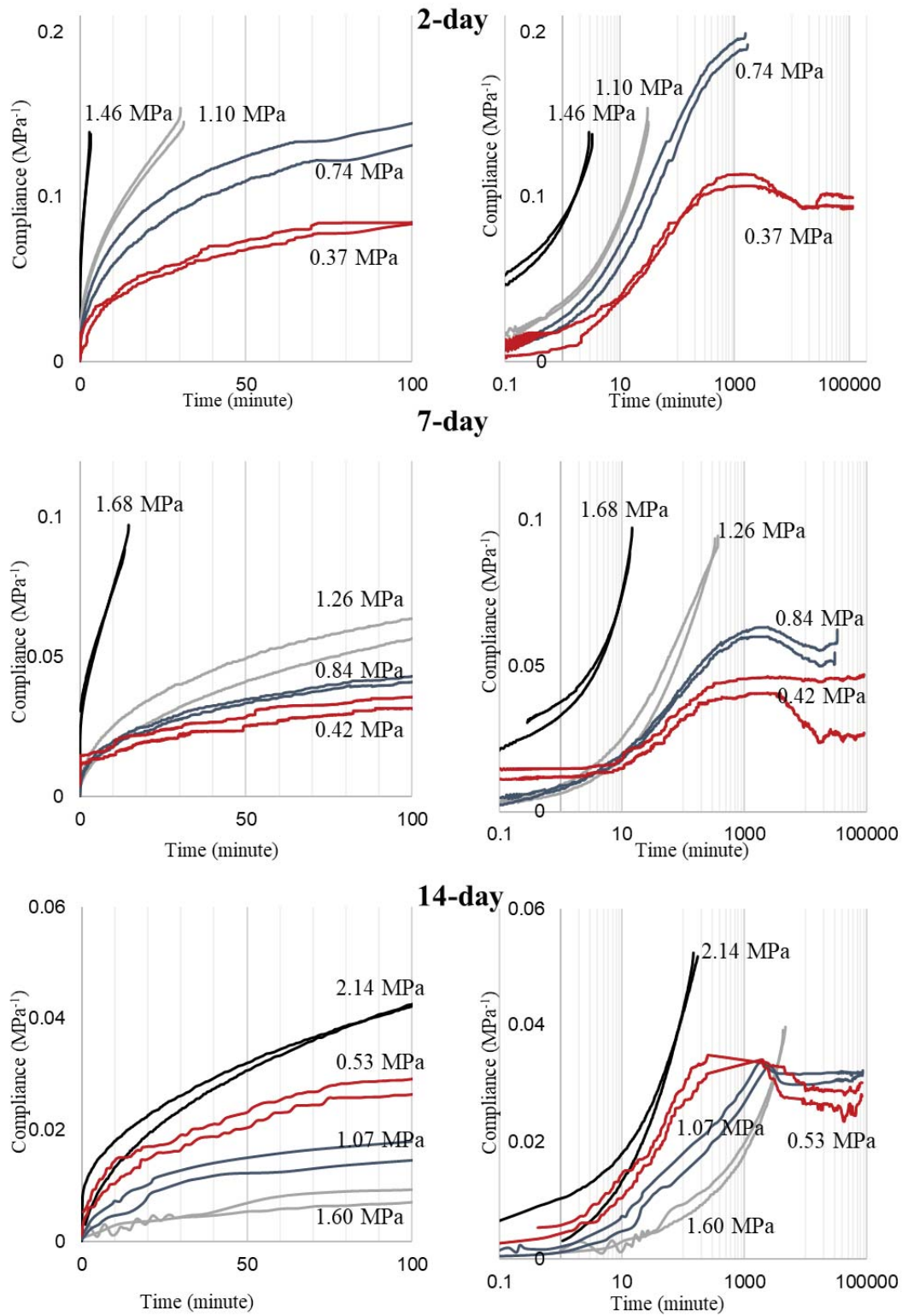
Figure 3.17 Experimental Compliance response of the TSL-2 for different curing times

The creep test results for three different curing times for each stress level are presented in Figure 3.18. Although 4 different stress levels were applied for each test set, only two creep stages were observed. During the primary creep stage, which is generally a short interval of the testing time, a rapid increase in creep strain was observed. A significant tertiary stage was not detected. During the secondary creep stage, the creep rate becomes almost constant as proposed in literature. Depending on the applied stress levels and the curing time, a wide range of rupture time was observed. 2-day cured specimens that are tested under 80% of their tensile strength (1.46 MPa) failed within 3 min. On the other hand, specimens that are tested under 20% of their tensile strength did not fail within the planned testing time. As it can be seen in Figure 3.18, the strain behaviour of the TSL exhibits a strong dependency with the applied stress levels and the curing time. In the small stress level tests, as the data were continuously recorded at short time intervals, strain readings were scattered in the small range. Moreover, if the tested specimen did not fail within 2000 min, a considerably small strain recovery was observed and then the strain converged to an asymptotic value. This behaviour can be affected from the macromolecular nature of the material (Guner and Ozturk, 2019). The evaluations and the detailed analyses of the experimental results will be given in the next section.
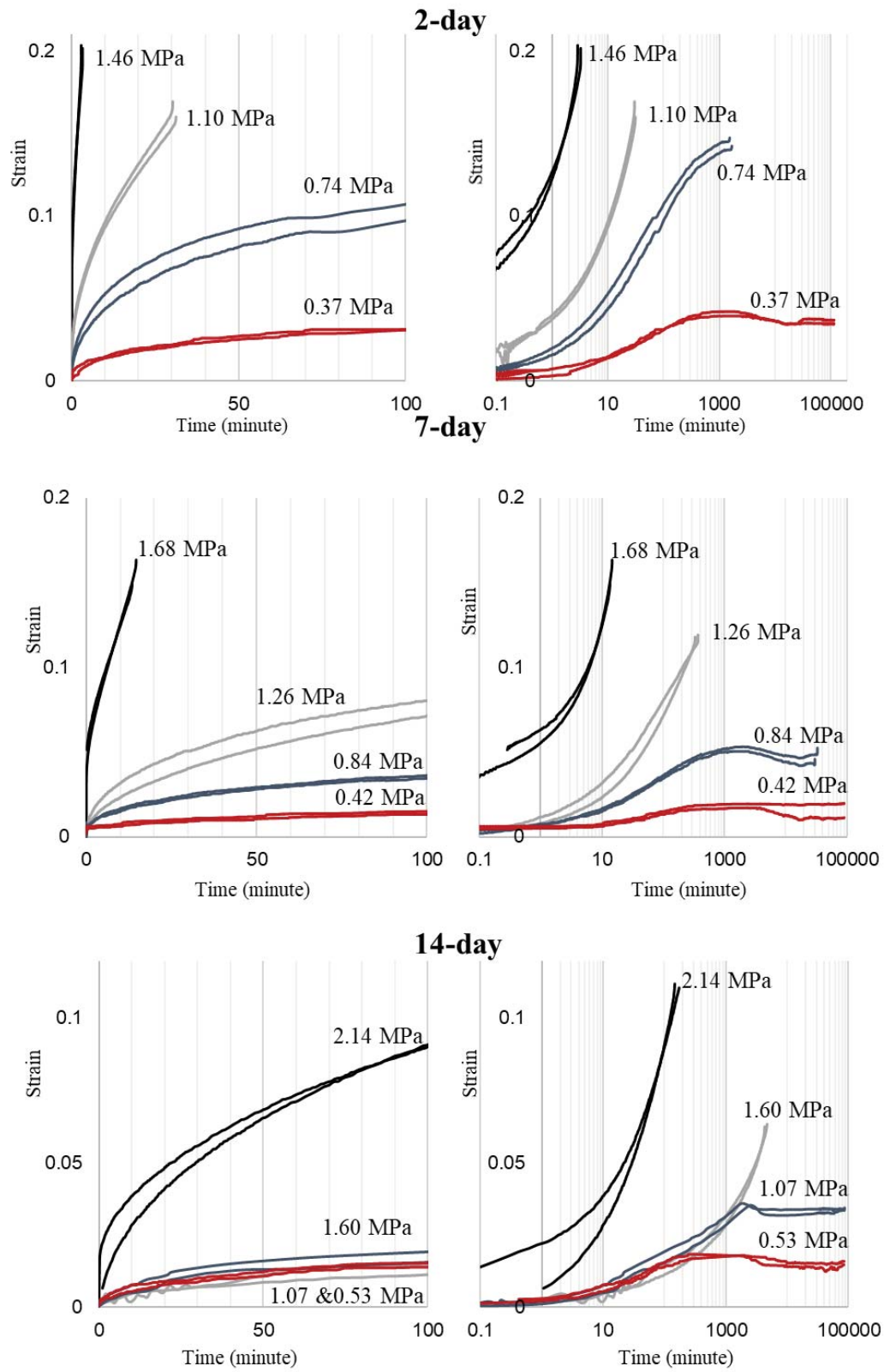
Figure 3.18 Experimental creep response of the TSL-2 for different curing times

CHAPTER 4

EVALUATIONS AND ANALYSES OF THE EXPERIMENTAL RESULTS

A detailed evaluation of creep test results is given in this section. For the 1, 7, 14, and 500-day experiments of the TSL-1 product, 30 out of 32 samples failed during the specified test period (2 months). The specimen ruptured in a period less than 10 days even for the cases where the effective loads are about 40% of the tensile strength. It can be concluded that TSL-1 is highly sensitive to creep behavior. It was observed from the tensile tests performed for each curing time that TSL-1 showed a drastic change in its mechanical material properties compared to TSL-2 depending on the curing time; and it has a higher tensile strength and elongation capability.

In the TSL-2 creep tests, the failure did not occur for the loads that was about 20% of the tensile strength value although the testing period was extended to 2.5 months. In addition, it was observed that the specimen having a curing time of 14-day could sustain without any rupture for about 2 months under the load that is 40% of the tensile strength value. It was concluded that TSL-2 product is also sensitive to creep behavior.

In brief, the laboratory tests reveal that TSL-2 exhibits a relatively lower time-dependent response in its creep behaviour although this product was observed to have a lower tensile strength and elongation capability compared to TSL-1.

4.1. Creep Rupture Envelopes

Creep tests are also commonly performed for service life estimation by constructing a creep rupture envelope. Creep rupture envelopes are widely used in polymer engineering. If the acting stress on the material is known, rupture time and/or strain amount at rupture can be estimated by using these envelopes. Therefore, it was decided to present creep rupture envelopes for the evaluation of the test results. These

envelopes were constructed for each curing time and each product within the scope of this study.

It is a best practice to plot creep rupture envelopes based on the critical design parameter. For instance, if the strain of the material is critical, strain versus time rupture curve is used, otherwise, stress versus time rupture curves are preferred. As TSLs have higher elongation capabilities compared to the conventional areal supports, it is intended in this section to investigate the time dependency of the load bearing capacity of the liner. Therefore, the creep rupture envelope was plotted for the stress case. Figure 4.1 and Figure 4.2 show the relationship between rupture time (hour) and curing time for different stress levels. It should be noted that the creep rupture envelope is presented by using active stress over ultimate tensile strength ratios of the TSL. These rupture envelopes might help support design engineers in estimating the effective permanent support time of the TSL.
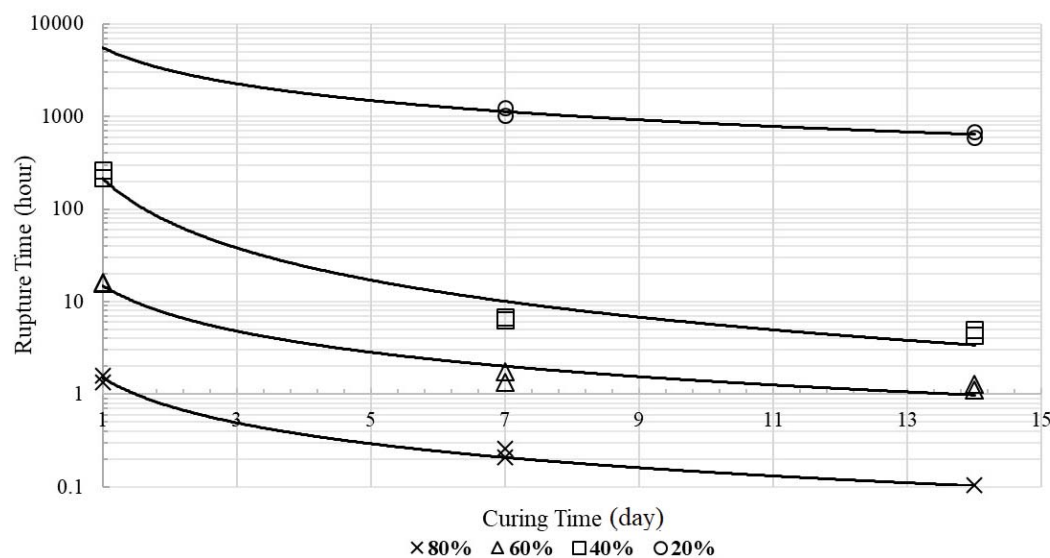
Figure 4.1 Creep rupture envelopes with different tensile strength percentage levels of TSL-1.

Figure 4.1 shows how rupture time of TSL-1 has a drastic drop at the increasing curing time for four different loads correlated with the percentiles of the tensile strength value. In addition, as expected, it is seen that the rupture time values also increase with the decrease in the strain value. Exponential functions can express the relationships

78

between curing time and rupture time at different stress percentile values. The derived equations are presented in ile strength ratio as constant.

Table 4.1.

Since TSL-2 does not fail in any of the tests performed under the load that is 20% of the tensile strength, creep rupture envelopes for only 3 different stress percentages are presented in Figure 4.2. The most significant difference observed in TSL-2 compared to TSL-1 is that the rupture time of the material increases due to the increasing curing time. In the TSL-1 experiments, the earliest rupture was observed in the specimens with 14-day curing time and 80% of the strength value while, in the TSL-2 experiments, the earliest rupture was observed in the sample with 2-day curing time at the same stress level. It can be concluded from this observation that the creep sensitivity decreases as the increase in the curing time of TSL-2. This decrease in the creep sensitivity is considered to be an advantage in TSL field applications.
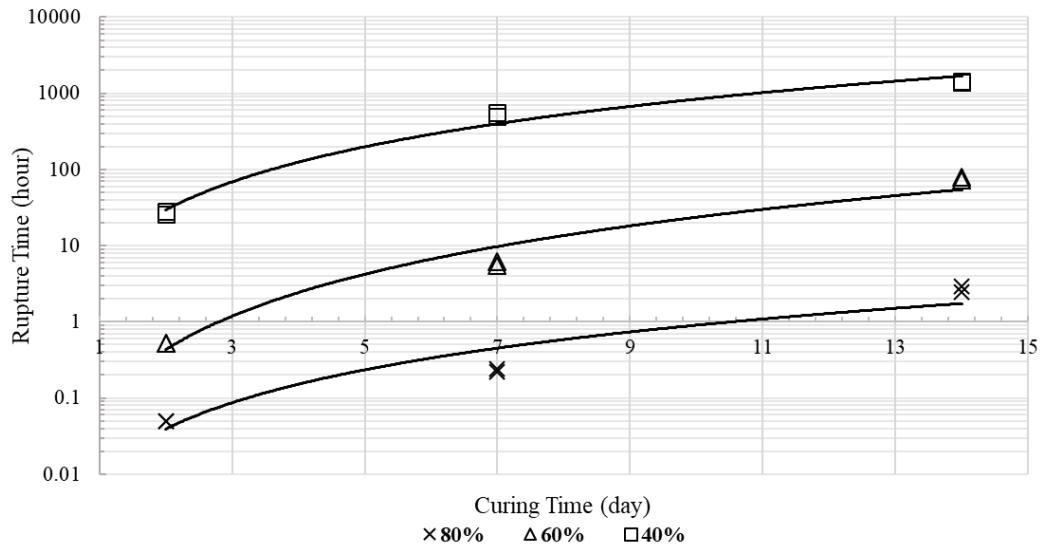
Figure 4.2 Creep rupture envelopes with different tensile strength percentage levels of TSL-2.

In the evaluation of the test results, a creep rupture envelope based on the curing time is presented as another creep rupture envelope type. Figure 4.3 shows the creep rupture envelopes based on the curing time for TSL-1. Contrary to the expectations on the

creep rupture envelopes based on the curing time presented for TSL-1, the increase in the curing time had a negative effect on the rupture time.

Rupture envelopes shifted to the left (causing a decrease in the rupture time) due to a stiffness increase as the curing time increases. In literature, mechanical property enhancement rate is relatively higher when evaluated for 1-day to 7-day curing time. A similar result is also obtained in this study where the rupture envelopes between 7-day and 14-day are close to each other for TSL-1. It should be noted that the samples under the load of 20% tensile strength and 1-day cured specimens did not fail within 2 months. Therefore, no test data could not be acquired for these experiments.
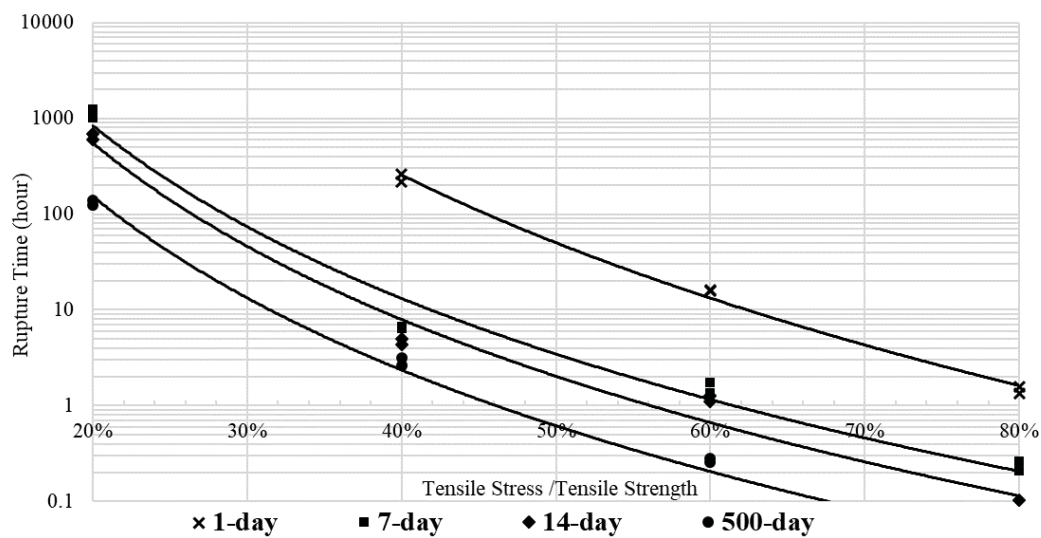
Figure 4.3 Creep rupture envelopes with different curing times of TSL-1.

Since the product lost its elongation capability under the constant load in the experiments carried out at the end of 500-day, specimens failed within a few hours even in the experiments where the tensile stress-strength ratio was 0.4.

For TSL-2, a very similar rupture behaviour was observed for the different curing times in the envelopes presented in Figure 4.4. In this basis, exponential expression was detected to offer the best-fit equations to represent this relationship at different stress percentages as shown in ile strength ratio as constant.
Table 4.1.
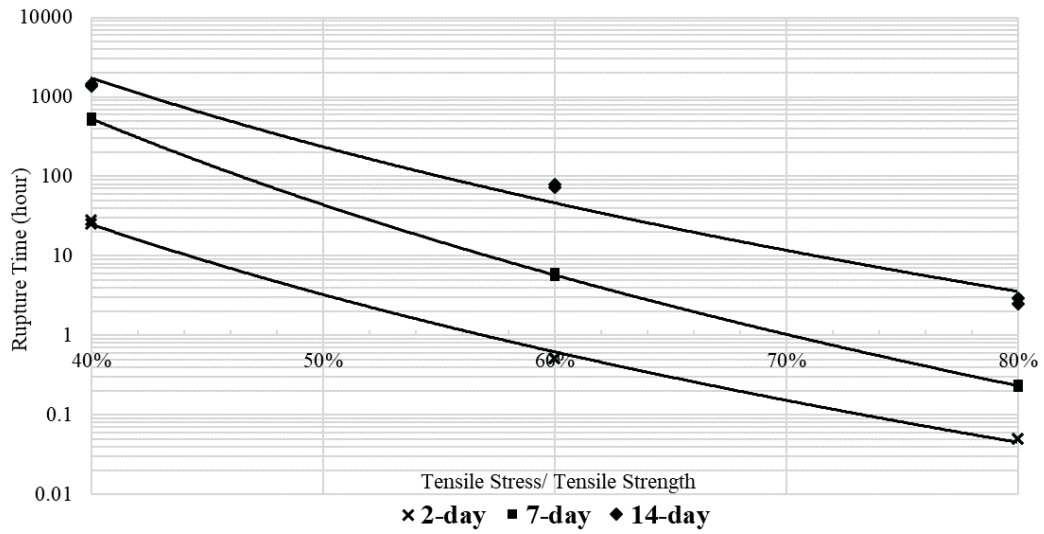
Figure 4.4 Creep rupture envelopes with different curing times of TSL-2

The applied tensile stress values increase at different curing times when the tensile stress / tensile strength parameter is the same. However, this ratio remains constant as the tensile strength increases depending on the curing time. Since the effect of the curing time on the creep behaviour was already investigated, instead of applying constant tensile stress values for different curing times, creep tests were performed by keeping the tensile stress/tensile strength ratio as constant.

Table 4.1 Equations and correlation coefficients of given rupture envelopes

TSL-1			TSL-2		
Stress Level (% of σt)	Equation[a]	SE	Stress Level (%)	Equation[a]	SE
80	$y = 1.461x^{-0.97}$	0.09	80	$y = 0.00023x^{3.538}$	0.16
60	$y = 15.956^{-1.13}$	0.38	60	$y = 0.00447x^{3.689}$	2.71
40	$y = 238.9x^{-1.775}$	16.01	40	$y = 28.121x^{1.483}$	47.17
20	$y = 5588.5x^{-0.820}$	120.39	20	-	-
Curing Time	Equation[b]	SE	Curing Time	Equation[b]	SE
1-day	$y = 0.5123x^{-6.706}$	15.91	2-day	$y = 0.0036x^{-9.714}$	0.84
7-day	$y = 0.00752x^{-7.407}$	64.68	7-day	$y = 0.0201x^{-11.104}$	17.40
14-day	$y = 0.00728x^{-7.074}$	25.46	14-day	$y = 1.825x^{-7.253}$	18.00
500-day	$y = 0.01849x^{-5.512}$	3.56			

a: x=Curing time in days, y=hours   **b:** x=Acting tensile stress / ultimate tensile strength, y=hours.

4.2. Trend Surface Analysis

In addition to the creep rupture envelopes, the equations in ile strength ratio as constant.

Table 4.1 were combined and 3D curves were plotted in TableCurve 3D software, including the complete set of data. These graphs are also called trend surface or response surface in the literature. These graphs provide a better visualization to understand the relationship between rupture time, curing time, and tensile stress/strength ratio. The trend surface graphs of TSL-1 and TSL-2 are shown in Figure 4.5 and Figure 4.6, respectively.
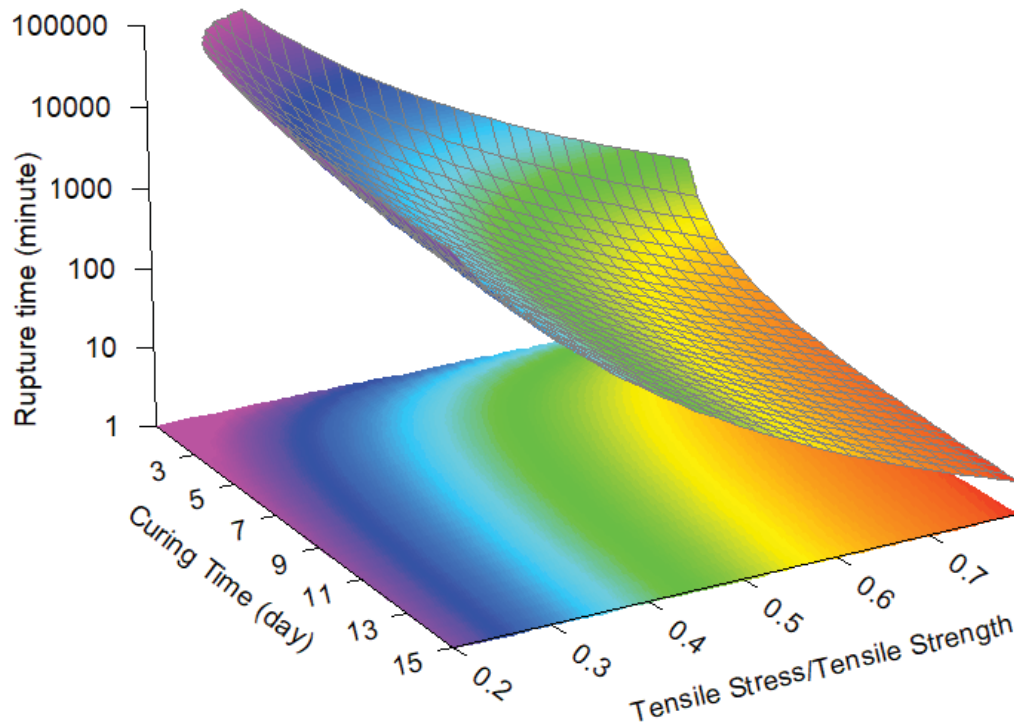
Figure 4.5 Trend surface of TSL-1

According to Figure 4.5, for the TSL-1, the rupture time decreases as the curing time increases under the same tensile stress/strength ratios. The earliest rupture point was observed at the highest stress level (80% of tensile strength) and 14-day curing time. On the other hand, according to the trend surface given for TSL-2 (Figure 4.6), the

rupture time increases as the curing time increases at the same stress rate. It should be noted that the rupture is not observed for the load that is of 20% tensile strength for the TSL-1 product.
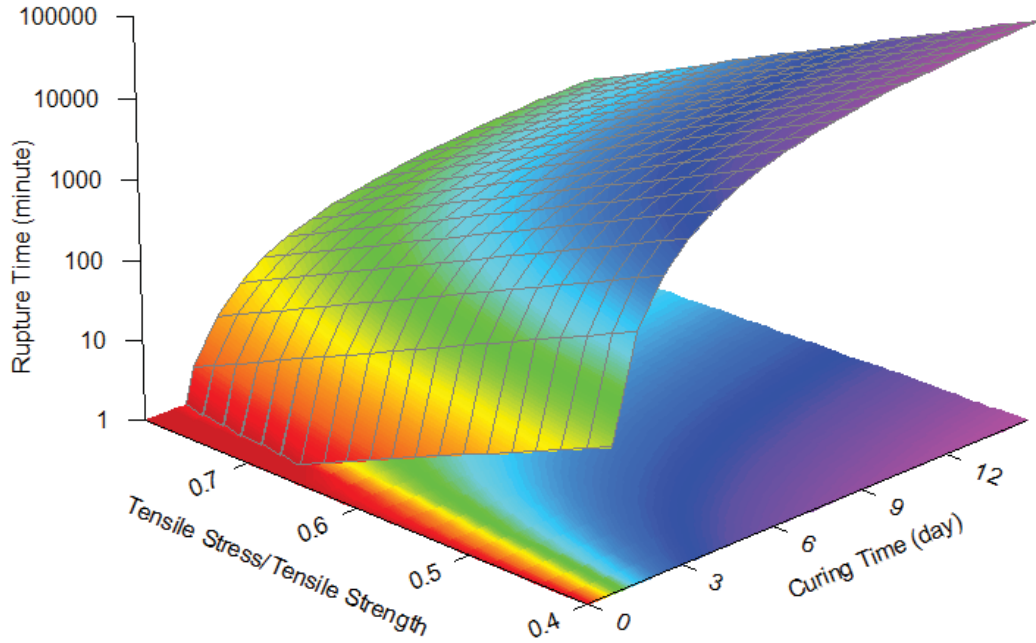
Figure 4.6 Trend surface of TSL-2

In addition, the equations presented in ile strength ratio as constant.

Table 4.1 were used to derive a holistic equation using a statistical package program (TableCurve 3D® v.4). The proposed equation for TSL-1 is;

$$Rupture\ Time\ (minute) = \exp\left[-1.96 + \frac{5.204}{\sqrt{Curing\ Time\ (day)}} - 6.92\ ln\left(\frac{Tensile\ Stress}{Tensile\ Strength}\right)\right] \quad (4.1)$$

The proposed equation for TSL-2 is;

$$Rupture\ Time\ (minute) = \exp\left[19.36 + \frac{8.5}{\sqrt{Curing\ Time\ (day)}} - 14.46\left(\frac{Tensile\ Stress}{Tensile\ Strength}\right)\right] \quad (4.2)$$

Design engineers might use Equations 4.1 and 4.2 in the future for a rough estimation of the rupture time of TSLs. In Figure 4.7, the predicted rupture time values and actual rupture time values are presented using these equations. Very close results were obtained for the rupture times over 100 minutes for TSL-1.

83
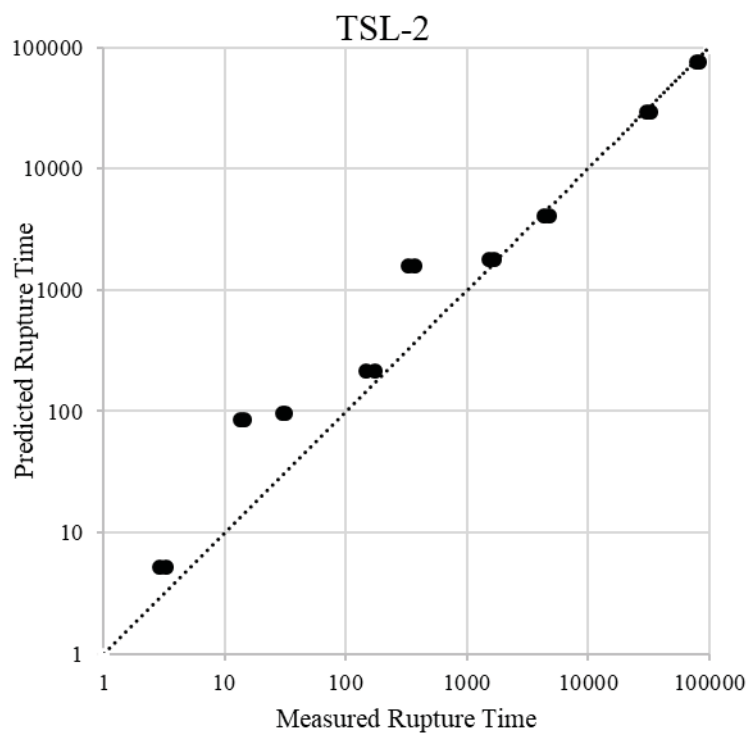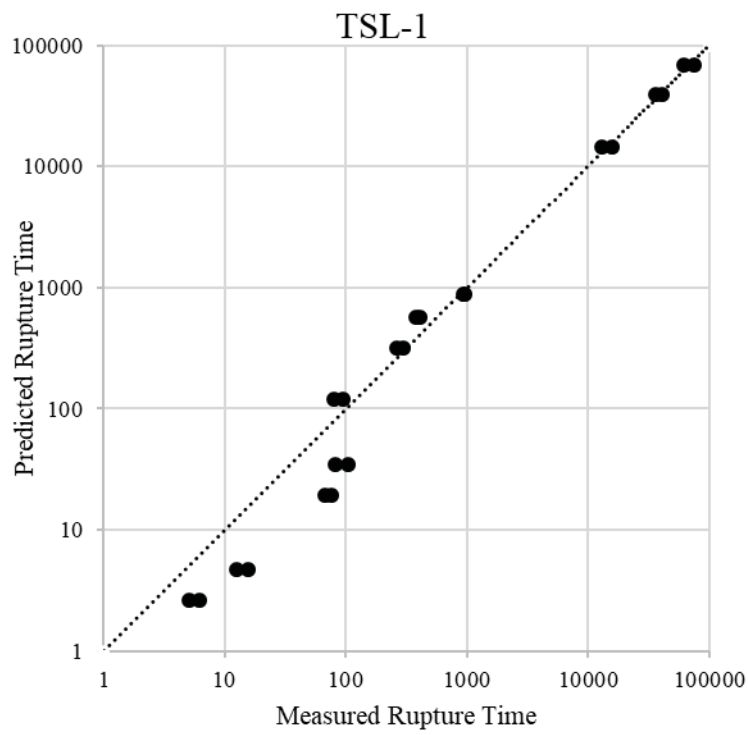
Figure 4.7 Measured versus predicted rupture time values

4.3. Construction of Practical Charts

As the next step in the evaluation of the laboratory results, the tensile stresses acting on the TSLs were analyzed based on the rupture times for different curing times. For this purpose, first of all, tensile stress/tensile strength ratios were converted to tensile stress values acting on the TSLs.

According to the tensile test results of TSL-1, the 14-day samples were detected to have almost 3.5 MPa ultimate tensile strength. On the other hand, Figure 4.8 shows that if the acting tensile stress is higher than 0.8 MPa for 14-day sample, TSL cannot resist more than 10 days. During the support design, design engineers should consider this behaviour and may use the proposed equations for designing TSL as a support member. It is understood that TSL-1 shows more resistance to the creep behaviour as the curing time increases according to the presented rupture envelopes. However, the resistance enhancement of the time-dependent deformation of TSL-1 is less than its tensile strength enhancement. This behaviour can be seen in Figure 4.8.
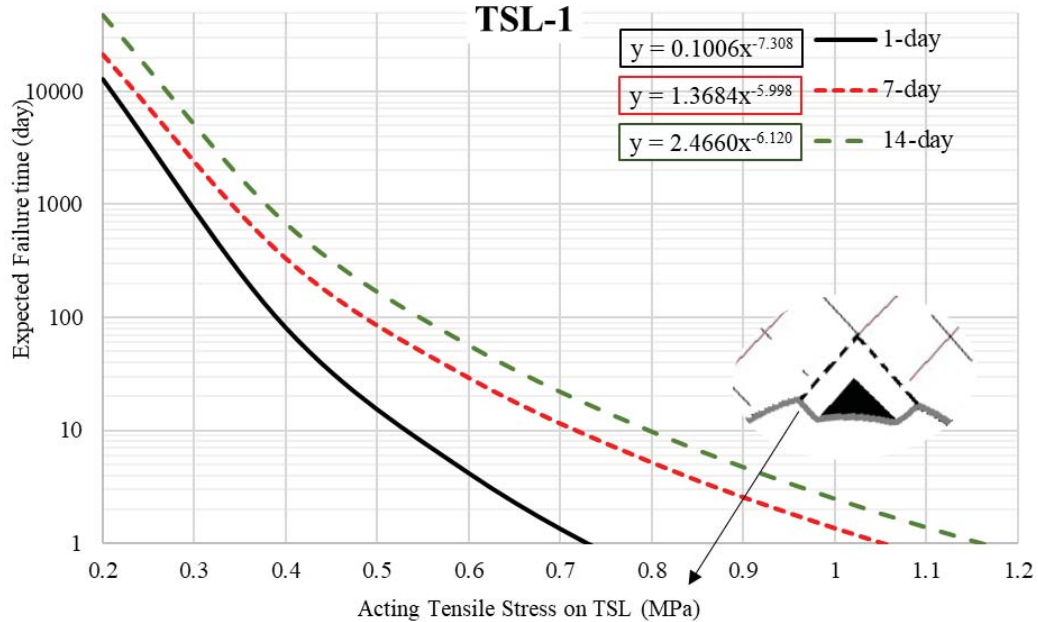
Figure 4.8 Tensile stress acting on TSL versus failure time relationships for TSL-1

According to Figure 4.8, the behaviour of the TSL-1 for the curing period of 7 and 14 days, is very similar. Although the 500-day experiment results for TSL-1 are not presented in this section, the obtained results are very similar to the results of 14-day values. Therefore, when a creep rupture envelope for the older curing period is required for TSL-1, design engineers can use 14-day curves basically. However, younger age (< 1 day-cured) TSLs cannot be extrapolated from the same curves. Therefore, early age (< 24 h) creep behaviour of TSLs should also be investigated considering the typical re-entry times (< 6 h) in a typical mining cycle.

The same study was carried out for the TSL-2 product (Figure 4.9). Since TSL-2 experiments with a curing time of 1-day cannot be performed, the results of 2-days are given in the same way on the graph. Although the tensile stress acting on TSL-2 reaches relatively higher values such as 1 MPa, it is predicted that the product can resist this tensile stress for approximately 100 days with the curing period of 14-day.
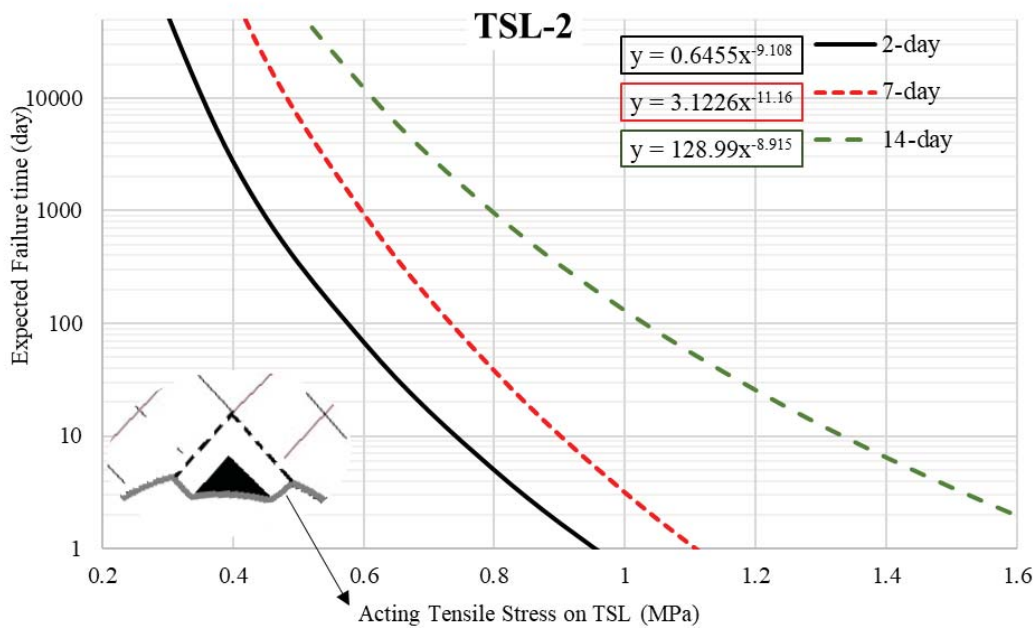
Figure 4.9 Tensile stress acting on TSL versus failure time relationships for TSL-2

It has been concluded that the TSL-2 product is more efficient than TSL-1, according to presented failure envelopes and considering the same acting stress values.

In the final stage of the evaluation of laboratory experiments, a different study was carried out in order to understand the dimensions of the block that a TSL under tension can hold. A regular tetrahedral block and cubic block scenarios were investigated to predict how long a typical wedge block may be sustained by the TSL. It should be noted that a couple of assumptions were made to construct the curves given in Figure 4.10 and Figure 4.11. These assumptions are given as follows:

- The weight of the block is directly transferred into tensioning the TSL (pure tension),

- No frictional resistance happens between displacing blocks,

- Tensile rupture will occur near to the perimeter of the block (no debonded zone).

Therefore, the maximum tensile load "T" to which TSLs are exposed is calculated as follows;

$$T \ (N) = Wc \ x \ t_{TSL} \ x \ \sigma_t \qquad (4.3)$$

Wc: Base circumference of the wedge block (4 x side length for cube block, 3 x side length for regular tetrahedral block)

t_{TSL} = Application thickness of the TSL

σ_t = Ultimate tensile strength of the TSL

During the calculations, the application thickness of TSLs was taken as 4 mm as in the experiments and the density of the rock block is assumed to be 2600 kg/m³. The constructed curves for 3 different curing time and different scenarios for TSL-1 are presented in Figure 4.10.

It is estimated that TSL-1 can carry a regular tetrahedron block with an edge length of 1 meter. On the other hand, it is clearly seen that TSL-1 product does not have the ability to carry a 1m³ block. The volume of the largest cube block was considered to

be that TSL-1 product can carry up to 5 years with a curing period of 14-day or more will be 0.125 m^3.

A 1-day cured cement-based TSL, supporting a regular tetrahedral block with a 1.2m side length can carry the load for 100 days. It is impossible to hold the 1.2m side length cube block under tension at all, and only 0.5m side length cube block can be carried for the same time (100 days). Therefore, one can simply calculate the geometry of the block that can be carried by a cement-based TSL from Figure 4.10. However, if the thickness of the TSL is increased, the curves will shift to the right (increasing the load-bearing capacity of the TSL); decreasing the TSL thickness will do the opposite.

A similar TSL-1 chart was also plotted for the TSL-2 product (Figure 4.11). It is clearly seen in the presented curves that TSL-2 can carry larger sized blocks for a longer time, compared to TSL-1.
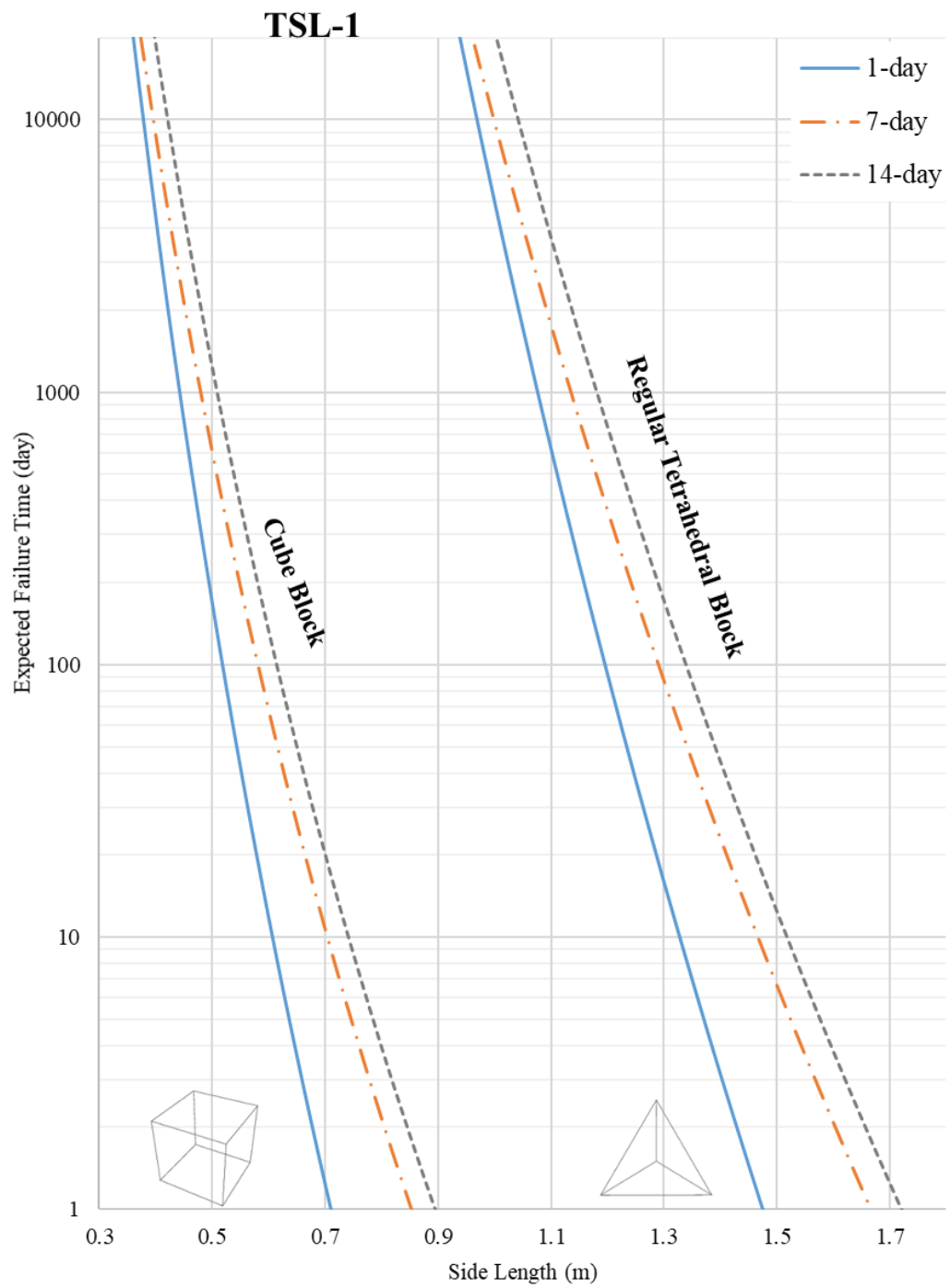
Figure 4.10 Holding time estimation of various wedge block dimensions for TSL-1 (Guner and Ozturk, 2018)
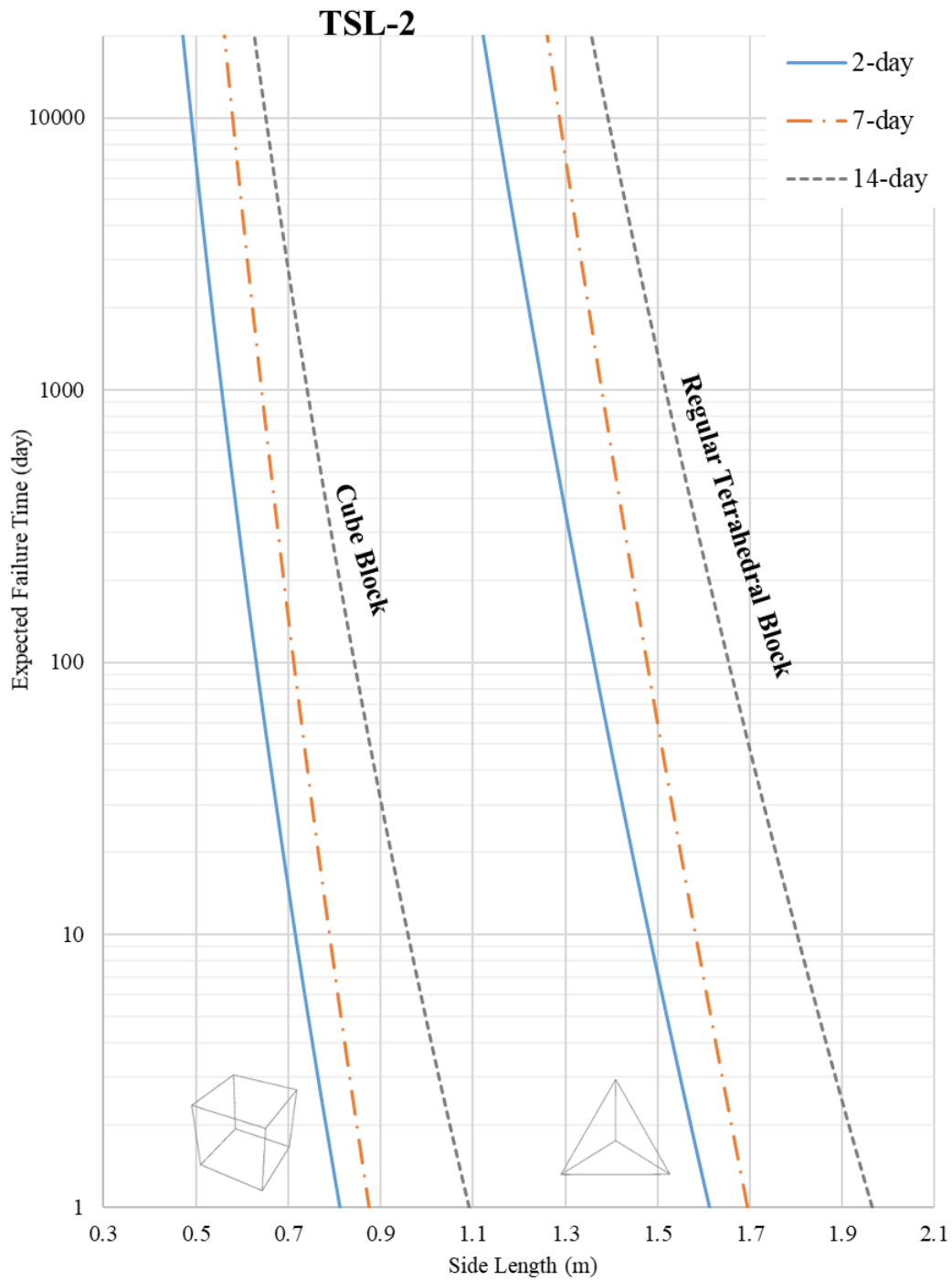
Figure 4.11 Holding time estimation of various wedge block dimensions for TSL-2

As shown in Figure 4.11, the curves drawn for 3 different curing times reveal that TSL-2 with 14-day curing time can carry regular tetrahedron blocks with a side length of 1.5 meters for a period up to 3 years. On the other hand, it is clearly seen that the

TSL-2 product does not have the ability to carry $1m^3$ blocks. The volume of the largest cube block was considered to be a block that TSL-2 product can carry up to 5 years with a curing period of 14-day or more will be 0.35 m^3.

The approach used in this study is demonstrative. It should be remembered that a more complicated liner design requires the parameters such as rock mass strength, geometry of interacting rock blocks, and frictional forces acting between displacing blocks.

As a result of laboratory studies, it was revealed that 2 different TSL products, which are widely used worldwide, are sensitive to the creep behavior. Both TSL products lost their effective support mechanisms when exposed to the loads that is about half of their ultimate tensile strengths. In this basis, the current study allows a better understanding of the importance of the TSL creep behavior. To achieve a comprehensive and effective support design with TSL, engineers should definitely consider that TSLs have time-dependent material behaviour.

It should be noted that the proposed rupture time equation here only takes tensile failure modes into consideration. Other failure modes need to be studied as well. Different application environments of TSLs require the investigation of creep behaviours under varying temperature and humidity conditions. Other TSLs should be investigated by specific creep tests for different curing times. This will enable researchers to simulate the application of TSL in a more representative way.

TSL field applications involve the use of sophisticated pumps operating at high pressures and spraying nozzles applied from a distance of 1–3m from the surface. TSLs sprayed on the rock surfaces on-site, in reality, might exhibit different deformation characteristics. The effect of molding versus spraying of TSLs in preparation might be more of a concern if the bonding characteristics of the liner are to be tested because of the positive effect of spraying application on bonding relative to molding. Hence, it is hypothesized that molding and spraying processes have a similar impact on tensile and creep testing (Guner and Ozturk, 2018).

In cases where some personnel are expected to work beneath freshly sprayed backs, it is important to remember that the TSL cures quickly to reach an adequate tensile strength. In this sense, curing rate of TSL in mining environment may enforce maintaining a fast operation in headings or stopes. Intuitively, one might think that knowing the ultimate tensile strength at the given age is good to define TSL performance. However, the time-dependent behaviour of TSLs also requires prediction of yield strength and deformation characteristics for the given loading conditions.

CHAPTER 5

CREEP MODELING

This section concentrates on constitutive modeling of nonlinear viscoelastic and viscoplastic material behaviors. The major difference between viscoelastic and viscoplastic behaviour can be observed during the unloading stage. Viscoelastic materials show a significant amount of delayed recovery in the unloading phase. On the other hand, a permanent residual plastic strain is observed for viscoplastic materials (Krishnaswamy *et al*. 1992). In an underground excavation condition, when wedge blocks slide out of their sockets, TSL becomes active and there is no way to return back to a passive mode (Tannant, 2001). In other words, "unloading" condition is not possible in a mining application practice of TSL. Therefore, step loading and stress unloading are not considered in the study scope so that and the stated difference in the unloading stage becomes insignificant for these two material behaviors. Moreover, viscoplastic models are widely used to investigate high-temperature material behaviour of metals since they do not asymptotically converge to a constant value as exponential functions during creep response.

5.1. Modeling Approaches

Time-dependent modeling in polymeric materials can be classified into either micromechanical or macromechanical approaches. Micromechanical approaches deal with crystalline and amorphous phases of polymers separately in the molecular level of the material. In practical structural applications, macromechanical models are preferred as the experimental behaviour under the simple loads are considered to define material properties that are also used in mathematical equations describing the time-dependent behaviour (Liu, 2007).

The modeling study aims the satisfy three major conditions given below:

i)   Constitutive model should be able to predict the liner response only for a wide range of uniaxial tensile loading conditions.

ii)   Modeling parameters should be easily derived from the values measured in experiments.

iii)   The generated model should be simple enough to be used in the future numerical studies.

Theoretical definition of the total creep strain function is given as:

$$\varepsilon_t(t) = \varepsilon_e + \varepsilon_v(t) \qquad (5.1)$$

In viscoelastic and viscoplastic modeling, constitutive relations are generally formulated using integral differential form (Lockett, 1972). The strain of the material at time t can be expressed with a hereditary integral as;

$$\varepsilon(t) = \int_0^t \psi(t - \tau) \frac{d\sigma(\tau)}{d\tau} \, d\tau \qquad (5.2)$$

where $\psi(t - \tau)$ is creep compliance function of the material and $d\sigma(\tau)/d\tau$ is the stress rate. Eq. (5.2) is simplified as given in Eq. (5.3) since the stress levels in the tests are kept constant in the experiments where creep tests are performed under uniaxial conditions.

$$\varepsilon(t) = \sigma \, \psi(t) \qquad (5.3)$$

When the material is exposed to a constant stress at t=0, an elastic strain (time-independent) occurs first, and then it is followed by the plastic or viscous strain component. Mechanically, this elastic part can be represented by a single spring element. It should also be pointed out that engineering strain is used in the modeling part.

5.1.1. Viscoplastic Modeling

Power-law functions are widely used to predict the creep curve using data obtained from creep tests at constant stress (Lockett, 1972). It offers a practical approach and requires less number of model parameters. Since creep strain keeps growing at a decreasing rate in power function models, this behaviour is considered as a viscoplastic. As observed in the creep tests, strain converges to an asymptotic value for a long testing duration. This behaviour occurs due to the micromoleculer nature of the material. Since this strain recovery and following asymptotic behaviours cannot be modeled by conventional power-law functions, the piecewise power-law functions were considered to be more appropriate in viscoplastic modeling.

The creep compliance equation $\psi(t)$ for typical power-law function, consists of both elastic (ψ_e) and viscous ($\psi_v(t)$) part and can be defined as;

$$\psi(t) = \frac{1}{E_0} + C_0 t^{C_1} \tag{5.4}$$

Where E_0 is the instantaneous elastic modulus, and C_0 and C_1 are material constants. These parameters are functions of stress.. The constitutive equation of the viscoplastic material can be obtained by substituting Eq. (5.4) into Eq. (5.2) as given in Eq. (5.5).

$$\varepsilon(t) = \int_0^t \left[\frac{1}{E_0} + C_0 \ (t - \tau)^{C_1} \right] \dot{\sigma}(\tau) \, d\tau \tag{5.5}$$

In the condition of creep tests, where stress is constant (σ_n) Eq. (5.5) becomes;

$$\varepsilon(t) = \varepsilon_e + \varepsilon_v(t) = \frac{\sigma_n}{E_0} + \sigma_n \ C_0 \ t^{C_1} \qquad t \leq t_{cr} \tag{5.6}$$

$$\varepsilon(t) = \varepsilon_e + \varepsilon_v(t) = \frac{\sigma_n}{E_1} + \sigma_n \ C_2 \ t^{C_3} \qquad t > t_{cr}$$

Where t_{cr} is the critical time to start strain recovery behavior. This value was taken constant in all studies performed for TSL-2. If the TSL ruptures before the critical time, the models includes only 3 stress-dependent parameters in that condition. 5 out of 12 models were constructed by piecewise power-law functions for TSL-2 and single

power-law function is used for TSL-1. Eq. (5.6) is implemented in a computer routine to generate model parameters. A good agreement was observed in short test durations since increasing testing times cause the strain values to reach asymptotic values and single power-law function, in that condition, is not capable to mimic the exact material behaviour. In brief, piecewise power functions are more capable compared to single power-law functions in representing strain recovery and asymptotic behaviours.

The model results obtained for both TSL products are given in the following section. The experimental data were obtained by averaging the results of two experimental repetition although there is not any observed drastic variation between the repetitions during the modeling phase.

5.1.2. Viscoelastic modeling

A combination of the spring-dashpot elements is generally used to achieve a realistic material response model (Lockett, 1972). In the viscoelastic modeling part, the nonlinear multi (generalized) Kelvin–Voigt modeling approach, which can also be obtained from rheological models, was followed. As testing duration varies from a few minutes to 2 months, the number of Kelvin elements was not kept constant. Each Kelvin element in the series represents the time intervals so that this model approach can be used properly for long testing periods. Although this approach is mainly based on linear viscoelastic modeling, the combination of one spring and multiple elements enables to predict the nonlinear time-dependent response of the material ranging from short to long testing durations.

For nonlinear viscoelastic modeling, the creep compliance equation $\psi(t)$ consists of both elastic (ψ_e) and viscous $(\psi_v(t))$ part, and can be given as;

$$\psi(t) = \frac{1}{E_0} + \sum_{i=1}^{n} \frac{1}{E_i} \left\{ 1 - e^{\left[-\frac{t}{\left(\frac{\eta_i}{E_i} \right)} \right]} \right\} \tag{5.7}$$

Where E_0 is the instantaneous elastic modulus, η_i and E_i are the dashpot viscosity and the spring stiffness of ith Kelvin element. η_i/E_i is the retardation time (τ_i). The constitutive equation of the viscoelastic material can be obtained by substituting Eq. (5.7) into Eq. (5.2) as shown in Eq. (5.8):

$$\varepsilon(t) = \int_0^t \frac{1}{E_0} + \sum_{i=1}^n \frac{1}{E_i} \left\{ 1 - e^{[-(t-\tau)/\tau_i]} \right\} \dot{\sigma}(\tau) \, d\tau \tag{5.8}$$

For the creep tests where the applied stress kept constant (σ_n) Eq. (5.8) becomes;

$$\varepsilon(t) = \varepsilon_e + \varepsilon_v(t) = \frac{\sigma_n}{E_0} + \sum_{i=1}^n \frac{\sigma_n}{E_i} \left[1 - e^{\left(-\frac{t}{\tau_i}\right)} \right] \tag{5.9}$$

The retardation times (τ_i) are taken as constant for different models. τ_1 was taken 0.2 min first and the following retardation times were taken 10 times of the previous value. A similar simplification was also performed in previous studies (Zhang and Moore, 1997; Liu, 2007). The number of Kelvin elements was found by an iteration routine where the optimal element number reduces the standard error of the model fits to 10^{-3}.

Eq. (5.9) was used to fit corresponding experimental creep curves using a computer routine providing a Levenberg-Marquardt algorithm. 4 nonlinear viscoelastic models were generated for each curing time. The model results obtained for the both TSL products are given in the next section. The raw experiment data used in the viscoplastic model stage were also used in viscoelastic modeling.

5.2. TSL-1 Modeling Results

Power law equations are widely used in the literature since they operate with a limited number of constants that determine the material behaviour during the viscoplastic modeling phase. In this basis, decrease in the constants may help the equation to be used more practically.

The change in the applied stress values generally causes significant variations in material behaviour for creep tests. Therefore, power-law equations sometimes become

insufficient for the estimation of the exact material behavior. Since strain recovery behaviour was not observed in TSL-1 experiments, the piecewise power-law functions were not used. Therefore, it was sufficient to have only 3 material constant values for each different curing time and stress level. In order to obtain viscoplastic model parameters, Eq. (21) is defined in a statistical software. Comparison of the predicted and the experimental creep curves for the viscoplastic model for the different curing times are presented in Figure 5.1. Generated material constants for single and piecewise power-law functions are presented in Table 5.1.

In samples where the stress level is 80% of its tensile strength, the strain growth did not reach asymptotic values. At this stress level, the results of the viscoplastic model are almost perfectly compatible with the results of the experiment. Acceptable results were obtained in the modeling studies carried out at the other constant load levels. It should be noted that instantaneous elastic modulus (E_0) values were kept constant for both viscoelastic and viscoplastic modeling stages. Therefore, E_0 values should be considered as the material property obtained from the experimental results rather than the modeling parameter.
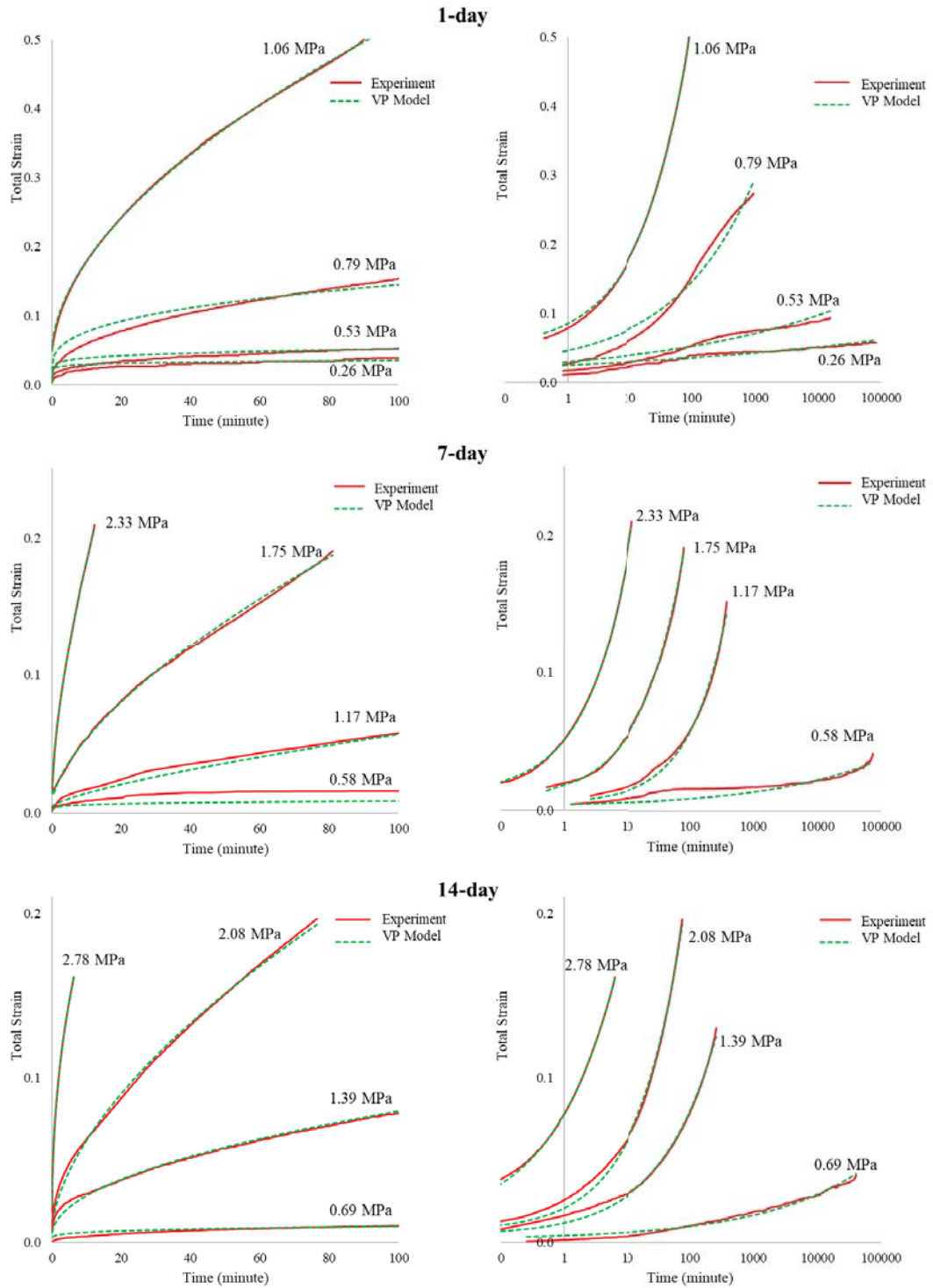
Figure 5.1 Comparison of experimental results and viscoplastic model for TSL-1

As seen in the results of the Viscoplastic model presented in Figure 5.1, the existing modeling technique was partially insufficient for some experiments performed with

the small stress levels. For this reason, it was also decided to perform a viscoelastic modeling technique in this study.

Table 5.1 Viscoplastic model coefficients at different stress levels and curing time for TSL-1

Curing Time (day)	σ_n (MPa)	E_0 (MPa)	C_0 (MPa^{-1})	C_1
1	0.26	65	0.0806	0.088
	0.53	52	0.0378	0.159
	0.79	38	0.0325	0.343
	1.06	21	0.0338	0.561
7	0.58	281	0.0038	0.242
	1.17	252	0.0015	0.733
	1.75	239	0.0061	0.644
	2.33	198	0.0169	0.639
14	0.69	412	0.0034	0.267
	1.39	347	0.0056	0.493
	2.08	303	0.0067	0.597
	2.78	268	0.0245	0.434

Since the viscoelastic model performed for TSL-1 cover a higher number of descriptive parameters compared to the viscoplastic model, it allows to achieve more realistic results. To obtain viscoplastic model parameters, Eq. (24) is defined in a statistical software (CurveExpert Professional). A comparison of the predicted and the experimental creep curves for the viscoelastic model for different curing times are presented in Figure 5.2. The material constants used in the construction of the viscoelastic models are presented in

Table 5.2. Compared to viscoplastic models, more realistic results were obtained in viscoelastic modeling part for experimental results under small stresses. In other words, the Multi Kelvin-Voigt modeling approach for TSL-1 was detected to be more successful in modeling the entire strain-time curve than viscoplastic approaches.

Figure 5.2 Comparison of experimental results and viscoelastic model for TSL-1

Table 5.2 Viscoelastic model coefficients at different stress levels and curing time for TSL-1

Curing Time (day)	σ (MPa)	E_0 (MPa)	E_1 (MPa)	E_2 (MPa)	E_3 (MPa)	E_4 (MPa)	E_5 (MPa)	E_6 (MPa)	E_7 (MPa)
1	0.26	65	6.57E+1	4.07E+1	1.51E+1	2.09E+1	3.59E+3	2.04E+1	-
	0.53	52	9.18E+1	2.21E+2	2.60E+1	1.58E+1	1.59E+2	1.63E+1	-
	0.79	38	1.95E+7	7.21E+1	1.75E+1	4.19E+0	-	-	-
	1.06	21	1.45E+8	2.10E+1	1.05E+1	1.30E+0	-	-	-
7	0.58	281	2.98E+2	7.27E+8	4.94E+1	1.02E+3	3.30E+2	1.68E+9	9.10E+0
	1.17	252	2.14E+8	2.64E+2	8.92E+1	3.50E+8	1.64E+0	-	-
	1.75	239	7.41E+2	1.23E+2	6.77E+1	4.25E+0	-	-	-
	2.33	198	1.60E+2	1.15E+2	6.68E+0	-	-	-	-
14	0.69	412	1.13E+10	9.62E+9	1.64E+2	7.73E+1	1.01E+2	3.59E+1	-
	1.39	347	1.44E+2	2.95E+2	8.93E+1	2.11E+1	3.70E+0	-	-
	2.08	303	2.35E+2	1.12E+2	1.39E+2	4.47E+0	-	-	-
	2.78	268	7.15E+1	6.27E+1	1.07E+1	-	-	-	-

The number of model constants differs from model to model as presented in

Table 5.2. The main reason here is that the experiment duration and the retardation time vary from a few minutes to two months. For example, the experiments performed under 0.26 MPa constant stress level for 1 day curing time were completed at around 20,000 minutes, and they were modeled using 6 series Kelvin elements. The available E_7 element in the table does not offer any mechanical meaning. In the next step, to avoid any confusion in the part that focus on coding of the model in the computer routines, it has been deemed appropriate to encode all models' Kelvin element numbers to be the highest number of Kelvin elements.

5.3. TSL-2 Modeling Results

It is observed from the laboratory studies of TSL-2 that if the tested specimen does not fail within 2000 minutes, a considerably small strain recovery is measured and then the strain converges to an asymptotic value. This behaviour is caused by the micromoleculer nature of the material. Since conventional power-law functions could

not model this strain recovery and the following asymptotic behaviours, the piecewise power-law functions were considered to be more appropriate in viscoplastic modeling. If the TSL ruptures before the critical time, the models includes only 3 stress-dependent parameters in that condition. 5 out of 12 models were constructed by piecewise power-law functions. Eq. (21) is applied to a computer routine to generate the model parameters. A good agreement was observed in the short test durations since the strain values converges to asymptotic values with the increasing test time and single power-law function becomes non-capable to mimic the exact material behaviour. In this basis, piecewise power functions are more capable than single power-law functions to capture strain recovery and asymptotic behaviours. Comparison of the predicted and the experimental creep curves in the viscoplastic model for different curing times are presented in Figure 5.3. The generated material constants for single and piecewise power-law functions are presented in Table 5.3.
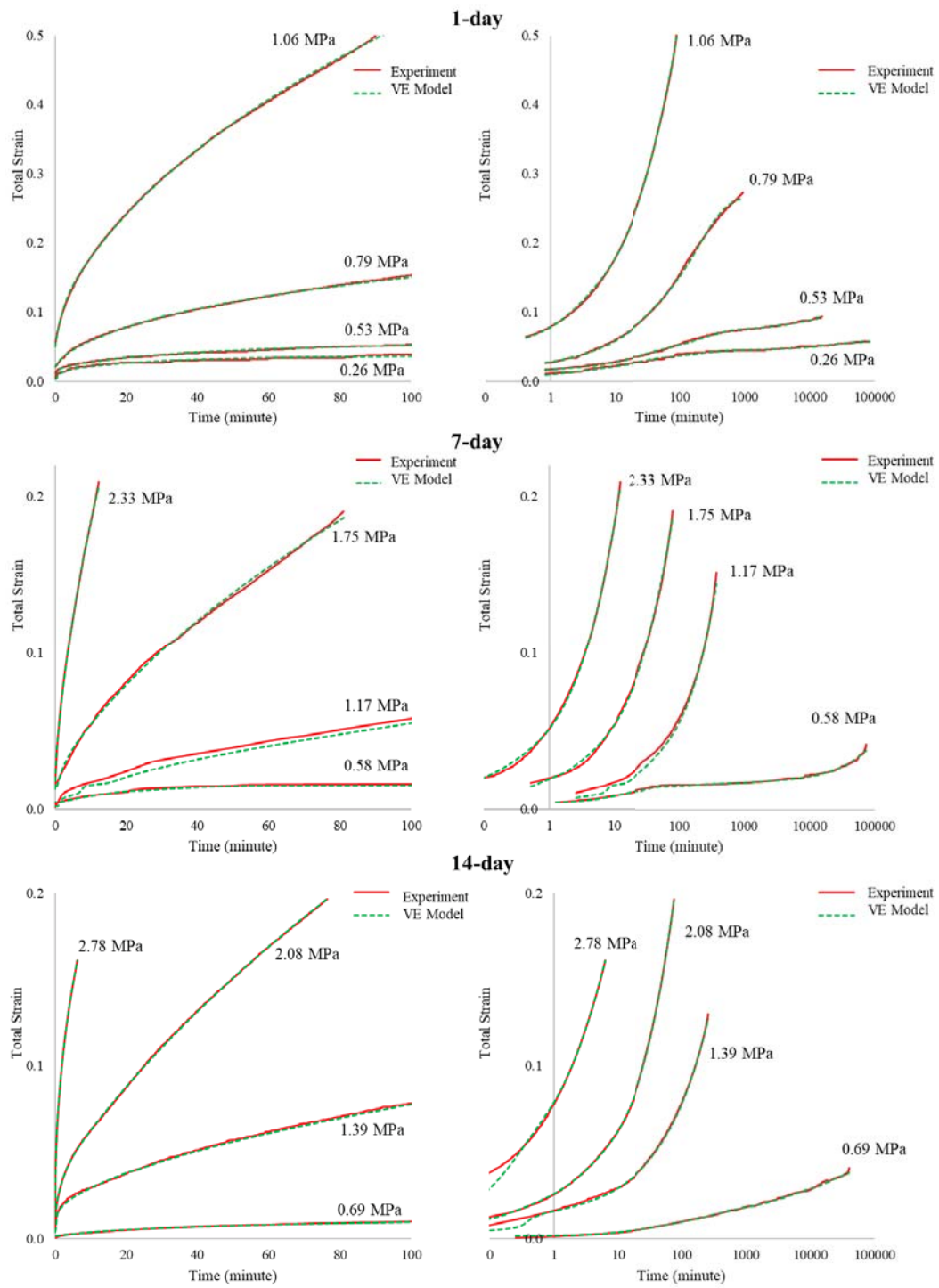
Figure 5.3 Comparison of experimental results and viscoplastic model for TSL-2

104

Table 5.3 Viscoplastic model coefficients at different stress levels and curing time for TSL-2

Curing Time (day)	σ_n (MPa)	E_0 (MPa)	C_0 (MPa^{-1})	C_1	E_1 (MPa)	C_2 (MPa^{-1})	C_3
2	0.37	205	0.021	0.26	10.70	30.20	-0.97
	0.74	140	0.049	0.20	-	-	-
	1.10	116	0.025	0.49	-	-	-
	1.46	28	0.048	0.63	-	-	-
7	0.42	482	0.011	0.21	25.90	88858	-2.22
	0.84	345	0.011	0.26	74.30	0.10	-0.10
	1.26	247	0.005	0.48	-	-	-
	1.68	42	0.009	0.77	-	-	-
14	0.53	6985	0.010	0.19	37.90	13.37	-0.99
	1.07	5620	0.004	0.28	31.30	0.00	-1.03
	1.60	3870	0.001	0.42	-	-	-
	2.14	177	0.004	0.46	-	-	-

In viscoelastic modeling part of TSL-2, the nonlinear multi Kelvin–Voigt modeling approach, which can also be obtained from rheological models, was followed. As testing duration varies from few minutes to 2 months, the number of Kelvin elements was not kept constant. Each Kelvin element in the series represents the time intervals so that this model offers a proper approach for the long testing periods. Eq. (24) was used to fit the corresponding experimental creep curves using a computer routine in which a Levenberg-Marquardt algorithm is embedded. 4 nonlinear viscoelastic models were generated for each curing time. Comparison of the predicted and the experimental creep curves for the viscoelastic models for different curing times are presented in Figure 5.4. The generated material constants for the Kelvin–Voigt elements are presented in Table 5.4. Although the viscoelastic model can be more capable of predicting the whole curve, it cannot simulate the specific parts where the strain decreases.
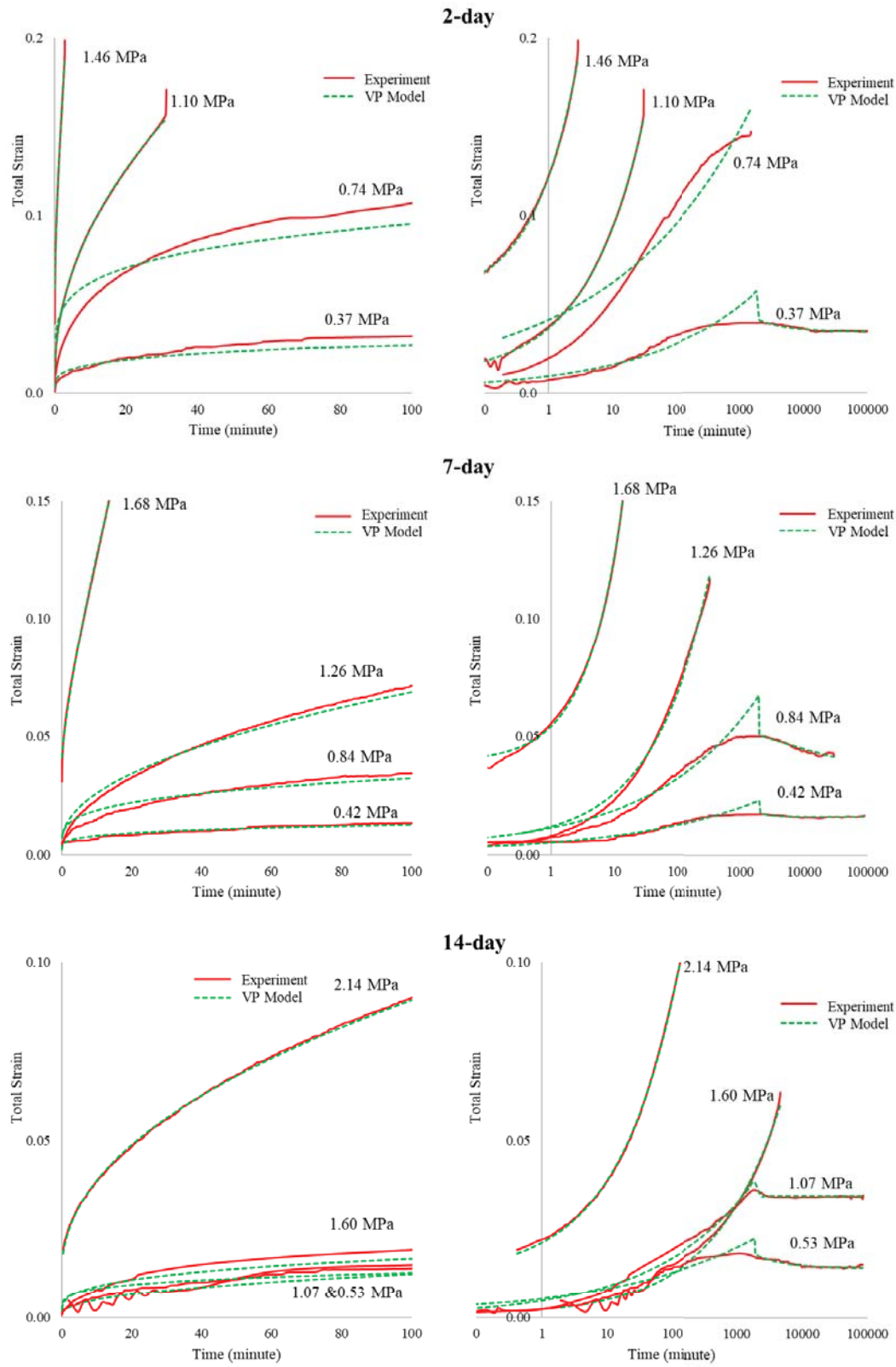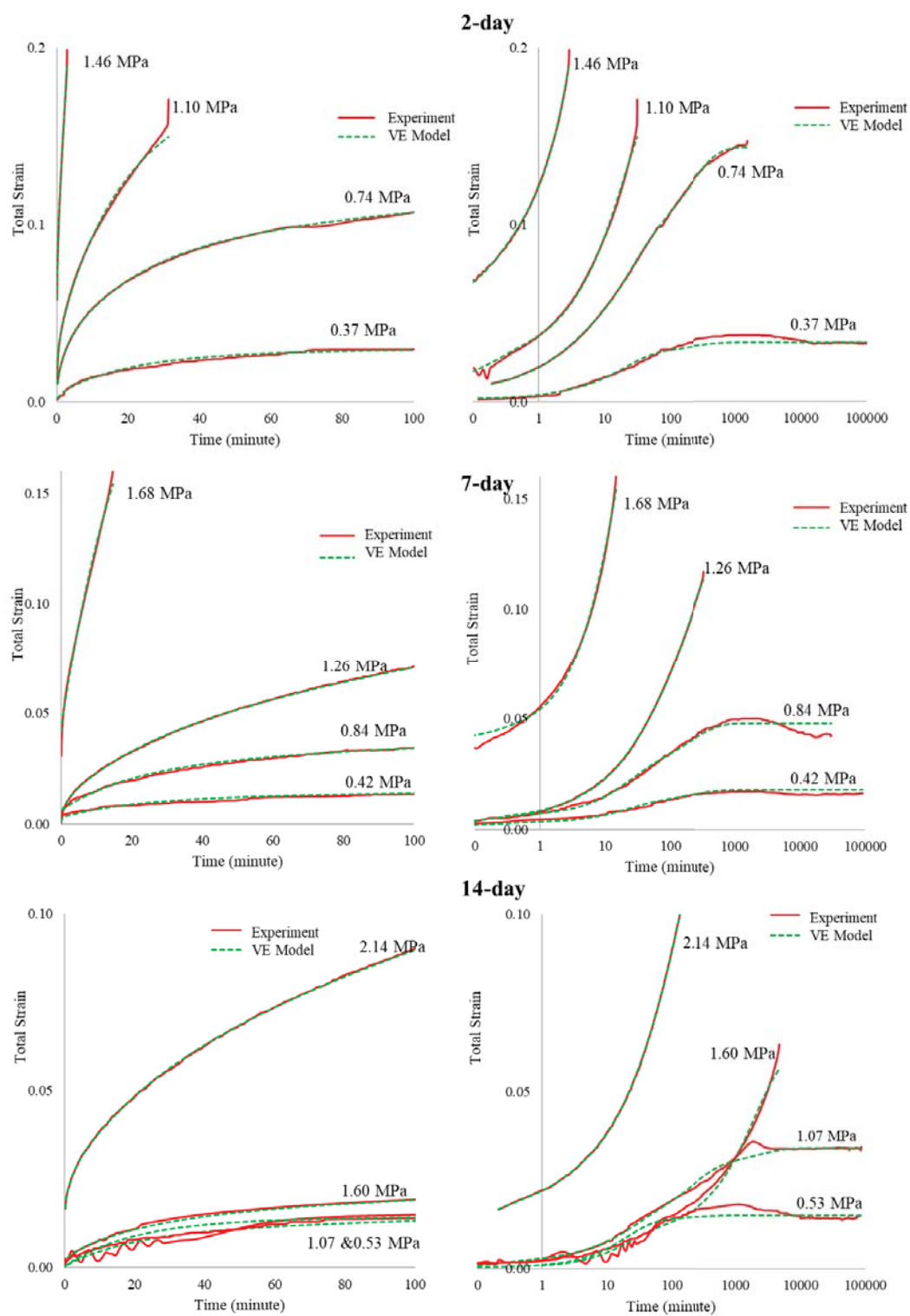
Figure 5.4 Comparison of experimental results and viscoelastic model for TSL-2

106

Table 5.4 Viscoelastic model coefficients at different stress levels and curing time for TSL-2

Curing Time (day)	σ_n (MPa)	E_0 (MPa)	E_1 (MPa)	E_2 (MPa)	E_3 (MPa)	E_4 (MPa)	E_5 (MPa)
2	0.37	205	3.26E+07	1.41E+02	1.65E+01	5.68E+01	-
	0.74	140	1.77E+02	4.14E+01	1.31E+01	1.23E+01	-
	1.10	116	6.59E+01	9.47E+01	7.78E+00	-	-
	1.46	28	5.10E+01	1.25E+02	1.94E+00	-	-
7	0.42	482	1.94E+02	2.45E+08	5.11E+01	6.15E+01	-
	0.84	345	2.17E+02	2.17E+08	4.38E+01	3.70E+01	-
	1.26	247	2.99E+09	2.72E+02	5.90E+01	1.24E+01	-
	1.68	42	4.20E+02	1.46E+09	7.92E+00	-	-
14	0.53	6985	1.51E+03	2.36E+09	4.01E+01	3.77E+02	8.00E+09
	1.07	5620	6.28E+02	8.86E+02	1.11E+02	6.81E+01	1.93E+02
	1.60	3870	2.10E+09	2.14E+09	1.65E+02	7.97E+02	3.27E+01
	2.14	177	3.70E+02	3.04E+02	1.07E+02	1.88E+01	-

It was concluded from the results of the model, which is performed for 2 different TSL products, that the Generalized Multi Kelvin–Voigt model or Viscoelastic model for elastic response and viscous flow is found to be more accurate than the piecewise power-law function. Although the viscoelastic models are not capable to mimic the strain recovery parts, the remaining behaviour can be predicted quite well. The major drawback of the piecewise viscoplastic model is that power-law functions are not capable to predict the asymptotic behaviour. Before the strain recovery part takes place, the model tends to overpredict the strain values. This situation leads to a sharp drop in strain which is not realistic in practice. For this reason, it was decided to use the values obtained in the Viscoelastic model approach when coding models in the computer routine and in the numerical modeling stages. Implementation of the model in the computer routine will be discussed in the next chapter.

It should be noted that damage-based creep models are generally associated with tertiary creep. The creep damage starts with an increase in creep strain rate at the end of secondary stage. Since a significant tertiary stage was not observed in this study,

damage-based creep models were not adopted. However, if the TSL is to be used in elevated temperature environment, tertiary creep stage might become significant so that damage-based creep model may also be considered.

CHAPTER 5

IMPLEMENTATION OF THE GENERATED CONSTITUTIVE RELATIONSHIPS TO THE SOFTWARE AND VERIFICATIONS

The behaviour of two different TSL products obtained from the structural modeling studies must be defined in software in which numerical modeling will be performed. Within the scope of this study, it was decided to use the software named ABAQUS, a commercial software package for finite element analysis. ABAQUS is frequently used in the fields of mechanical, materials, and civil engineering. Although there are different creep models defined in the interface of the software used, the existing models were insufficient for the creep behaviour modeling of TSLs on a macro scale. Since the inadequacy of the software in creep modeling is known at the beginning of the study, it was decided to include the implementation of the generated constitutive relationships in the software and the related verifications.

ABAQUS software allows to find out solutions for static and dynamic problems in different specific command-based sections. In this basis, it consists of three core products: ABAQUS /CAE, ABAQUS /Standard, and ABAQUS /Explicit. These cores contain logical sub-definition commands.

The software includes the modeling, analysis, solution management and result evaluation stages in an interface called ABAQUS / CAE. In this interface, geometry can be imported and simplified, or geometry can be created directly. In addition, multiple models can be created in a single CAE file. In other words, this core provides a preprocessing and postprocessing environment for the analysis.

6.1. Generation of User Subroutines

In ABAQUS software, 5 different creep laws are available. These laws are the power, the hyperbolic-sine, the Anand, the Darveaux, and the double power. Although, these

default creep models provide a significant convenience to the user, material creep behaviours are typically of very complex form to fit experimental data in some practical cases. Therefore, the creep laws are frequently userdefined via the use of user subroutine CREEP and included in a generic time-dependent material formulation. Multi Kelvin or Voigt model is not standard model in ABAQUS and hence needed to be incorporated via the CREEP user subroutine

User subroutines should be written as C, C ++ or Fortran code and is included in a model where the analysis is executed. In this basis, the "Intel Parallel Studio" software and the ABAQUS must be connected in order to define generated subroutines. Fortran language was preferred in the subroutine process.

Since the viscoelastic models give more representative results compared to the viscoplastic models, it was decided to work with the viscoelastic model (multi Kelvin-Voigt) approaches in the user subroutine studies.

In laboratory and structural modeling studies, strain-time relationships were determined for 3 different curing times and 4 different constant stress levels for each TSL product. In the user subroutine stage, it was decided to prepare different routines for each curing time, as TSL products have very different creep responses in different curing times.

Another important purpose of generating user subroutines is to simulate the behaviour of the TSLs in cases of intermediate stress levels where the experiments are not carried out. For this reason, the relationships between the Kelvin constants obtained from the structural models and the different stress values for each curing time were found out. Afterward, these relationships were defined in the routine; and the subroutine was provided to give fair results for variable stress levels. In the subroutine generation process, multi Kelvin-Voigt models given in Eq. (5.9) were used.

6.1.1. Implementation of Instantaneous Elastic Modulus subroutine

Elastic material behaviour must be defined first in order to create a creep model in the ABAQUS software. In the laboratory tests, as the constant load is applied, the elastic

strain (ε_e) occurs instantaneously in the specimen at $t=0$. This elastic strain value depends not only on the curing time of the TSL, but also on the applied stress level in the experiments under the same curing time. The parameter controlling the elastic strain behaviour is called the instantaneous elastic modulus (E_0), as mentioned in the previous sections.

The instantaneous elastic modulus values presented in the previous chapter vary in proportion to the applied stress level. For this reason, before the creep subroutine is generated, the instantaneous elastic modulus values, which are the elastic material parameters of TSL, must be defined with a different subroutine. In this context, the user subroutine has been prepared to specify the predefined field variables called "UFIELD" in the ABAQUS. Details of user subroutine UFIELD is presented in ABAQUS documentation. UFIELD user subroutine interface is as follows:

```
SUBROUTINE UFIELD (FIELD,KFIELD,NSECPT,KSTEP,KINC,TIME,NODE,
    1 COORDS,TEMP,DTEMP,NFIELD)
     INCLUDE 'ABA_PARAM.INC'
     DIMENSION FIELD(NSECPT,NFIELD), TIME(2), COORDS(3),
    1 TEMP(NSECPT), DTEMP(NSECPT)
     user coding to define FIELD
     RETURN
     END
```

The targeted elastic strain behaviour is obtained by inputting the function of the instantaneous elastic modulus value depending on the applied stress value (σ_n) in the field part that needs to be defined by the user. The changes in the instantaneous elastic modulus values obtained in the previous section depending on the applied stresses are presented in Figure 6.1 and Figure 6.2. The functions describing these changes are coded into the subroutine and this stage is completed.
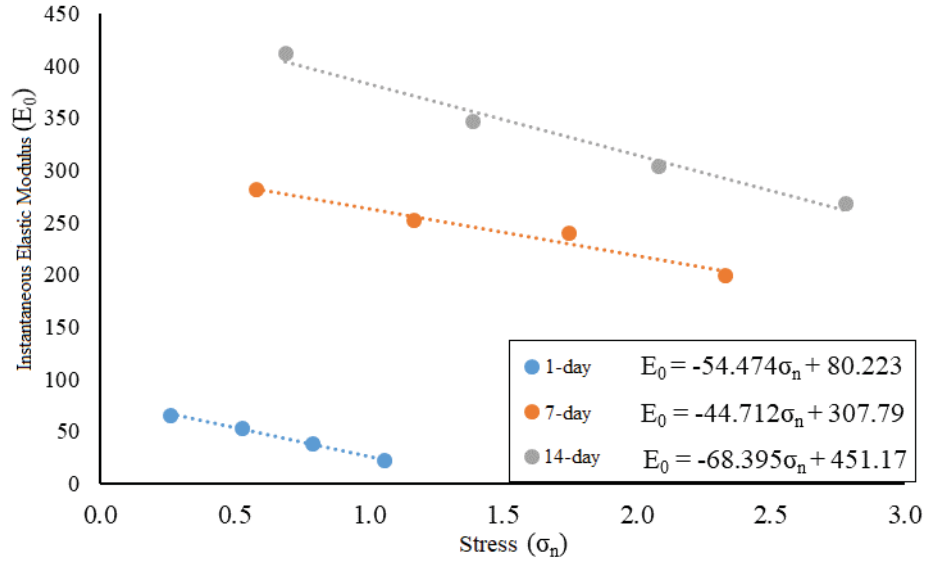
Figure 6.1 Instantaneous elastic modulus and applied stress relationships of TSL-1
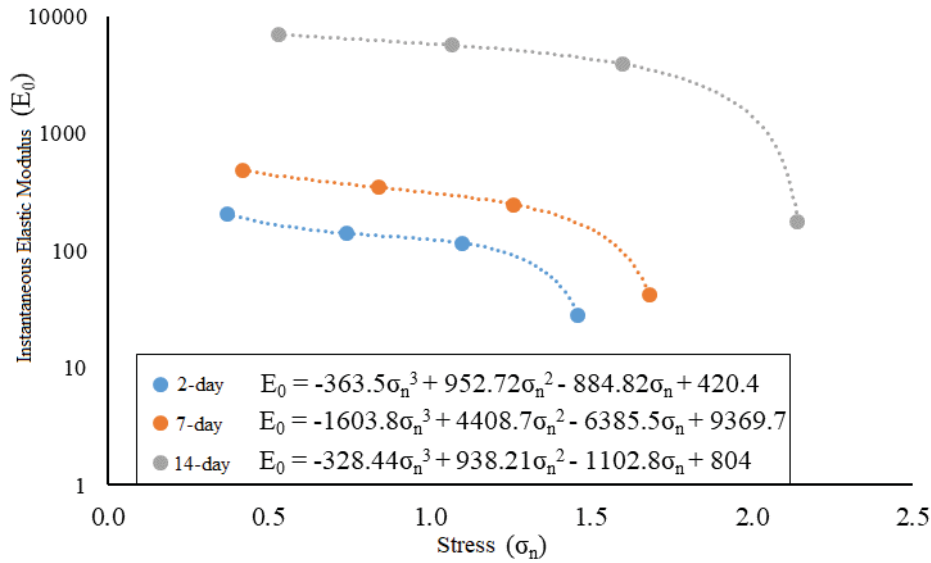
Figure 6.2 Instantaneous elastic modulus and applied stress relationships of TSL-2

Since ABAQUS performs finite element analysis with time steps, a time step must be specified to define the simulation time of the instantaneous elastic strain of the material. Since the instantaneous strain change occurs when the samples are sustained under constant load, creep is not active in this step. It is recommended that small time-step compared to the creep time be used in elastic part. Therefore, this time step in which the sample takes instantaneous strain was taken as 0.01 minutes.

6.1.2. Implementation of Creep Subroutine

After the elastic strain behaviour of TSLs were introduced to the software, a subroutine part was performed to define the creep behavior. At this stage, 6 models were created in total, different for each curing time and each TSL product. Multi Kelvin-Voigt model parameters obtained in the structural model section were used at this stage. Developed subroutines are presented in Appendix D. The interface of the creep subroutine defined in the ABAQUS software is:

```
SUBROUTINE CREEP(DECRA,DESWA,STATEV,SERD,EC,ESW,P,QTILD,
1 TEMP,DTEMP,PREDEF,DPRED,TIME,DTIME,CMNAME,LEXIMP,LEND,
2 COORDS,NSTATV,NOEL,NPT,LAYER,KSPT,KSTEP,KINC)
INCLUDE 'ABA_PARAM.INC'
CHARACTER*80 CMNAME
DIMENSION DECRA(5),DESWA(5),STATEV(*),PREDEF(*),DPRED(*),
1 TIME(3),EC(2),ESW(2),COORDS(*)
user coding to define DECRA, DESWA
;DECRA(1): Equivalent deviatoric creep strain increment
RETURN
END
```

ABAQUS provides both explicit and implicit time integration scheme of creep behaviour defined in CREEP subroutine. The choice of the time integration scheme depends on the procedure type, the procedure definition, and requested analysis type (linear or nonlinear). Implicit time integration scheme is commonly used and generally more effective when the response duration is long relative to typical relaxation times for the material. Simple high-temperature structural design applications usually do not need implicit integration, but more complicated problems such as geotechnical-geomechanical applications often are integrated more efficiently by the implicit method provided in the program. If implicit integration is used with this subroutine, nonlinear equations must be solved at each time step must be defined in the subroutine.

At the start of a new increment, the subroutine is called once for each integration point to calculate the estimated creep strain based on the state at the start of the increment. Subsequently, it is called twice for each iteration if explicit integration is used: once to calculate the creep strain increment at the start of the increment and once to calculate it at the end of the increment. This is needed to test the validity of the time increment with respect to the user-specified maximum allowable difference in the creep strain increment. The subroutine must use the corresponding values of time, temperature, field variables, and solution-dependent state variables in the calculation of the creep strain increment. For implicit integration ABAQUS uses a local iteration procedure to solve the nonlinear constitutive equations, and the subroutine is called multiple times. The exact number of calls depends on the convergence rate of the local iteration procedure and, hence, will vary from point to point. During these iterations it is possible for the values of the state variables to be far from their final values when the equations are solved. Therefore, the coding in the subroutine must adequately protect against arithmetic failures (such as floating point overflows) even when variables are passed in with physically unreasonable values.

The input/output depends on the kind of material: In this study elastic properties of the material are assumed as isotropic. A typical solution step is as follows: the Von Mises stress goes in and the equivalent deviatoric creep strain increment and its derivative with respect to the Von Mises stress for a given Von Mises stress come out. Typical workflow for creep analysis in ABAQUS is presented in Figure 6.3. Verification of the model was made by comparing the defined subroutines with the experimental results and these verification steps are presented in the next section.
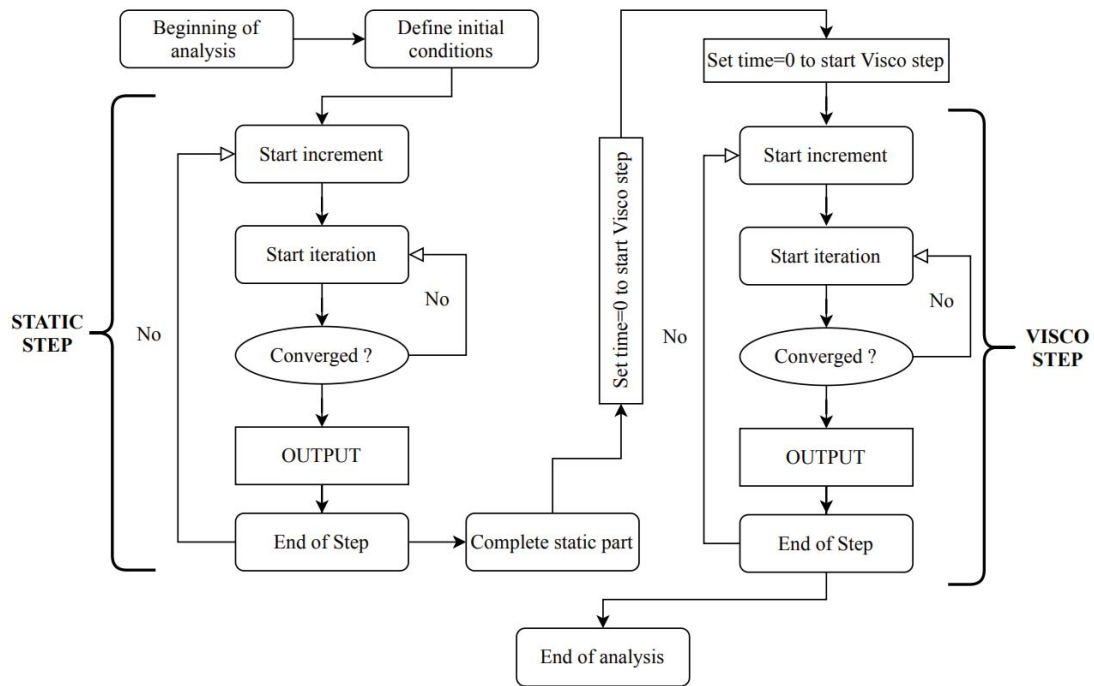
Figure 6.3 Typical workflow for creep analysis in ABAQUS

6.2. Creep Test Simulations and Verification of Models

For creep test simulation, primarily, the sample geometry was created with the same dimensions as the samples used in laboratory experiments. In accordance with the modeling procedure described in the previous section, creep test models were prepared and analyzed with the generated subroutines. The main purpose of the simulation is to develop a real-like creep model in a computational environment to able to mimic different cases of TSL applications.

The mesh structure of the tensile creep sample formed in this context is presented in Figure 6.4. The meshed geometry consists of rectangles with 20 nodes and 1488 elements (C3D20R). The C3D20R element is a general-purpose quadratic brick element, with reduced integration (2x2x2 integration points). A reference point (RP) is added a few cm away to the top of the specimens, and it is bounded to the top surface to apply the constant stress. The bottom part of the specimen, the part held by the clamp in experiments, was fixed in 6 degree of freedoms (encastre). The upper part of

the specimen is also fixed except for y direction (u2) in all degree of freedoms (u1, u3, ur1, ur2, ur3).

Figure 6.4 The mesh geometry of the specimen

In FE creep test validation, first of all, the simulations of experiments were carried out for 4 stress levels in which the experiments were performed. It should be noted that validations were carried out with different implemented subroutines for each product. At the end of the analysis, the experimental data were compared with the implemented model and finite element model results and highly consistent results were obtained. The software outputs showing the total strain values and strain distributions at the point of rupture in the Finite Element validation models prepared for two different TSLs are presented in Figure 6.5 and Figure 6.7. E_{22} values show the total strain value of the sample in the direction of the y-axis; constant stress is applied. Constant Poisson ratio value entered into the software as 0.4. The specimen gets strain on other directions in accordance with this value. It was also observed that the amount of stress applied during the model did not change as intended. In addition, all strain time behaviors recorded at the time of the experiment, presented in mathematical models and taken as model output are compared. These comparisons made under 4 different stress values for TSL-1 and TSL-2 are presented in Figure 6.6 and Figure 6.8.

The second aim of this study is to obtain realistic creep behaviour results for cases where experiments were not performed. Therefore, in addition to the model validation studies, additional validation models for TSL-2 were performed to ensure that the creep behaviour was consistent in the intermediate stress levels.
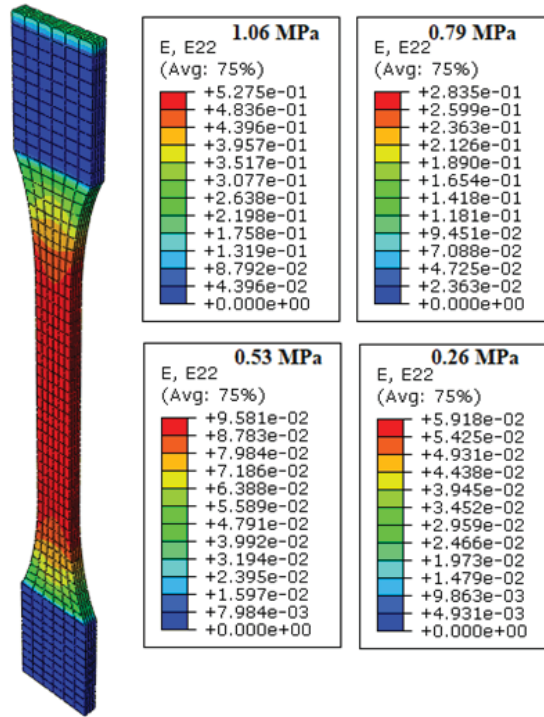
Figure 6.5 Strain distributions at the moment of rupture for TSL-1 (1-day)
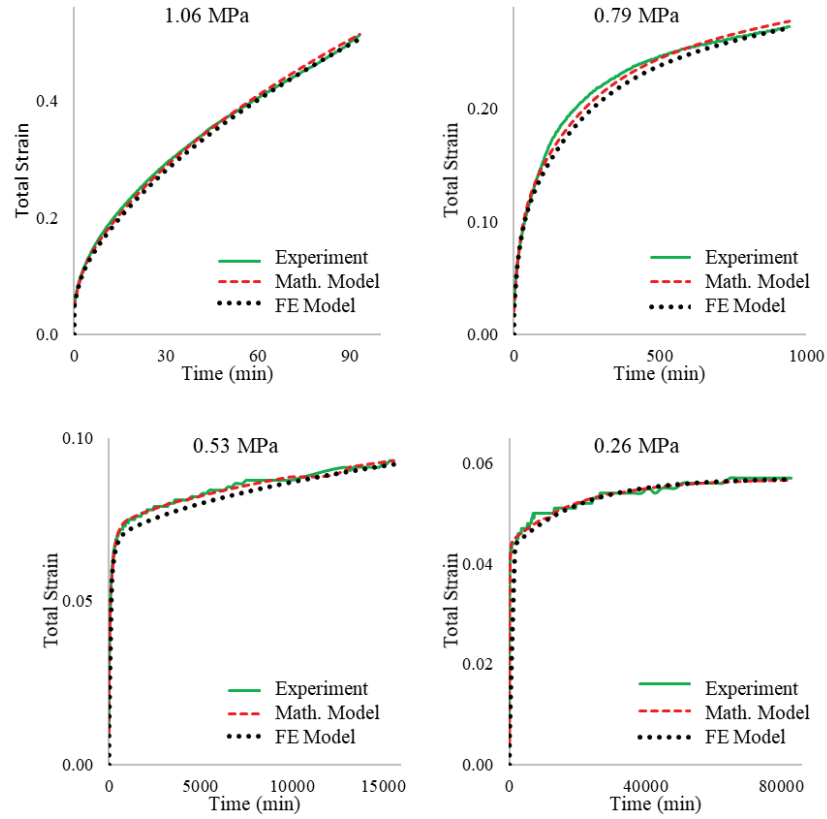
Figure 6.6 FE verification model comparisons for TSL-1 (1-day)
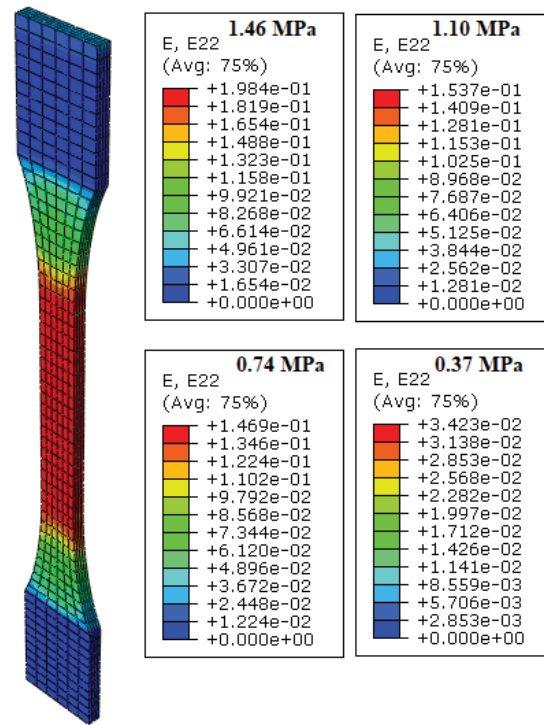
Figure 6.7 Strain distributions at the moment of rupture for TSL-2 (2-day)
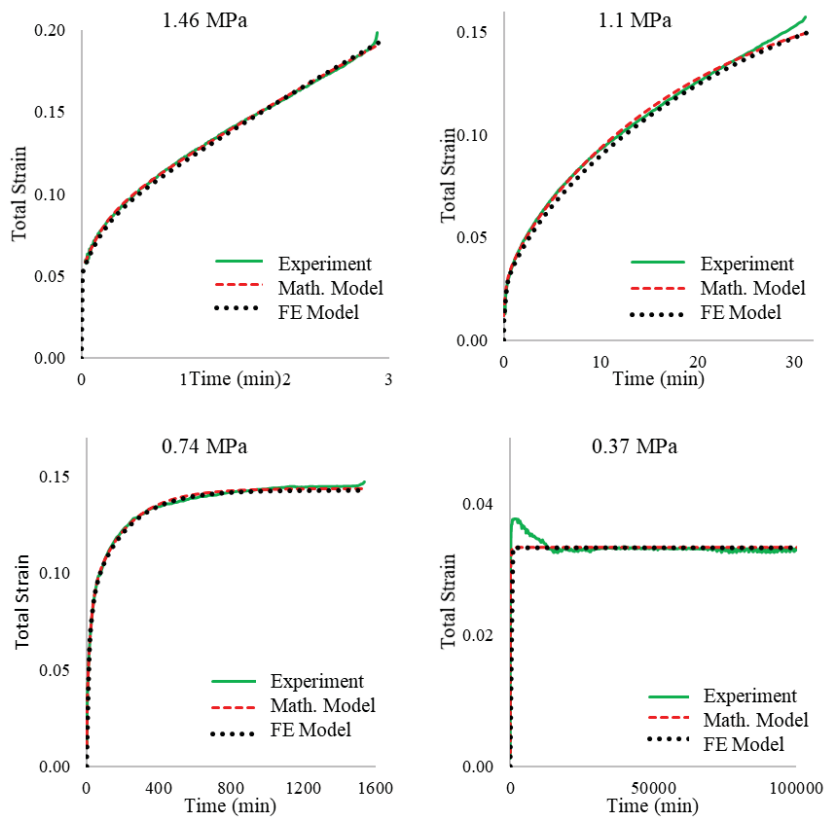
Figure 6.8 FE verification model comparisons for TSL-2 (2-day)

118

For additional validation models, constant stress values of 1.27,0.92, and 0.56 MPa were applied to the sample, respectively. The strain-time graphs of the models under these stress values are presented in Figure 6.9. As testing duration varies from a few minutes to 2 months, for the better understanding of the behaviour, the first 100 minutes and the whole graph (log scale) are presented separately. Besides, the failure envelope obtained at the end of the experiments can be seen in the graphs.
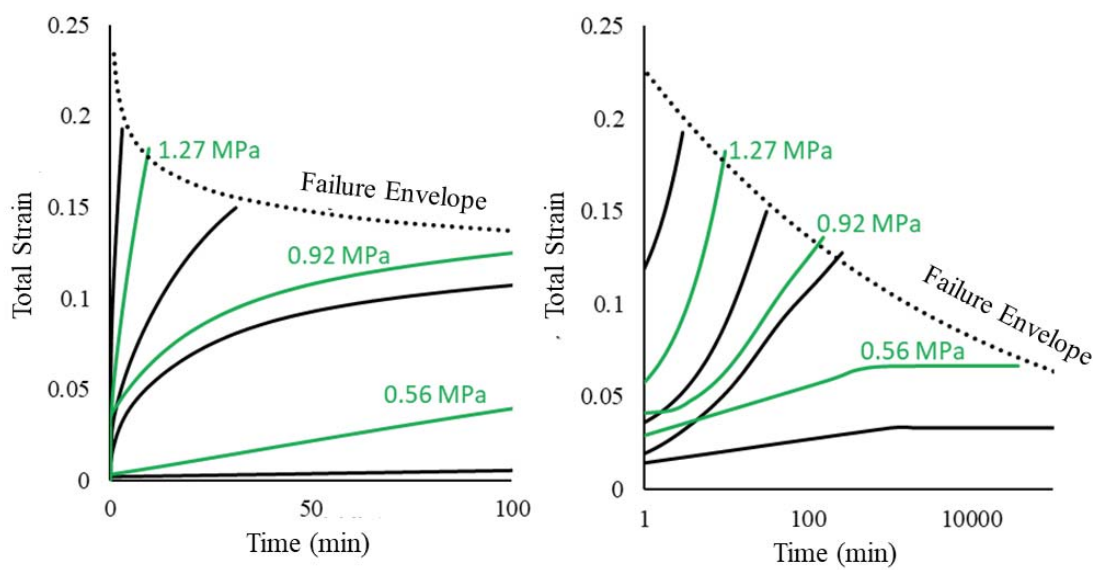
Figure 6.9 FE creep modeling for intermediate stress levels (TSL-2)

As a result of the validation models, The correlation between the experimental creep strain, Multi Kelvin creep model, and numerical creep strain obtained using ABAQUS Finite Element Analysis was found to be adequate.

119

CHAPTER 6

NUMERICAL ANALYSIS OF THE SUPPORT BEHAVIOUR OF TSL IN A CIRCULAR OPENING

This section presents the time-dependent behaviour analysis of the circular tunnel models opened in 4 different in rock masses by using ABAQUS software. Time-dependent squeezing behaviors of various openings were defined in the program in such a way that they would have 1%, 2.5%, 5% and 10% closure at the end of 12 months in accordance with the literature. Later, the TSL was activated in the model, and the support behaviour of the material against the tunnel closure during the 12-month period was examined.

The main purpose of the numerical models is to examine the ability of TSLs to support the rock mass so that time-dependent behaviour of TSLs can be revealed for different practical cases. It is shown in detail in the analysis of experimental results that TSLs can play an active role in carrying wedge blocks. In addition to the block-scale support feature, it is also important to examine the impact of rock mass of a TSL in a global scale.

In the modeling phase, the tunnel with circular cross-section to be analyzed has a 5 m diameter and is located at 400 m depth, and vertical and horizontal stresses states are equal (hydrostatic). By considering the symmetry conditions in the tunnel section, only the quarter of the tunnel was modeled in the numerical modeling studies. In the models, it is required to minimize the boundary effect when selecting finite element mesh dimensions. For this reason, the model geometry was created at least 5 times larger than the tunnel diameter.

Since the models are symmetrical along the length of the tunnel, plane unit deformation conditions are considered. In other words, unit deformations perpendicular to the model plane are considered to be zero. This condition is called as

plane strain in the literature and provides a considerable drop in the solution times of the problems.

In the model, one-way movement is allowed in the right and lower boundaries, which also have symmetry axes (roller supports). In other words, the boundary condition added to the right boundary of the model allows a movement only in the y-plane, and the boundary condition added to the lower edge only allows a movement in the x-plane. In addition, vertical ground pressure is applied to the upper boundary, and horizontal ground pressure is applied to the left edge of the model. Since the medium is hydrostatic, horizontal and vertical stresses are applied equally to the limits. The model geometry and the boundary conditions are presented in Figure 7.1.
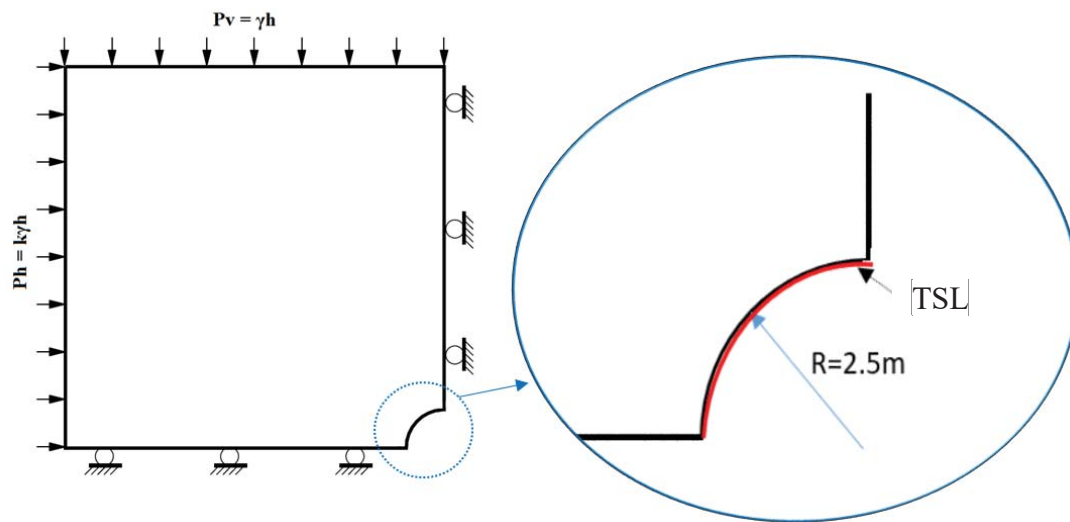
Figure 7.1 Model geometry and boundary conditions

In the modeling part, 4 different ground behaviors are simulated separately. The critical points in the presented graph of Hoek and Marinos (2000), squeezing behaviour of non-reinforced tunnels are based on the selection of different ground behaviors (Figure 7.2).

According to Figure 7.2, 10% strain value is defined as extreme squeezing problem limit and 1% strain value is defined as low squeezing problem. In the created models

showing the time-dependent tunnel closure behavior, these critical 4 values were taken as basis in the 12-month real time simulation of the tunnel.
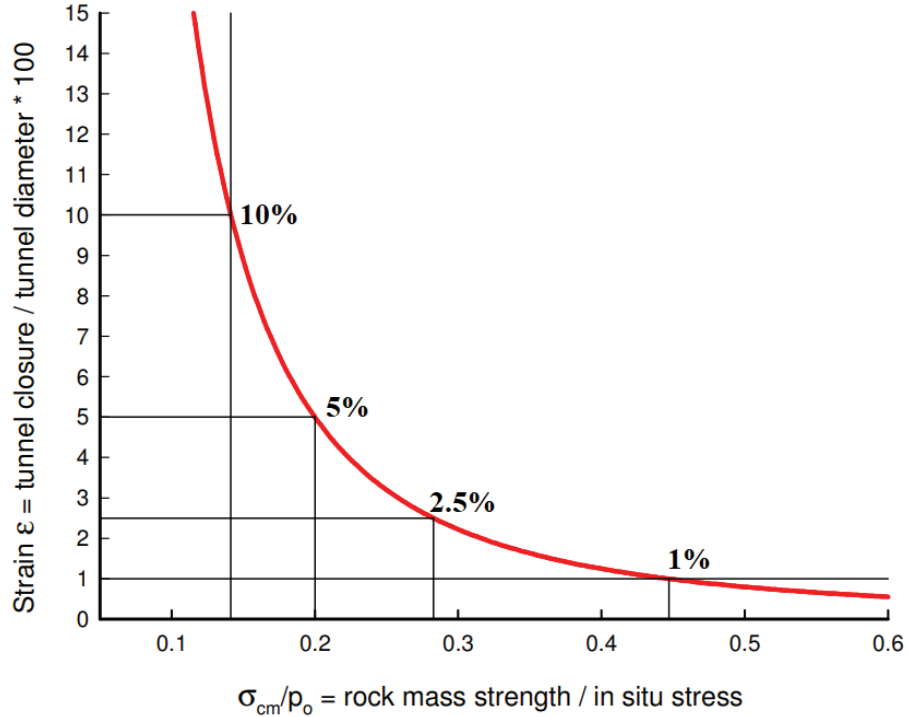
Figure 7.2 Squeezing behaviour of non-reinforced tunnels (After Hoek and Marinos, 2000)

The power or Findley's law creep model is relatively simple to use, so it is widely used in structural time-dependent problems. However, these model types have specific and limited range of applications. Since the stress state remains constant in the creep models in this study, the time-hardening version of power-law creep model was used to simulate the time-dependent closure behaviour of underground opening in ABAQUS. The basic equation of this behaviour is as follows;

$$\dot{\varepsilon}^{cr} = A(\sigma^{cr})^n t^m \tag{7.1}$$

Where $\dot{\varepsilon}^{cr}$ is the uniaxial equivalent creep strain rate, σ^{cr} is the uniaxial equivalent deviatoric stress or Mises equivalent stress, A, n, and m are user defined material parameters. For physically reasonable behavior, A and n must be positive, and m should be between -1 and 0. General creep strain equation for the time-hardening of

the model can be obtained by integrating Equation (7.1) with respect to time as follows:

$$\varepsilon^{cr} = \frac{A}{m+1}(\sigma^{cr})^n t^{m+1} \qquad (7.2)$$

To find out the constants (A, n, and m), the theoretical and measured tunnel closure curves in the literature were evaluated. In this sense, using the creep strain behaviour presented in Equation (7.2), four different tunnel closure behaviours were modelled. The mechanical and physical properties, and creep model constants of the four different rock masses are presented in Table 7.1.

Table 7.1 Rock mass properties and material constants of various models

Constant Parameters			
Poisson's ratio	0.45	Tunnel Diameter (m)	5
Depth (m)	400	UCS (MPa)	60
Unit weight (MN/m^3)	0.025	σ_h/σ_v	1

Variable Parameters						
ε_{final} (%)	E_{rm} (MPa)	σ_{rm} (MPa)	A (10^{-5})	n	m	GSI
1	3840	4.5	1.9	0.62	-0.67	54
2.5	2445	2.8	4.5	0.841	-0.74	46
5	1510	2.0	14.1	0.89	-0.84	40
10	1010	1.5	27.0	1.03	-0.89	36

The model consists of two parts as the rock mass and the liner. These two parts are tied together, and the tunnel boundary is defined as master surface where the liner is introduced as slave surface. So, there is not detachment or slip between liner and tunnel boundary. The liner and the ground are discretized using a 4-node bilinear plane

strain quadrilateral mesh type (CPE4). The rock mass or tunnel consists of 1225 elements, and TSL consists of 30 elements. The mesh density is increased linearly from the boundaries to the tunnel wall, as shown in Figure 7.3.
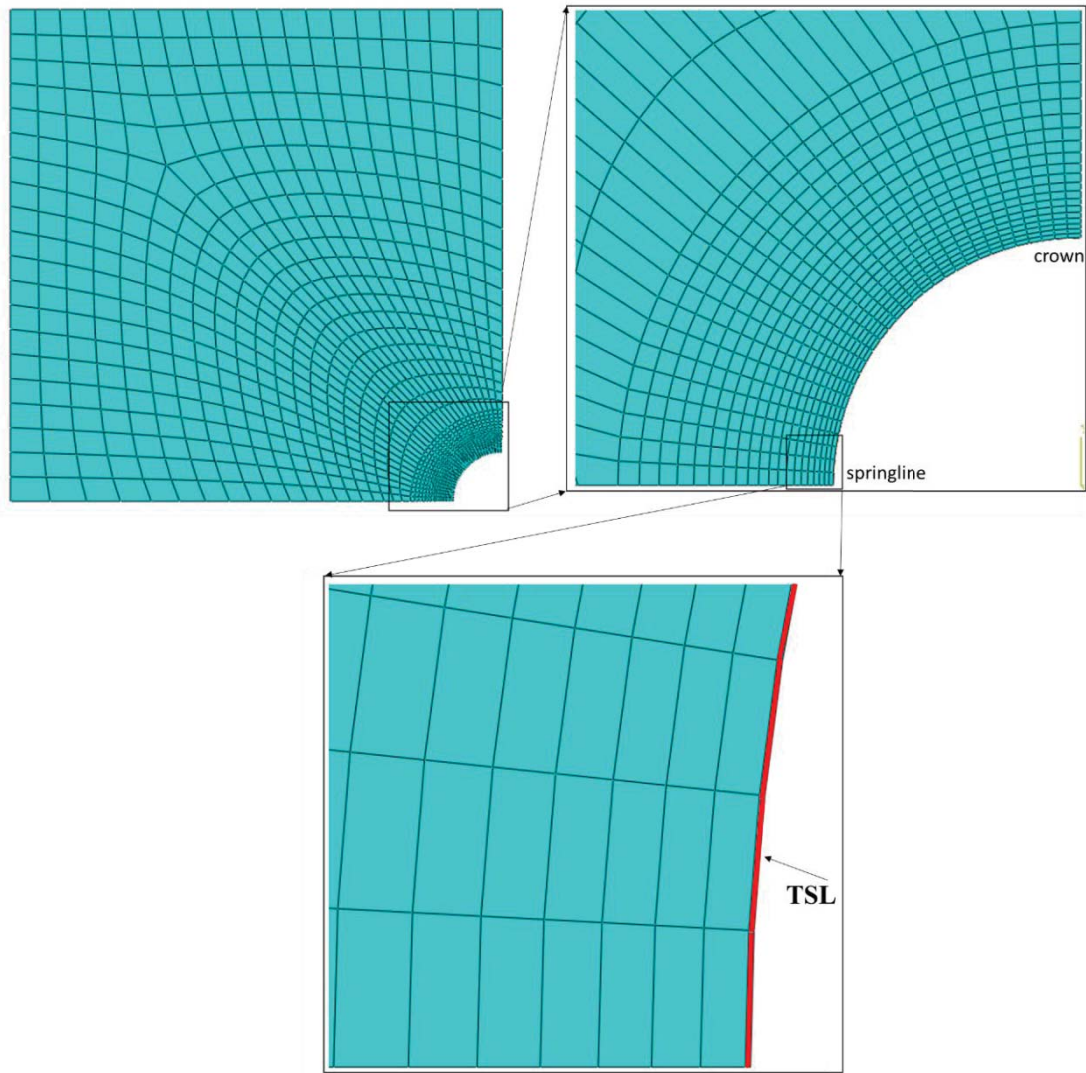
Figure 7.3 Meshing of the model

The modeling process of the unreinforced tunnel behaviour was carried out primarily. At this stage, the parameters presented in Table 7.1 were used. The created models were defined in 3 stages to define initial, elastic, and visco phases. The models were created in a way that the iteration stages of the program performed a real time performance (hours).

In the initial part, boundary conditions were introduced to the model. In the elastic part, the linear elastic behaviour of the rock mass was modeled where this phase took extremely small time compared to the visco part. In the visco part, which is the main part of the model, was performed. The stress and strain values of the rock mass at the end of the elastic part were compared with the analytical solutions, and 99.9% similarity was obtained in the results. Time hardening creep law was defined in the software and was used in the visco stage. In the verification part of this stage, the theoretical time-dependent tunnel closure behaviour used to find the model constants were compared with the time-dependent curves in the tunnel walls.

At the end of the analysis conducted for the unreinforced tunnel, the tunnel closure behaviour was determined by using the displacement values obtained in the tunnel wall over a 12 months period (program output) as illustrated in Figure 7.4.
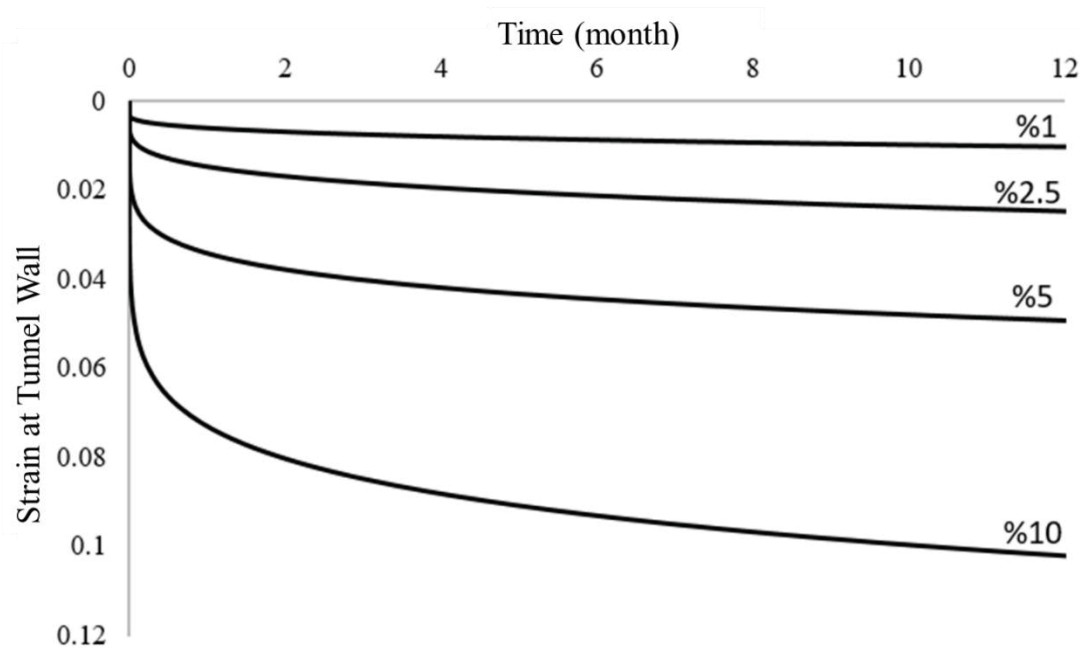
Figure 7.4 Time-dependent behaviors in four different models

In the tunnels opened without any support or internal pressure, it was ensured to obtain that the closure on the crown and the springline during the Visco phase as targetted. For example, the contour plots of the stress and strain values of the non-reinforced tunnel model, which reached 10% strain after simulating for a 12 months period, can

126

be viewed in Figure 7.5. As seen in these contour plots, the stress and strain values formed in the tunnel crown are approximately 20 MPa (S_{11}) and 10% (E_{11}), respectively. Since the model was created in a hydrostatic stress state, similar values were observed in the springline.
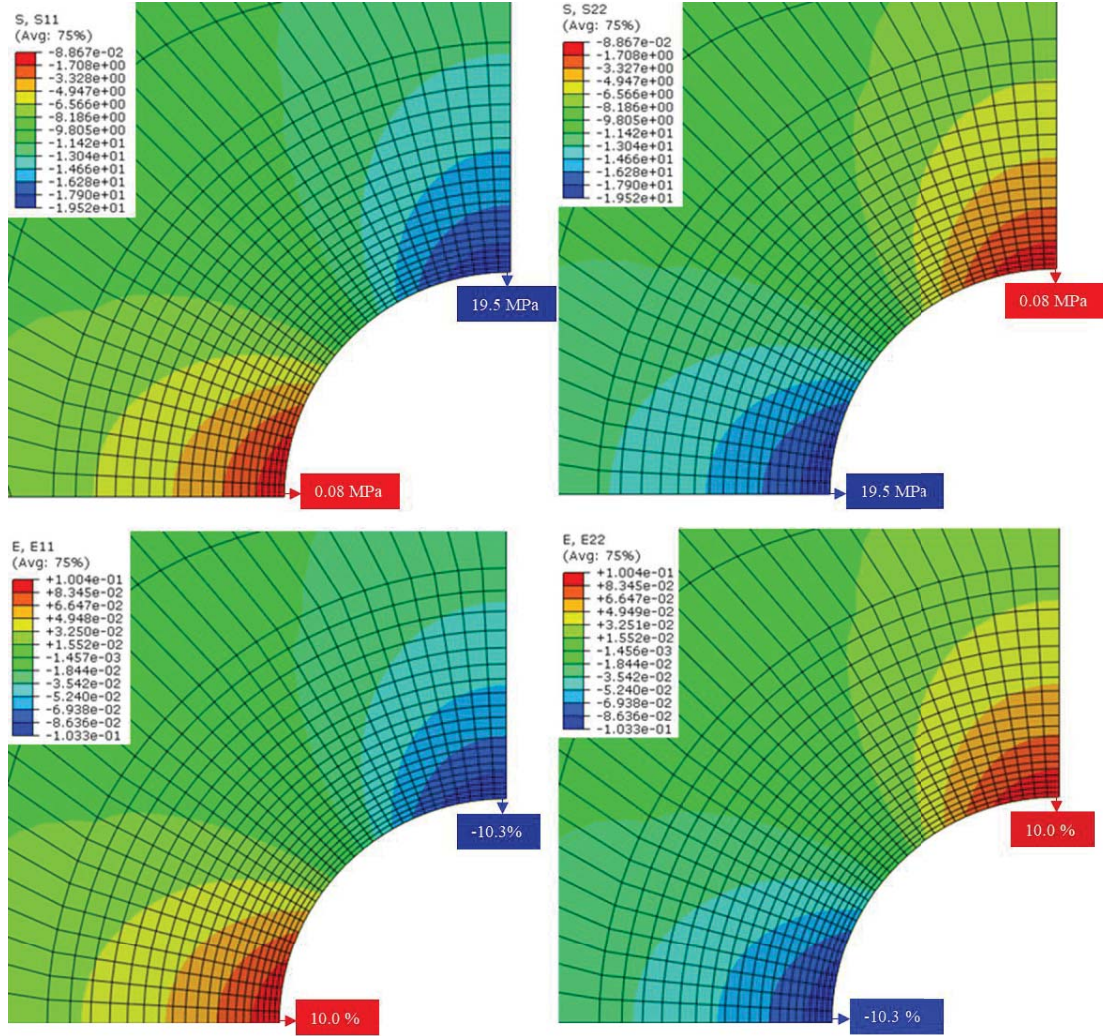
Figure 7.5 Stress and strain distributions of the unreinforced tunnel model (10% strain, GSI 36)

Following the analysis for the unsupported case, the analyzes were conducted with a subroutine so as to investigate the effect of TSL on the tunnel support. The Eq. (5.9) is implemented to software in order to simulate the TSL behaviour. Although different subroutines were created for different various curing times, 7- and 14-day models were not used at this stage. In the models of unsuported tunnel case, it was observed that,

at the end of 7 and 14 days, the openings get an approximate value of 70% of the strain that can be received at the end of a 1-year period. For this reason, the activation times of the elements, which represent the liner with a curing time of 7 or 14 days, must also be 7 or 14 days in real-time. By considering the ground reaction curve of the tunnels with 4 different closure behaviors given in Figure 7.4, it was concluded that the use of subroutines created for these curing times would be functionless.

In order to simulate the support analysis of the TSL, the model must behave unsupported until the time when the liner is activated. In the analysis, "model change method" recommended by the ABAQUS software was used. This method enables the support to be activated at the different stages, and this condition is frequently used in software-based rock engineering studies. Besides, the contact behaviour between the TSL and the tunnel was defined with the "TIE" command in the model. In other words, the cases such as debonding and slipping of the TSLs from the tunnel surface was not taken into consideration.

The model consists of one initial and four stages as listed below.

- Initial stage: Boundary conditions and interactions are defined (this stage cannot be renamed, edited, or deleted).
- Step 1: The linear elastic behaviour of the rock mass is provided to represent initial elastic deformation at $t=0$ (very small step times compared to the creep time is used).
- Step 2: The rock mass is provided to behave time-dependent material (time-hardening creep) until the liner was activated.
- Step 3: Initial elastic deformation on TSL at $t=0$ is modeled elastically.
- Step 4: The tunnel and TSL are modeled together for 12 months in real time.

At this stage, it was decided to examine the effect of TSL thickness on the support behavior. For this reason, a lined tunnel model analysis was performed as 5 and 10 mm TSL thicknesses.

128

In the models created with TSL support, the aim is to observe the decrease in the strain values formed on the tunnel crown and springline. The strain values obtained at the end of 12 months under reinforced and unreinforced conditions for 4 different tunnel behaviors, and the effects of TSL on strain values are presented in Table 7.2. Although the horizontal, vertical and maximum strain values are very close to each other in the table, they are presented separately. The support behaviors presented belong to the TSL application with a thickness of 5 mm.

Table 7.2 Comparison of model results (5 mm TSL)

Crown									
	ε_{11} (%)			ε_{22} (%)			ε_{max} (%)		
Model			Change (%)			Change (%)			Change (%)
	Without TSL	With TSL		Without TSL	With TSL		Without TSL	With TSL	
%1	-1.1154	-1.1151	0.03	1.00423	1.00389	0.03	1.00665	1.0063	0.03
%2.5	-2.6273	-2.6256	0.07	2.48396	2.48227	0.07	2.48979	2.48809	0.07
%5	-5.2394	-5.2351	0.08	5.01678	5.01248	0.09	5.02847	5.02416	0.09
%10	-10.276	-10.263	0.12	9.98432	9.97203	0.12	10.0074	9.9951	0.12
Springline									
	ε_{11} (%)			ε_{22} (%)			ε_{max} (%)		
Model			Change (%)			Change (%)			Change (%)
	Without TSL	With TSL		Without TSL	With TSL		Without TSL	With TSL	
%1	1.00591	1.00556	0.03	-1.1171	-1.1167	0.03	1.00664	1.0063	0.03
%2.5	2.48799	2.48629	0.07	-2.6314	-2.6297	0.07	2.48977	2.48807	0.07
%5	5.02485	5.02055	0.09	-5.2474	-5.2431	0.08	5.02842	5.02411	0.09
%10	10.0002	9.98793	0.12	-10.292	-10.279	0.12	10.0073	9.99497	0.12

According to the analysis results, it has been observed that the TSL product can reduce the strain values by only 0.12% even in the tunnel models with the weakest rock mass characteristics and the highest closure values. As expected, when the quality of the rock mass increases, the effect of TSLs also decreases.

Following the small changes observed in the models as a result of the application of 5-mm TSL, the same analyzes were performed on the models with a thickness of 10 mm, where this thickness is considered high in the field application. The vertical, horizontal, and maximum strain values observed in the tunnel crown and springline at the end of 12 months in the models are presented in Table 7.3.

Table 7.3 Comparison of model results (10 mm TSL)

Crown									
Model	ε_{11} (%)		Change (%)	ε_{22} (%)		Change (%)	ε_{max} (%)		Change (%)
	Without TSL	With TSL		Without TSL	With TSL		Without TSL	With TSL	
%1	-1.1154	-1.1148	0.05	1.00423	1.00365	0.06	1.00665	1.00607	0.06
%2.5	-2.6273	-2.6243	0.11	2.48396	2.4811	0.12	2.48979	2.48692	0.12
%5	-5.2394	-5.2319	0.14	5.01678	5.0095	0.15	5.02847	5.02118	0.15
%10	-10.276	-10.255	0.20	9.98432	9.96354	0.21	10.0074	9.98658	0.21
Springline									
Model	ε_{11} (%)		Change (%)	ε_{22} (%)		Change (%)	ε_{max} (%)		Change (%)
	Without TSL	With TSL		Without TSL	With TSL		Without TSL	With TSL	
%1	1.00591	1.00533	0.06	-1.1171	-1.1164	0.05	1.00664	1.00606	0.06
%2.5	2.48799	2.48512	0.12	-2.6314	-2.6284	0.11	2.48977	2.4869	0.12
%5	5.02485	5.01756	0.15	-5.2474	-5.2400	0.14	5.02842	5.02113	0.15
%10	10.0002	9.97942	0.21	-10.292	-10.270	0.20	10.0073	9.98645	0.21

As a result of the analyzes performed at 10 mm TSL thickness, it was seen that TSL product could not contribute to global tunnel stability. Even in the models performed with the weakest rock mass characteristics and the highest closure, it has been shown that TSL can reduce strain values by only about 0.21%. In addition to the comparisons made at the end of 12 months, closure behaviour of the tunnels with and without TSL were also compared, but no distinctive results were obtained. The ability of TSL to

reduce rock mass strain in different tunnel behaviors and different application thicknesses is presented graphically in Figure 7.6.
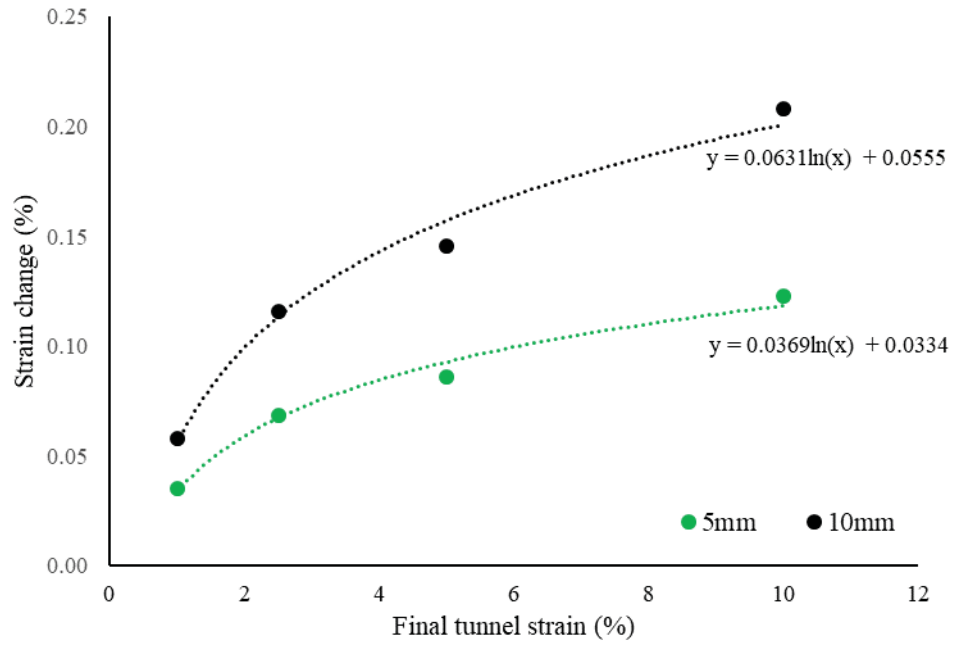

Figure 7.6 Global support performance of TSL

CHAPTER 7

CONCLUSIONS AND RECOMMENDATIONS

This study consists of laboratory, mathematical and numerical modeling parts. The laboratory part covers 46 valid tensile and 56 valid creep tests under the ambient temperature to obtain creep behaviours of two TSL products with different curing time conditions. The tests were performed under 4 different constant stress levels for each curing time. These stress values were determined by tensile testing and were performed just before the creep tests. As a result of these tests, creep rupture envelopes were constructed to estimate the rupture time and the strain amount at rupture of the TSL. These envelopes are commonly used to estimate the service life of the material. In time-dependent modeling part, both viscoplastic (power law) and viscoelastic (Multi Kelvin-Voigt) models were developed for each stress level and curing time. Afterwards, the developed time-dependent models were implemented in a subroutine in ABAQUS. In the numerical modeling part, circular openings with 4 different rock mass environments were introduced to ABAQUS software to reveal the material's time-dependent behavior. Time-dependent squeezing behaviors of various openings were defined in the program in such a way that they would have various closures at the end of 12 months in accordance with the literature. By this way, the support behaviour of the TSL against the tunnel closure during the 12-month period was examined.

The main conclusions and the recommendations obtained at the different stages of the study carried out in this context are as follows:

  i. Results and recommendations regarding the sample preparation process;
- Mixing time and speed of TSLs directly affect their mechanical properties. High speed mixing may cause air bubbles, and therefore air might get

entrapped in the TSL batch mixture. In addition, since tack free time is very limited, long mixing time causes lumps in the batch.

- The optimum mixing time and mixing speed for the tested TSL products were taken as 6 min and 120 rpm, respectively.

- In the sample preparation part, shrinkage of the samples might occur due to different chemical compositions of TSLs. In field applications, this problem may cause a decrease in the thickness of the liner.

- Die cutting technique is relatively easier to implement as a specimen preparation method due to its advantage in creating more homogenous and representative TSL specimens. In molding technique, corners and the gauge section of the Type IV samples do not get filled by the fresh TSL mixture naturally, and large air bubbles are frequently observed.

- Specimens prepared by die cutter have higher ultimate tensile strength and yield strength values and also have small standard deviations between repetitive tests, compared to molding technique.

- If the TSL is not brittle, Type I specimens prepared with die cutter are recommended for laboratory tensile and creep testing.

- The sample preparation process was repeated many times under laboratory conditions, and it was tried to prepare the sample closest to the product obtained in field conditions (spraying method). Similar creep behaviors are thought to be observed in the samples prepared by spraying and molding-die cutting method. However, this needs to be verified by further researches. In further laboratory studies, if the bonding characteristic between the TSL-rock interface is significant, it is thought that more representative test results can be obtained by preparing TSL samples with spraying methods as in the field.

- Laboratory experiments were carried out with non-reactive type TSLs. Since the reactive TSLs can only be applied with strict safety precautions, the majority of the commercially available TSL products on the market are in the modified non-reactive class. If a laboratory experiment with a reactive TSL will be carried out, the safety data sheet must be read carefully. Since the

reactive TSLs cure very fast, the gas output is observed during this chemical reaction. This gas must not be inhaled, and the environment must be ventilated. Besides, as the reactive TSLs cure very quickly, the mixing time and mixing speed should be optimized. Also, the molding process must be done much faster during the sample preparation.

ii.   Conclusions and recommendations regarding the laboratory experiments;

- Tested TSL products are extremely sensitive to creep behavior. For this reason, the ultimate strength parameter should not be considered as a design parameter. Also, creep behaviour varies sharply depending on the curing time.

- According to the creep compliance graphs presented, both TSL products exhibit nonlinear creep behaviors.

- According to the laboratory studies lasting about 18 months, the creep strain at rupture and the rupture time values varying between 3% to 60%, and 2 minutes to >2 months, respectively.

- As the curing time increases with the same stress levels for TSL-1 (cement based), the rupture time decreases, while the opposite behaviour has been observed for TSL-2 (polymer based). The strain values of the samples at the moment of rupture change inversely with the curing time.

- In the 1, 7, and 14-day experiments of TSL-1 (cement based), 22 of 24 samples showed a rupture behaviour within the specified test period (2 months). The product was failed in less than 10 days, even at the stress level corresponding to 40% of the tensile strength. In creep tests corresponding to 20% of polymer-based TSL-2's strength, no rupture was observed although the material was tested more than 2-months. Besides, the sample with a curing time of 14 days can resist for approximately 2 months under the load that is 40% of the strength value.

- Although the TSL-2 (polymer based) has a relatively low tensile and elongation capacity, it is concluded that TSL-2 product can be used more

efficiently. Because, it is less sensitive to creep behavior, and this can considered as an advantage in field applications.

- Creep rupture envelopes are used to evaluate the long-term performance of products and to estimate their lifetimes. For this reason, separate envelopes have been created for different curing times of TSL products. By using the presented rupture envelopes, researchers and design engineers will be able to estimate the service life of TSLs.

- In the study conducted by considering the block that TSLs can carry under tension in underground applications, assuming to have a regular tetrahedron and cube geometry, were examined and useful graphics were created. It is estimated that TSL-1 (cement based) can carry regular tetrahedron blocks with an edge length of 1 meter. It is considered that the volume of the largest cube block that TSL-1 (cement based) can carry up to 5 years with the curing time of 14 days and beyond will be 0.125 m^3. On the other hand, it is estimated that 14 day cured TSL-2 (polymer based) can carry regular tetrahedron blocks with a side length of 1.5 meters for a period up to 3 years. It is considered that the volume of the largest cube block that 14-day or older aged TSL-2 can carry up to 5 years will be 0.35 m^3. It is also clearly seen that TSLs do not have the ability to carry 1m^3 block.

- The time-dependent material behaviour is as important as the ultimate tensile strength, therefore, design engineers should take less than 20 % of the ultimate tensile strength of the TSL as a practical guide. For an order of increase in the service time (stand-up time) of the TSL, an order of decrease in the ultimate tensile strength of TSL should be applied.

- In this study, the laboratory experiments were carried out under ambient conditions. It is known that for polymer and cementitious materials, the creep is accelerated by increasing the temperature. Therefore, the different application environments (deep mines or permafrost conditions) of the TSLs require the investigation of creep behaviors under varying temperature and humidity conditions.

- In experiments, time and displacement values were recorded continuously. Firstly, it was decided to record 8 data per second, but it was decided to decrease this value to 1 data per minute during the experimental periods of up to 2 months. In future studies, instead of recording data with fixed time intervals, it is recommended that the data should be recorded according to the change in displacement values (i.e., data per 0.01 mm displacement).

- In some field applications, the TSLs are used in conjunction with shotcrete. Further laboratory studies recommended for investigating the combined creep behaviour of the TSL and shotcrete.

iii. Conclusions and recommendations from creep modeling studies;

- In the viscoplastic modeling, although the high stress level models achieved very consistent results, this method was insufficient as the strain-time relationship has an asymptotic behaviour especially at smaller creep strain values.

- Strain recovery behaviour was observed during the creep tests of polymer-based TSL-2 product. For this reason, time-dependent behaviours are simulated with piecewise models instead of typical viscoplastic modeling. Piecewise power-law functions are suitable to simulate strain recovery part; on the other hand, these functions cannot simulate asymptotic behaviours.

- Although viscoplastic modeling approach is more practical than viscoelastic modeling, more consistent results were obtained in viscoelastic method. For this reason, the values obtained from the Viscoelastic model approach were preferred in the numerical models.

- The number of model constants shows a variation in different models for the viscoelastic approach. The main reason for this situation is that the experimental duration and the resultant retardation time varies.

- The compliance behaviour of tested TSLs for different stress levels is not identical and it is not similar either. Therefore, creep strain behaviour must be represented by different functions of time at each stress level and each

curing time. For this reason, constitutive modeling for tested TSLs can only be described by nonlinear and non-separable models in terms of the applied stress, time, and curing time.

For further studies, if compliance behaviours of tests are identical, generic constitutive modelling is strongly recommended.

iv. Conclusions and recommendations from creep model implementations:

- Since the instantaneous elastic modulus (E_0) values obtained from the experimental results vary for the applied stresses even for the same curing period, stress-dependent E_0 functions should be defined as a field variable. The user subroutine USDFLD should be created in order to obtain variable E_0.

- In the user subroutine part, different routines were implemented for each curing time, as TSL products have different behaviors during variable curing times.

- Experiment simulations were performed in the subroutine verification. The behaviours obtained from these simulations were compared with the experimental results, and it was ensured that the subroutine was working. In addition, the simulations were carried out for the intermediate stress values which the experiments were not performed for, and it was observed that the implemented subroutine gives some reasonable results in the different stresses.

- Since a significant tertiary stage was not observed in the laboratory tests of this study, damage-based creep models were not adopted. However, if the TSL is to be used in elevated temperature environment, tertiary creep stage might become significant so that damage-based creep model may also be considered.

v. Conclusions and recommendations from numerical models:

- The time hardening creep law can be used to simulate the time-dependent behaviour of different rock masses. This modeling law gives more realistic results in the time-dependent closing behaviour of the tunnels and is recommended to the researchers working in this field where the stress state is constant.

- Time-dependent squeezing behaviors in the tunnel directly affect TSL's global support mechanism. In the tunnels with high squeezing behavior, the work done by TSLs is relatively higher.

- It was observed that TSLs with 5 mm application thickness can reduce the strain values by only 0.12%, even in the tunnel models with the weakest rock mass characteristics and the highest closures. An effective support behaviour was not observed (0.21% reduction) in the models with a thickness of 10 mm, where this thickness can be considered to be high in the field applications.

- It is believed that the time-dependent support behaviour of TSLs can be understood better by the numerical modeling of the support mechanism provided by the TSLs on the scale of the block, rather than the support they provided on a global scale.

- Further laboratory-field experiments and numerical studies are recommended for the investigation of the combined support performance of the surface support members used in conjunction with the field applications. Their creep behaviour and interaction with each other may provide essential findings to evaluate their long term efficiency.

- For the numerical evaluation of the support mechanism provided by the TSLs on the scale of the block, the discontinuum approaches can be tried to be applied in future works.

REFERENCES

ABAQUS, FEA., 2017. Abaqus Inc. Providence, Rhode Island, United States.

Ahn, T., (2011), "Thermal and Mechanical Stuides of Thin Spray-on Liner (TSL) for Concrete Tunnel Linings." Phd. Thesis of the University of Western Ontario.

Archibald, J. F. (2004). Canadian laboratory and field testing. In Surface support in mining (Potvin, Y., Stacey, D. and Hadjigeorgiou, J. (eds)). Perth, Australia: Australian Centre for Geomechanics, pp. 73–87

Archibald, J.F. (2001). Assessing acceptance criteria for and capabilities of liners for mitigating ground falls. In: MASHA Health and Safety Conference Sudbury.

Archibald, J.F. Espley S.J. St. Lausch P. (1997). Field and Laboratory Response of Mineguard Spray-on Polyurethane Liners. Proc. Int. Symp. on Rock Support, Lillehammer, pp. 475-490.

Archibald, J.F., Degagne D.O. (2000). Recent Canadian Advances in the Application of Spray-on Polymeric Linings Mining Health and Safety Conference, Sudbury, Ontario.

Archibald, J.F., Lausch P. (1999). "Thin Spray-on Linings for Rock Failure Stabitization". Proc. 37th US Rock Mechanics Symp., Vail. Rock Mechanics for Industry, Balkema, Rotterdam, pp. 617-624.

ASTM D2990-09 (2010) Standard Test Methods for Tensile, Compressive, and Flexural Creep and Creep-Rupture of Plastics, American Society for Testing and Materials (ASTM), West Conshohocken, PA, USA. Doi: 10.1520/D2990-09.

ASTM D-638-10, (2010), "Standard Test Method for Tensile Properties of Plastics-1," ASTM International, West Conshohocken, PA, USA DOI: 10.1520/D0638-10

Aydan, Ö. (1989). The stabilisation of rock engineering structures by rockbolts (PhD dissertation).

Aydan, Ö. (2018). Rock reinforcement and rock support. CRC Press. 16-33. 484 p.

Bailey, R. W. (1929). Creep of steel under simple and compound stresses and the use of high initial temperature in steam power plants. Sectional Meeting of the World Power Conference, Tokyo. pp. 1089.

Brinson, H. F., Brinson, L. C. (2015). Polymer engineering science and viscoelasticity. New York, NY: Springer. 177-185. 482 p.

Carstens, R. (2005) Thin sprayed liners-adding or destroying value. In: 1st international seminar on strategic versus tactical approaches in mining. SymposiumSeries 40. SAIMM. Johannesburg, pp. 327–335.

Carstens, R., and Oosterhuizen, A.O. (2004). "Application of a thin sprayed liner (TSL) in VCR gullies behind advancing stope panels at Savuka Gold Mine". SANIRE 2004 Conference, Johannesburg, RSA.

Chen, L., Zhou, Z., Liu, G., Cui, X., Dong, Q. and Cao, H., (2020). Effects of substrate materials and liner thickness on the adhesive strength of the novel thin spray-on liner. Advances in Mechanical Engineering, 12(2), doi: 10.1177/1687814020904574

Coates, D.F., (1966). Rock mechanics principles. Mines Branch Monograph. Department of Energy, Mines and Resources, Canada.

Curran, J.H, Corkum B, Hammah RE (2004) Three-dimensional analysis of underground wedges under the influence of stresses. In Gulf Rocks 2004, the 6th North America Rock Mechanics Symposium (NARMS). American Rock Mechanics Association.

DeMaio, A. M. (2006). The role of bonding on the tensile creep behavior of paper (PhD dissertation, Georgia Institute of Technology).

Dirige, A., Archibald, J. (2009). Numerical Modeling Simulations of Spray-on Liners Support Potential in Highly Stressed and Rockburst Prone Rock Conditions". Proceedings of the 3rd CANUS Rock Mechanics Symposium, Toronto

EFNARC, (2008). Specification and Guidelines on Thin Spray-on Liners for Mining and Tunneling. ENC 250TSL v7.2 25-07-08,

Espley, S, Tannant D.D, Baiden, G, Kaiser, P.K. (1999). Design Criteria for Thin Spray-on Membrane Support for Underground Hardrock Mining. Canadian Ins. of Mining and Metallurgy Annual Meeting, Calgary.

Espley, S.J, Gustas R, Heilig J, Moreau LH (2001) Thin spray-on liner research and field trials at INCO. In: Section 25 international seminar and field trials on surface support liners: membrane- shotcrete and mesh. Perth.

Esterhuizen, A.P., Bosman J.D., (2009) "Practical Experience with The use of Thin Sprayed Liners At two Rivers Platinum Mine", 43rd U.S. Rock Mechanics Symposium and 4th U.S.-Canada Rock Mechanics Symposium, Asheville.

Ferreira, P.H., Piroddi, A., (2012). The application of GRP and thin spray liner support products in a typical block cave mining method to enhance safety and productivity. The Southern African Institute of Mining and Metallurgy, v112. pp.141-150.

Findley, W.N, Lai J.S, Onaran K (1989). Creep and Relaxation of Nonlinear Viscoelastic Materials. Dover Publications, New York 50-77. 343 p.

Finn, D.J., Teasdale, P., and Windsor, C.R. (1999). In situ trials and field testing of two polymer restraint membranes, Rock Support and Reinforcement Practice in Mining, ed. E. Villaescusa, C.R. Windsor and A.G. Thompson, A.A. Balkema, 1999. pp. 139–153.

Finn, D. (2001). Polymer Membrane Test. Surface Support Liners: Membranes, Shotcrete and Mesh, Australian Centre for Geomechanics, Australia. Sect.20.

Fowkes, N, Teixeira, J.A, and Stacey, T.R. (2008) Crack repair using an elastic filler. J Mech Phys Solids 56(9) pp. 2749–2758, doi: 10.1016/j.jmps.2008.06.001

Gilbert, S, Saydam, S, and Mitra, R. (2010) Laboratory investigation of the potential use of thin spray-on liners in underground coal mines, The symposium of extracting the science: a century of mining research. Littleton, CO, USA.

Göbel, L., Königsberger, M., Osburg, A. and Pichler, B., (2018). Viscoelastic behavior of polymer-modified cement pastes: Insight from downscaling short-term macroscopic creep tests by means of multiscale modeling. Applied Sciences, 8(4), p.487. doi: 10.3390/app8040487

Guner, D. (2014) Experimental and numerical analysis of effect of curing time on tensile strength and elastic material properties of thin spray-on liners. MSc Dissertation, Middle East Technical University.

Guner, D. and Ozturk, H., (2017). Tensile-creep test specimen preparation practices of surface support liners. In IOP Conference Series: Earth and Environmental Science (Vol. 95, No. 4, p. 042004). IOP Publishing.

Guner, D. and Ozturk, H., (2018). Creep behaviour investigation of a thin spray-on liner. International Journal of Rock Mechanics and Mining Sciences, 108, pp. 58-66. doi: 10.1016/j.ijrmms.2018.05.007

Guner, D. and Ozturk, H., (2019). Experimental and modelling study on nonlinear time-dependent behaviour of thin spray-on liner. Tunnelling and Underground Space Technology, 84, pp. 306-316. doi: 10.1016/j.tust.2018.11.037

Guner, D. and Ozturk, H.,(2016). Experimental and Numerical Analysis of the Effects of Curing Time on Tensile Mechanical Properties of Thin Spray-on Liners. Rock Mechanics and Rock Engineering, 49, pp. 3205-3222. doi: 10.1007/s00603-016-0997-x

Hadjigeorgiou, J, (2003). Proceedings of the Third International Seminar on Surface Support Liners: Thin Spray-On Liners, Shotcrete, and Mesh, Quebec City, Canada, s. 10, pp. 1-22.

Hannon, A., (2009) "Thın Sprayed Lıners (TSLs) and a Safe Workıng Place". The Southern African Institute of Mining and Metallurgy Hard Rock Safe Safety Conference, Sun City. pp. 99-114.

Hawker, R (2001) Tekflex—new areas of application. Surface support liners: membranes, shotcrete and mesh. Australian Centre for Geomechanics, Perth (Sect. 17)

Hoek, E. and Marinos, P., (2000). Predicting tunnel squeezing problems in weak heterogeneous rock masses. Tunnels and tunnelling international, 32(11), pp.45-51.

Hoek, E., and Wood, D. F. (1987). Support in underground hard rock mines. Underground support systems, 35, 1-6.

Hoek, E., Kaiser, P. K., and Bawden, W. F. (2000). Support of underground excavations in hard rock. CRC Press.152-156, 215 p.

Hyams, D.G., (2011). CurveExpert Professional: software.

Jensen, P. (2013). Managing the Engineering, Health & Safety Aspects of Thin Spray- On Liner Application. Msc. Thesis, Luleå University of Technology.Department of Civil, Environmental and Natural Resources Engineering.

Komurlu, E, Kesimal A (2014) Improved performance of rock bolts using sprayed polyurea coating. Rock Mech Rock Eng. doi:10. 1007/s00603-014-0696-4

Komurlu, E., Demir, AD, (2017). A Numerical Modelling Study on Performance of Thin Spray-on (TSL) Liners. 25th International Congress and Exhibition of Tukey (IMCET 2017), Antalya, Turkey, pp. 105-112

Krishnaswamy, P., Tuttle, M. E., Emery, A. F., and Ahmad, J. (1992). Finite element modeling of the time-dependent behavior of nonlinear ductile polymers. Polymer Engineering & Science, 32(16), 1086-1096. doi: 10.1002/pen.760321606.

Kuijpers, J. (2001). "Evaluation of Membrane Support Behaviour". Surface Support Liners: Membranes, shotcrete and Mesh. Australian Centre for Geomechanics, Perth. Sect.21.

Kuijpers, J. S and Toper, Z. (2002). Towards a Better Understanding of the Support Function of Thin Sprayed Liners. 2nd International Seminar on Surface Support Liners: Thin Sprayed Liners, Shotcrete, Mesh and Lace, SAIMM, Sandton.

Kuijpers, J. S., Sellers, E. J., Toper, A. Z., Rangasamy, T., Ward, T., Van Rensburg, A. J., Yilmaz, H., Stacey T. R. (2004). "Required technical specifications and standard testing methodology for thin sprayed linings".   SIMRAC Final Report.   Research agency: CSIR Division of Mining Technology. Project No: SIM 020206, Report No-0404.

Lacerda, L, Rispin M (2002) Current ground support membrane applications in North American underground mines. In: 2nd international seminar on surface support liners: thin sprayed liners, shotcrete, mesh. Johannesburg.

Lacerda, L.(2004), "Shotcrete and Other Surface Support Liners", SME Annual Meeting, Denver, Colorado.

Lau, V, Saydam, S, Cai, Y, Mitra, R, (2008) Laboratory Investigation of Support Mechanism for Thin Spray-on Liners. 12th International Conference of International Association for Computer Methods and Advances in Geomechanics (IACMAG) Goa, India, pp. 1381-1388.

Laurence, D. (2001). Membrane trials at an Australian Underground coal mine. Surface Support Liners: Membranes, Shotcrete and Mesh. Australian Centre for Geomechanics, Perth. Sect.22.

Leaderman, H. (1941). Elastic and creep properties of filamentous materials, PhD dissertation, Massachusetts Institute of Technology.

Lee, C., Chang, S.H., Lee, K. and Kim, D., (2015). Numerical study on contact behavior of TSL (Thin Spray-on Liner). Journal of Korean Tunnelling and Underground Space Association, 17(6), pp. 665-674. doi: 10.9711/KTAJ.2015.17.6.665

Lee, K., Kim, D., Chang, S. H., Choi, S. W., Park, B., and Lee, C. (2018). Numerical approach to assessing the contact characteristics of a polymer-based waterproof membrane. Tunnelling and Underground Space Technology, 79, 242-249. doi: 10.1016/j.tust.2018.05.015

Lewis, B. (2001). Mondi Rock-HoldTM the development of this structural membrane support. Surface Support Liners: Membranes, shotcrete and Mesh. Australian Centre for Geomechanics, Perth. Sect.18.

Li, Z, Saydam, S, Mitra, R, Chalmers, D (2015) Investigation on Adhesion Strength of Thin Spray- on Liners in an Underground Coal Mine. Coal Operators' Conference, pp. 191-197.

Li, Z., Nocelli, B. and Saydam, S., (2017). Effect of rock strength and surface roughness on adhesion strength of thin spray-on liners. International Journal of Rock Mechanics and Mining Sciences, 91, pp.195-202.

Li, Z., Tenney, J., Chalmers, D., Mitra, R., and Saydam, S. (2016). Application of thin spray-on liners to enhance the pre-drained coal seam gas quality. Energy Exploration & Exploitation, 34(5), 746-765. doi: 10.1177/0144598716659599

Liu, H. (2007). Material modelling for structural analysis of Polyethylene (Master's thesis, University of Waterloo).

Lockett, F. J. (1972). Nonlinear viscoelastic solids. Academic Press.25-28. 195 p.

Ludwik, P., Elemente der technologischen mechanik, 1909. Verlag Von Julius Springer, Leipzig, p.32.

Lukey, C. E. Spinks, E. Baafi, I. Porter, J. Nemcik, 2008. "Polymer-Based Alternative to Steel Mesh for Coal Mine Strata Reinforcement". 13th Australian Tunnelling Conference Melbourne, 327-330.

Malan, D.F., Napier, J.A.L. (2008). Numerıcal Modelling of Tunnel Liner and Fracture Interaction. 6th. International Symposium on Ground Support in Mining and Civil Engineering Construction, SA.

Mason, D.P., and Abelman, H. (2009). Support provided to rock excavations by a system of two liners. Int J Rock Mech Min Sci 46:1197–1205. doi: 10.1016/j.ijrmms.2009.01.006.

Mason, D.P., and Stacey, T.R. (2008). Support to rock excavations provided by sprayed liners. Int J Rock Mech Min Sci 45:773–788. doi: 10.1016/j.ijrmms.2007.09.001.

MasterRoc TSL 865 Technical Data Sheet.. BASF. From: https://assets.master-builders-solutions.basf.com/en-us/basf-masterroc-tsl-865-tds.pdf. [Accessed 28 April 2020].

Morton, E. C., Thompson, A. G., Villaescusa, E., and Roth, A. (2007). Testing and analysis of steel wire mesh for mining applications of rock surface support. In 11th ISRM Congress. International Society for Rock Mechanics and Rock Engineering.

Mpunzi, M. (2012). The Properties and Performance of Selected Thin Spray on Liners for Rock Support. Dissertation, University of Witwatersrand.

Mpunzi, P., R. Masethe, M. Rizwan, T.R. Stacey, (2015) Enhancement of the tensile strengths of rock and shotcrete by thin spray-on liners. Tunnelling and Underground Space Technology 49, 369–375. doi: 10.1016/j.tust.2015.05.013

Naismith, W.A., and Steward, N.R. (2002). Comparative Performance Testing of Ultra-Thin Structural Liners. 2nd Int. Seminar on Surface Support Liners: Thin Sprayed Liners, Shotcrete, Mesh. SAIMM, Sandton.

Nater, P., Mena-Cabrera, A. (2010). Thin Sprayed Liners - an Approach With Numerical Models. International Society for Rock Mechanics. Eurock 2010.

Nomikos, P.P., Yiouta-Mitra, P.V, Sofianos, A.I. (2006) Stability of asymmetric roof wedge under non-symmetric loading. Rock Mech Rock Eng, 39(2), 121-129. doi: 10.1007/s00603-005-0058-3.

Norton, F. H. (1929). The Creep of Steel at High Temperature. McGraw Hill, New York. 90 p.

O'Donnell, J.D.P., Tannant, D.D. (1998). Field pull tests to measure insitu capacity of shotcrete. Canadian Institute of Mining and Metallurgy Annual General Meeting, Montreal; 1998.

Ozturk, H. (2005). Adhesion between thin spray-on liners and rock or concrete. Dissertation. University of Alberta.

Ozturk, H., (2011), Elastic Material Properties of Thin Spray-on Liner. The Journal of the chamber of Mining Engineers of Turkey, Vol.50, No.2, 41-45.

Ozturk, H. (2012a). Work of adhesion of thin spray-on liners. Rock Mech Rock Eng. Volume 45, Issue 6, pp. 1095-1102. doi:10.1007/s00603-012-0238-x.

Ozturk, H. (2012b). Fracture mechanics interpretation of thin spray-on liner adhesion tests. Int J Adhes Adhes Sci 34:17–23. doi:10.1016/j.ijadhadh.2012.01.001

Ozturk, H. and Guner, D., (2017). Failure analysis of thin spray-on liner coated rock cores. Engineering Failure Analysis, 79, pp.25-33. doi: 10.1016/j.engfailanal.2017.03.024

Ozturk, H. and Guner, D., (2019). Laboratory and distinct element analysis of the deformability behaviour of thin spray-on liners. International Journal of Rock Mechanics and Mining Sciences, 123, p.104118. doi: 10.1016/j.ijrmms.2019.104118.

Ozturk, H., Tannant D.D. (2004) Influence of rock properties and environmental conditions on adhesive bond to a thin liner. Surface Support in Mining. Australian Centre for Geomechanics. pp. 135-139.

Ozturk, H., Tannant D.D. (2010) Thin spray-on liner adhesive strength test method and effect of liner thickness on adhesion. Int J Rock Mech Min Sci; 47, 808-815. doi:10.1016/j.ijrmms.2010.05.004

Pappas, D.M., Barton, T.M., Eric, S.W. (2003) The long-term performance of surface support liners for ground control in an underground limestone mine. In: 3rd International seminar on surface support liners: thin spray-on liners, shotcrete and mesh, Quebec City, Canada. (Sect. 22).

Paraskevopoulou, C. (2016). Time-dependency of rocks and implications associated with tunneling. PhD dissertation, Queen's University (Canada).

Pickett, A., Thomas, A. (2013) Where are we now with sprayed concrete lining in tunnels? http://shotcrete.org/media/Archive/2013Fal_GoinUnderground.pdf. Accessed 11.11 .2019.

Potvin, Y. (2002). "Towards a common understanding of TSL applications in mines". 2nd Int. Seminar on Surface Support Liners: Thin Sprayed Liners, Shotcrete, Mesh. SAIMM, Sandton, RSA, Sect.A1, pp. 1-9.

Potvin, Y. (2006). Australian Rockfall Research Reveals Industry Advancement. Canadian Mining Journal. http://www.canadianminingjournal.com/features/Australian-rockfall-research-reveals-industry-advancement Accessed 08.11 .2019.

Potvin, Y., Stacey, T. R., Hadjigeorgiou, J., and Yilmaz, H. (2004). "Thin spray-on liners (TSLs) – a quick reference guide, Part 1 in Surface Support in Mining" Potvin, Stacey and Hadjigeorgiou Eds, Australian Centre for Geomechanics, Perth, Australia, pp. 3-43.

Prandtl, L. (1928). Ein Gedankenmodell zur kinetischen Theorie der festen Körper. ZAMM-Journal of Applied Mathematics and Mechanics/Zeitschrift für Angewandte Mathematik und Mechanik, 8(2), 85-106.

Qiao, Q, Nemcik J, Porter I, and Baafi E (2015) Compressive Strength Testing of Toughskin Thin Spray-On Liner. Coal Operators' Conference, pp. 198-203.

Qiao, Q., (2015). Experimental and numerical analysis of thin spray-on liner materials for use in underground mines. Phd. Thesis of the University of Wollongong

Qiao, Q., Nemcik, J., Porter, I., and Baafi, E. (2014) Laboratory investigation of support mechanism of thin spray-on liner for pillar reinforcement. Geotechnique Letters, doi: 10.1680/geolett.14.00076

Rabcewicz, L. V. (1965). The new Austrian tunnelling method. Water Power, 511-515.

Richardson, J., Mitra, R., Saydam, S., (2009). Investigation of Thin Spray-On Liners using Numerical Modeling". ARMA, American Rock Mechanics Association, Asheville.

Saydam, S. Yilmaz, H. and Stacey T.R, (2004) A New Testing Approach for Thin Spray-on Liners: Double-Sided Shear Strength (DSS) Test. Surface Support in Mining, Eds. Y. Potvin, T.R. Stacey, J. Hadjigeorgiou, Australian Centre for Geomechanics. Pages: 151-156.

Severs, E. T. (1962). Rheology of polymers. Reinhold Pub. Corp. 78-80. 180 p.

Shan, Z., (2017). Geotechnical assessment of thin spray-on liners for underground coal mine roof support. PhD. dissertation, University of Wollongong (Australia).

Smith, N. (2012). The use and application of Thin Spray Liners (TSLs) in Mining. Seventh International Symposium, Rockbolting and Rock Mechanics in Mining. Aachen, Germany, 197-204.

Spearing, A.J.S., and Gelson J. (2002) Developments and the future of thin reactive liners since the previous conference in Australia. 2nd Int. Seminar on Surface Support Liners: Thin Sprayed Liners, Shotcrete, Mesh. SAIMM, Sandton, RSA, Sect.13.

Spearing, A.J.S., Borejszo, G., and Campoli, A. (2009). "The application of a structural thin support liner (TSL) on mines". 43rd U.S. Rock Mechanics Symposium and 4th U.S.-Canada Rock Mechanics Symposium.

Spearing, A.J.S., Ohler J., Attogbe E. (2001) The effective testing of thin support membranes for use in underground mines. Surface Support Liners:

Membranes, Shotcrete and Mesh, Australian Centre for Geomechanics , Australia

Stacey, T.R, and Kasangula, M. (2003) Results from Testing of TSL's Using a Simple, Low Cost Laboratory Test. 3rd Int. Seminar on Surface Support Liners: Thin Spray-On Liners, Shotcrete and Mesh, Quebec City, Canada. Sect.17

Stacey, T.R. (2001). Review of membrane support mechanisms, loading mechanisms, desired membrane performance, and appropriate test methods. J. S. Afr. Inst. Min. Metall. 2001;101(7):343–351.

Steyn, J., R.J. Gerber, A.T., Harrison, Ferreira P.H. 2008. Investıgatıon of the Characteristics of Thin Sprayed Liners and Their use as an Additional Support Medium in Block Cave Mining. The Southern African Institute of Mining and Metallurgy, 1-19

Swan, G., Spencer, E.J., Graham, C., Hastings D., Rayner T.J., Livingstone D., McDonald N.W. and Bond, B. (2012). Towards Proving the Feasibility of a New, Composite Polymer Liner. Eurock, Stockholm.

Systat Software, Inc. (2001). TableCurve 3D Software, ver. 4.0. Chicago: Systat, Inc

Tannant, D.D,, and Ozturk, H. (2003) Evaluation of test methods for measuring adhesion between a liner and rock. 3rd Int. Seminar on Surface Support Liners: Thin Spray-On Liners, Shotcrete and Mesh, Quebec City, Canada. Sect.13.

Tannant, D.D., (2001), Thin Spray-on Liners for Underground Rock Support. 17th International Mining Congress and Exhibition of Turkey, pp. 57-68.

Tannant, D.D., and Wang, C. 2003, Thin Tunnel Liners Modelled with Particle Flow Code. Engineering Computations, Vol.21, pp. 318-341. doi: 10.1108/02644400410519811.

Tannant, D.D., Swan, G., Espley, S., Graham, C. 1999. Laboratory test procedures for validating the use of thin sprayed-on liners for mesh replacement, CIM AGM, Calgary, 8 p.

TEKFLEX LP Liquid/Powder-Version Technical Data Sheet. 2019. Minova CarboTech GmbH, Germany. https://www.minovaglobal.com/emea-cis/our-

products/sprayed-membranes-and-coatings/tekflex/tekflex-lp/. [Accessed 28 April 2020].

Thompson, A.G., Villaescusa, E., and Windsor, C.R. (2012). Ground support terminology and classification: an update. Geotech Geol Eng. 2012;30:553–580. doi: 10.1007/s10706-012-9495-4.

Villaescusa, E. (2014). Geotechnical Design for Sublevel Open Stoping. London: CRC Press. 395. 502 p.

Villaescusa, E., Thompson, A., and Windsor, C. (2019). Probabilistic estimate of rock mass static and dynamic demands for underground excavation stabilisation. Journal of Rock Mechanics and Geotechnical Engineering, 11(3), 481-493. doi: 10.1016/j.jrmge.2018.08.009.

Wei, Q., Zhang, N., Feng, X., Xie, Z., Wu, J., and Cao, J. (2019). Influence of Polypropylene Fiber on Tensile Property of a Cement-Polymer Based Thin Spray-On Liner. Applied Sciences, 9(14), 2876. doi: 10.3390/app9142876.

Wojno L. and Kuijper J.S., (1997). "Spray-on, user Friendly and Flexible Support for Mine Excavations." Proc. Int. Symp. An Rock Support, Lillehammer, pp. 671-683.

Yilmaz, H. (2007). Shear-bond strength testing of thin spray-on liners. J S Afr Inst Min Metall 107(8):519–530

Yilmaz, H. (2011). Development of testing methods for comparative assessment of Thin Spray-on Liner (TSL) shear and tensile properties. PhD dissertation, University of the Witwatersrand, (South Africa).

Yilmaz, H., Saydam, S., and Toper, A.Z. (2003). Emerging support concept: thin spray-on liners. International Mining Congress and Exhibition of Turkey-IMCET, ISBN 975- 395-605-3. pp. 65-72

Zhang, C., and Moore, I. D. (1997). Nonlinear mechanical response of high density polyethylene. Part II: Uniaxial constitutive modeling. Polymer Engineering & Science, 37(2), 414-420. doi: 10.1002/pen.11684.

Zhang, Q., Le Roy, R., Vandamme, M. and Zuber, B., (2014). Long-term creep properties of cementitious materials: Comparing microindentation testing

with macroscopic uniaxial compressive testing. Cement and concrete research, 58, pp. 89-98. doi: Get rights and content

Zhenjun, S., Porter, I., Nemcik, J., and Baafi, E. (2014) Comparing the reinforcement capacity of welded steel mesh and a thin spray-on liner using large scale laboratory tests. Int Journal of Mining Science and Technology. doi:10.1016/j.ijmst.2014.03.015

Zhou, G., Li, S., Ma, Y., Ding, J. and Zhang, M., (2019). Synthesis and properties of a reinforcing dust-cementing material for thin spray-on liners in mine roadways. Advances in Materials Science and Engineering. doi: 10.1155/2019/8486534.

APPENDICES

A. SPECIMEN GEOMETRY TYPE AND PREPARATION TECHNIQUE DETERMINATION

T-I-D: Type I geometry, specimens prepared by die cutting technique

T-I-M: Type I geometry, specimens prepared by molding technique

T-IV-D: Type IV geometry, specimens prepared by die cutting technique

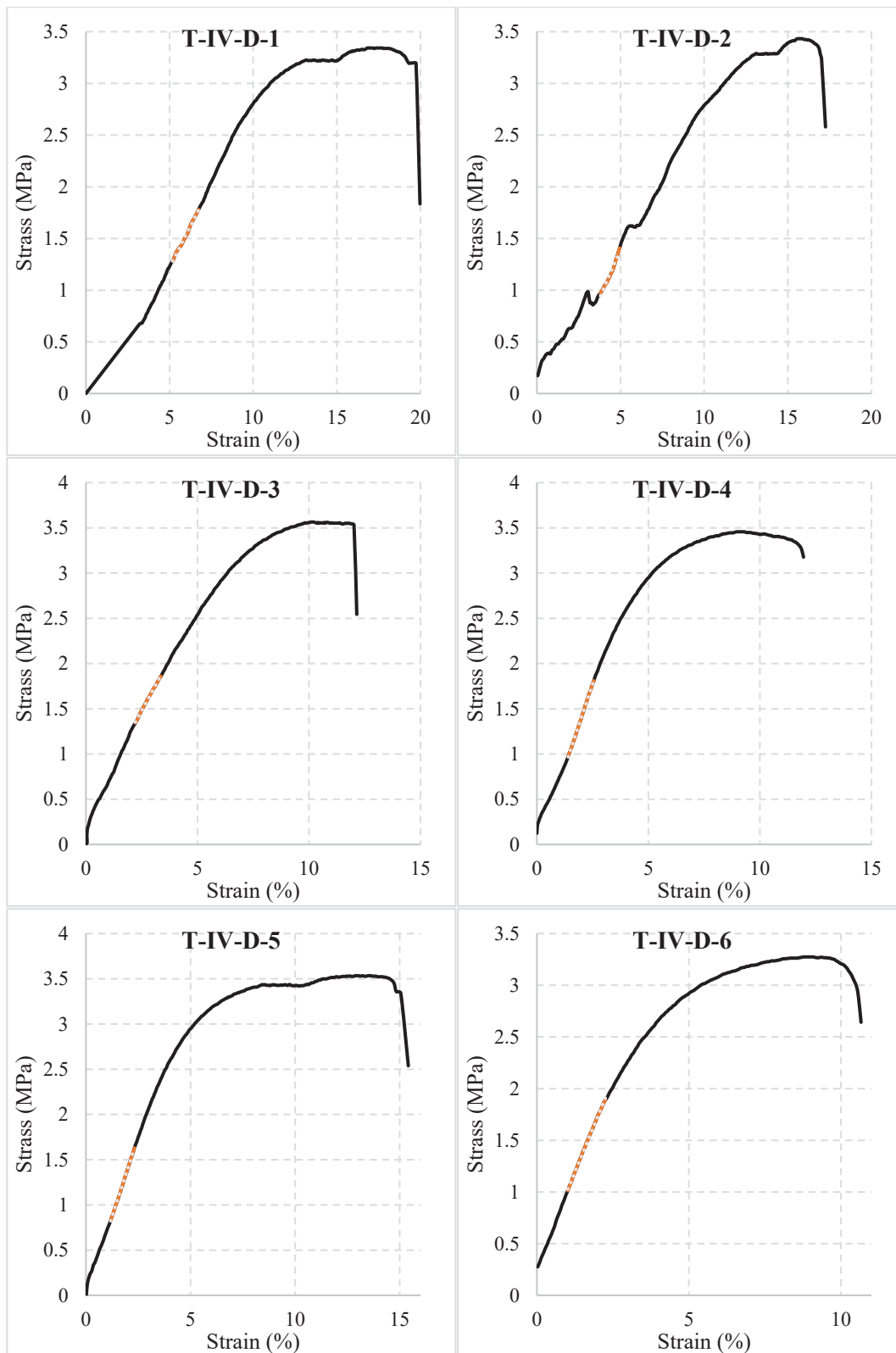**T-IV-M:**   Type IV geometry, specimens prepared by molding technique
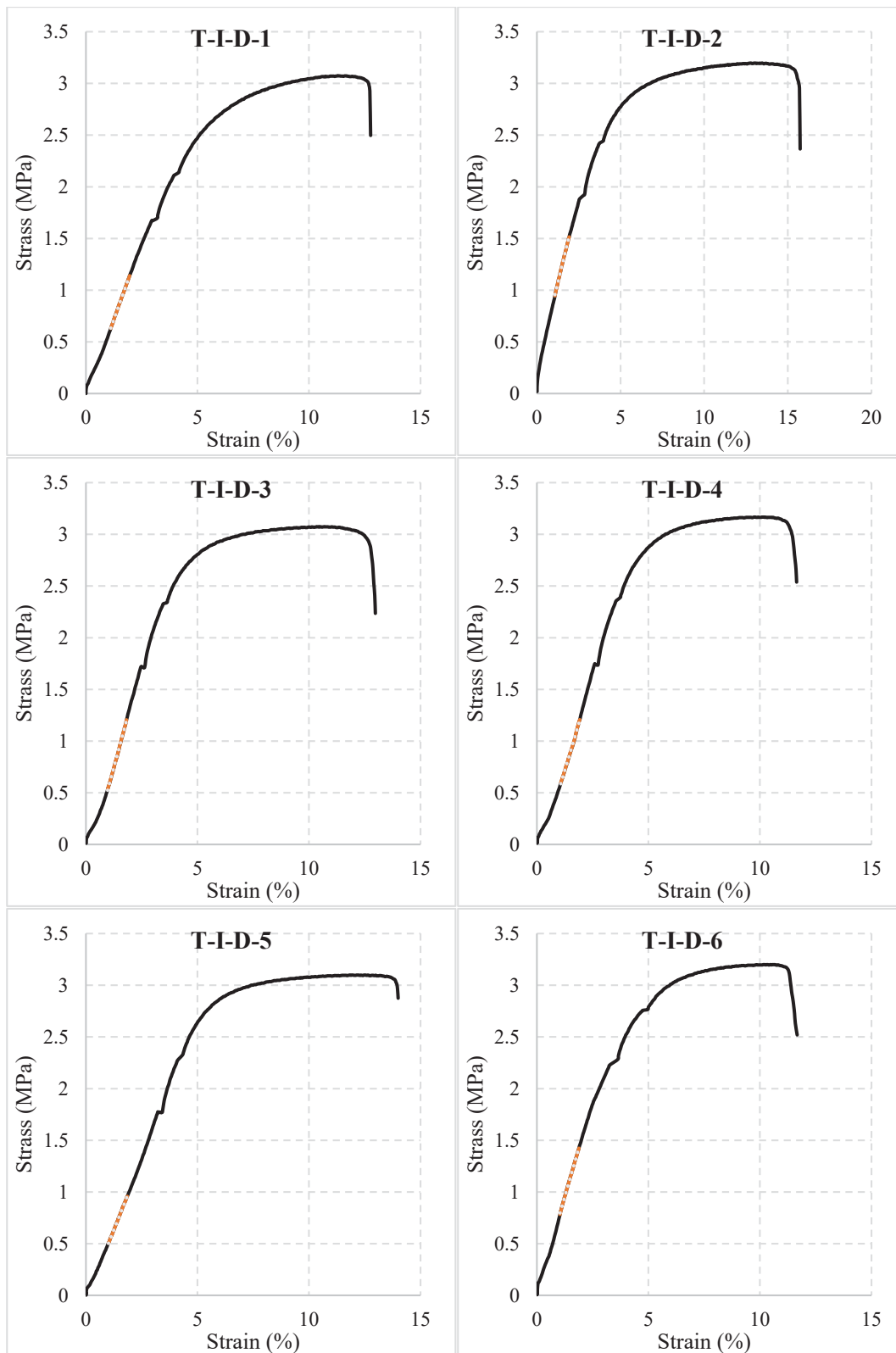
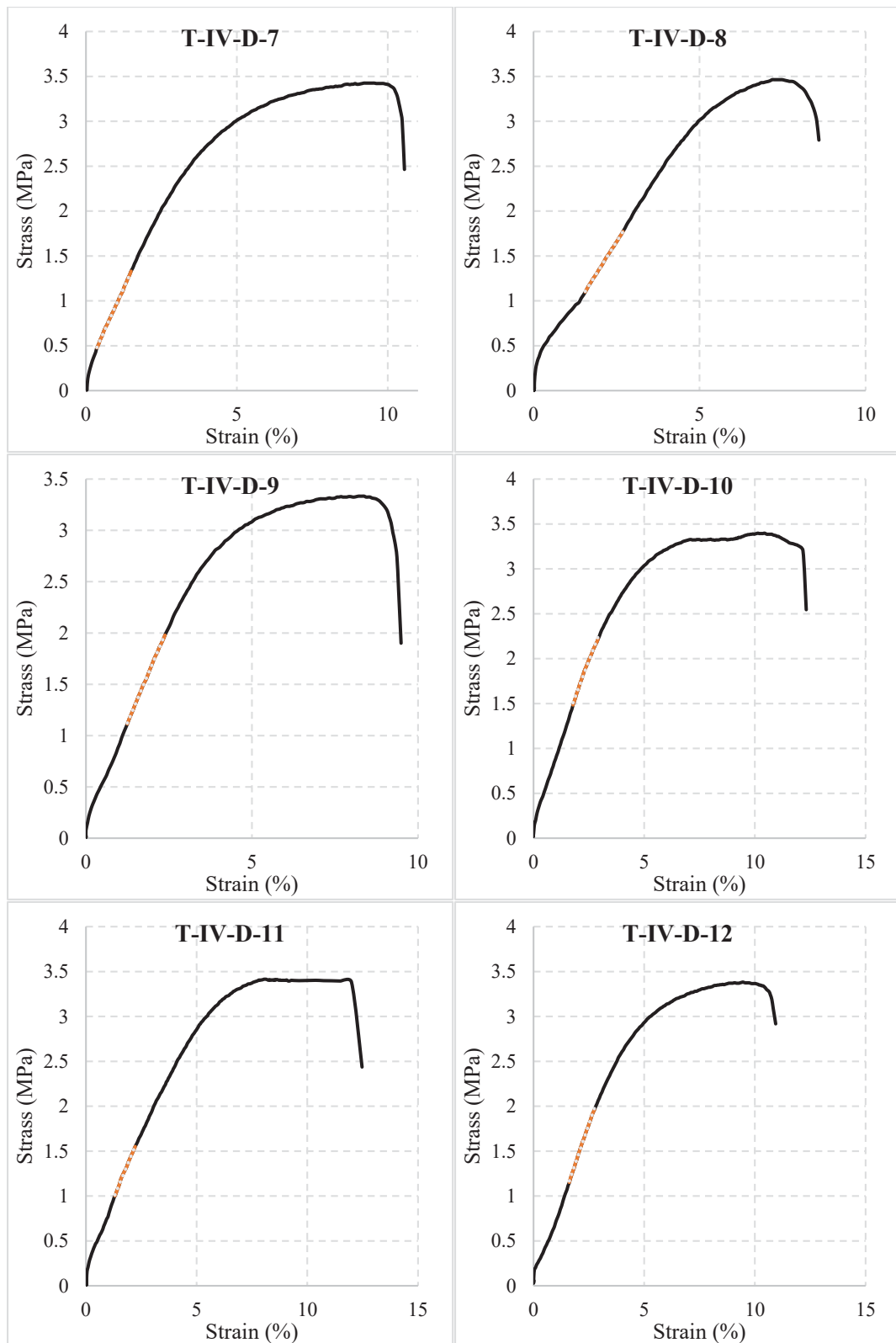Figure A.1 Stress- Strain Curves for Type-I Specimens Prepared by Die Cutter (Test No. 1-6)
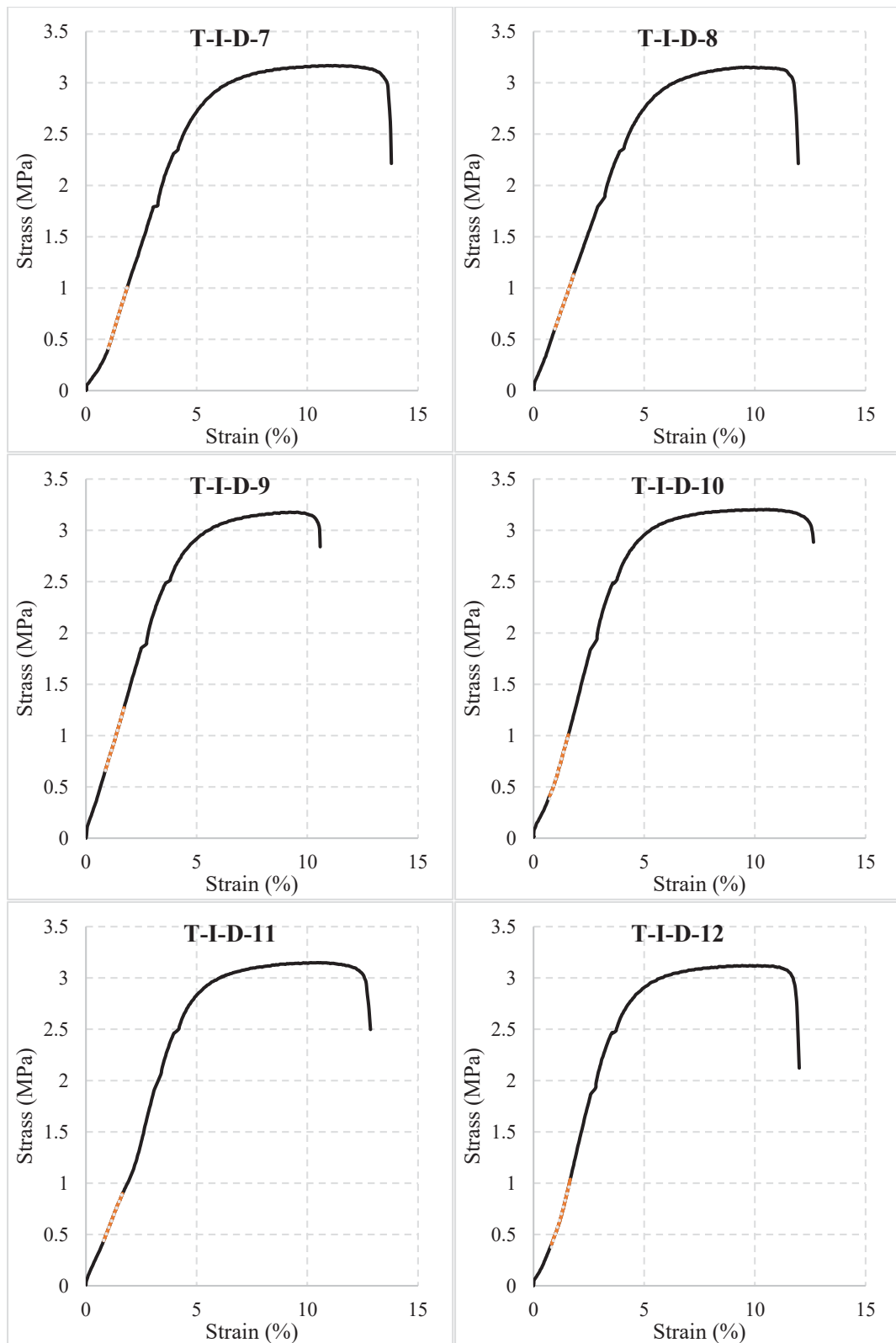
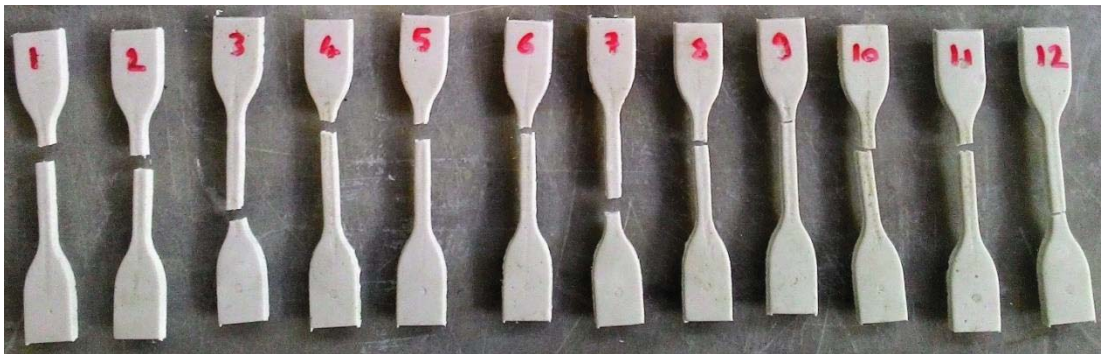Figure A.2 Stress- Strain Curves for Type-I Specimens Prepared by Die Cutter (Test No. 7-12)

Table A. 1. Tensile Test Results for Type-I Specimens Prepared by Die Cutter

T-I-D

Test No	Ult. Tensile Strength (MPa)	Tensile Modulus (MPa)	Elongation at break (%)	Yield Strength (MPa)
1	3.08	62.24	13.32	2.11
2	3.20	67.74	15.69	2.14
3	3.08	80.38	12.78	2.15
4	3.17	74.46	12.87	2.21
5	3.10	63.77	13.97	2.23
6	3.20	73.67	11.30	2.25
7	3.17	69.80	13.63	2.31
8	3.15	62.48	12.54	2.32
9	3.18	72.83	11.55	2.21
10	3.20	78.54	12.61	2.24
11	3.15	71.04	12.66	2.27
12	3.12	74.21	12.22	2.31
Avg.	**3.15**	**70.93**	**12.93**	**2.23**
Std. Dev.	**0.05**	**5.96**	**1.16**	**0.07**
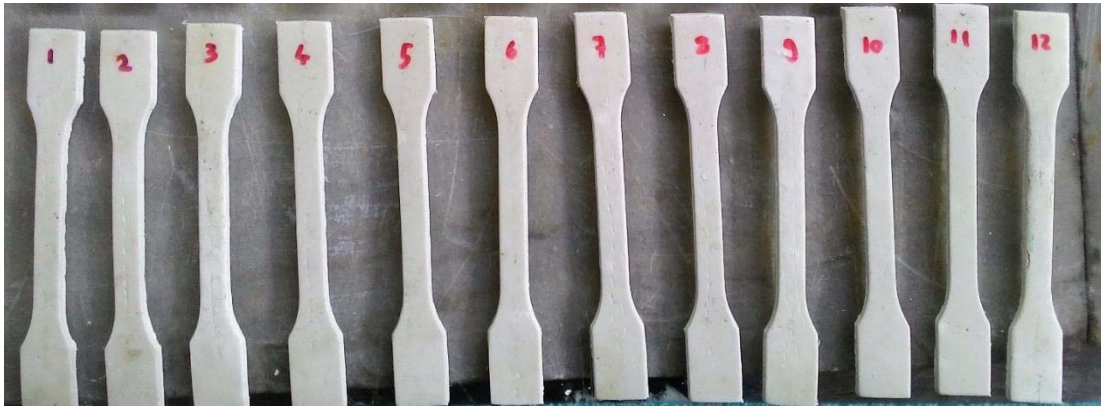
(a)

(b)

Figure A.3 Specimen Photos for Type-I Specimens Prepared by Die Cutter Before (a) and After (b) the Test
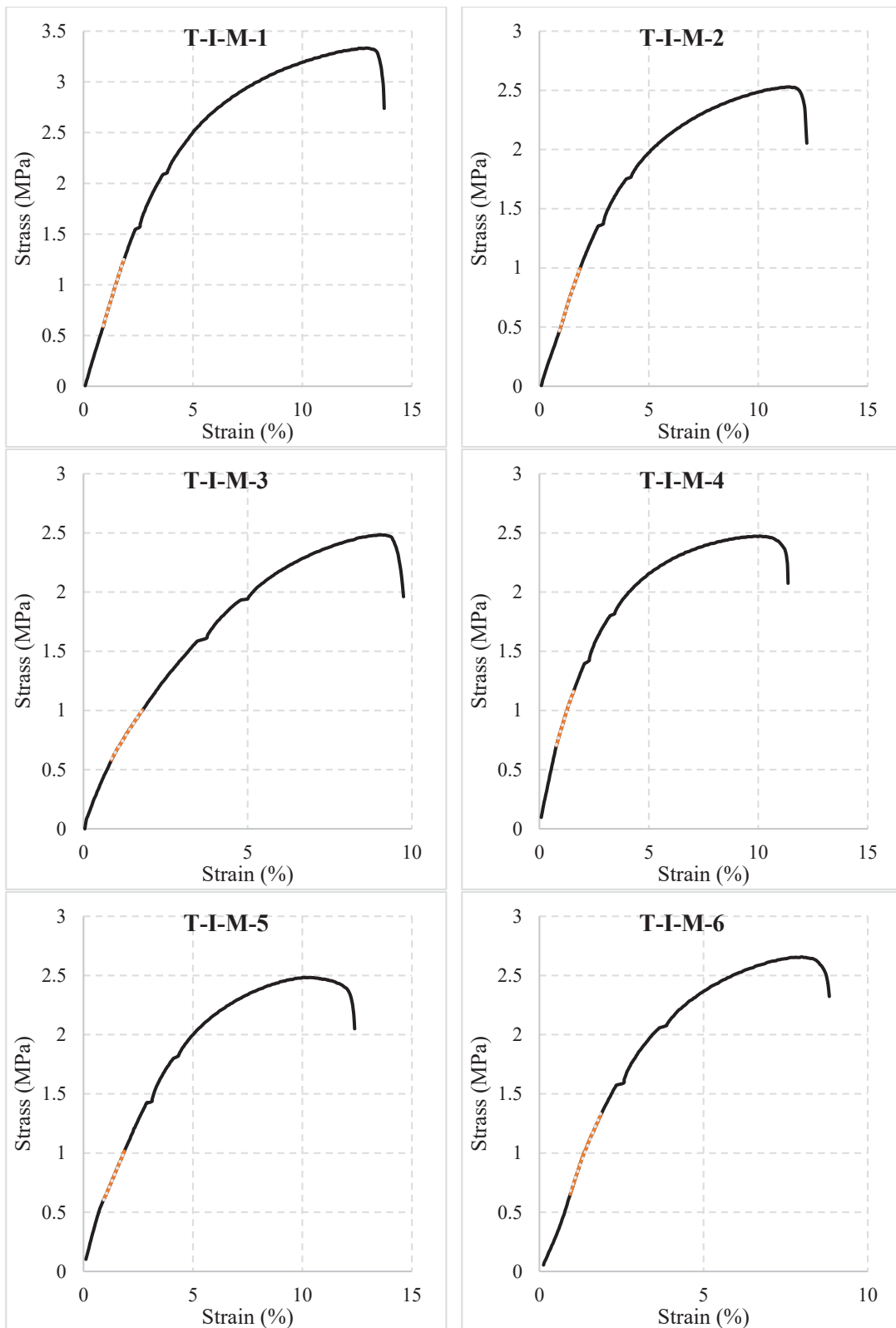
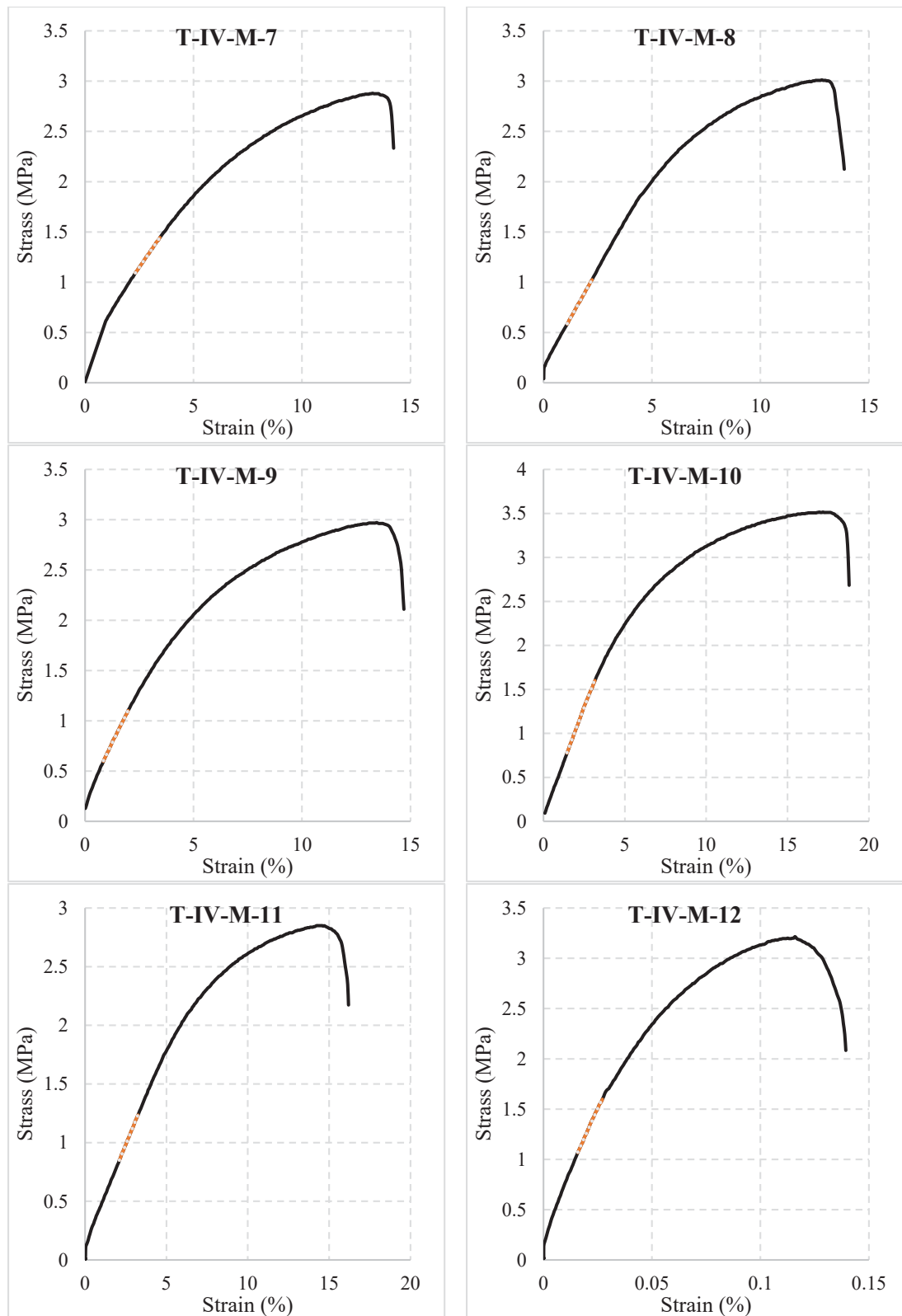Figure A.4 Stress- Strain Curves for Type-I Specimens Prepared by Molding (Test No. 1-6)
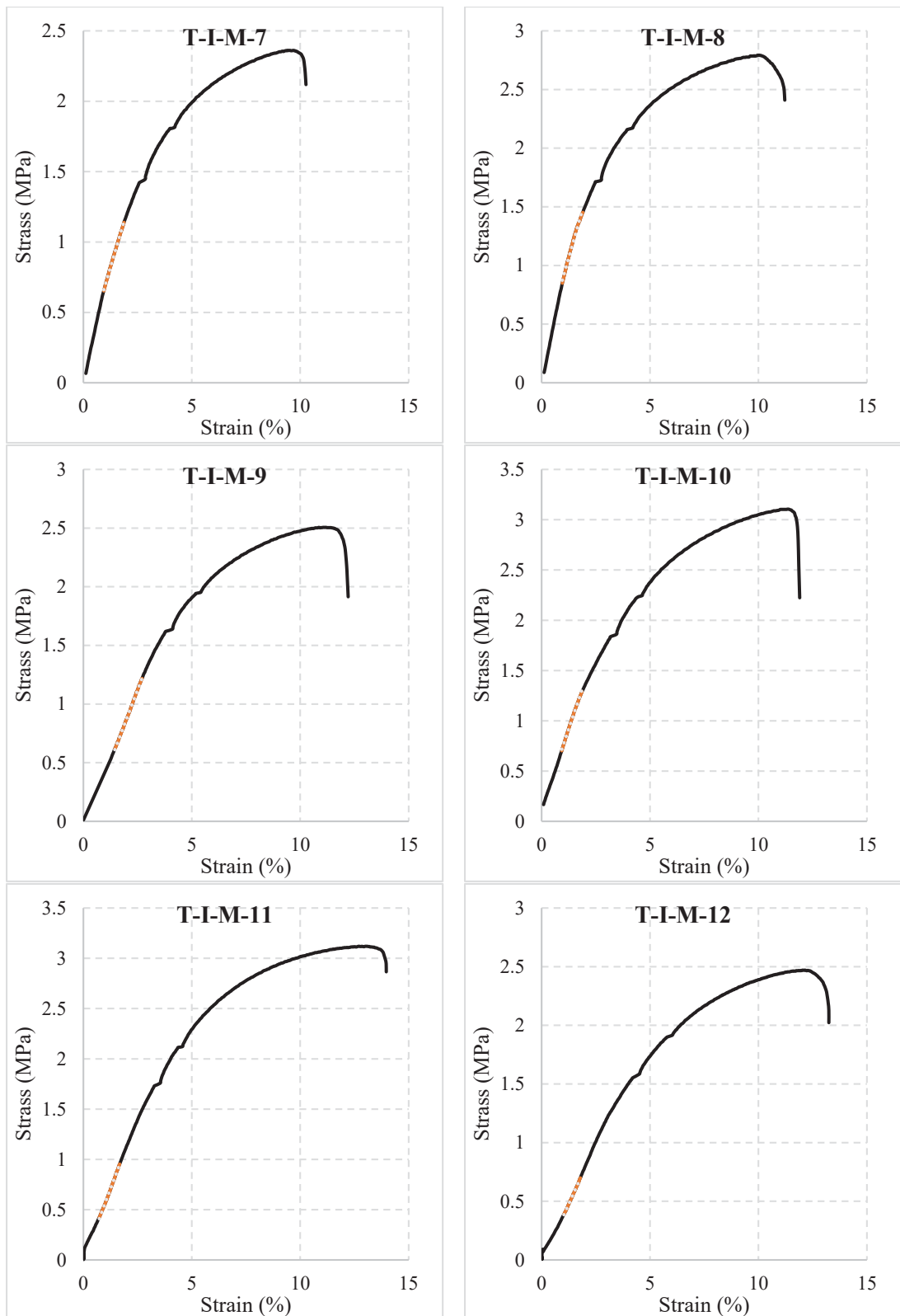
Figure A.5 Stress- Strain Curves for Type-I Specimens Prepared by Molding (Test No. 7-12)

Table A. 2. Tensile Test Results for Type-I Specimens Prepared by Molding

		T-I-M		
Test No	Ult. Tensile Strength (MPa)	Tensile Modulus (MPa)	Elongation at break (%)	Yield Strength (MPa)
1	3.33	69.83	13.71	2.10
2	2.53	55.35	12.14	1.75
3	2.49	42.34	9.71	1.92
4	2.47	53.16	11.35	1.77
5	2.48	43.74	12.35	1.93
6	2.66	63.95	8.83	1.94
7	2.36	49.27	10.12	1.64
8	2.79	76.33	11.21	1.70
9	2.51	46.51	11.35	1.54
10	3.10	67.70	11.75	1.82
11	3.12	58.27	13.98	2.17
12	2.47	43.77	13.24	1.87
Avg.	**2.69**	**55.85**	**11.65**	**1.85**
Std. Dev.	**0.32**	**11.44**	**1.58**	**0.18**
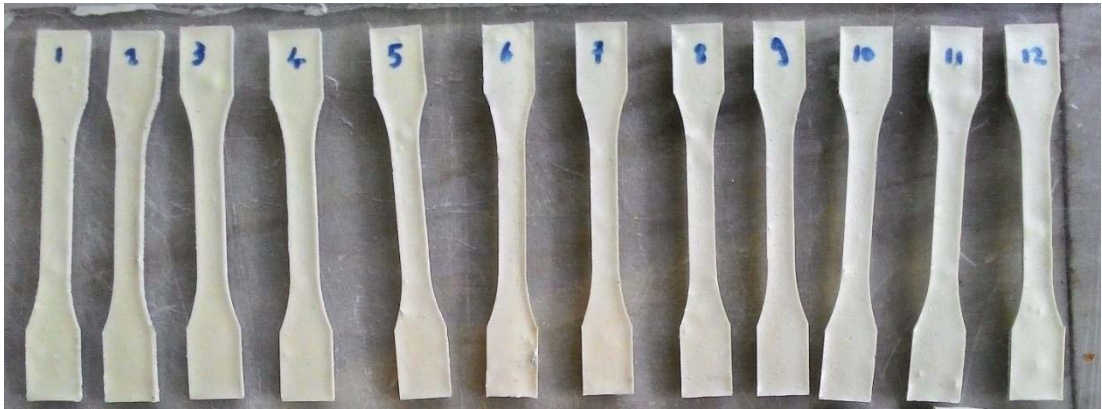
(a)

(b)

Figure A.6 Specimen Photos for Type-I Specimens Prepared by Molding Before (a) and After (b) the Test

Figure A.7 Stress- Strain Curves for Type-IV Specimens Prepared by Die Cutter (Test No. 1-6)

Figure A.8 Stress- Strain Curves for Type-IV Specimens Prepared by Die Cutter (Test No. 7-12)

Table A. 3. Tensile Test Results for Type-IV Specimens Prepared by Die Cutter

T-IV-D

Test No	Ult. Tensile Strength (MPa)	Tensile Modulus (MPa)	Elongation at break (%)	Yield Strength (MPa)
1	3.34	53.58	11.75	2.74
2	3.43	49.40	12.65	2.62
3	3.56	55.97	12.11	3.02
4	3.46	59.08	12.05	2.75
5	3.53	68.15	15.01	2.68
6	3.27	66.94	10.65	2.46
7	3.42	60.84	10.47	2.75
8	3.46	59.91	12.41	2.99
9	3.33	61.02	11.19	2.57
10	3.40	57.70	12.17	2.74
11	3.41	59.98	12.25	2.74
12	3.38	60.25	10.82	2.54
Avg.	**3.42**	**59.40**	**11.96**	**2.72**
Std. Dev.	**0.08**	**5.12**	**1.21**	**0.17**

(a)

(b)

Figure A.9 Specimen Photos for Type-IV Specimens Prepared by Die Cutter Before (a) and After (b) the Test
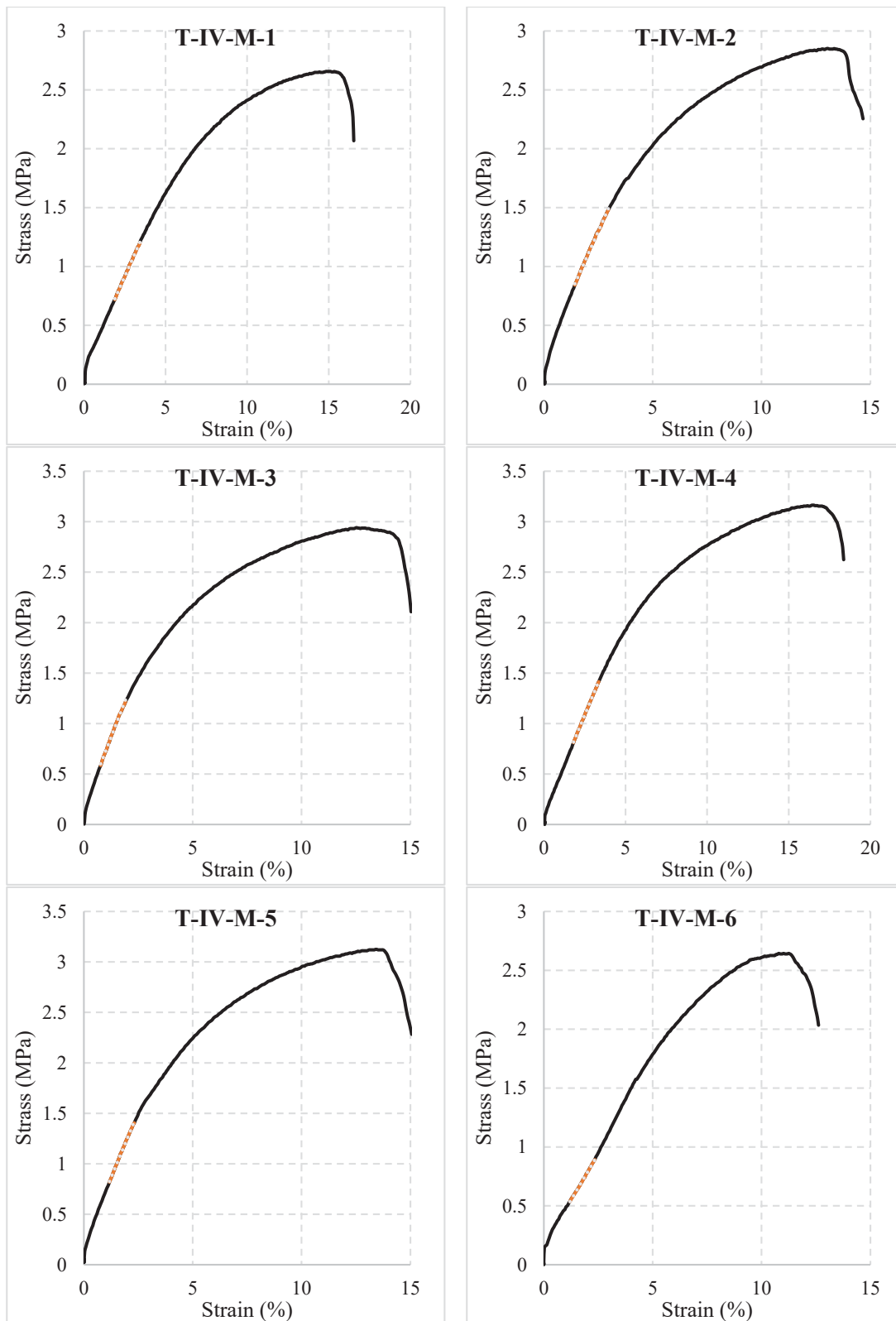
Figure A.10 Stress- Strain Curves for Type-IV Specimens Prepared by Molding (Test No. 1-6)

Figure A.11 Stress- Strain Curves for Type-IV Specimens Prepared by Molding
(Test No. 7-12)

Table A. 4. Tensile Test Results for Type-IV Specimens Prepared by Molding

T-IV-M

Test No	Ult. Tensile Strength (MPa)	Tensile Modulus (MPa)	Elongation at break (%)	Yield Strength (MPa)
1	2.66	31.26	16.36	1.85
2	2.85	52.01	14.09	1.85
3	2.94	58.45	14.69	1.98
4	3.16	38.25	17.50	2.23
5	3.12	56.80	13.41	1.96
6	2.64	35.58	12.10	2.40
7	2.88	28.27	14.11	2.23
8	3.01	38.90	13.40	2.29
9	2.97	36.68	14.17	2.20
10	3.52	57.72	18.40	2.24
11	2.85	33.79	15.79	2.06
12	3.22	55.75	14.25	2.61
Avg.	**2.99**	**43.62**	**14.86**	**2.16**
Std. Dev.	**0.24**	**11.52**	**1.82**	**0.23**
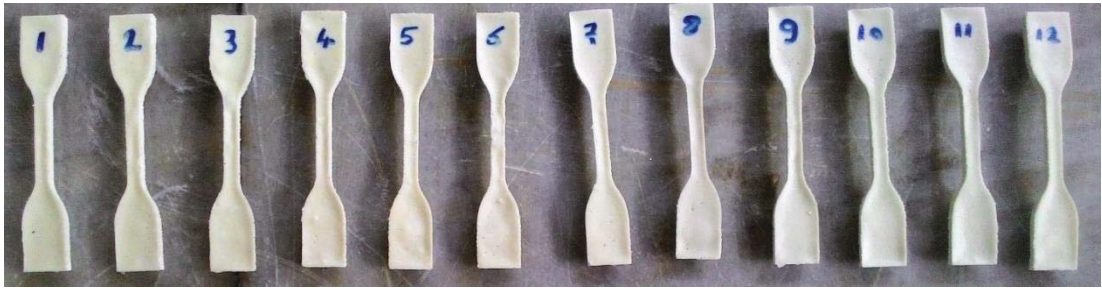
(a)
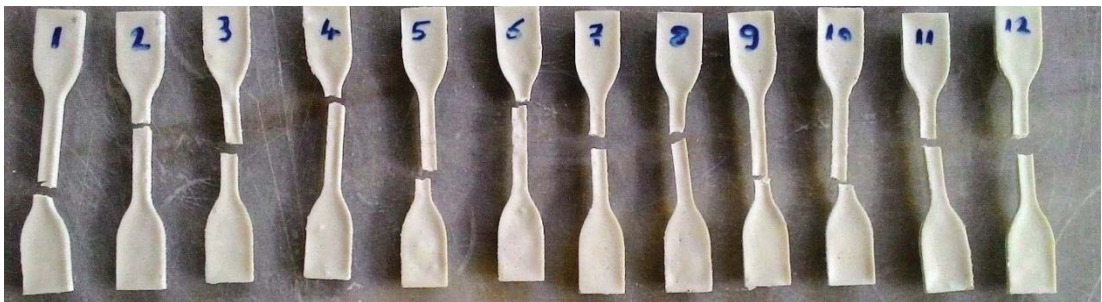
(b)

Figure A.12 Specimen Photos for Type-IV Specimens Prepared by Molding Before (a) and After (b) the Test

B. TSL-1 TEST RESULTS

TSL-1 TENSILE TEST RESULTS

Table B. 1. Tensile Test Results for 1-day Cured TSL-1

Test No.	1-Day	
	Failure Load (N)	Ultimate Tensile Strength (MPa)
1	68.38	1.23
2	71.42	1.34
3	69.75	1.34
4	71.51	1.35
5	70.04	1.23
6	69.45	138
7	70.73	1.36
Avg.	**70.14**	**1.32**
Std. Dev.	**1.08**	**0.06**

(a)   (b)
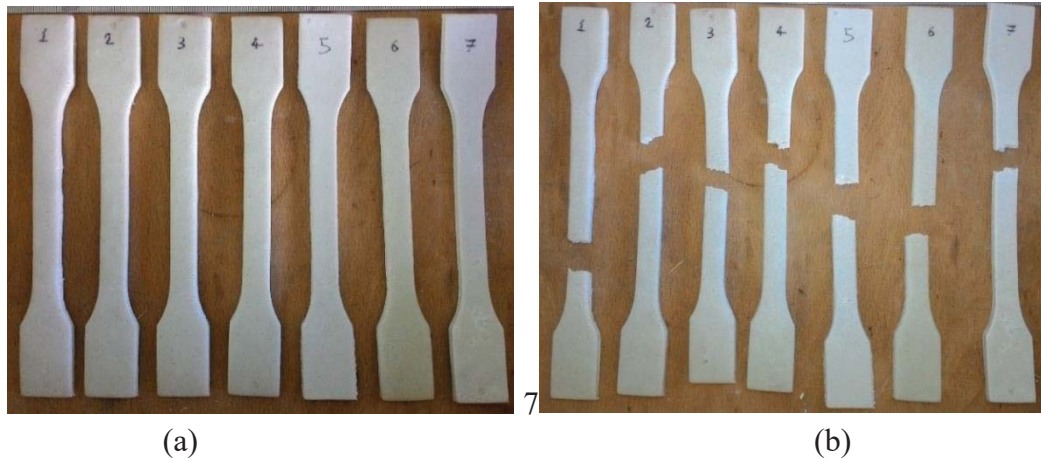
Figure B. 1. Specimen Photos Before (a) and After (b) Tensile tests (TSL-1, 1-day)

173

Table B. 2. Tensile Test Results for 7-day Cured TSL-1

| Test No. | 7-Day | |
	Failure Load (N)	Ultimate Tensile Strength (MPa)
1	166.08	2.99
2	161.87	2.96
3	151.47	2.82
4	164.42	2.95
5	161.08	2.88
6	160.20	2.86
Avg.	**160.88**	**2.91**
Std. Dev.	**5.10**	**0.07**

(a)

(b)

Figure B. 2. Specimen Photos Before (a) and After (b) Tensile tests (TSL-1, 7-day)

Table B. 3. Tensile Test Results for 14-day Cured TSL-1

| Test No. | 14-Day | |
	Failure Load (N)	Ultimate Tensile Strength (MPa)
1	185.51	3.48
2	197.38	3.67
3	190.12	3.58
4	180.41	3.34
5	180.90	3.33
6	173.24	3.29
7	186.88	3.37
8	189.82	3.73
Avg.	**185.51**	**3.47**
Std. Dev.	**7.65**	**0.15**

<center>(a)</center> <center>(b)</center>

Figure B. 3. Specimen Photos Before (a) and After (b) Tensile tests (TSL-1, 14-day)

Table B. 4. Tensile Test Results for 500-day Cured TSL-1

Test No.	500-Day	
	Failure Load (N)	Ultimate Tensile Strength (MPa)
1	188.11	3.55
2	196.40	3.71
3	192.57	3.63
4	185.17	3.49
5	198.31	3.74
6	191.30	3.61
7	198.95	3.75
8	209.15	3.95

9	206.60	3.90
Avg.	**196.28**	**3.70**
Std. Dev.	**8.00**	**0.15**
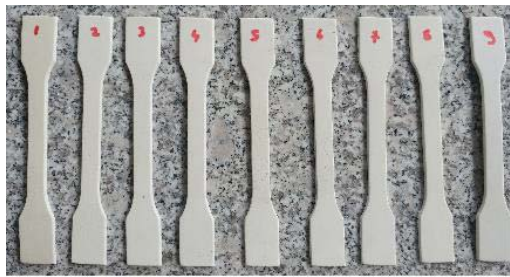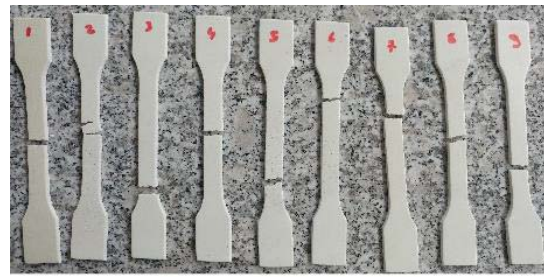
(a)   (b)

Figure B. 4. Specimen Photos Before (a) and After (b) Tensile tests (TSL-1, 500-day)
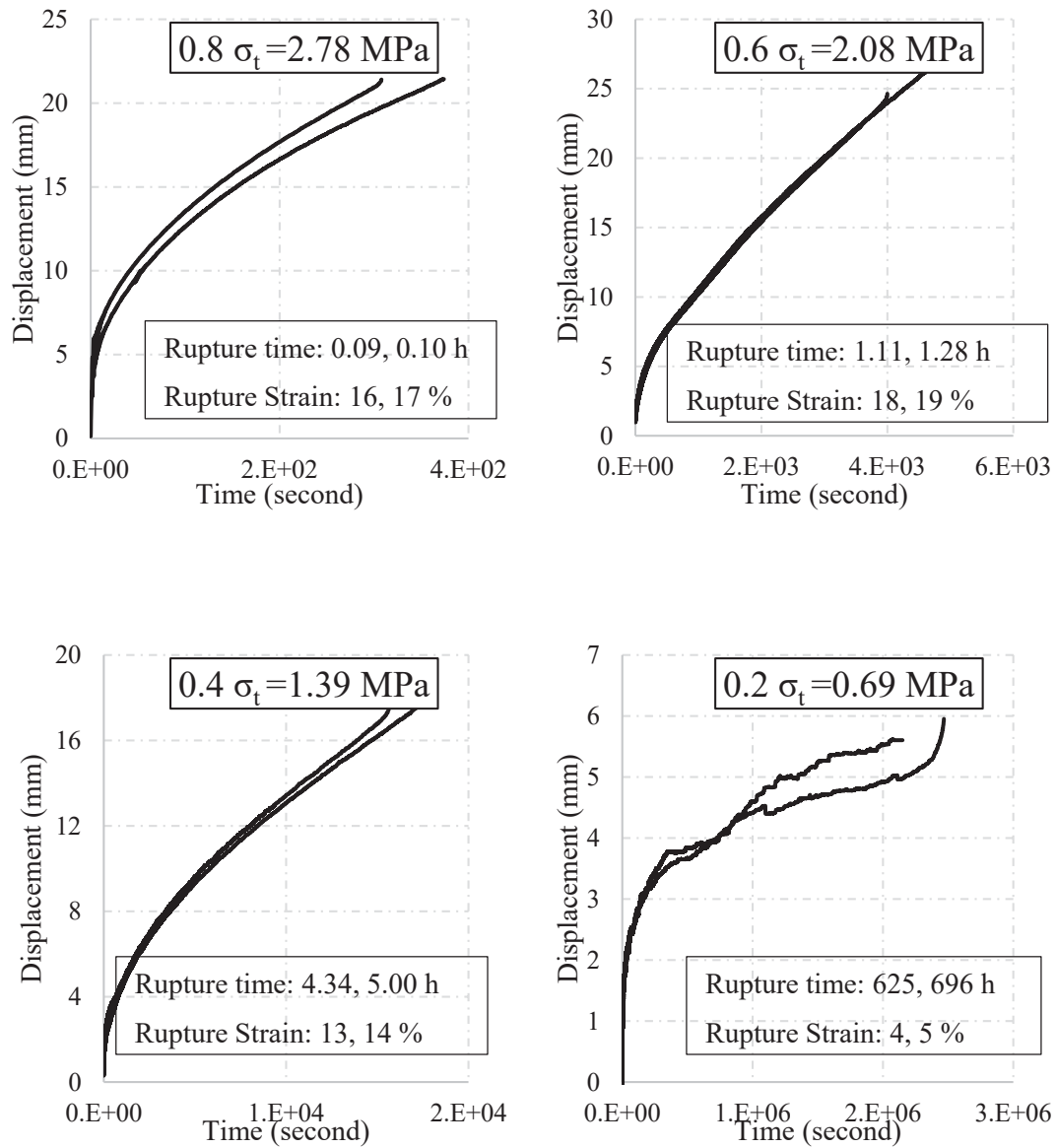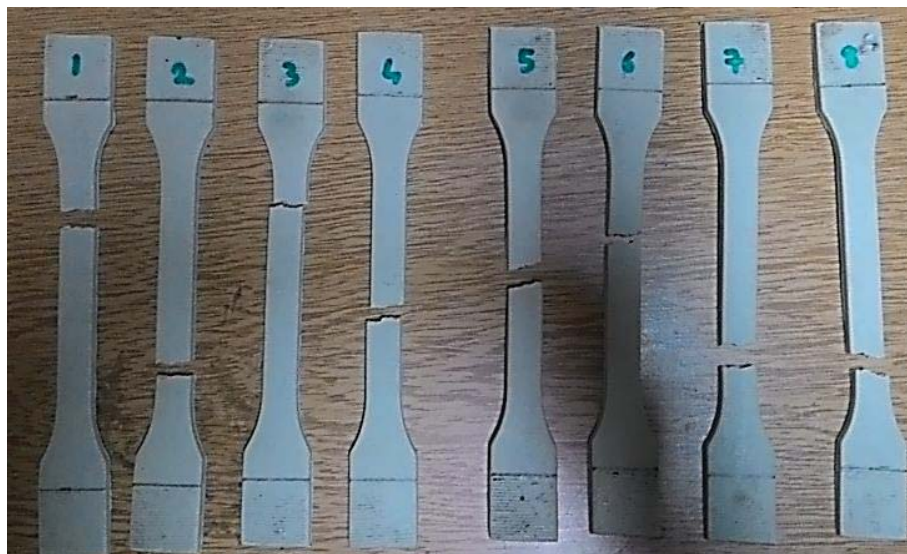
TSL-1 CREEP TEST RESULTS

1-Day Raw Data
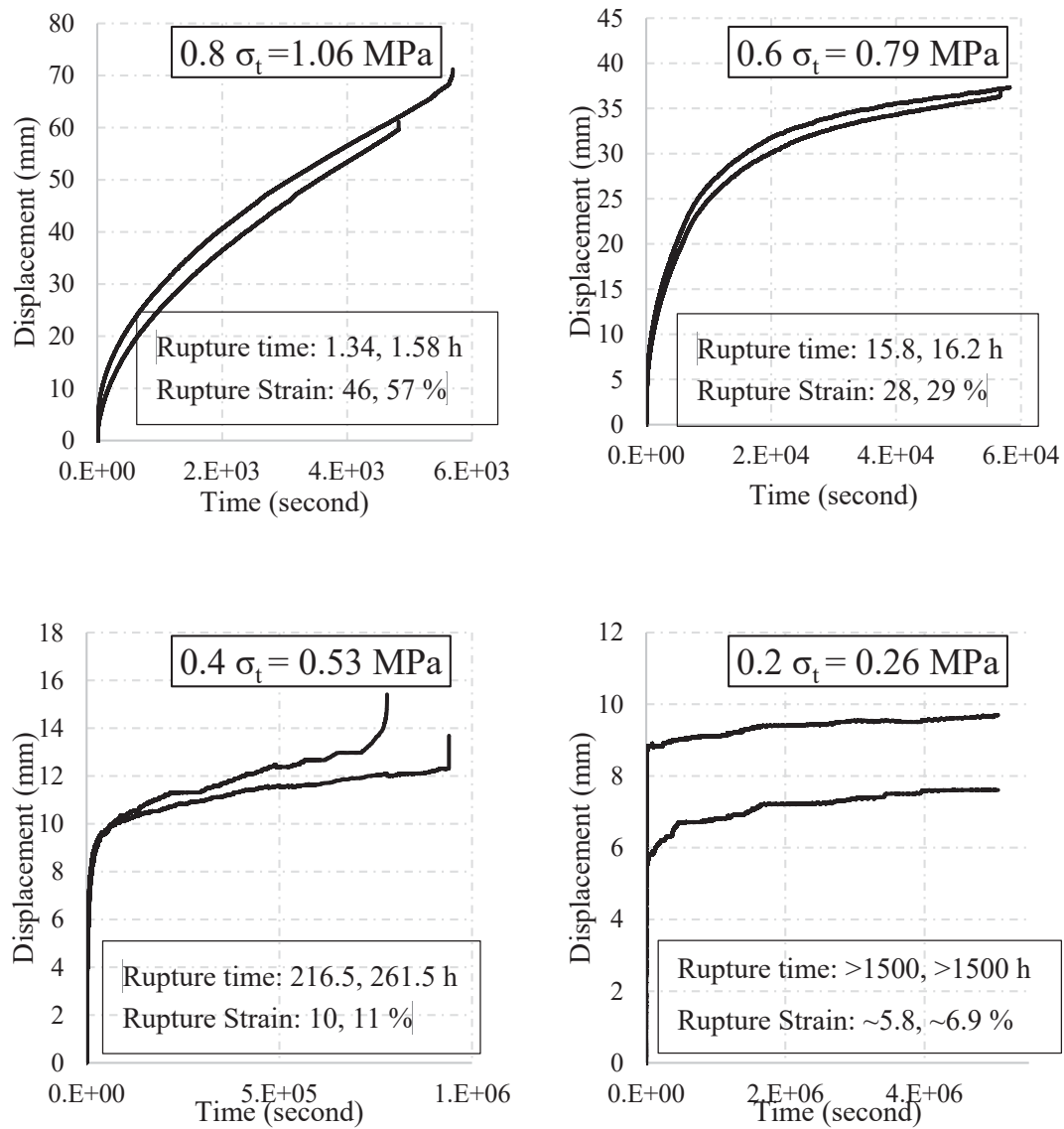
Figure B. 5. Raw Experimental Data from 1-day Creep Tests for Various Stress Levels (TSL-1)
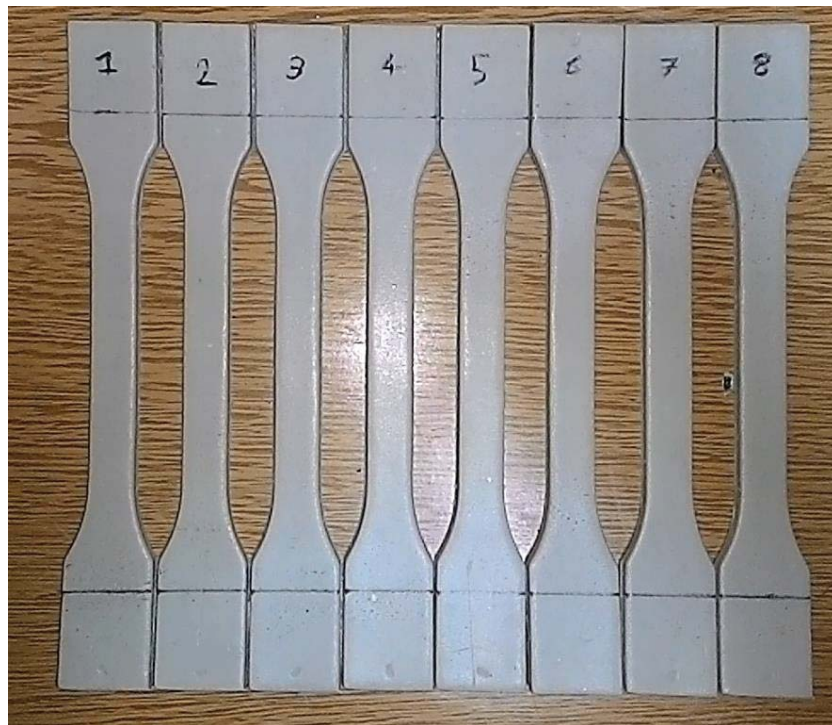
(a)
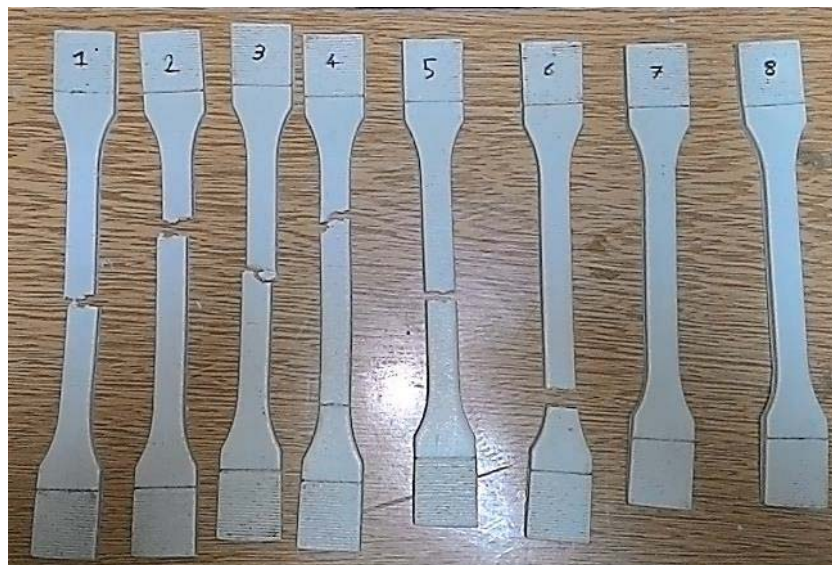
(b)
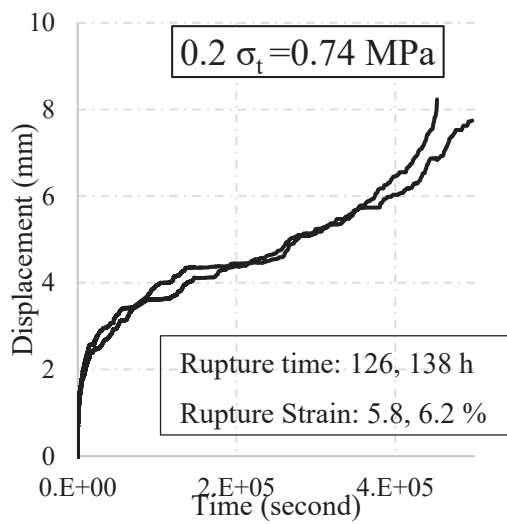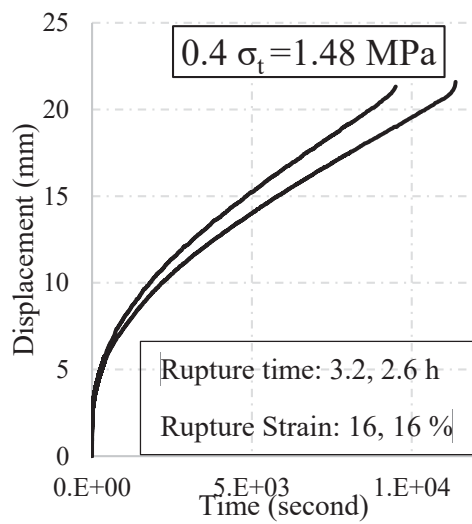Figure B. 6. Specimen Photos Before (a) and After (b) Creep Tests (TSL-1, 1-day)

7-Day Raw Data
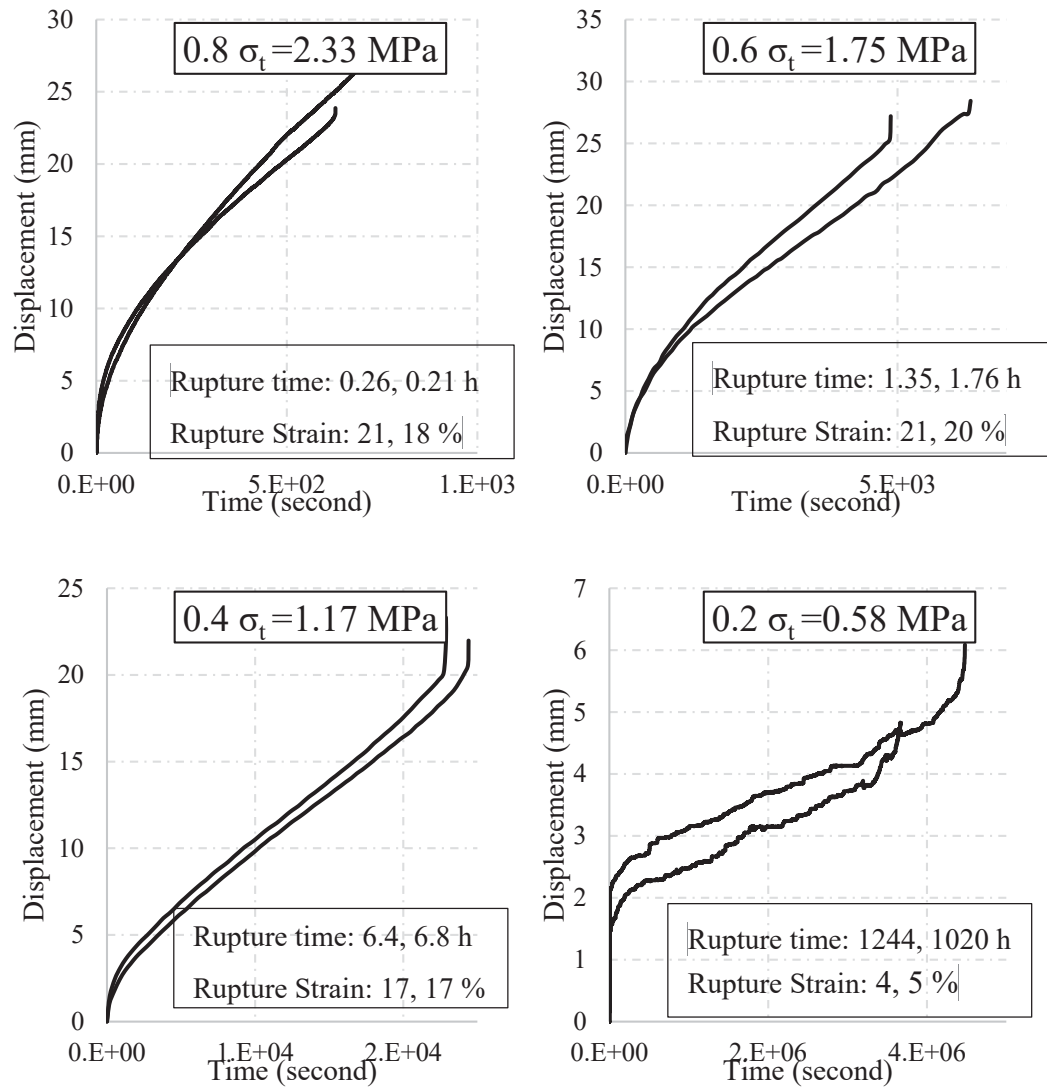
Figure B. 7. Raw Experimental Data from 7-day Creep Tests for Various Stress Levels (TSL-1)
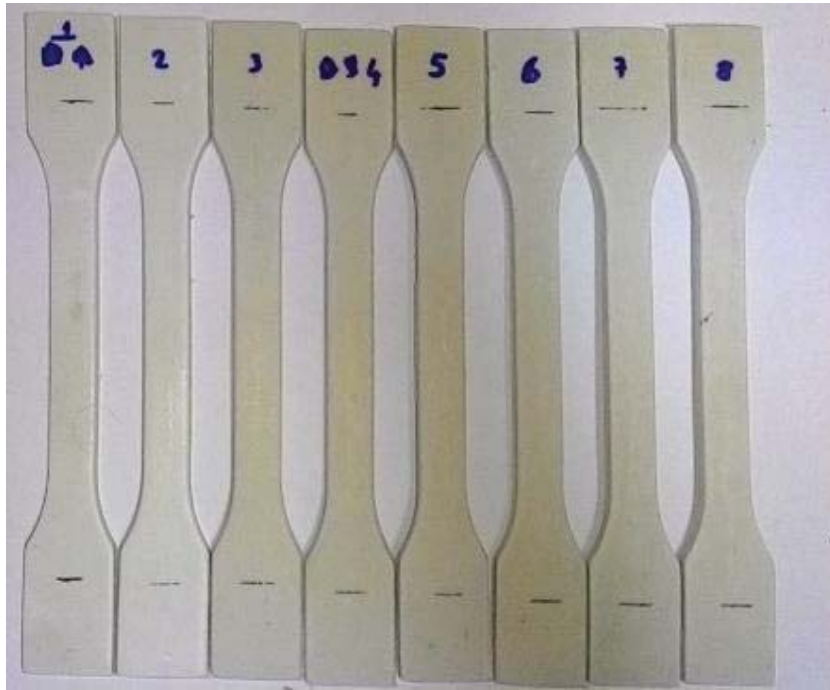
(a)
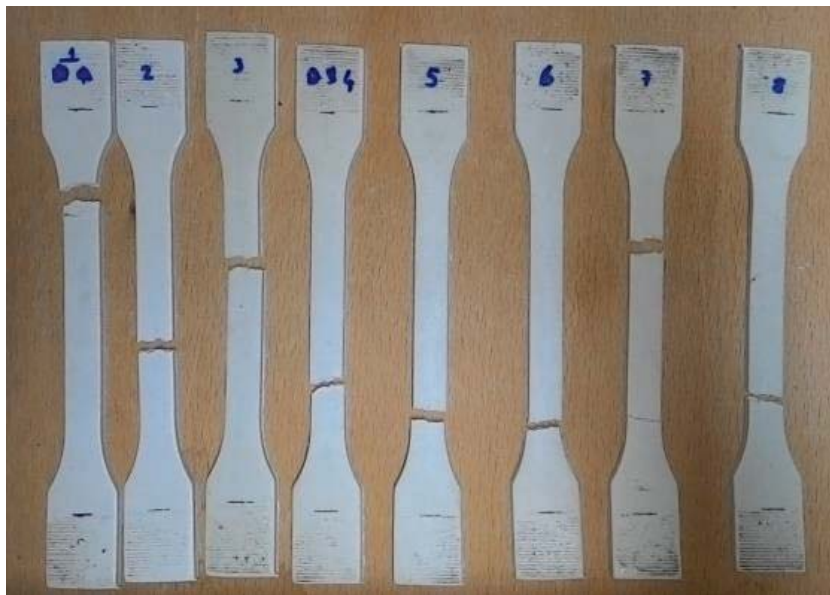
(b)

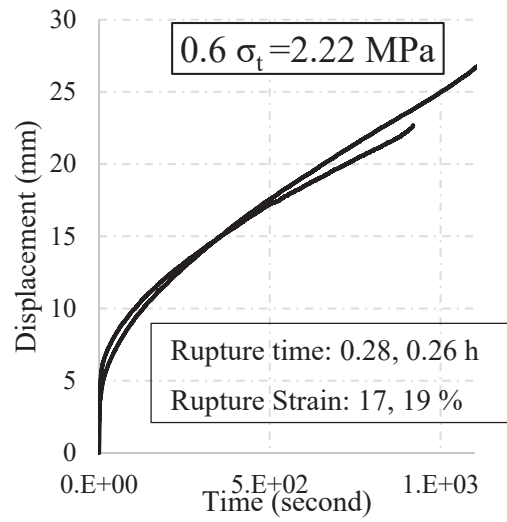Figure B. 8. Specimen Photos Before (a) and After (b) Creep Tests (TSL-1, 7-day)

14-Day Raw Data

Figure B. 9. Raw Experimental Data from 14-day Creep Tests for Various Stress Levels (TSL-1)

(a)

(b)

Figure B. 10. Specimen Photos Before (a) and After (b) Creep Tests (TSL-1, 14-day)
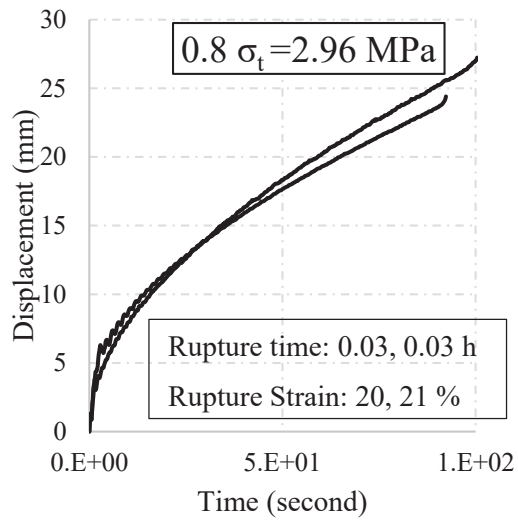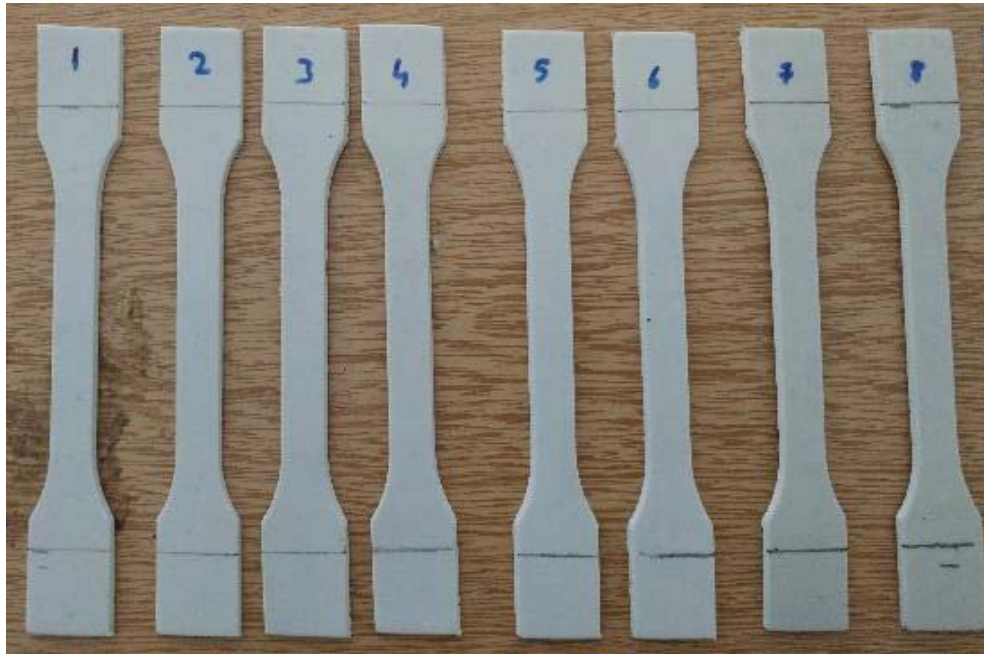
500-Day Raw Data

Displacement (mm) vs Time (second), 0.8 σ_t=2.96 MPa, Rupture time: 0.03, 0.03 h, Rupture Strain: 20, 21 %

0.6 σ_t=2.22 MPa, Rupture time: 0.28, 0.26 h, Rupture Strain: 17, 19 %

0.4 σ_t=1.48 MPa, Rupture time: 3.2, 2.6 h, Rupture Strain: 16, 16 %

0.2 σ_t=0.74 MPa, Rupture time: 126, 138 h, Rupture Strain: 5.8, 6.2 %

Figure B. 11. Raw Experimental Data from 500-day Creep Tests for Various Stress
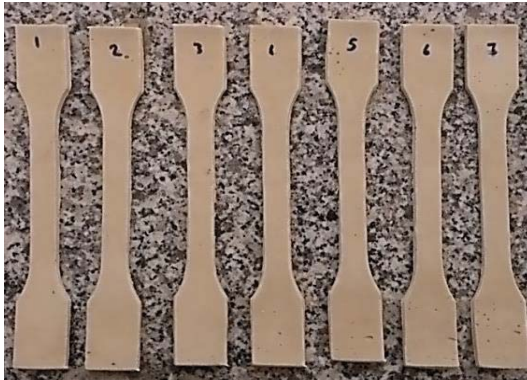Levels (TSL-1)

(a)

(b)

Figure B. 12. Specimen Photos Before (a) and After (b) Creep Tests (TSL-1, 500-day)

C. TSL-2 TEST RESULTS

TSL-2 TENSILE TEST RESULTS

Table C. 1. Tensile Test Results for 2-day Cured TSL-2

Test No.	2-Day	
	Failure Load (N)	Ultimate Tensile Strength (MPa)
1	90.45	1.76
2	95.65	1.89
3	93.78	1.84
4	94.67	1.88
5	92.41	1.81
6	92.31	1.82
7	93.39	1.85
Avg.	**93.24**	**1.84**
Std. Dev.	**1.71**	**0.04**

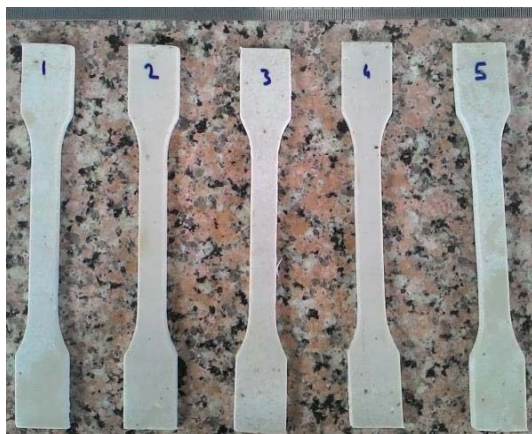(a)   (b)

Figure C. 1. Specimen Photos Before (a) and After (b) Tensile tests (TSL-2, 2-day)

Table C. 2. Tensile Test Results for 7-day Cured TSL-2

| Test No. | 7-Day | |
	Failure Load (N)	Ultimate Tensile Strength (MPa)
1	108.40	2.15
2	107.71	2.09
3	105.16	2.08
4	104.18	2.03
5	110.17	2.13
Avg.	**107.13**	**2.10**
Std. Dev.	**2.44**	**0.05**
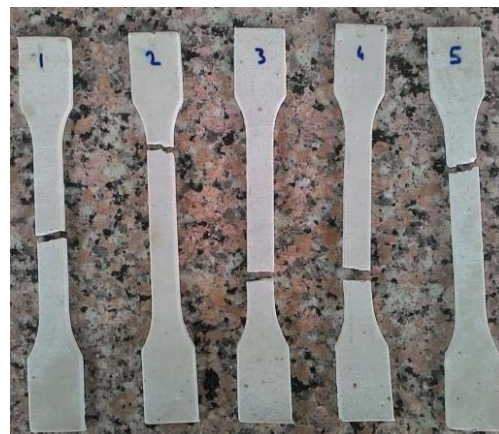
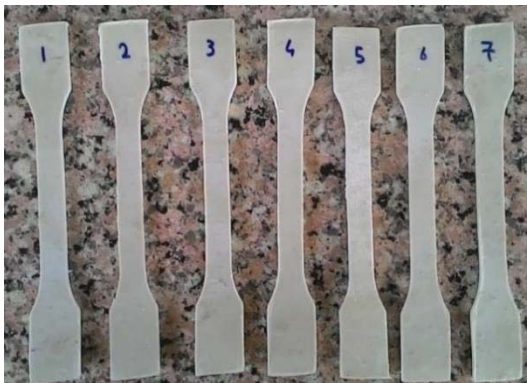(a)   (b)

Figure C. 2. Specimen Photos Before (a) and After (b) Tensile tests (TSL-2, 7-day)

Table C. 3. Tensile Test Results for 14-day Cured TSL-2

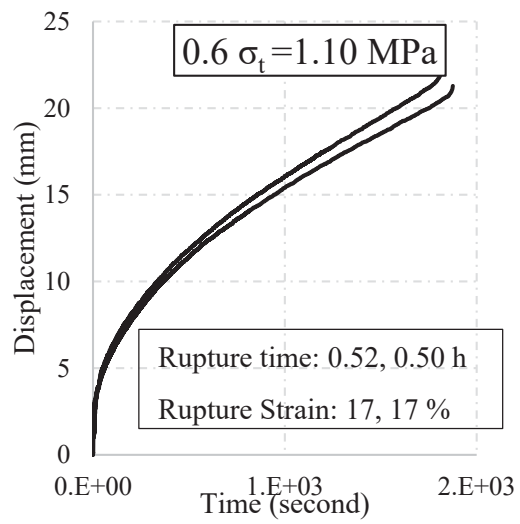| Test No. | 14-Day | |
	Failure Load (N)	Ultimate Tensile Strength (MPa)
1	127.73	2.50
2	131.06	2.51
3	129.39	2.51
4	149.11	2.96
5	144.01	2.96
6	140.87	2.70
7	135.87	2.52
Avg.	**136.86**	**2.67**
Std. Dev.	**8.07**	**0.21**
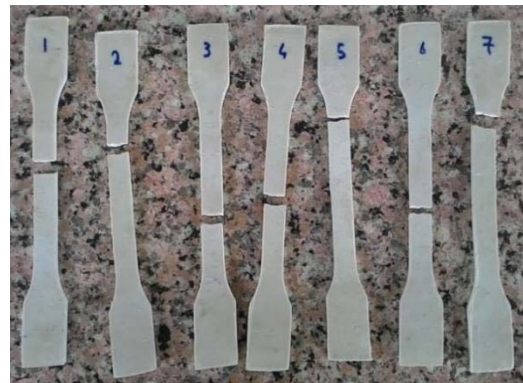
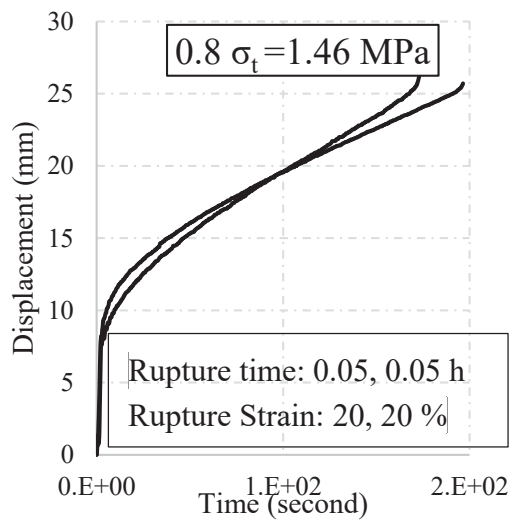(a)   (b)

Figure C. 3. Specimen Photos Before (a) and After (b) Tensile tests (TSL-2, 14-day)

TSL-2 CREEP TEST RESULTS

2-Day Raw Data

Figure C. 4. Raw Experimental Data from 2-day Creep Tests for Various Stress Levels (TSL-2)

(a)

(b)

Figure C. 5. Specimen Photos Before (a) and After (b) Creep Tests (TSL-2, 2-day)
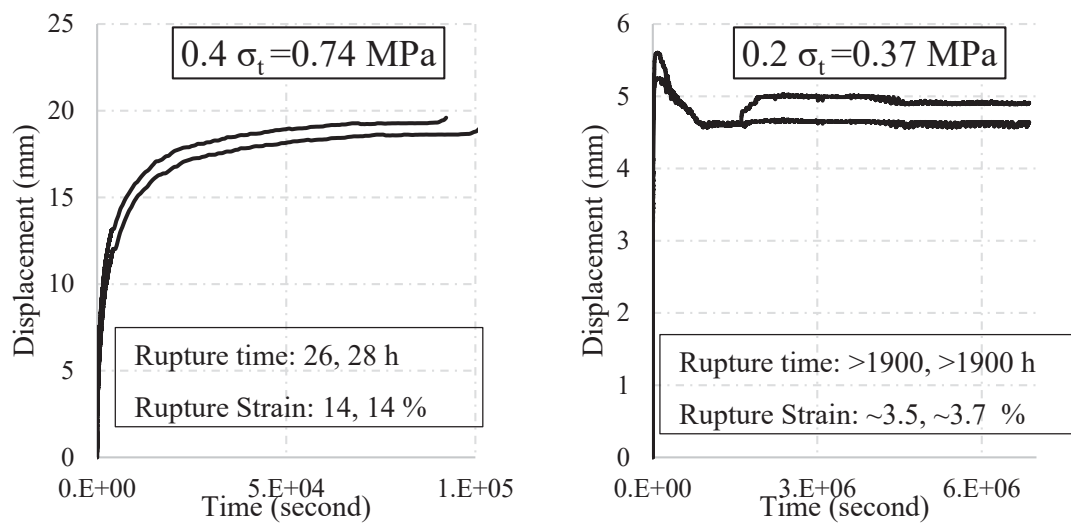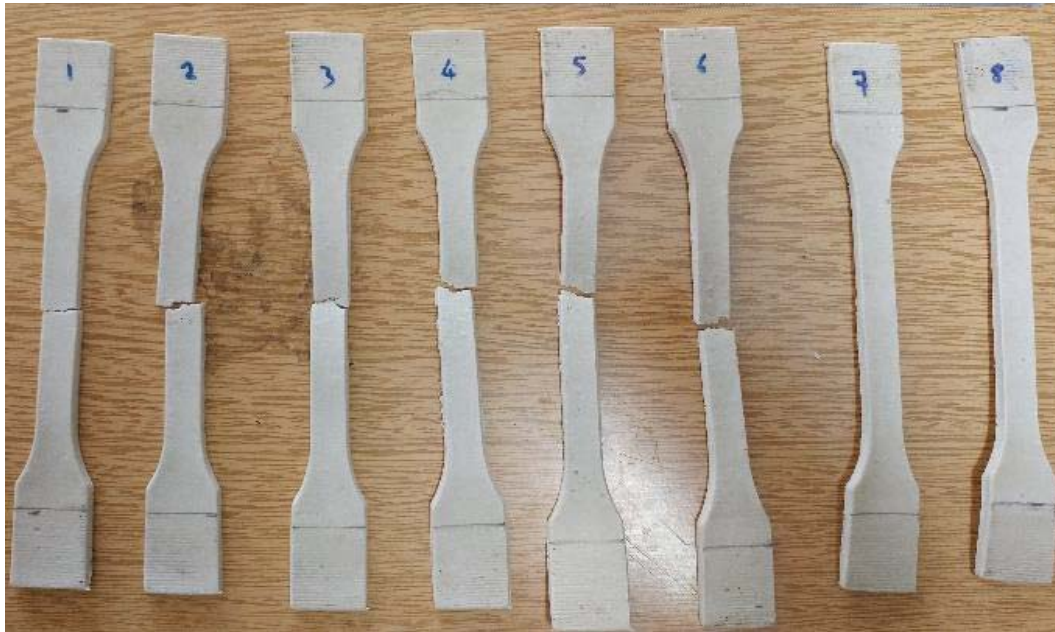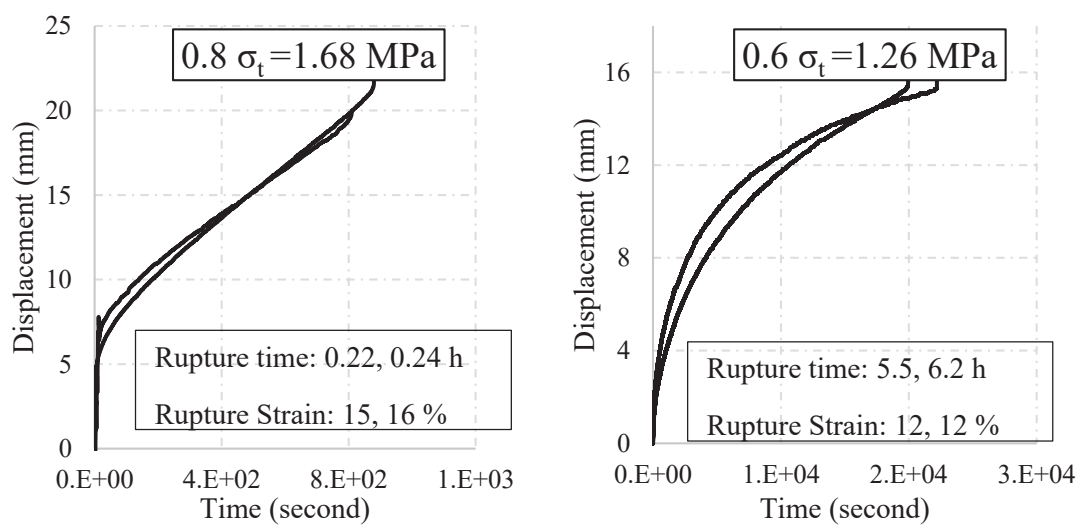
7-Day Raw Data

Figure C. 6. Raw Experimental Data from 7-day Creep Tests for Various Stress
Levels (TSL-2)

(a)

(b)

Figure C. 7. Specimen Photos Before (a) and After (b) Creep Tests (TSL-2, 7-day)
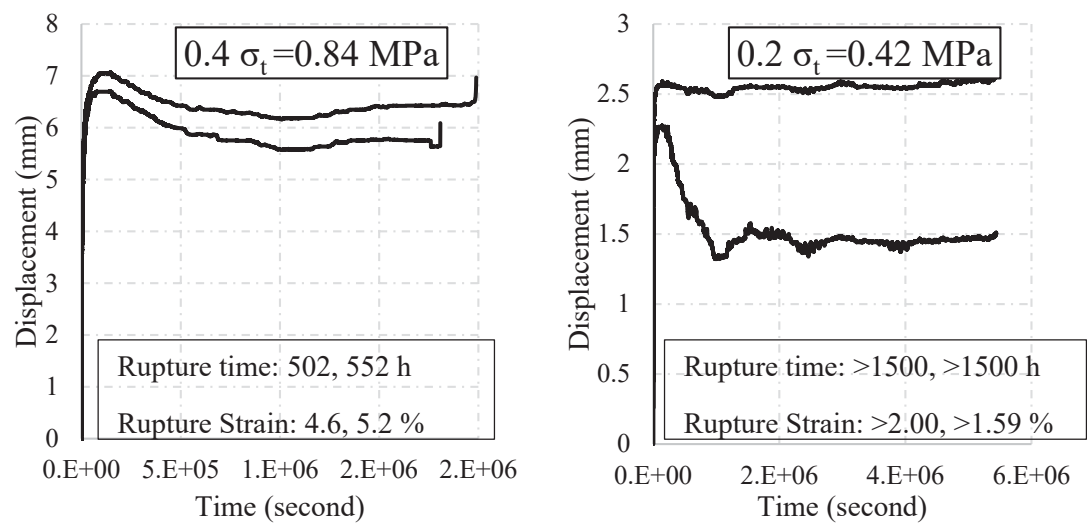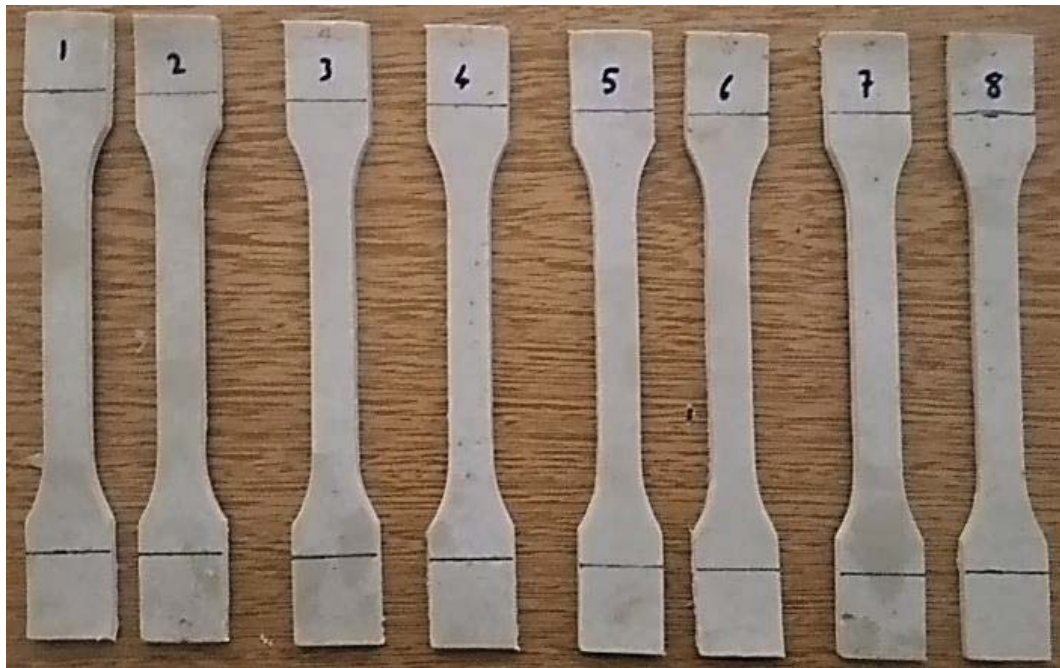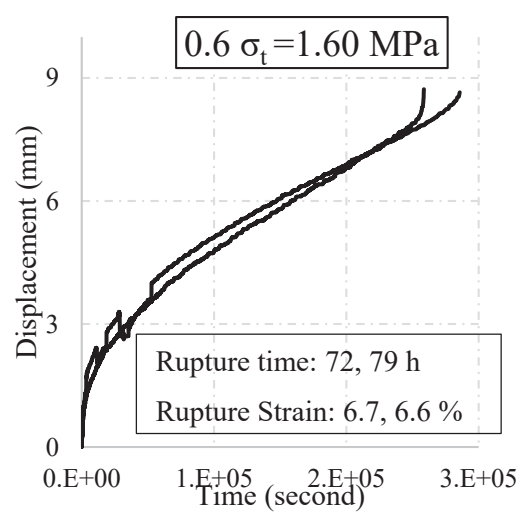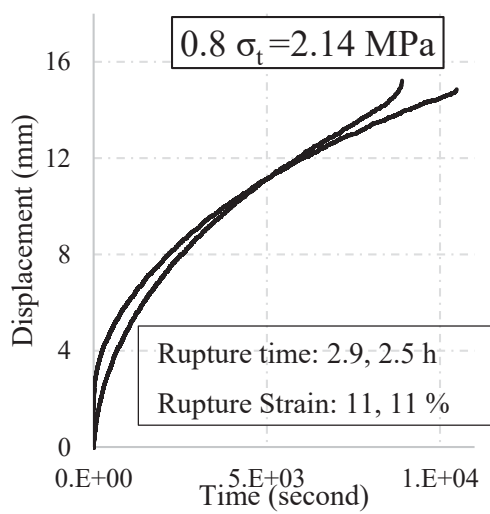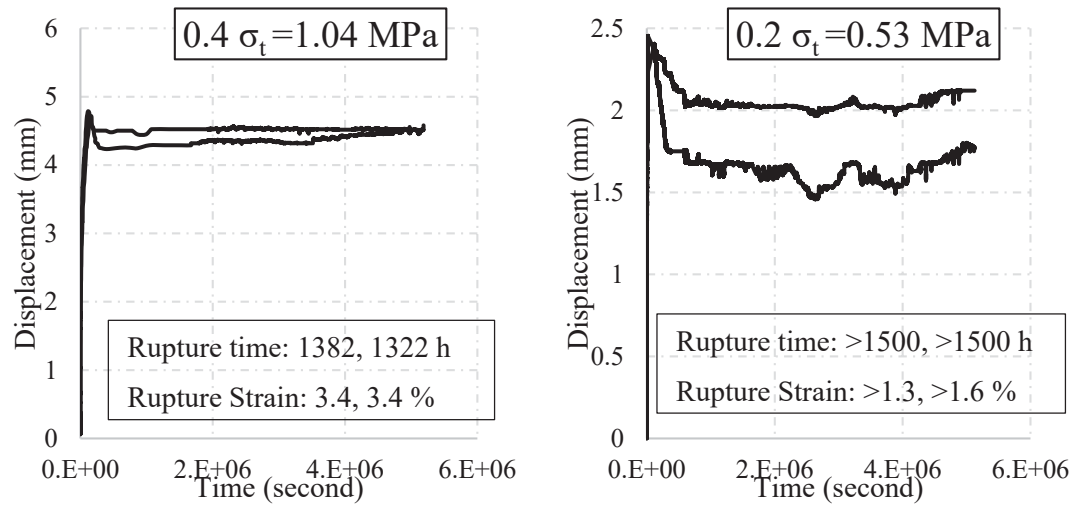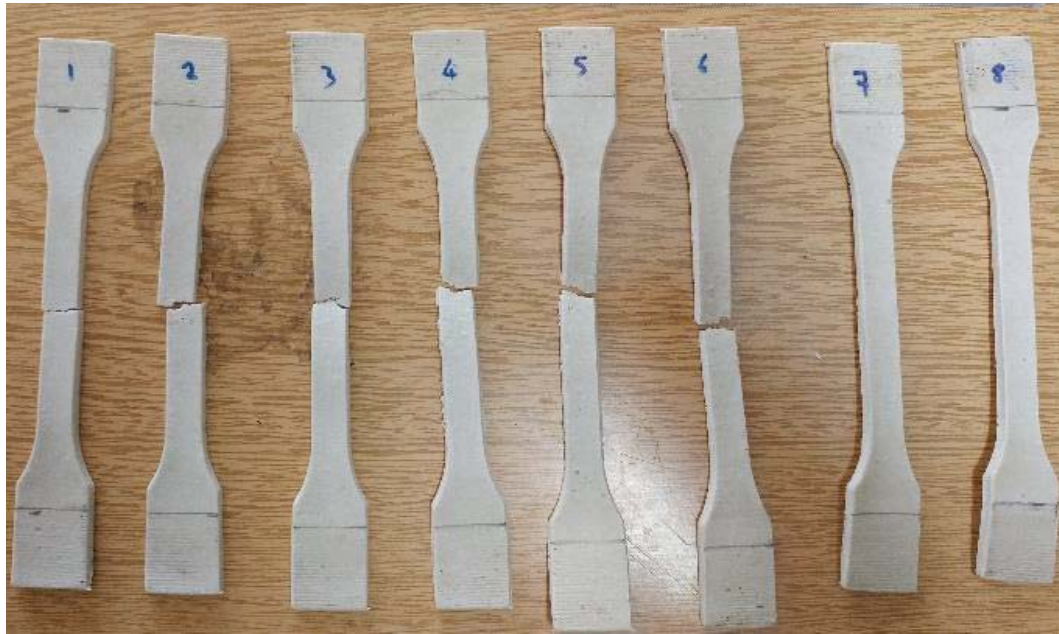
14-Day Raw Data

Figure C. 8. Raw Experimental Data from 14-day Creep Tests for Various Stress Levels (TSL-2)

(a)

195

(b)

Figure C. 9. Specimen Photos Before (a) and After (b) Creep Tests (TSL-2, 14-day)

D. IMPLEMENTED SUBROUTINES

TSL-1 Subroutine

```fortran
SUBROUTINE USDFLD(FIELD,STATEV,PNEWDT,DIRECT,T,CELENT,
1 TIME,DTIME,CMNAME,ORNAME,NFIELD,NSTATV,NOEL,NPT,LAYER,
2 KSPT,KSTEP,KINC,NDI,NSHR,COORD,JMAC,JMATYP,MATLAYO,LACCFLA)
 INCLUDE 'ABA_PARAM.INC'
 CHARACTER*80 CMNAME,ORNAME
 CHARACTER*3  FLGRAY(15)
 DIMENSION FIELD(NFIELD),STATEV(NSTATV),DIRECT(3,3),
     1 T(3,3),TIME(2)
 DIMENSION ARRAY(15),JARRAY(15),JMAC(*),JMATYP(*),COORD(*)
 DOUBLE PRECISION S11, S22, S33, S12, S23, S31
 call GETVRM('S',ARRAY,JARRAY,FLGRAY,JRCD,JMAC,JMATYP,MATLAYO,
 1 LACCFLA)
   sss= MAX(ARRAY (1) , ARRAY(2), ARRAY (3))
         FIELD(1) = (54.474*sss)+80.223
 RETURN
 END
         SUBROUTINE CREEP(DECRA,DESWA,STATEV,SERD,EC,ESW,P,QTILD,
1 TEMP,DTEMP,PREDEF,DPRED,TIME,DTIME,CMNAME,LEXIMP,LEND,
2 COORDS,NSTATV,NOEL,NPT,LAYER,KSPT,KSTEP,KINC)
 INCLUDE 'ABA_PARAM.INC'
 CHARACTER*80 CMNAME
 DIMENSION DECRA(5),DESWA(5),STATEV(*),PREDEF(*),DPRED(*),
 1 TIME(3),COORDS(*),EC(2),ESW(2)
C DEFINE CONSTANTS
    IF (QTILD .LT. 0.53) THEN
    E1=10**(0.5372*QTILD + 1.6779)
             E2= 669.26*QTILD - 133.31
             E3= 40.481*QTILD + 4.5748
             E4= -18.889*QTILD + 25.811
             E5= -12704*QTILD + 6892
             E6= -15.444*QTILD + 24.436
    ELSE IF (QTILD .GE. 0.53 .AND. QTILD .LE. 0.79) THEN
             E1=10**(20.493*QTILD - 8.8985)
             E2=-574.35*QTILD + 525.8
             E3=-32.808*QTILD + 43.418
             E4=-44.669*QTILD + 39.475
             E5=-595.44*QTILD + 474.58
             E6=-46.4*QTILD + 40.842
             ELSE IF (QTILD .GT. 0.79) THEN
             E1=10**(3.2214*QTILD + 4.7458)
             E2=-189.04*QTILD + 221.41
             E3=-25.926*QTILD + 37.981
             E4=-10.696*QTILD + 12.636
             E5= -10.696*QTILD + 12.636
             E6=-10.696*QTILD + 12.636
    ENDIF
             T1= (1/(E1*0.2))*(EXP(-TIME(3)/0.2))
       T2= (1/(E2*2.0))*(EXP(-TIME(3)/2.0))
```

197

```
      T3= (1/(E3*20))*(EXP(-TIME(3)/20))
              T4= (1/(E4*200))*(EXP(-TIME(3)/200))
    T5= (1/(E5*2000))*(EXP(-TIME(3)/2000))
    T6= (1/(E6*20000))*(EXP(-TIME(3)/20000))
    DECRA(1) = DTIME* QTILD* (T1+T2+T3+T4+T5+T6)
              RETURN                 END
```

TSL-2 Subroutine

```fortran
 SUBROUTINE USDFLD(FIELD,STATEV,PNEWDT,DIRECT,T,CELENT,
  1 TIME,DTIME,CMNAME,ORNAME,NFIELD,NSTATV,NOEL,NPT,LAYER,
  2 KSPT,KSTEP,KINC,NDI,NSHR,COORD,JMAC,JMATYP,MATLAYO,LACCFLA)
  INCLUDE 'ABA_PARAM.INC'
  CHARACTER*80 CMNAME,ORNAME
  CHARACTER*3  FLGRAY(15)
  DIMENSION FIELD(NFIELD),STATEV(NSTATV),DIRECT(3,3),
  1 T(3,3),TIME(2)
  DIMENSION ARRAY(15),JARRAY(15),JMAC(*),JMATYP(*),COORD(*)
  DOUBLE PRECISION S11, S22, S33, S12, S23, S31
  call GETVRM('S',ARRAY,JARRAY,FLGRAY,JRCD,JMAC,JMATYP,MATLAYO,
  1 LACCFLA)
    sss= MAX(ARRAY (1) , ARRAY(2), ARRAY (3))
          FIELD(1) = (-152.88*sss + 262.52)
  RETURN
  END
          SUBROUTINE CREEP(DECRA,DESWA,STATEV,SERD,EC,ESW,P,QTILD,
  1 TEMP,DTEMP,PREDEF,DPRED,TIME,DTIME,CMNAME,LEXIMP,LEND,
  2 COORDS,NSTATV,NOEL,NPT,LAYER,KSPT,KSTEP,KINC)
  INCLUDE 'ABA_PARAM.INC'
  CHARACTER*80 CMNAME
  DIMENSION DECRA(5),DESWA(5),STATEV(*),PREDEF(*),DPRED(*),
  1 TIME(3),COORDS(*),EC(2),ESW(2)
C DEFINE CONSTANTS
    IF (QTILD .LT. 0.74) THEN
   E1=10**(-14.234*QTILD + 12.78)
             E2=10**(-1.4394*QTILD + 2.6816)
             E3=10**(-0.2729*QTILD + 1.3187)
             E4=10**(-1.7929*QTILD + 2.4181)
             ELSE IF (QTILD .GE. 0.74 .AND. QTILD .LE. 1.1) THEN
              E1=10**(-1.1885*QTILD + 3.1263)
              E2=10**(1.0002*QTILD + 0.8763)
              E3=10**(-0.6277*QTILD + 1.5812)
              E4=10**(-0.5572*QTILD + 1.5036)
              ELSE IF (QTILD .GT. 1.1) THEN
              E1=10**(-0.31*QTILD + 2.1599)
              E2=10**(0.3357*QTILD + 1.6073)
              E3=10**(-1.6736*QTILD + 2.7317)
              E4=10**(-1.6736*QTILD + 2.7317)
     ENDIF

             T1= (1/(E1*0.2))*(EXP(-TIME(3)/0.2))
     T2= (1/(E2*2.0))*(EXP(-TIME(3)/2.0))
        T3= (1/(E3*20))*(EXP(-TIME(3)/20))
             T4= (1/(E4*200))*(EXP(-TIME(3)/200))

   DECRA(1) = DTIME* QTILD* (T1+T2+T3+T4)
             RETURN
             END
```

CURRICULUM VITAE

PERSONAL INFORMATION

Surname, Name	: Güner, Doğukan
Nationality	: Turkish (TC)
Date and Place of Birth	: 30 September 1988, Konya
Phone	: +90 312 210 2676
E-mail	: dogukan@metu.edu.tr

EDUCATION

Degree	Institution	Year of Graduation
M.S.	METU, Mining Engineering	2014
BS	METU, Mining Engineering	2011
High School	Meram Anatolian High School, Konya	2006

WORK EXPERIENCE

Year	Place	Enrollment
2011-Present	METU Dept. of Mining Engineering	Research Assistant

FOREIGN LANGUAGES

Advanced English, Basic Italian

PUBLICATIONS

Journal Publications

1. Ozturk H., Guner D. (2019). Laboratory and distinct element analysis of the deformability behaviour of thin spray-on liners. International Journal of Rock Mechanics and Mining Sciences. doi: 10.1016/j.ijrmms.2019.104118

2. Guner D., Ozturk H. (2019). Experimental and modelling study on nonlinear time-dependent behaviour of thin spray-on liner. Tunnelling and Underground Space Technology, 84, 306-316. doi: 10.1016/j.tust.2018.11.037.

3. Guner D., Ozturk H. (2018). Creep behaviour investigation of a thin spray-on liner. International Journal of Rock Mechanics and Mining Sciences. 108, 58-66. doi: 10.1016/j.ijrmms.2018.05.007.

4. Ozturk H., Guner D. (2017). Failure analysis of thin spray-on liner coated rock cores. Engineering Failure Analysis, 79, 25-33. doi: 10.1016/j.engfailanal.2017. 03.024.

5. Guner D., Ozturk H, Erkayaoglu M. (2017). Investigation of the elastic material properties of Class G cement. Structural Concrete, 18(1), 84-91. doi: 10.1002/suco.201600020.

6. Guner D., Ozturk H. (2017). Püskürtme İnce Kaplamaların Mekanik Özelliklerinin Kür Süresine Göre Değişiminin İncelenmesi. Çukurova Universitesi Mühendislik-Mimarlik Fakultesi Dergisi, 32(1), 121-132.

7. Guner D., Ozturk H. (2016). Experimental and numerical analysis of the effects of curing time on tensile mechanical properties of thin spray on liners. Rock Mechanics and Rock Engineering, 49(8), 3205-3222. doi: 10.1007/s00603-016-0997-x.

Conference Publications

1. Guner D., Ozturk H. (2019). A 5-parameter isothermal creep model for polymeric liners. Proceedings of GSRD International Conference, Budapest, Hungary.

2. Guner D., Ozturk H. (2019). Finite element simulation on tensile creep behaviour of underground support liner. XVI International Congress "Machines. Technologies. Materials", Varna, Bulgaria.

3. Guner D., Ozturk H. (2018). Creep modelling study of a surface support liner. 3rd International Conference on Energy Engineering and Smart Materials, Milan, Italy.

4. Guner D., Ozturk H. (2018). Time-dependent material behaviour of aged surface support liner. 6th International Geomechanics Conference, Varna, Bulgaria.

5. Guner D., Ozturk H. (2017). Tensile/Creep Test specimen preparation practices of surface support liners. The World Multidisciplinary Earth Sciences Symposium (WMESS), Prague, Czech Republic.

6. Guner D., Ozturk H. (2017). Creep behaviour of a polymer-based underground support liner. The 2nd International Conference on Energy Engineering and Smart Materials, 1884(1), Doi: 10.1063/1.5002518, Lyon, France.

7. Guner D., Ozturk H. (2017). Isothermal creep behaviour investigation of thin spray-on liners. 51ST US Rock Mechanics / Geomechanics Symposium, San Francisco, CA.

8. Guner D., Ozturk H. (2017). Comparison of mechanical properties of thin spray-on liners under tension and compression. 25th International Mining Congress of Turkey, 81-88, Antalya, Turkey.

9. Guner D., Ozturk H. (2016). Scale effect of thin spray on liners for pillar reinforcement. Eighth International Symposium on Ground Support in Mining and Underground Construction, Lulea, Sweden.

10. Yardimci AG.,Tutluoglu L., Karpuz C., Ozturk H., Guner D. (2016). Quality assessment of backfill performance for an underground iron mine in Turkey. Eighth International Symposium on Ground Support In Mining and Underground Construction, Lulea, Sweden.

11. Guner D., Ozturk H. (2016). New performance criterion for thin spray on liners: tensile toughness. 50TH U.S. Rock Mechanics/Geomechanics Symposium, Houston, Texas.

12. Guner D., Ozturk H. (2015). Effect of curing time on elastic material behaviour of thin spray on liners. 23rd Mine Planning and Equipment Selection-Smart Innovation In Mining, 1041-1050, Johannesburg, SA.

13. Guner D., Ozturk H. (2015). Importance of displacement measurement location of polymeric dogbone tensile test specimens. 4th International Symposium Frontiers In Polymer Science, Riva del Garda, Italy.

14. Guner D., Ozturk H. (2015). Comparison of mechanical behaviour of g class cements for different curing time. 24th International Mining Congress and Exhibition, 445-451, Antalya, Turkey.

15. Guner D., Ozturk H. (2014). Effect of curing time on geomechanical properties of a ductile thin spray on liner. 6th International Geomechanics Conference, 168-175, Varna, Bulgaria.

16. Tutluoglu L, Karpuz C, Ozturk H, Guner D, Yardimci AG. (2013). Geotechnical considerations for mining method selection of a potential underground iron ore mine in mideastern Turkey. 22nd Mine Planning and Equipment Selection Conference, 491-500., Doi: 10.1007/978-3-319-02678-7, Dresden, Germany.

17. Guner D., Ozturk H. (2013). Tensile strength properties of underground support liners. 3rd International Symposium Frontiers In Polymer Science, Sitges, Spain.

HOBBIES

Basketball, Movies, Theater, Gourmet